Agronomy Research

Established in 2003 by the Faculty of Agronomy, Estonian Agricultural University

Aims and Scope:

Agronomy Research is a peer-reviewed international Journal intended for publication of broad-spectrum original articles, reviews and short communications on actual problems of modern biosystems engineering incl. crop and animal science, genetics, economics, farm- and production engineering, environmental aspects, agro-ecology, renewable energy and bioenergy etc. in the temperate regions of the world.

Copyright & Licensing:

Agronomy Research online:

Agronomy Research is available online at: https://agronomy.emu.ee/

Acknowledgement to Referees:

The Editors of *Agronomy Research* would like to thank the many scientists who gave so generously of their time and expertise to referee papers submitted to the Journal.

Abstracted and indexed:

SCOPUS, EBSCO, DOAJ, CABI Full Paper and Clarivate Analytics database: (Zoological Records, Biological Abstracts and Biosis Previews, AGRIS, ISPI, CAB Abstracts, AGRICOLA (NAL; USA), VINITI, INIST-PASCAL.)

Subscription information:

Institute of Technology, EMU
Fr.R. Kreutzwaldi 56,
51006 Tartu,
ESTONIA
e-mail: timo.kikas@emu.ee

Journal Policies:

Estonian University of Life Sciences, Latvia University of Life Sciences and Technologies, Vytautas Magnus University Agriculture Academy, Lithuanian Research Centre for Agriculture and Forestry, and Editors of *Agronomy Research* assume no responsibility for views, statements and opinions expressed by contributors. Any reference to a pesticide, fertiliser, cultivar or other commercial or proprietary product does not constitute a recommendation or an endorsement of its use by the author(s), their institution or any person connected with preparation, publication or distribution of this Journal.

ISSN 1406-894X

CONTENTS

Agronomy Research **21**(S3), 1433–1450, 2023
https://doi.org/10.15159/AR.23.092

Identification of Mexican maize races (*Zea mays* L.) with drought tolerance using osmotic potential experiments for genetic breeding

J.A. Batista-Rascon[1], J.C. Jiménez-Galindo[2,*], N. Ramírez-Cabral[3], G. Castellanos-Pérez[1] and J.J. Figueroa-Gonzalez[3]

[1]Autonomous University of Chihuahua, Agrotechnological Sciences Faculty, V. Carranza y Escorza s/n, Col. Centro, Chihuahua, 31000 Chihuahua, México
[2]Agriculture and Livestock Research, National Institute of Forestry, Av. Hidalgo No 1213, Cuauhtémoc, 31500 Chihuahua, México
[3]National Institute of Forestry, Agriculture and Livestock Research, Km. 24.5 Carretera Zacatecas-Fresnillo Calera de Víctor Rosales, Zacatecas. C.P. 98500, México
[*]Correspondence: cruz2477@yahoo.com.mx

Received: July 13rd, 2023; Accepted: September 23rd, 2023; Published: October 23rd, 2023

Abstract. Maize (*Zea mays* L.) is the third most important cereal crop worldwide after wheat and rice per cultivated area with 249,225,876 hectares and the most important crop for number of harvested grain tons with 1,482,997,259 in 2021. Some native Mexican maize races could be a source for drought tolerance to improve commercial cultivars and hybrids. The experiments were conducted using various osmotic pressures (OP) induced by polyethylene glycol (PEG-6000) (0, -0.05, -0.15, -0.30 and -0.49 MPa) simulating an increase of drought stress in ten maize genotypes. The main objectives of this study were the evaluation of germination and seedling growth components in response to drought stress and the identification of sources of drought tolerance in Mexican maize races. Apachito-r showed an increased germination in 110.4%, Cristalino-079 had a decreased germination in 98.7% and Cristalino-279 reduced its germination in a 91.1% compared to the control. Apachito-r outstands in root length at -0.05 OP increasing 200.1% and at -0.49 increasing 129.8%. The values for stem length were decreasing as the OP was increasing and only Apachito-r showed a significant difference at -0.30 MPa decreasing 39.8% respect to its control. Cristalino-279 showed significant difference in the variable root fresh weight and its value outstand at -0.15 increasing 267.2%, at -0.30 increasing 281.6% and at -0.49 MPa increasing 189.3% compared to the control in water. The variable root dry weight had the highest value for Apachito-r at -0.05 MPa increasing in a 189.4%, decreasing at -0.15 in 72% and at -0.30 MPa in a 79.8% and increasing at -0.49 MPa in 112.3%. Also noteworthy are E-zapata-r increasing 190.5% and Cristalino-061 increasing 142.9% at -0.30. E-zapata-r at -0.49 increased 115.1%. Cristalino-279 showed significant difference in the variable stem fresh weight and its value outstand at -0.05, -0.15 and -0.30 MPa increasing 146.7%, 103.7% and 60.2% respectively. Finally, in stem dry weight the tendency was to decrease as OP was increasing, however Cristalino-279 showed differences at -0.30 decreasing in 89.5% and at -0.49 MPa increasing in a 143.5% respect to the control. The most drought tolerant genotypes were Cristalino-279, Apachito-r, Azul and 8-carreras-PP. The most tolerant genotypes showed greater root length, greater root fresh and dry weight, better germination and greater stem length.

Resistant and susceptible genotypes are ideal material to understand the physical and chemical mechanisms related to drought tolerance. Cristalino-279 shows the best level of drought tolerance at all levels of osmotic pressure, this genotype can be used as a source of drought tolerance for the improvement of commercial maize.

Key words: native maize races, drought tolerance, osmotic pressure, polyethylene glycol.

INTRODUCTION

Worldwide, maize (*Zea mays* L.) is the third most important cereal crop, after wheat and rice (Huang et al., 2015) per cultivated area with 249,225,876 hectares harvested in 2021 (FAOSTAT, 2023); and the most important crop in the world, per grain harvested tons, with 1,482,997,259 (Shiferaw et al., 2011; FAOSTAT, 2023). Maize is listed as an essential crop for world food security, for humans and in animal consumption (Campos et al., 2004; Prasanna, 2012). Moreover this crop is a staple grain with economic and social importance (Ureta et al., 2020; Magorokosho & Tongoona, 2003; Iqbal et al., 2021).

Climate change is increasing average temperatures, modifying patterns of precipitation and reduction water availability, this phenomena is likely to increase in frequency and intensity in the coming decades (Hendrix & Glaser, 2007; Lobell & Burke, 2008). Due to climate change, grain yield and quality will decrease, because of the increment of biotic and abiotic stresses, among these, dry and heat stresses are the most remarkable affecting negatively growth and yield traits of maize (Sabagh et al., 2018; Zenda et al., 2018; Islam et al., 2019; Dong et al., 2020; Raj et al., 2020; Liu et al., 2022; SINGH et al., 2022).

Mainly, farmers grow the maize under rain-fed conditions (Hellin et al., 2014). Biradar et al. (2006) mentioned that globally more than 50% of the total cultivated area of maize is under rain-fed conditions.

Some native Mexican maize races have been reported as tolerant to drought, such is the case of Apachito, Cristalino de Chihuahua and Azul (Ruiz Corral et al., 2008; Ruiz Corral et al., 2013). Other genotypes from other regions of the world have been identified such as hybrids with good response under drought conditions as H3, H4, H8, H11, H15, H19, H27 and H29 (Qayyum et al., 2012). Tohono O'odham Z16 maize was reported with high drought tolerance (Shisanya & Hornetz, 1997). Arun-2 the most drought tolerant maize was reported by (Magar et al., 2019). Genotypes BC678 and BC404 were reported as resistant to drought stress (Khayatnezhad & Gholamin, 2012). Ahmad et al. (2015) found two hybrids with good drought tolerance 6525 and 32B33. Naghavi et al. (2013) found three genotypes with highest tolerance to drought KSC-720, KSC-710-GT and KSC-700. ND476 genotype were reported with high level of drought tolerance (Dong et al., 2020). And from the tested genotypes by (Iqbal et al., 2021), genotype 249 and genotype 252 were the best genotypes for maize improvement for tolerance to drought stress.

The loss in maize production is accounted approximately 16% in lowland tropics (Edmeades et al., 2006) and it reached up to 60% in severely drought-affected regions/ seasons (Ribaut et al., 2009). Current trends of climatic change show a likehood of increase water scarcity and reduce maize productivity by 15–30% (Lobell et al., 2014).

Recommended drought tolerance adaptation strategies include farmers' increased use of tolerant maize genotypes (Hellin et al., 2014). Among different plant adaptive strategies to water stress (WS), drought avoidance is one of the most important, can be used for enhancing crop yield under WS conditions (Blum, 2011). This can be achieved in a variety of ways, including adjustment of growth rate and growth pattern of shoot and root (Comas et al., 2013). It is already known that the ability of the plant for water uptake depends on root system, root structure, and access to water in soil which in turn determine the functionality of plant shoot. Thus, extent of drought avoidance or tolerance in plants can be determined by a number of biometric attributes such as leaf number and structure, root length and branching pattern, leaf waxy layer, leaf rolling etc. (Blum, 2011; Comas et al., 2013). Since crop sensitivity at the germination growth stage governs overall success of a crop, it is advocated that biometric attributes at the early growth stages can be used as indicator for crop performance at later growth stage or as a selection criteria for improving crop resistance against drought (Lobell et al., 2008; Reynolds & Tuberosa, 2008; Blum & Blum, 2011; Comas et al., 2013). This argument can be supported by the fact that several germination and seedling growth indices are frequently used as predictors to appraise drought tolerance in crop plants (Comas et al., 2013; Ayalew et al., 2015).

One of the most plausible techniques to simulate uniform drought includes the use of metabolically inactive compound such as Polyethylene glycol which has been widely employed by a number of workers to study the effects of WS in different groups of plants (Waheed, 2014; Ahmad et al., 2015; Islam et al., 2019; Zeng et al., 2019; Badr et al., 2020; Raj et al., 2020; Bukhari et al., 2021; Badr et al., 2020; Suhartono, 2021). Some efforts have been carried out in different crops to find sources of tolerance to drought, such is the case of (Jimenez-Galindo et al., 2018) that found that the tolerant bean genotypes, detected with PEG-6000, T-cafe and R-bufa, showed more root length and root dry weight. Therefore these traits could help us indirectly to select tolerant genotypes in beans (Jiménez Galindo & Acosta Gallegos, 2013). In addition (Ortega-Ortega et al., 2023) found that tolerant genotypes detected with PEG-6000 bioassays of oat to drought have higher germination rate with respect to their control in water, longer roots, and higher root fresh weight, root dry weight, shoot fresh weight, and shoot dry weight. In this case Teporaca genotype was the most tolerant genotype and had the best response in field experiments with irrigation-drought experiments.

The main objective of this research is to assess drought tolerance in a collection of native Mexican maize races to identify the best sources of drought tolerance at early stages.

MATERIALS AND METHODS

Plant material

Ten genotypes with diverse genetic backgrounds into six Mexican maize races (*Zea mays* L.) recollected by INIFAP at Chihuahua State, were used, to study drought tolerance on germination, and root and stem development characters using polyethylene glycol (Table 1). The Apachito, Cristalino de Chihuahua and Azul races, tolerant to drought, were selected (Ruiz Corral et al., 2008; Ruiz Corral et al., 2013). In addition, we studied the races: Gordo, Palomero, E-Zapata-r and 8-Carreras-PP with unknown response to drought tolerance.

Table 1. Agronomic traits of ten genotypes of maize, evaluated for drought tolerance

Genotype	Origin	Drought response	Race	Seed color
Apachito-r	INIFAP	Tolerant[1, 2]	Apachito	Pink
Gordo	INIFAP	Unknown	Gordo	White
Palomero	INIFAP	Unknown	Palomero de Chihuahua	Yellow
E-Zapata-r	INIFAP	Unknown	Unknown	White
Cristalino-282	INIFAP	Tolerant[2]	Cristalino de Chihuahua	Yellow
Azul	INIFAP	Tolerant[2]	Azul	Black
Cristalino-079	INIFAP	Tolerant[2]	Cristalino de Chihuahua	Yellow
Cristalino-279	INIFAP	Tolerant[2]	Cristalino de Chihuahua	White
Cristalino-061	INIFAP	Tolerant[2]	Cristalino de Chihuahua	White
8-carreras-PP	INIFAP	Unknown	8-carreras	White

[1]Apachito race was reported as tolerant to dry conditions by (Ruiz Corral et al., 2008). [2]Apachito, Cristalino de Chihuahua and Azul races were reported as tolerant to dry conditions by (Ruiz Corral et al., 2013).

Experimental design

Two experiments were conducted in Lab where seeds were incubated at 28 °C in a complete randomized design in a factorial arrangement. Factorial combinations of ten maize genotypes and five osmotic pressures levels were evaluated with three repetitions. The experimental plot was one petri dish of 10 cm in diameter. Ten seeds of each accession were used per repetition with a layer of filter paper, to which 8 mL of the previously PEG-6000 prepared dilutions were added. Obtaining a total of 10 genotypes and 5 levels of osmotic pressure of 0.0, -0.05, -0.15, -0.30 and -0.49. To carry out the evaluation, dilutions of polyethylene glycol (PEG-6000) were prepared in distilled water at 0, 50, 100, 150, and 200 g of PEG-6000 per liter of distilled water, to reach an osmotic pressure (OP) of 0.0, -0.05, -0.15, -0.30 and -0.49, respectively, based on the equation provided by (Michel & Kaufmann, 1973). The variables germination, root and stem length, root fresh weight, stem fresh weight, root dry weight and stem dry weight were measured. Seeds were considered germinated when the root or stem was approximately 10 mm in length or more. After seven days, the roots and stems of the seedlings were measured in centimeters and on the same day the fresh root and stem were weighed on a precision balance in grams. The root and stem tissue were cut and placed in a stove at 45 °C for seven days to record the root and stem dry weight in grams. All data were expressed as percent reduction or increase respect to their own control in water with 0.0 OP.

Statistical analysis

An analysis of variance (ANOVA) was made using the GLM (General Linear Model) procedure (PROC GLM) of SAS. Sources of variation were genotype, stress level, and genotype × stress level interaction. Genotypes, osmotic pressure and genotype × osmotic pressure interaction were considered fixed effects. Besides, an individual ANOVA by stress level was also carried out. We used Tukey at $p < 0.05$ for mean comparisons. In addition, Principal Component Analyzes was performed with all traits using the SAS Software for Windows 9.0 statistical package (SAS Institute. Inc. Cary, N.C., USA, 2002). Previously, all data were standardized with mean = 0 and standard deviation = 1. The first component was used to ordering genotypes because it explained most of the variability across Osmotic Pressure levels (OP1 = 44.7%, OP2 = 36.5%, OP3 = 45.0% and OP4 = 40.3% of the explained variability) and was considered as an index of tolerance to drought.

RESULTS AND DISCUSSION

Of the ten maize races under study, three stand out in percentage of germination: Apachito-r which had an increased germination in 110.4%, Cristalino-079 with a decreased germination of 98.7% and Cristalino-279 that reduced its germination in 91.1% compared to control at high osmotic pressure at -0.49 OP. No significant differences were obtained at -0.05, -0.15 and -0.30 MPa between maize races (Figs 1 –7).

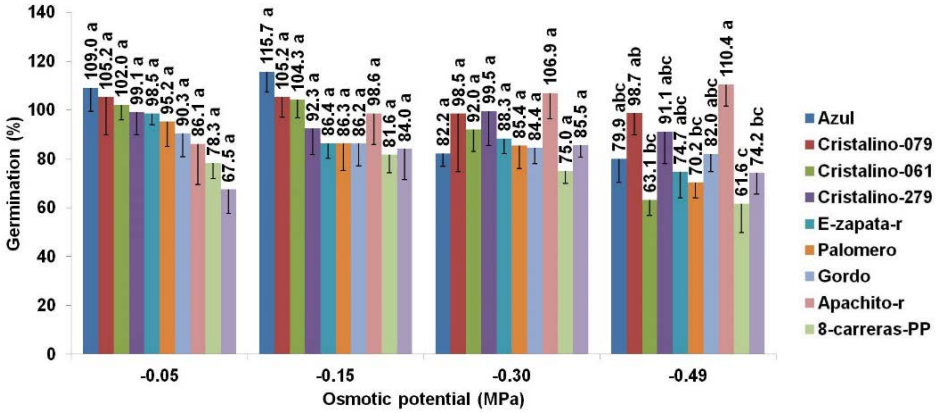

Figure 1. ANOVA for germination (%) effects by the osmotic potential of percentage data of ten maize genotypes evaluated in vitro conditions under different osmotic potentials generated by increasing concentration of PEG-6000. The control group is not shown because it is the 100% for each variety and for each trait. The *LSD* for the interaction (genotype*PEG) was calculated with the formula *LSD* = Distribution T (α-DF) * √EMS * 2 / n repetitions.

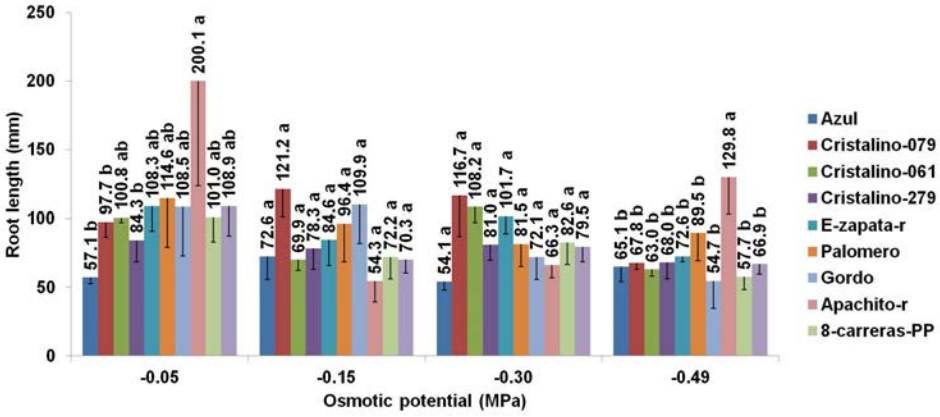

Figure 2. ANOVA for root length effects by the osmotic potential of percentage data of ten maize genotypes evaluated in vitro conditions under different osmotic potentials generated by increasing concentration of PEG-6000. The control group is not shown because it is the 100% for each variety and for each trait. The *LSD* for the interaction (genotype*PEG) was calculated with the formula *LSD* = Distribution T (α-DF) * √EMS * 2 / n repetitions.

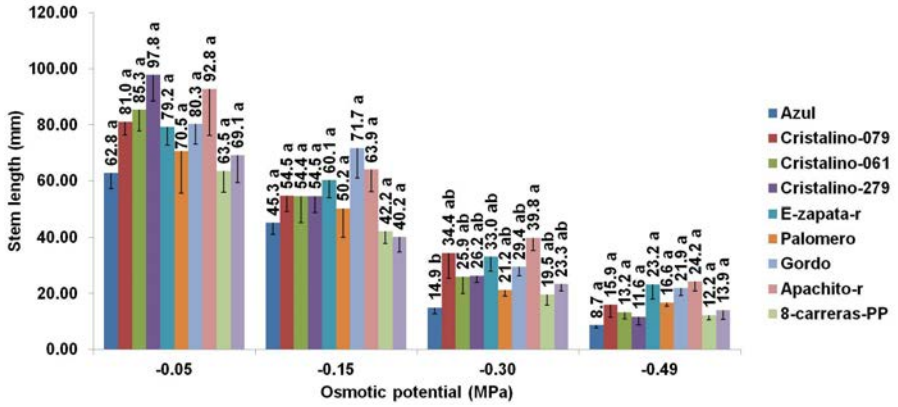

Figure 3. ANOVA for stem length effects by the osmotic potential of percentage data of ten maize genotypes evaluated in vitro conditions under different osmotic potentials generated by increasing concentration of PEG-6000. The control group is not shown because it is the 100% for each variety and for each trait. The *LSD* for the interaction (genotype*PEG) was calculated with the formula *LSD* = Distribution T (α-DF) * √EMS * 2 / n repetitions.

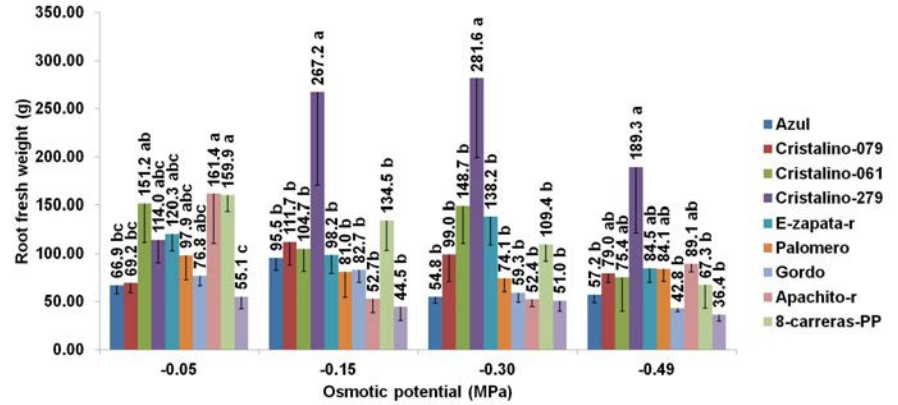

Figure 4. ANOVA for root fresh weight effects by the osmotic potential of percentage data of ten maize genotypes evaluated in vitro conditions under different osmotic potentials generated by increasing concentration of PEG-6000. The control group is not shown because it is the 100% for each variety and for each trait. The *LSD* for the interaction (genotype*PEG) was calculated with the formula *LSD* = Distribution T (α-DF) * √EMS * 2 / n repetitions.

Apachito-r outstands in root length at -0.05 OP increasing 200.1% compared to control. No significant differences were found at -0.15 and -0.30 between maize races; and at -0.49 only Apachito-r was different to the other races, increasing 129.8% respect to its control in water. The values for stem length were decreasing as the OP was increasing and only Apachito-r showed a significant difference at -0.30 MPa decreasing 39.8% respect to its control. Cristalino-279 showed significant difference in the variable root fresh weight and its value outstand at -0.15 increasing 267.2%, at -0.30 increasing 281.6% and at -0.49 MPa increasing 189.3% compared to the control in water. The variable root dry weight had the highest value for Apachito-r at -0.05 MPa increasing in

189.4%, decreasing at -0.15 in 72% and at -0.30 MPa in a 79.8% and increasing at -0.49 MPa in 112.3%. Also noteworthy are E-zapata-r increasing 190.5% and Cristalino-061 increasing 142.9% at -0.30. E-zapata-r at -0.49 increasing 115.1% compared to the control. Cristalino-279 showed significant difference in the variable stem fresh weight and its value outstand at -0.05, -0.15 and -0.30 MPa increasing 146.7%, 103.7% and 60.2% respectively. Finally, in stem dry weight the tendency was to decrease as OP was increasing, however Cristalino-279 showed differences at -0.30 decreasing in 89.5% and at -0.49 MPa increasing in 143.5% (Figs 1–7).

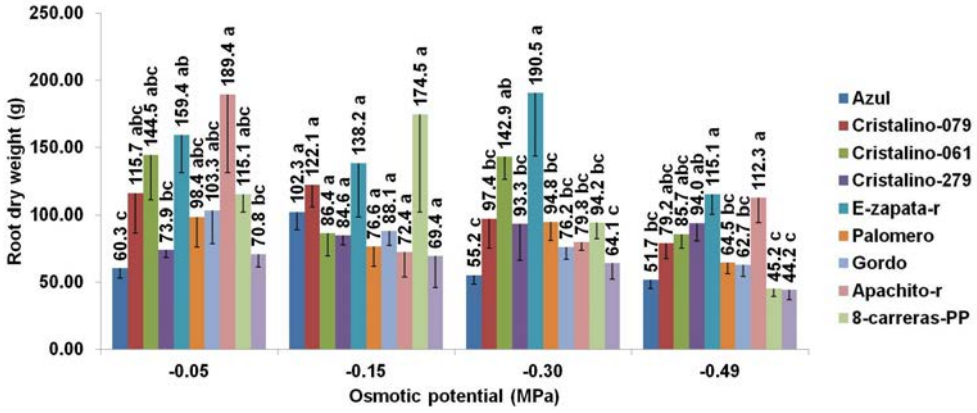

Figure 5. ANOVA for root dry weight effects by the osmotic potential of percentage data of ten maize genotypes evaluated in vitro conditions under different osmotic potentials generated by increasing concentration of PEG-6000. The control group is not shown because it is the 100% for each variety and for each trait. The *LSD* for the interaction (genotype*PEG) was calculated with the formula *LSD* = Distribution T (α-DF) * √EMS * 2 / n repetitions.

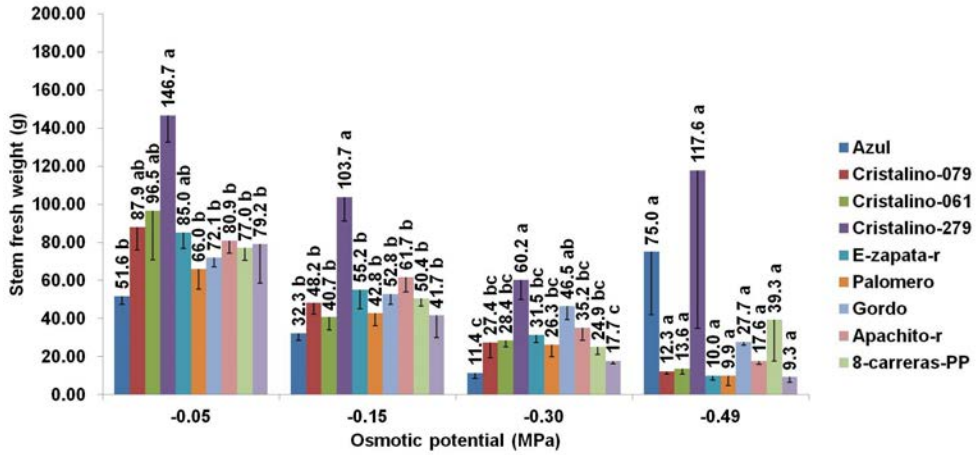

Figure 6. ANOVA for stem fresh weight effects by the osmotic potential of percentage data of ten maize genotypes evaluated in vitro conditions under different osmotic potentials generated by increasing concentration of PEG-6000. The control group is not shown because it is the 100% for each variety and for each trait. The *LSD* for the interaction (genotype*PEG) was calculated with the formula *LSD* = Distribution T (α-DF) * √EMS * 2 / n repetitions.

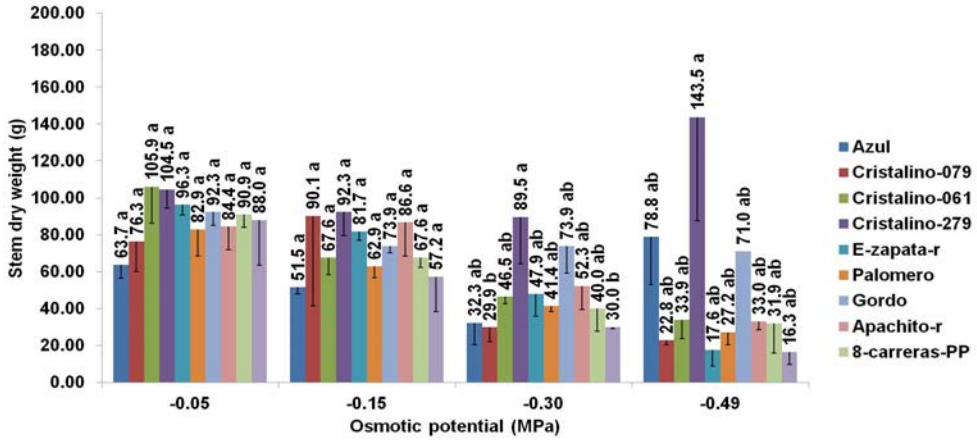

Figure 7. ANOVA for stem dry weight effects by the osmotic potential of percentage data of ten maize genotypes evaluated in vitro conditions under different osmotic potentials generated by increasing concentration of PEG-6000. The control group is not shown because it is the 100% for each variety and for each trait. The *LSD* for the interaction (genotype*PEG) was calculated with the formula *LSD* = Distribution T (α-DF) * √EMS * 2 / n repetitions.

Many studies have been carried out to search sources of drought tolerant maize using PEG-6000 (Bashir et al., 2016; Khayatnezhad et al., 2010; Magar et al., 2019). Sabagh et al. (2018) mention that due to drought stress, yield of maize reduce significantly, especially in Arid and Semi-Arid regions around the world. The use of drought tolerant maize genotypes has potential to stabilize the grain yield of maize (Sabagh et al., 2018). Therefore, developing cultivars tolerant to drought stress is challenging for breeders to face the future climate changing conditions (Sabagh et al., 2018; Iqbal et al., 2021). The main traits that have been used to evaluate drought tolerance with PEG-6000 are: germination, root length, stems length, fresh and dry weight of the root, fresh and dry weight of the stem (Bashir et al., 2016; Jimenez-Galindo et al., 2018; Ortega-Ortega et al., 2023). Other researchers have been measured number of crown roots, number of seminal roots, primary root length, number of lateral roots fresh root weight, dry root weight and these genetic variations can be used to develop high yielding drought tolerant maize genotypes through selection and conventional breeding approaches (Qayyum et al., 2012). Mexico is the primary center of origin and diversity for maize (*Zea mays* L.) (Hellin et al., 2014; SINGH et al., 2022). For this reason, it is extremely important to search for the best sources of drought tolerance in maize races from northern Mexico where the maize genotypes have been mostly exposed to severe droughts, perhaps for thousands of years. However, few studies have been carried out with maize races from Mexico.

On the other hand, when evaluating root growth, it was also observed that the Apachito-r genotype showed greater length in root growth at -0.05 and -0.49 of OP. Our results are agree with (Zeng et al., 2019) that mention that the growth and development of maize roots are closely related to drought tolerance. While when evaluating the length of its stem, significant differences were only found at -0.30 of OP. These results are consistent, because the Apachito-r genotype has been reported as adaptable to drought stress conditions, but only in some period of its production cycle (Ruiz Corral et al., 2013), although no significant differences were found at all OP concentrations.

When evaluating the total fresh weight of the root, a greater weight was observed at -0.05 of OP, in the races: Cristalino-061, Apachito-r and 8-carreras-PP. In addition, the higher weight found in the Cristalino-279 genotype at -0.15, -0.30 and -0.49 from OP. However, it is necessary to highlight that not all the genotypes of the Cristalino de Chihuahua race presented a good response to drought as mentioned by (Ruiz Corral et al., 2013), highlighting only the Cristalino-279 genotype. Maize selection by farmers and by environmental factors led to the evolution of a large number of distinct Mexican maize races (Perales & Golicher, 2014). This is probably due to the great variability of Cristalinos de Chihuahua that has been preserved in the mountains of the state by the Tarahumaras. This native group, and with the help of the environment, have selected genotypes for different colors and their response to biotic and abiotic factors. This is also consistent because Mexico is the main center of origin for bean and maize (SINGH et al., 2022), as mentioned by (Jiménez-Galindo et al., 2023) where it is mentioned that maize Mexican races, have been exposed for thousands of years to adverse biotic and abiotic factors. We are agree with (Eagles & Lothrop, 1994) that mention that Mexican maize races is of ancient origin and has a distinct morphology, karyotype, and isozyme frequency. Previous research describes that the Cristalino de Chihuahua maize race tolerates varying degrees of WS during its production stages, and it is a race that commonly grows in conditions of low humidity and with high temperatures around 31 °C (Ruiz Corral et al., 2013). Therefore, it can be considered that the higher fresh weight of the root, which was observed in the Cristalino-279 genotype, is because of its greater tolerance to drought stress compared to Apachito-r, Cristalino-061 and 8-Carreras- PP, during root development.

In contrast, when evaluating root dry weight, the maize races with the highest weight were: Apachito-r, E. Zapata-r and Cristalino-061, the three maize genotypes, showed significant differences at -0.05 from OP; E. Zapata-r and Cristalino-061 at -0.30 and Apachito-r and E. Zapata-r at -0.49 of OP. Although it is known that the Cristalino-279 genotype obtained greater root weight when fresh, but not dry, it could be suggested that the root of Cristalino-279 in contrast to the races: Apachito-r, Cristalino-061 and E. Zapata-r, maintains a greater amount of water in its root, possibly because drought stress has induced the expression of proteins such as aquaporins (Chávez Suárez et al., 2014), these proteins regulate and transport water, under conditions of abiotic stress, such as drought. Therefore, it could be suggested that the lower amount of dry weight of the Cristalino-279 genotype is due to the fact that the evaporation rate was higher when subjected to dehydration, since possibly its roots are capable of retaining a greater amount of water, in contrast to the other races that obtained higher root dry weight.

Principal Component Analysis

On the other hand, when performing the principal component analysis, to evaluate the effects of the increasing osmotic potential (PEG-6000) of the maize genotypes in vitro, the principal component (PC1) explains 44.7% at -0.05 MPa, 36.5% at -0.15 MPa, 45.0% at -0.30 MPa and 40.3% at -0.49 MPa of OP. The PC1, when considered as an index of tolerance to drought, it was observed, that the maize races evaluated, with greater tolerance to drought at -0.30 and -0.49 of OP, were Cristalino-279, Azul and 8-carreras-PP, in contrast to Apachito-r, E-Zapata-r and Palomero, which proved to be maize races with greater susceptibility to drought at -0.49 MPa.

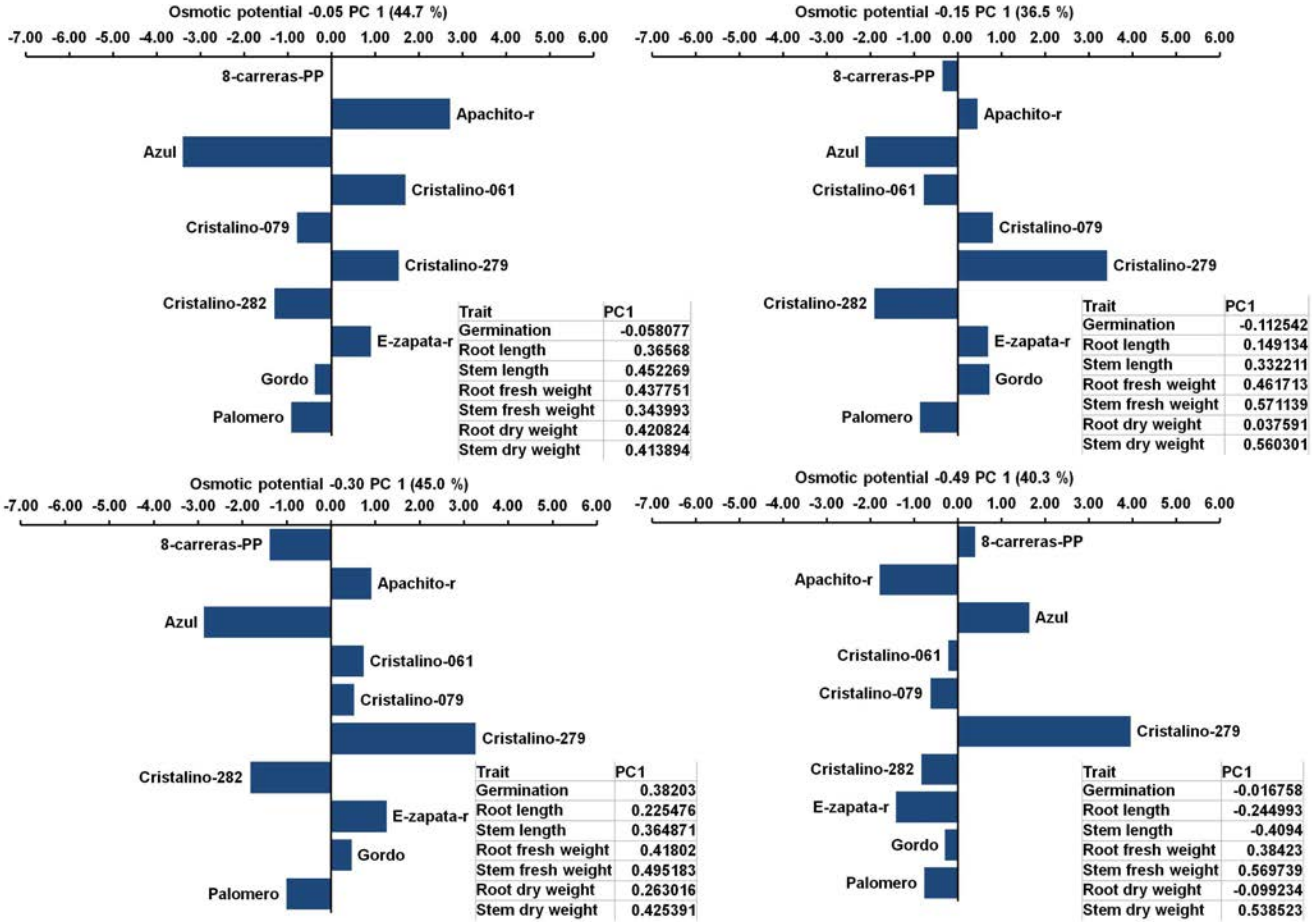

Figure 8. Effect of osmotic potential in ten maize genotypes evaluated *in vitro* under osmotic potential generated by an increasing concentration of PEG-6000.

Apachito-r responds well at -0.05, -0.15 and -0.49 MPa. Therefore, it is observed that the best genotype for tolerance to drought was Cristalino-279, which maintained tolerance at all different levels of OP evaluated. Fig. 8 shows whether the genotypes respond positively or negatively as the OP level increases. Cristalino-279 responds positively (Fig. 8).

Research has been reported that in maize germination under drought stress, enzymes such as isocitrate lyase (ICL) and malate synthase (MS) are expressed, these belong to the glyoxylate cycle, which is activated under different phonological stages of the plant kingdom, including germination (Ihle & Dure III, 1972; Longo et al., 1975). Furthermore, it has also been shown that both ICL and MS are responsible for inhibiting the action of abscisic acid (ABA), a phytohormone responsible for seed dormancy; in contrast, the germination phytohormone gibberellic acid (GA) is activated (Paek et al., 1998). Therefore, it is probable that Apachito-r, Cristalino-079 and Cristalino-279 genotypes stand out in germination, under drought stress conditions, induced with PEG-6000, due to a higher expression of the enzymes ICL and MS, allowing a greater AG activity in the seeds. The drought tolerance mechanism may be associated with accumulation of osmoprotectants as proline and soluble sugars (Mohammadkhani & Heidari, 2008). The accumulation of soluble sugars is strongly correlated to the acquisition of drought tolerance in plants (Hoekstra et al., 2001).

However, the enzymatic activity of the Mexican maize races mentioned should be studied in the future.

On the other hand, when evaluating the fresh weight of the stem, the best genotype in all the levels induced by drought with PEG-6000, was the Cristalino-279 genotype. Similarly, when evaluating stem dry weight, significant differences were observed at -0.30 and -0.49 of OP, which favor higher, stem dry weight again to the Cristalino-279 genotype. As can be seen, in this evaluated parameter of dry and fresh weight of the stem, Cristalino-279 again obtained greater weight, due to the fact that the Cristalino race is reported as one of those that best adapts to drought stress conditions (Ruiz Corral et al., 2013). Although the other selected races are high-yielding, it is consistently shown that the Cristalino-279 genotype excels in stem weight, both fresh and dry, which could suggest that in addition to retaining a greater amount of water in the stem, could also be a great producer of biomass and therefore, the possibility that it excels in grain yield, although the necessary evaluations are still to be carried out to verify this parameter. Finally, it can be suggested that the races with the highest yield, in different parameters evaluated, were both Apachito-r and Crisitalino-279, both maize races, reported in previous studies (García-Lara & Serna-Saldivar, 2019), also native to the Sierra de Chihuahua. We are agree with (Wen et al., 2012) about the knowledge of genetic diversity within and among maize races is essential for using them in plant breeding.

The maize races with the best response for the variable root length, under drought conditions at -0.49 OP, were the genotypes: Cristalino-279, Azul and 8-carreras-PP. Apachito-r responds well at -0.05, -0.15 and -0.30 (Fig. 9).

Figure 9. Effect of osmotic potential in ten genotypes of maize evaluated *in vitro* under osmotic potential generated by an increasing concentration of PEG-6000. Green arrows show longer roots at -0.49 of OP, and red arrows show shorter roots at -0.49 MPa.

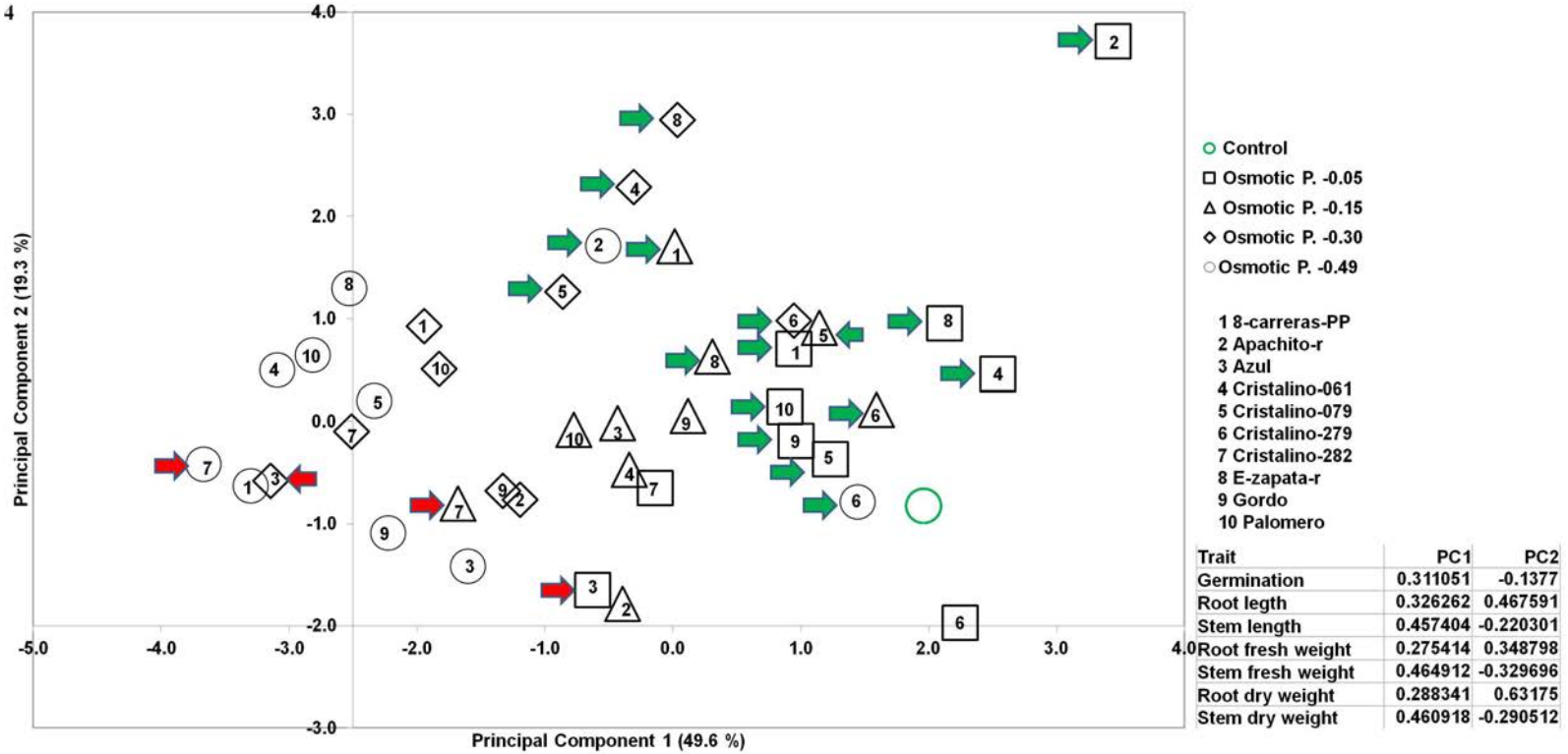

Trait	PC1	PC2
Germination	0.311051	-0.1377
Root legth	0.326262	0.467591
Stem length	0.457404	-0.220301
Root fresh weight	0.275414	0.348798
Stem fresh weight	0.464912	-0.329696
Root dry weight	0.288341	0.63175
Stem dry weight	0.460918	-0.290512

Figure 10. Plot of PC1 vs PC2 for ten maize genotypes and four levels of OP. Green arrows show genotypes with best response to OP, and red arrows show the genotypes with the poor response when OP was increasing.

On the other hand, when performing the principal component analysis at the four OP levels (-0.05, -0.15, -0.30 and -0.49), between PC1 (49.6%) and PC2 (19.3%). It was observed that the genotypes with the best response to the OP at -0.05 were Apachito-r, E-Zapata-r, Cristalino-061, 8-carreras-PP, Palomero, Gordo and Cristalino-079 but when subjected to OP values of -0.15, the best were 8-Carreras-PP, Cristalino-079, Cristalino-279 and E-Zapata-r and, although when increasing the OP to -0.30, the more tolerant were E-zapata-r, Critalino-061, Cristalino-279 and Cristalino-079. Finally, it was shown that when increasing the OP to -0.49, the genotypes with the highest resistance proved to be in order of greater than less tolerance to drought: Cristalino-279 and Apachito-r. In contrast, it was shown that the genotypes most susceptible to drought for OP levels of -0.05, -0.15, -0.30 and -0.49 were: Azul, Cristalino-282, Azul and Cristalino-282, respectively (Fig. 10).

Cristalino-279 shows the best level of drought tolerance at all levels of osmotic pressure, this genotype will help to develop maize drought resistance breeding in Mexico and the world. In addition, to carry out genetic research and improvement in maize we are preparing a MAGIC population, with this races, to study the genomic regions for biotic and abiotic stresses, among them drought tolerance, and in addition grain quality and agronomic traits in a future. Now we have the first recombination with crosses Cacahuacintle × Bofo × Cristalino-079 × Cristalino-279 × Azul × Cristalino-282 × Apachito-r × Apachito-b.

CONCLUSIONS

The most drought tolerant genotypes were Cristalino-279, Apachito-r, Azul and 8-carreras-PP. In contrast to Cristalino-282, the genotype most susceptible to drought. The most tolerant genotypes showed greater root length, greater root fresh and dry weight, better germination and greater stem length. Susceptible genotypes have shorter root length, lower fresh and dry root weight, lower germination and shorter stem length. Resistant and susceptible genotypes are ideal material to understand the physical and chemical mechanisms that are related to drought tolerance. Cristalino-279 shows the best level of drought tolerance at all levels of osmotic pressure and this genotype can be used as a source of drought tolerance for the improvement of commercial maize. In future research we should focus on mapping the genomic regions responsible of drought tolerance using PEG method for phenotyping MAGIC populations from Mexican maize races.

ACKNOWLEDGMENTS. Armando Batista thanks the Agrotechnological Sciences Faculty of Universidad Autónoma de Chihuahua for the support and help given for the realization of the present research. As well as to the National Institute of Agricultural, Forestry and Livestock Research (INIFAP), campus Cuauhtémoc for their economic support and assistance.

FUNDING. This work was supported by National Institute of Forestry, Agriculture and Livestock Research of México. Grant number: 1-1.6-9385034743-A-M.2-2 'Regiones genómicas asociadas a la resistencia a plagas de almacén en una población MAGIC de maíz'.

REFERENCES

Ahmad, Z., Waraich, E.A., Ahmad, R., Iqbal, M.A. & Awan, M.I. 2015. Studies on screening of maize (*Zea mays* L.) hybrids under drought stress conditions. *Journal of Advance Botany and Zoology* **2**, 1–5. doi: 10.15297/JABZ.V2I4.01

Ayalew, H., Ma, X. & Yan, G. 2015. Screening wheat (*Triticum* spp.) genotypes for root length under contrasting water regimes: potential sources of variability for drought resistance breeding. *Journal of Agronomy and Crop Science* **201**, 189–194. doi: https://doi.org/10.1111/jac.12116

Badr, A., El-Shazly, H.H., Tarawneh, R.A. & Börner, A. 2020. Screening for drought tolerance in maize (*Zea mays* L.) germplasm using germination and seedling traits under simulated drought conditions. *Plants* **9**, 565. doi: https://doi.org/10.3390/plants9050565

Bashir, N., Mahmood, S., Zafar, Z.U. & Rasul, S. 2016. Is drought tolerance in maize (*Zea mays* L.) cultivars atthe juvenile stage maintainedat the reproductive stage. *Pak. J. Bot* **48**, 1385–1392.

Biradar, C.M., Thenkabail, P.S., Turral, H., Noojipady, P., Li, Y., Velpuri, M., Dheeravath, V., Vithanage, J., Schull, M. & Cai, X. 2006. A Global Map of Rainfed Cropland Areas at the end of last millennium using Remote Sensing and Geospatial Techniques. *Proceedings* **6418**, 546–550. doi: https://doi.org/10.1117/12.713204

Blum, A. 2011. Drought resistance-is it really a complex trait? *Functional Plant Biology* **38**(10) 753–757. doi: https://doi.org/10.1071/FP11101

Blum, A. 2011. Drought Resistance and Its Improvement. In: Plant Breeding for Water-Limited Environments. *Springer, New York, NY*. doi: https://doi.org/10.1007/978-1-4419-7491-4_3

Bukhari, B., Sabaruddin, Z., Sufardi, S. & Syafruddin, S. 2021. Drought test resistance of maize varieties through PEG 6000. *IOP Conference Series: Earth and Environmental Science, IOP Publishing* **644**, pp. 012040. doi:10.1088/1755-1315/644/1/012040

Campos, H., Cooper, M., Habben, J., Edmeades, G. & Schussler, J. 2004. Improving drought tolerance in maize: a view from industry. *Field crops research* **90**, 19–34. doi: https://doi.org/10.1016/j.fcr.2004.07.003

Comas, L.H., Becker, S.R., Cruz, V.M.V., Byrne, P.F. & Dierig, D.A. 2013. Root traits contributing to plant productivity under drought. *Frontiers in plant science* **4**, 442. doi: https://doi.org/10.3389/fpls.2013.00442

Chávez-Suárez, L., Álvarez-Fonseca, A. & Ramírez-Fernández, R. 2014. Aspectos de interés sobre las acuaporinas en las plantas. *Cultivos Tropicales* **35**, 45–54.

Dong, A., Yang, Y., Liu, S., Zenda, T., Liu, X., Wang, Y., Li, J. & Duan, H. 2020. Comparative proteomics analysis of two maize hybrids revealed drought-stress tolerance mechanisms. *Biotechnology & Biotechnological Equipment* **34**, 763–780. doi: https://doi.org/10.1080/13102818.2020.1805015

Eagles, H. & Lothrop, J. 1994. Highland maize from central Mexico-its origin, characteristics, and use in breeding programs. *Crop science* **34**, 11–19. doi: https://doi.org/10.2135/cropsci1994.0011183X003400010002x

Edmeades, G., Bänziger, M., Campos, H. & Schussler, J. 2006. Improving tolerance to abiotic stresses in staple crops: a random or planned Process?, Plant breeding: the Arnel R. Hallauer international symposium, Blackwell Publishing Ames, Iowa, USA. pp. 293–309.

FAOSTAT. Statistical Database. In Food and Agriculture Organization of the United Nations; FAO: Rome, Italy, 2022. Available online: http://faostat.fao.org/ (accessed on 20 May 2023).

García-Lara, S. & Serna-Saldivar, S.O. 2019. Corn history and culture. *Corn*, pp. 1–18. doi: https://doi.org/10.1016/B978-0-12-811971-6.00001-2

Hellin, J., Bellon, M.R. & Hearne, S.J. 2014. Maize landraces and adaptation to climate change in Mexico. *Journal of Crop Improvement* **28**, 484–501. doi: https://doi.org/10.1080/15427528.2014.921800

Hendrix, C.S. & Glaser, S.M. 2007. Trends and triggers: Climate, climate change and civil conflict in Sub-Saharan Africa. *Political geography* **26**, 695–715. doi: https://doi.org/10.1016/j.polgeo.2007.06.006

Hoekstra, F.A., Golovina, E.A. & Buitink, J. 2001. Mechanisms of plant desiccation tolerance. *Trends in plant science* **6**, 431–438. doi: https://doi.org/10.1016/S1360-1385(01)02052-0

Huang, Q., Zhao, Y., Liu, C., Zou, X., Cheng, Y., Fu, G., Xu, J., Zhang, X. & Lu, G. 2015. Evaluation of and selection criteria for drought resistance in C hinese semiwinter rapeseed varieties at different developmental stages. *Plant Breeding* **134**, 542–550. doi: https://doi.org/10.1111/pbr.12291

Ihle, J.N. & Dure, III L.S. 1972. The Developmental Biochemistry of Cottonseed Embryogenesis and Germination: III. Regulation of the Biosynthesis of Enzymes Utilized in Germination. *Journal of Biological Chemistry* **247**, 5048–5055. doi: https://doi.org/10.1016/S0021-9258(19)44937-5

Iqbal, M., Suwarno, W.B. & Azrai, M. 2021. Selection of maize genotypes for drought tolerance improvement. *IOP Conference Series: Earth and Environmental Science, IOP Publishing* **911**, pp. 012002. doi: 10.1088/1755-1315/911/1/012002

Islam, N.U., Ali, G., Dar, Z., Maqbool, S., Khulbe, R. & Bhat, A. 2019. Effect of Peg Induced Drought Stress on Maize (*Zea mays* L.) Inbreds. *Plant Arch* **19**, 1677–1681.

Jimenez-Galindo, J.C., Alvarez-Iglesias, L., Revilla-Temino, P., Jacinto-Soto, R., Garcia-Dominguez, L.E., de La Fuente-Martinez, M., Malvar-Pintos, R.A., Ordas-Lopez, B., Vander Wal, A.J. & Osorno, J.M. 2018. Screening for Drought Tolerance in Tepary and Common Bean Based on Osmotic Potential Assays. *Plant* **6**, 24. doi: 10.11648/j.plant.20180602.11

Jiménez-Galindo, J.C., Castillo-Rosales, A., Castellanos-Pérez, G., Orozco-González, F., Ortega-Ortega, A., Padilla-Chacón, D., Butrón, A., Revilla, P. & Malvar, R.A. 2023. Identification of Resistance to the Corn Weevil (*Sitophilus zeamais* M.) in Mexican Maize Races (*Zea mays* L.). *Agronomy* **13**(2), 312. doi: https://doi.org/10.3390/agronomy13020312

Jiménez-Galindo, J.C. & Acosta-Gallegos, J.A. 2013. Rendimiento de frijol común (*Phaseolus vulgaris* L.) y Tépari (*Phaseolus acutifolius* A. Gray) bajo el método riego-sequía en Chihuahua. *Revista mexicana de ciencias agrícolas* **4**, pp 557–567.

Khayatnezhad, M. & Gholamin, R. 2012. The effect of drought stress on leaf chlorophyll content and stress resistance in maize cultivars (*Zea mays*). *African Journal of Microbiology Research* **6**, 2844–2848.

Khayatnezhad, M., Gholamin, R., Jamaatie-Somarin, S. & Zabihi-Mahmoodabad, R. 2010. Effects of peg stress on corn cultivars (*Zea mays* L.) at germination stage. *World Appl. Sci. J.* **11**, 504–506.

Liu, S., Liu, X., Zhang, X., Chang, S., Ma, C. & Qin, F. 2022. Co-Expression of ZmVPP1 with ZmNAC111 Confers Robust Drought Resistance in Maize. *Genes* **14**(1), 8. doi: https://doi.org/10.3390/genes14010008

Lobell, D.B. & Burke, M.B. 2008. Why are agricultural impacts of climate change so uncertain? The importance of temperature relative to precipitation. *Environmental Research Letters* **3**, 034007.doi: 10.1088/1748-9326/3/3/034007

Lobell, D.B., Burke, M.B., Tebaldi, C., Mastrandrea, M.D., Falcon, W.P. & Naylor, R.L. 2008. Prioritizing climate change adaptation needs for food security in 2030. *Science* **319**, 607–610. doi: 10.1126/science.1152339

Lobell, D.B., Roberts, M.J., Schlenker, W., Braun, N., Little, B.B., Rejesus, R.M. & Hammer, G.L. 2014. Greater sensitivity to drought accompanies maize yield increase in the US Midwest. *Science* **344**, 516–519. doi: 10.1126/science.1251423

Longo, G.P., Bernasconi, E. & Longo, C.P. 1975. Solubilization of enzymes from glyoxysomes of maize scutellum. *Plant Physiology* **55**, 1115–1119. doi: https://doi.org/10.1104/pp.55.6.1115

Magar, M.M., Parajuli, A., Shrestha, J., Koirala, K.B. & Dhital, S.P. 2019. Effect of PEG induced drought stress on germination and seedling traits of maize (*Zea mays* L.) lines. *Türk Tarım ve Doğa Bilimleri Dergisi* **6**, 196–205. doi: https://doi.org/10.30910/turkjans.556607

Magorokosho, C. & Tongoona, P. 2003. Selection for drought tolerance in two tropical maize populations. *African Crop Science Journal* **11**, 151–161. doi: 10.4314/acsj.v11i3.27566

Michel, B.E. & Kaufmann, M.R. 1973. The osmotic potential of polyethylene glycol 6000. *Plant physiology* **51**, 914–916. doi: https://doi.org/10.1104/pp.51.5.914

Mohammadkhani, N. & Heidari, R. 2008. Drought-induced accumulation of soluble sugars and proline in two maize varieties. *World Appl. Sci. J.* **3**, 448–453.

Naghavi, M.R., Aboughadareh, A.P. & Khalili, M. 2013. Evaluation of drought tolerance indices for screening some of corn (*Zea mays* L.) cultivars under environmental conditions. *Notulae Scientia Biologicae* **5**, 388–393. doi: https://doi.org/10.15835/nsb539049

Ortega-Ortega, A., Jiménez-Galindo, J., Parra-Quezada, R., Jacobo-Cuellar, J., Ruiz-Anchondo, T.D., Salmerón-Zamora, J., Zamudio-Flores, P. & Malvar, R. 2023. Osmotic stress tolerance in forage oat varieties (*Avena Sativa* L.) based on osmotic potential trials. *Agronomy Research* **21**(S1), 335–346. doi: https://doi.org/10.15159/AR.23.005

Paek, N.C., Lee, B.-M., Bai, D.G. & Smith, J.D. 1998. Inhibition of germination gene expression by Viviparous-1 and ABA during maize kernel development. *Molecules & Cells (Springer Science & Business Media B.V.)* **8**(3), 336–342.

Perales, H. & Golicher, D. 2014. Mapping the diversity of maize races in Mexico. *PloS one* **9**(12), e114657. doi: https://doi.org/10.1371/journal.pone.0114657

Prasanna, B. 2012. Diversity in global maize germplasm: characterization and utilization. *Journal of biosciences* **37**, 843–855. doi: https://doi.org/10.1007/s12038-012-9227-1

Qayyum, A., Ahmad, S., Liaqat, S., Malik, W., Noor, E., Saeed, H.M. & Hanif, M. 2012. Screening for drought tolerance in maize (*Zea mays* L.) hybrids at an early seedling stage. *African Journal of Agricultural Research* **7**(24), 3594–3604.

Raj, R.N., Gokulakrishnan, J. & Prakash, M. 2020. Assessing drought tolerance using PEG-6000 and molecular screening by SSR markers in maize (*Zea mays* L.) hybrids. *Maydica* **64**, 1–7.

Reynolds, M. & Tuberosa, R. 2008. Translational research impacting on crop productivity in drought-prone environments. *Current opinion in plant biology* **11**, 171–179. doi: https://doi.org/10.1016/j.pbi.2008.02.005

Ribaut, J.M., Betran, J., Monneveux, P. & Setter, T. 2009. Drought Tolerance in Maize. In: Bennetzen, J.L., Hake, S.C. (eds) Handbook of Maize: Its Biology. Springer, New York, NY. doi: https://doi.org/10.1007/978-0-387-79418-1_16

Ruiz-Corral, J.A., Durán-Puga, N., Sanchez-Gonzalez, J.d.J., Ron-Parra, J., González-Eguiarte, D.R., Holland, J. & Medina-García, G. 2008. Climatic adaptation and ecological descriptors of 42 Mexican maize races. *Crop Science* **48**, 1502–1512. doi: https://doi.org/10.2135/cropsci2007.09.0518

Ruiz-Corral, J.A., Sánchez-González, J.d.J., Hernández-Casillas, J.M., Willcox, M.C., Ramírez-Ojeda, G., Ramírez-Díaz, J.L. & González-Eguiarte, D.R. 2013. Identificación de razas mexicanas de maíz adaptadas a condiciones deficientes de humedad mediante datos biogeográficos. *Revista mexicana de ciencias agrícolas* **4**, 829–842.

Sabagh, A.E., Hossain, A., Barutçular, C., Khaled, A., Fahad, S., Anjorin, F.B., Islam, M.S., Ratnasekera, D., Kizilgeçi, F. & Yadav, G. 2018. Sustainable maize (*Zea mays* L.) production under drought stress by understanding its adverse effect, survival mechanism and drought tolerance indices. *Journal of Experimental Biology and Agricultural Sciences* **6**(2), 282–295. doi: http://dx.doi.org/10.18006/2018

SAS Institute. Base SAS 9.4 Procedures Guide: Statistical Procedures. Version 9.4; SAS Institute: Cary, NC, USA, 2016.

Shiferaw, B., Prasanna, B.M., Hellin, J. & Bänziger, M. 2011. Crops that feed the world 6. Past successes and future challenges to the role played by maize in global food security. *Food security* **3**, 307–327. doi: https://doi.org/10.1007/s12571-011-0140-5

Shisanya, C.A. & Hornetz, B. 1997. Phenological and Physiological Evaluation of the Potential of Tohono O'odham Z16 Maize as a New Crop for the Semi-Arid Areas of SE-Kenya. *Der Tropenlandwirt-Journal of Agriculture in the Tropics and Subtropics* **98**(1), 94–115.

Singh, G.M., Gosavi, G., Srinathareddy, S., Patel, S.S., Solanki, P.S., Zhang, F., Xu, J., Mishra, V. & Sharma, S. 2022. Impact of Drought on Maize Yield and Exploration of In-Situ Maize Crop Genetic Resources for Drought Tolerance. *Preprints.* doi: https://doi.org/10.20944/preprints202212.0210.v1

Suhartono, A.A. 2021. Selection of maize plants resistant to drought stress in the vegetative phase using polyethylene glycol (PEG 6000). *AMA Agric Mech Asia Afr Lat Am* **52**(1), 2255–2261.

Ureta, C., González, E.J., Espinosa, A., Trueba, A., Piñeyro-Nelson, A. & Álvarez-Buylla, E.R. 2020. Maize yield in Mexico under climate change. *Agricultural Systems* **177**, 102697. doi: https://doi.org/10.1016/j.agsy.2019.102697

Waheed, A. 2014. Screening and selection of tomato genotypes/cultivars for drought tolerance using multivariate analysis. *Pak J of Bot* **46**(4), 1165–1178.

Wen, W., Franco, J., Chavez-Tovar, V.H., Yan, J. & Taba, S. 2012. Genetic characterization of a core set of a tropical maize race Tuxpeño for further use in maize improvement. *PLoS One* **7**, e32626. doi: https://doi.org/10.1371/journal.pone.0032626

Zenda, T., Liu, S., Wang, X., Jin, H., Liu, G. & Duan, H. 2018. Comparative proteomic and physiological analyses of two divergent maize inbred lines provide more insights into drought-stress tolerance mechanisms. *International journal of molecular sciences* **19**, 3225. doi: https://doi.org/10.3390/ijms19103225

Zeng, W., Peng, Y., Zhao, X., Wu, B., Chen, F., Ren, B., Zhuang, Z., Gao, Q. & Ding, Y. 2019. Comparative proteomics analysis of the seedling root response of drought-sensitive and drought-tolerant maize varieties to drought stress. *International Journal of Molecular Sciences* **20**, 2793. doi: https://doi.org/10.3390/ijms20112793

Agronomy Research **21**(S3), 1451–1463, 2023
https://doi.org/10.15159/AR.23.103

Comparative approach for assessing the soil quality in an urban conservation unit

G.S.D. Berna, C.R. Pereira, E. de Oliveira* and C.M. Hüther

Universitdade Federal Fluminense, Programa de Pós-graduação em Engenharia de Biossistemas, Rua Passo da Pátria 156 sala 236, 24.210-240 Niterói, Brasil
*Correspondence: eltonoliveira@id.uff.br

Received: August 16th, 2023; Accepted: October 30th, 2023; Published: November 6th, 2023

Abstract. This study aimed to verify the quality of the soil according to different stages of forest regeneration. Urban conservation units can be of great importance in land management and in the sustainable development process of cities. Monitoring soil quality in these spaces can help to define strategies in the forest recovery process. A management performance evaluation method and consequent soil quality was applied, using data envelopment analysis (DEA). Soil was collected in the three stages of forest regeneration observed, land with established forests, reforested land, and open land, at three different depths. In the set of 54 analyzed observations, soils with low levels of fertility were verified. However, an area with reforested land showed the best performance in maximizing the selected variables and consequently better soil quality scores. The open lands showed the lowest performance in soil conservation. In this way, the revealed performance scores accompanied the Sum of Exchangeable Bases and Organic Matter values. This quality score can help to define soil management strategies, which may be applicable to a wider audience and wider contexts in environmental management.

Key words: degraded area, environmental management, forest regeneration, quality scores, soil management, sustainable development.

INTRODUCTION

Globally, the forested area decreased by 420 million hectares (ha) between 1990 and 2020 (FAO, 2020). Changes in land use such as conversion of forests to agriculture, human settlements and other infrastructure developments are the main causes of forest loss (Fekete & Nehren, 2023). However, recent global initiatives to reforest degraded lands considerably reduce these losses to 4.7 million ha per year during 2010 and 2020 (Ahirwal et al., 2021).

Tropical forests stored 55% of the total carbon (C) stocks, where the soil is responsible for about 32% of the total, and the conversion of forests to non-forest land generally results in low quality, loss of C reservoir and soil biodiversity (Sarvade et al., 2016; Das et al., 2021).

Therefore, it is important to develop a good knowledge of these changes, mainly to understand how they affect soil functioning and losses of natural forest ecosystems (Xiao et al., 2022). These degradations are a potential generator of changes, which can have one of the most adverse consequences in the forest ecosystem (Huang et al., 2019), where soil properties can be altered by changes in land use and can act as an indicator parameter of soil quality.

For this, it is interesting to study the physical and chemical characteristics of soils that are in different stages of forest regeneration and, consequently, different vegetation cover, in order to understand their relationship with soil quality in these environments. Through an evaluation method that reveals a performance score of forest regeneration and consequent soil quality, using data envelopment analysis, the present study can contribute to soil conservation and improvement in the reforestation process, which among many others benefits through increases the carbon stock, establishes the earth's ecological flow, supports the biogeochemical cycle of water, meets part of the Sustainable Development Goals of the United Nations and mitigates the impact of climate change (FAO, 2020). These modifications are reflected sensitively by considerable alterations in soil formation and degradation processes, in soil properties and soil functions (Várallyay, 2010).

According to Maróstica et al. (2021), an index of green areas can be adopted as a decision-making parameter for the expansion of green areas in the city, such as the implementation of parks, seeking greater environmental equity. Thus, this study can help define management strategies in a conservation unit, applying an evaluation and monitoring system for land use and management in forest regeneration. Espada et al. (2018) draw attention to forest management as a tool for environmental conservation and for improving people's quality of life, contributing to the development of sustainable territories. Therefore, the objective of this study was to verify the quality of the soil in function of different stages and managements of forest regeneration through the evaluation of the physical and chemical attributes of the soil in the Conservation Unit Parque Natural Municipal da Água Escondida, in Morro da Boa Vista, in Niteroi, RJ.

MATERIALS AND METHODS

This study was carried out in Morro Boa Vista, Niterói, State of Rio de Janeiro, which is part of the Água Escondida Municipal Natural Park Conservation Unit, coordinates UTM, 22º53'22"S 43º06'22". Study in the Conservation Unit has Authorization from the Secretary of Environment, Water Resources and Sustainability - SMARTH, for Scientific Research in a Municipal Conservation Unit, under number Nº01/2022, Process Nº 250000056/2022.

The climate of the study site is characterized as Aw (tropical savannah climate), according to the Köppen classification (Gorthi et al., 2022), with two well-defined seasons, a hot and rainy summer; a dry winter with lower temperatures, with January being the rainiest month (average of 147 mm) and August the driest (41 mm) (Aragão et al., 2022). At the highest point of this Hill there is a structure with 6 (six) transmission antennas of the State Security Secretariat, which is 209 meters above sea level. The soils are shallow in the most rugged areas and in areas with low slopes they are moderately developed and deep (Wang et al., 2022).

In the study area there are three different soil cover compositions, called treatments(T), being: T1. lands with established forests; T2. reforested lands; T3. open land, where soil samples were later collected (Fig. 1).

Figure 1. Aerial view of the study site located in the Conservation Unit Parque Natural Municipal da Água Escondida, in Morro da Boa Vista, Niterói, RJ, Brazil.
Source: The authors.

The soil had the following characteristics at the time of collection: normally not very thick, yellowish to pinkish yellow in color, sandy in appearance on the surface, sometimes saprolite, permeable, weakly developed soils and can be classified as Acrisol (WRB, 2022), with greater stability on the slopes, and quite stable to excavations, even on steeper terrain. Showing shallow variations in the most rugged areas, but moderately developed in areas with low slopes. The presence of colluvial slopes with talus deposits was also observed, which are strongly inclined depositional surfaces, consisting of hillside deposits, with sediments primarily medium sands to silts, as also verified in a study carried out by Rowell et al. (2018).

Regarding soil analysis, in each of the three treatments, six soil samples were collected at three different depths: 0–10; 20–30 and 40–50 cm, making a total of 54 samples. The samples, for each treatment, were collected close to tree individuals, in the planting line of the seedlings and between the planting lines.

After collection in the field, samples were weighed and sent to the IBRA Agronomic Testing Laboratory in Sumaré, SP. Chemical and physical analyses were performed, including Calcium, Magnesium, Sodium, Phosphorus, and pH. The organic carbon was determined by the volumetric method of potassium dichromate ($K_2Cr_2O_7$). The carbon in the organic matter in the sample was oxidized to CO_2, and the chromium (Cr) in the extracting solution was reduced (from Cr^{+6} to Cr^{+3}). Excess dichromate was titrated with ammonium ferrous sulphate. The results were expressed in g dm^{-3} (Li et al., 2022). To calculate the soil organic matter content, the value of C (%) was multiplied by

1.724 (assuming that the soil organic matter contains 58% carbon). In the evaluation of the soil texture, the organic fraction was not considered, since this presents less stability compared to the mineral fraction and can be altered with the change of land use. Thus, in addition to allowing assessments of the ionic exchange capacity, soil texture is of great relevance in the mechanisms of nutrient uptake by the roots, such as nutrient diffusion and mass flow (Freire et al., 2013).

To compare the performance of each treatment, the DEA (Data Envelopment Analysis) methodology was chosen. This methodology incorporates multiple variables for the calculation of a single score, with a value between 0 and 1, where the higher, the better the treatment performance, facilitating the intended analysis (Banker et al., 1984). Based on the results of the soil analysis, 6 variables were selected (Hydrogen Potential (pH), Phosphorus (P), Potassium (K), Calcium (Ca), Magnesium (Mg) and Soil Organic Carbon (SOC), as they are essential elements, as intrinsic components in the structure and metabolism of plants, essential for growth, development, or reproduction in their life cycle (Taiz et al., 2017). Neimane et al. (2019) also highlighted the quantitative variables referring to the levels of Ca, Mg, P and K in the monitoring of soils in reforested areas. The dynamics of organic carbon and mineral macronutrients are influenced by several factors including vegetation cover. Forest species have a greater capacity for nutrient cycling than annual cycle plants, as the root system is permanent and deep, absorbing elements from subsurface layers and returning them to the soil through litter (Mafra et al., 2008). Although these nutrients go through a continuous cycle through all organisms, they predominantly enter the biosphere through the root systems of plants, therefore, they were considered as outputs because they are identified as products to be maximized.

In the DEA methodology, the observations were called DMUs (Decision Making Units). Each observed point, where soil samples were collected, was considered a DMU, in a total of 54. Thus, we chose to use the DEA BCC model of unitary input directed to outputs. Where the unit input indicates the existence of the DMU. Functioning as a multicriteria tool, not as a classic efficiency measurement technique (Gomes et al., 2012; Oliveira et al., 2014). To apply the DEA model, the SIAD version 3.0 program - Integrated Decision Support System (Angulo Meza et al., 2005) was used.

The analyzed variables Sum of Exchangeable Bases, Sand Content and Organic Matter (OM) were not included in the model used to generate the performance score but were considered as explanatory variables. The Sum of Exchangeable Bases (V value) refers to the sum of the bases (calcium, magnesium, potassium, and sodium) in exchangeable form expressed as milligram equivalents per 100 g of soil, can be expressed in percentage (V%) and is already an indicative index of soil quality, where a value above 50% characterizes eutrophic soil. Organic matter (OM), in turn, plays an important role in the maintenance and sustainability of natural ecosystems, as it is responsible for storing a good part of soil nutrients, including SOC, and is a source of diverse transformations, mediated by soil organisms (Sales et al., 2018). In the evaluation of the texture, soils with a sandy texture may present less water retention and adsorption of ions when compared to soils with a clayey texture. For these reasons, the use of these variables in the DEA model can cause inconsistencies or mathematical distortions (Dyson et al., 2001).

Then, the generated scores were related to variables, also extracted from the results of soil analysis, however, external to the DEA model; through dispersion diagrams, similar to those applied in Lin et al. (2022), in order to assist the intended analysis. These diagrams were divided into four quadrants. Where, the points observed in quadrant 1 have the highest and in quadrant 3 the lowest, scores and values linked to the external variables in question, in each of the 54 points observed (Fig. 2).

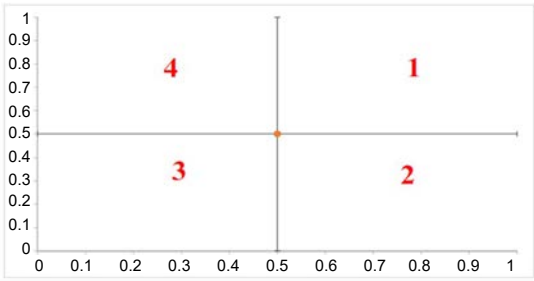

Figure 2. Representation of the applied dispersion diagram.
Adapted from Lin et al. (2022).

RESULTS AND DISCUSSION

Each observed point was considered a DMU, resulting from the combination between the treatment, the planting sector, distance between the planting row and the collection depth, for each of the 54 analyzed soil samples. Among the scores generated by SIAD, the standard score was considered as the performance soil quality score analyzed (Table 1).

The macronutrients calcium (Ca), magnesium (Mg), potassium (K), phosphorus (P) and soil organic carbon (SOC) showed their maximums in Treatment 2, reforested land, indicating the best soil quality in this treatment (Table 2).

Average of the performance score of the set of observations was 82.3%, the minimum was 61%. Sectors with a performance score of 100% include in Treatment 1, DMU 09; in Treatment 2, DMUs 20 and 23 and in Treatment 03, DMUs 34 and 37 (Table 3). However, treatment 2 had the best average quality score (86.3%) (Table 2).

Table 1. Performance scores revealed by the DEA method applied to each of the 54 DMUs

DMU*	Depth (0–10 cm)		Depth (20–30 cm)		Depth (40–50 cm)	
	score	(%)	score	(%)	score	(%)
1SFAB	0.84	84	0.84	84	0.94	94
1SFC	0.87	87	0.81	81	0.89	89
1SFlAB	0.61	61	0.69	69	1.00	100
1SFlC	0.83	83	0.70	70	0.78	78
1S17AB	0.86	86	0.71	71	0.70	70
1S17C	0.89	89	0.73	73	0.73	73
2SAAB	0.71	71	1.00	100	0.85	85
2SAC	0.85	85	1.00	100	0.86	86
2SEAB	0.86	86	0.83	83	0.83	83
2SEC	0.85	85	0.80	80	0.78	78
2S2AB	0.95	95	0.82	82	0.88	88
2S2C	1.00	100	0.81	81	0.84	84
3S9AB	1.00	100	0.89	89	0.92	92
3S9C	0.98	98	0.84	84	0.89	89
3S13AB	0.84	84	0.80	80	0.90	90
3S13C	0.74	74	0.71	71	0.70	70
3S19AB	0.83	83	0.69	69	0.67	67
3S19C	0.74	74	0.71	71	0.64	64
Minimum	0.61	61	0.69	69	0.64	64
Average	0.85	85	0.80	80	0.82	82
Maximum	1.00	100	1.00	100	1.00	100
S D	0.10	10	0.10	10	0.10	10

* Numbers 1, 2 and 3 (treatments); SF, SF1 and S17 (sectors); SA, SE and S2 (sectors); S9, S13 and S19 (sectors); AB (planting row) and C (between rows).

Table 2. Variables (outputs) and performance scores in each treatment

	Ca, (cmolc dm^{-3})	Mg, (cmolc dm^{-3})	K, (cmolc dm^{-3})	P, (mg dm^{-3})	SOC, (g dm^{-3})	pH	Scores, (%)
Treatment 1							
Minimum	4.0	1.0	0.4	0.2	4.0	2.0	61.0
Average	7.8	4.2	1.0	1.4	9.0	4.0	80.2
Maximum	20.0	12.0	1.7	4.2	16.0	6.0	100.0
S D	4.1	2.8	0.5	1.1	3.9	0.7	10.2
Treatment 2							
Minimum	4.0	2.0	0.2	0.2	4.0	3.9	71.0
Average	16.4	10.8	2.0	2.6	10.7	4.1	86.3
Maximum	29.0	20.0	5.1	9.0	18.0	4.5	100.0
S D	7.2	5.1	1.5	2.5	4.0	0.2	7.9
Treatment 3							
Minimum	4.0	1.0	0.2	0.1	4.0	3.7	64.0
Average	11.0	7.0	1.1	1.5	8.1	4.1	80.4
Maximum	24.0	18.0	4.1	8.1	14.0	4.7	100.0
S D	6.6	6.3	1.2	2.0	3.1	0.3	11.0
T1. T2 e T3							
Minimum	4.00	1.00	0.20	0.10	4.00	2.00	61.0
Average	11.74	7.35	1.36	1.86	9.28	4.06	82.3
Maximum	29.00	20.00	5.10	9.00	18.00	6.00	100.0
S D	6.99	5.58	1.23	2.02	3.78	0.47	10.0

T1– established forest; T2 – forest in regeneration; T3 – open area.

Table 3. Variables selected as outputs for the applied DEA model and DMU performance score

DMU*	Ca, cmolc dm^{-3}	Mg, cmolc dm^{-3}	K cmolc dm^{-3}	P, mg dm^{-3}	SOC, g dm^{-3}	pH	Score, %
1	14	12	1.3	1.4	6	4.2	84
2	7	3	1.4	2.0	4	4.0	84
3	20	7	1.7	3.5	14	4.6	94
4	8	4	1.3	1.2	15	4.0	87
5	5	2	0.5	0.3	10	3.9	81
6	4	1	0.4	0.2	9	3.8	89
7	6	2	0.5	1.1	4	2.0	61
8	7	3	0.6	2.2	5	4.0	69
9	8	4	0.7	4.2	6	6.0	100
10	13	6	1.3	2.3	10	4.3	83
11	7	3	0.8	1.0	6	4.0	70
12	6	3	1.6	1.2	5	4.3	78
13	7	6	1.4	1.0	15	3.9	86
14	5	3	0.6	0.4	9	3.7	71
15	4	3	0.4	0.7	8	3.7	70
16	9	9	1.7	1.9	16	3.8	89
17	5	3	0.6	0.4	10	3.7	73
18	5	2	0.4	0.2	10	3.7	73
19	4	2	0.2	0.2	7	3.9	71
20	23	16	4.3	7.2	17	4.4	100
21	17	11	2.0	1.5	7	4.2	85

Table 3 (continued)

22	12	12	1.2	1.0	4	4.2	85
23	29	20	4.0	9.0	18	4.5	100
24	19	13	2.3	3.6	9	4.2	86
25	13	8	0.9	5.1	13	4.2	86
26	10	6	0.7	4.9	12	4.1	83
27	15	5	0.5	2.8	12	4.1	83
28	10	9	0.9	2.0	14	4.0	85
29	12	7	0.6	1.3	12	3.9	80
30	6	5	0.4	1.3	11	3.9	78
31	26	17	4.2	3.8	13	4.3	95
32	13	13	2.5	0.6	9	4.0	82
33	25	10	1.3	0.3	5	4.0	88
34	25	20	5.1	2.1	15	4.5	100
35	16	11	3.0	0.6	9	4.0	81
36	21	10	2.3	0.2	6	4.0	84
37	24	18	4.1	4.7	12	4.7	100
38	19	15	1.8	0.9	7	4.3	89
39	19	17	0.9	0.1	4	4.3	92
40	22	18	3.9	0.3	12	4.6	98
41	16	10	2.1	0.1	5	4.2	84
42	16	13	1.4	0.2	4	4.4	89
43	10	6	0.6	2.2	14	3.9	84
44	9	5	0.5	1.1	13	3.8	80
45	9	4	1.0	8.1	8	3.9	90
46	8	4	0.7	2.2	9	3.9	74
47	6	2	0.3	1.0	9	3.7	71
48	6	2	0.2	0.7	8	3.7	70
49	10	4	0.6	2.7	8	4.5	83
50	6	2	0.4	0.8	6	3.9	69
51	4	1	0.3	0.2	6	3.8	67
52	6	3	0.5	1.3	9	3.9	74
53	4	1	0.3	0.4	8	3.8	71
54	4	1	0.2	0.3	4	3.8	64
Minimum	4	1	0.2	0.1	4	2.0	61
Average	11.7	7.3	1.36	1.86	9.3	4.06	82.3
Maximum	29	20	5.1	9.0	18	6.0	100
S D	7.0	5.6	1.23	2.02	3.8	0.47	10

*1 to 18, Treatment 1 (T1); 19 to 36, Treatment 2 (T2) and 37 to 54; Treatment 3 (T3). Ca (calcium), Mg (magnesium), K (potassium), P (phosphorus), SOC (soil organic carbon), pH (hydrogen potential).

Among the observations performance score showed an average of 82.3%while the average pH was 4.06, proving to be strongly acidic. Regarding the texture, we can observe the classification in Table 4.

The area with established forest had the highest level of total sand (84%), with an average of 64.3% and soil with a sandy texture. Treatment 2 presented the lowest sand content 54.6% (Table 4). The mean, across all 54 observations of the performance score is 82.3%, and the sand content is 59.7%, these define the quadrant divisions of the diagram in Fig. 3, A (Table 5).

Table 4. Soil textural classification

T1			T2			T3		
DMU*	Sand, %	Texture Type	DMU	Sand, %	Texture Type	DMU	Sand, %	Texture Type
1	53	Medium	19	66	Medium	37	54	Medium
2	84	Sandy	20	68	Medium	38	32	Clay
3	72	Medium	21	62	Medium	39	43	Clay
4	78	Medium	22	58	Medium	40	52	Medium
5	71	Medium	23	63	Medium	41	48	Medium
6	63	Medium	24	53	Medium	42	43	Clay
7	73	Medium	25	58	Medium	43	62	Medium
8	76	Medium	26	56	Medium	44	62	Medium
9	79	Medium	27	46	Clay	45	60	Medium
10	68	Medium	28	55	Medium	46	60	Medium
11	80	Sandy	29	50	Medium	47	61	Medium
12	74	Medium	30	58	Medium	48	60	Medium
13	58	Medium	31	53	Medium	49	78	Sandy
14	51	Medium	32	50	Medium	50	75	Medium
15	45	Clay	33	43	Clay	51	78	Medium
16	58	Medium	34	57	Medium	52	76	Medium
17	30	Clay	35	37	Clay	53	71	Medium
18	46	Clay	36	51	Clay	54	74	Medium
Minimum	30.0			36.9			32.3	
Average	64.3			54.6			60.3	
Maximum	84.2			67.9			77.9	
S D	14.8			7.9			13.4	

* T1 – established forest; T2 – forest in regeneration; T3 – open area.

Table 5. Means of performance scores, V% value, sand content and available organic matter (OM), in each treatment

T1	V%	Sand, g kg^{-1}	OM, g dm^{-3}	Scores, %
Minimum	11.0	300.0	7.0	61
Average	34.1	643.1	15.5	80
Maximum	57.0	842.0	27.0	100
S D	15.65	147.97	6.44	10
T2				
Minimum	5.0	369.0	7.0	8
Average	23.1	545.8	18.4	80
Maximum	53.0	679.0	31.0	100
S D	16.1	79.40	6.80	24
T3				
Minimum	14.0	323.0	7.0	64
Average	30.1	603.3	13.9	79
Maximum	51.0	779.0	24.0	98
S D	10.75	133.52	5.40	10
T1, T2 and T3				
Minimum	5.0	300.0	7.0	61
Average	29.1	597.4	15.9	82.3
Maximum	57.0	842.0	31.0	100
S D	14.8	128.0	6.4	10

T1 – established forests; T2 – forest in regeneration; T3 open area.

The analysis of the performance score in relation to the sand content is shown in Fig. 3, (A), where quadrant 2, with the highest concentration of points (35.2%), shows that the observations with the best performance are in regions with lower sand contents. Quadrant 4, which has the highest sand content and lowest performance scores, has 29.3% of the observed points. Pointing out the influence of sand content in the process of conservation of these soils.

The analysis of the performance score in relation to organic matter (OM) is shown in Fig. 3, (B). The average of the performance score is 82.3%, and the average of the OM is 15.9 g dm^{-3} and define the quadrants of this diagram. Quadrants 1 and 3, with 61.1% of the observations, points to the best performance of the soil regeneration process, in places with higher levels of organic matter. In forest ecosystems, a variety of abiotic and biotic soil-forming factors drive soil organic matter and nutrient cycling with a profitable outcome in mitigating climate change (Camponi et al. 2022).

The relationship between the performance score and the V% value is revealed in Fig. 3, (C). The quadrants of this diagram are defined by the mean of the performance score (82.3%) and by the mean of the V% value (29.1). The observations contained in the first quadrant represent 27.8% and in the third quadrant 29.6%, making up 57.4% of the total points observed. Confirming the positive relationship between the revealed performance score and the V% value.

Like the studies by Mafra et al. (2008) and Sales et al. (2018), this study used the applied DEA model, serve to discriminate the treatments evaluated in the set of 54 observations, in which both authors obtained analysis of soil nutrients in reforested areas. These authors evaluated soil organic carbon and macronutrient elements to analyze soil characteristics in terms of their ability to store nutrients in response to the different management conditions adopted. Lehocká et al. (2009) also evaluated soil quality through indicators extracted from chemical and physical analysis, in different management systems.

This study corroborates the work of Neto et al. (2007), who also use DEA to evaluate the biological performance of intercropped planting systems and concludes that the DEA method is effective in discriminating the best cultivation systems.

When collecting and analyzing the soil in layers, Mafra et al. (2008) revealed the carbon stock is more present in reforestation areas than in field or forest areas and the levels of P, K, Ca and Mg, also, obtained the highest averages in the regenerating sector, as well as in the present study. It can be seen in the T2 treatment that the enrichment with plant species from different strata, herbaceous, shrubby, and arboreal, in the forest restoration process carried out, may have provided interactions that favored better availability of nutrients and consequent soil quality detected, on soil profile analyzed in this study. An approach involving the diversity and distribution of plant species, within each studied area, could help to understand this trend.

In Table 3, which shows the variables and scores revealed, an average performance was 82.3%, in the treatment of regenerating forest. This result indicates that among the three treatments, treatment in the process of regeneration presents the best soil quality, corroborating with the studies of Mafra et al. (2008) and Sales et al. (2018). Thus, this quality score can help define soil management strategies, which may be applicable to other soil assessment situations in environmental management (Espada et al., 2017).

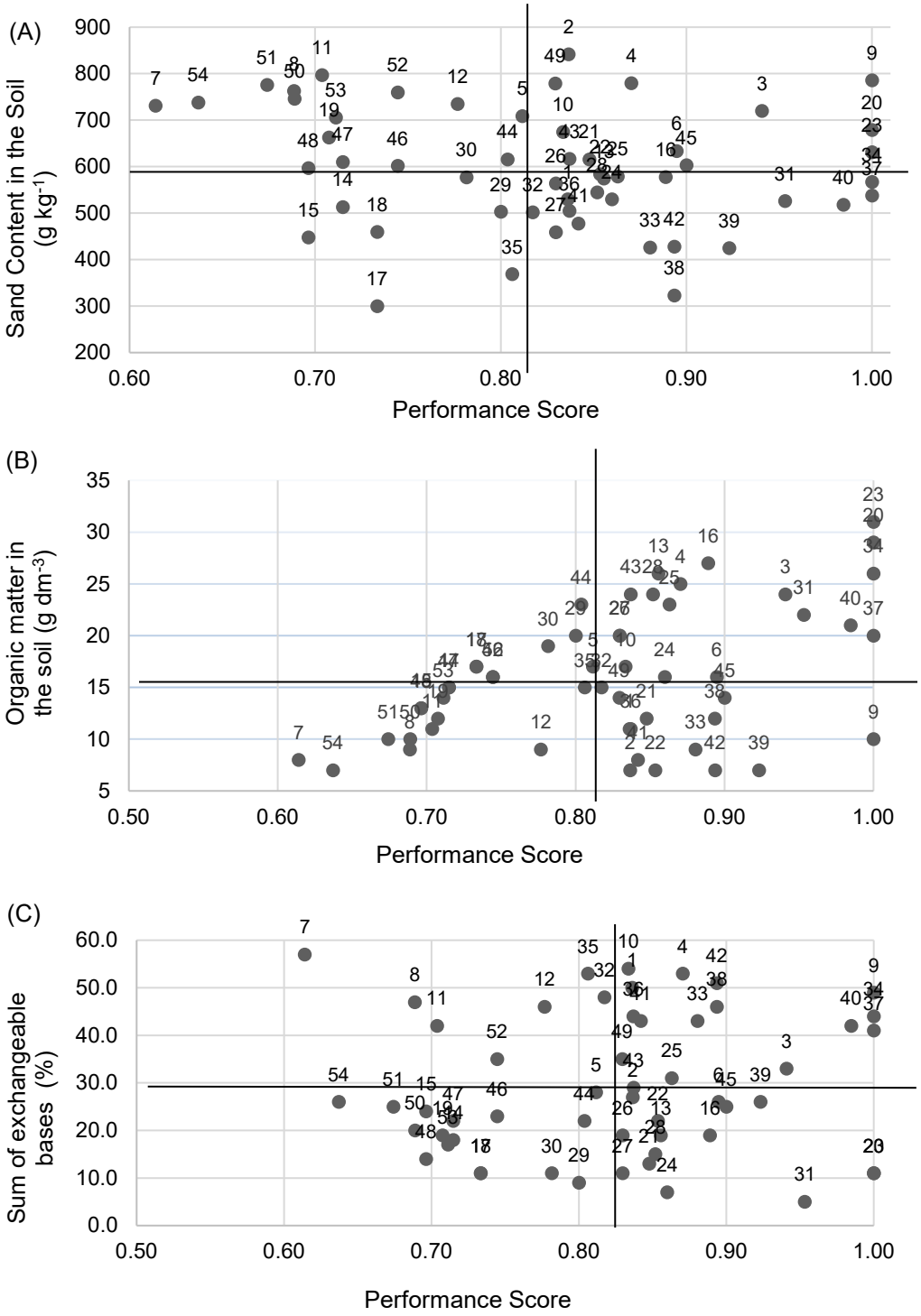

Figure 3. Scatter diagram of the performance score in relation to the explanatory variables: (A) Sand Content, (B) Organic Matter and (C) Sum of Exchangeable Bases.

Source: prepared by the authors.

It was considered that there may have been influence of the slope in relation to the loss of organic carbon and macronutrients. The treatment with an open area and with a higher percentage of sand content showed the lowest levels of the variables studied, in agreement with the work by Rocha (2021) who found a greater loss of soil nutrients through leaching in areas with greater slope. Lowe et al. (2021), also found that a soil with a steeper slope may have a greater loss of macronutrients, correlated with the loss of silt and clay.

CONCLUSIONS

The analyzed soils, in general, presented low levels of fertility. However, the treatment with regenerating area (T2), obtained the highest average in the performance score and consequent higher soil quality, obtaining the highest levels of SOC and macronutrients in the soil. In addition, the revealed performance scores accompanied the V % and organic matter values. The treatment with the worst performance was the one with open land (T3), which presented the lowest levels of the analyzed variables. The initiative of aggregating representative variables of the soil analysis in a single quality score can contribute to directing actions and defining strategies for soil management (Espada et al., 2018).

ACKNOWLEDGEMENTS. We wish to thank CILN (Niterói Cleaning Company), PMN (Municipality of Niterói) and FAPERJ/ PDPA (Applied Projects Development Program).

REFERENCES

Ahirwal, J., Kumari, S., Singh, A.K., Kumar, A. & Maiti, S.K. 2021. Changes in soil properties and carbon fluxes following afforestation and agriculture in tropical forest. *Ecological Indicators* **123**. https://doi.org/10.1016/j.ecolind.2021.107354

Angulo Meza, L., Biondi Neto, L., Mello, J.C.C.B.S. & Gomes, E.G. 2005. ISYDS - Integrated System for Decision Support (SIAD - Sistema Integrado de Apoio à Decisão): a software package for data envelopment analysis model. *Pesquisa Operacional* **25**, 493–503.

Aragão, J.R.V., Zuidema, P.A. & Groenendijk, P. 2022. Climate-growth relations of congeneric tree species vary across a tropical vegetation gradient in Brazil. *Dendrochronologia* **71**. https://doi.org/10.1016/j.dendro.2021.125913

Banker, R.D., Charnes, A. & Cooper, W.W. 1984. Some models for estimating technical scale inefficiencies in DEA. *Management Science* **30**(9), 1078–1092.

Camponi, L., Cardelli, V., Cocco, S., Serrani, D., Salvucci, A., Cutini, A., Agnelli, A., Fabbio, G., Bertini, G., Roggero, P.P. & Corti, G. 2022. Effect of coppice conversion into high forest on soil organic C and nutrients stock in a Turkey oak (Quercus cerris L.) forest in Italy. *Journal of Environmental Management* **312**. https://doi.org/10.1016/j.jenvman.2022.114935

Das, D.S., Dash, S.S., Maity, D. & Rawat, D.S. 2021. Population structure and regeneration status of tree species in old growth Abies pindrow dominant forest: A case study from western Himalaya, India. *Trees, Forests and People* **5**. https://doi.org/10.1016/j.tfp.2021.100101

Dyson, R.G., Allen, R., Camanho, A.S., Podinovisk, V.V., Sarrico, C.S. & Shale, E.A. 2001. Pitfall and protocols in DEA. *European Journal of Operational Research* **132**, 245–259. https://doi.org/10.1016/S0377-2217(00)00149-1

Espada, A.L.V., Sobrinho, M.V., Rocha, G.M. & Vasconcellos, A.M.A. 2018. Community Forest Management from Partnership in Brazilian Amazonia: The Case of Flona do Tapajós. *Revista Brasileira de Gestão e Desenvolvimento Regional* **14**(1), 135–165 (in Portuguese). ttps://www.rbgdr.net/revista/index.php/rbgdr/article/view/3472/644

Fekete, A. & Nehren, U. 2023. Assessment of social vulnerability to forest fire and hazardous facilities in Germany. *International Journal of Disaster Risk Reduction* **87**. https://doi.org/10.1016/j.ijdrr.2023.103562

FAO - Food and Agriculture Organization of the United Nations. 2020. Global Forest Resources Assessment – Key findings. Rome. https://doi.org/10.4060/ca8753en (accessed 03 November 2022).

Freire, L.R., Balieiro, F.C., Zonta, E., Anjos, L.H.C., Pereira, M.G., Lima, E., Guerra, J.G.M., Ferreira, M.B.C., Leal, M.A.A., Campos, D.V.B & Polidoro, J.C. 2013. *Liming and Fertilization Manual of the State of Rio de Janeiro*. Embrapa, Seropédica, RJ: Editora Universidade Rural, 430 pp. (in Portuguese).

Gomes, E.G., Abreu, U.G.P., Mello, J.C.C.B.S., Carvalho, T.B. & Zen, S. 2012. Unitary input DEA model to identify beef cattle production systems typologies. *Pesquisa Operacional* **32**(2), 389–406.

Gorthi, S., Singh, R., Chakraborty, S., Li, B. & Weindorf, D.C. 2022. Identification of Köppen climate classification and major land resource area in the United States using a smartphone application. *Geoderma Regional* **30**. https://doi.org/10.1016/j.geodrs.2022.e00567

Huang, L., Liao, F.H., Lohse, K.A., Larson, D.M., Fragkias, M., Lybecker, D.L. & Baxter, C.V., 2019. Land conservation can mitigate freshwater ecosystem services degradation due to climate change in a semiarid catchment: The case of the Portneuf River catchment, Idaho, USA. *Science of the Total Environment* **651**, 1796–1809. https://doi.org/10.1016/j.scitotenv.2018.09.260

Li, H., Gong, K., Jin, X., Owens, G. & Chen, Z., 2022. Mechanism for the simultaneous removal of Sb (III) and Sb (V) from mining wastewater by phytosynthesized iron nanoparticles. *Chemosphere* **307**. https://doi.org/10.1016/j.chemosphere.2022.135778

Lin, T.Y., Chiu, Y. & Xu, W.Z. 2022. Environmental efficiency and sustainability of food production and consumption in the EU. *Sustainable Production and Consumption* **34**, 440–452. https://doi.org/10.1016/j.spc.2022.09.028

Lehocká, Z., Klimeková, M., Bieliková, M. & Mendel, L. 2009. The effect of different tillage systems under organic management on soil quality indicators. *Agronomy Research* **7**(Special issue I), 369–373.

Lowe, M.A, McGrath, G. & Leopold, M. 2021. The Impact of Soil Water Repellency and Slope upon Runoff and Erosion. *Soil & Tillage Research* **205**. https://doi.org/10.1016/j.still.2020.104756

Mafra, A.L., Guedes, S.F.F., Filho, O.K., Santos, J.C.P., Almeida, J.A. & Rosa, J.D. 2008. Organic carbon and soil chemical attributes in forest areas. *Árvore* **32**(2), 217–224 (in Portuguese).

Maróstica, J.R., Cortese, T.T.P., Locosselli, G.M. & Kniess, C.T. 2021. Urban sustainability and green areas indicators in the city of São Paulo. *Revista Brasileira de Gestão e Desenvolvimento Regional* **17**(1), 450–463.

Neimane, S,S. Celma S., Butlers, A. & Lazdiņa, D. 2019. Conversion of an industrial cutaway peatland to a Betulacea family tree species plantation. *Agronomy Research* **17**(3), 741–753. https://doi.org/10.15159/AR.19.111

Neto, F.B, Gomes, E.G., Nunes, G.H.S. & Júnior, A.P.B. 2007. Multidimensional analysis of carrot-lettuce intercroppings under different combinations of population densities. *Pesquisa Agropecuária Brasileira* **42**(12), 1697–1704 (in Portuguese). https://doi.org/10.1590/S0100-204X2007001200005

Oliveira, E., Andrade, F.V.S., Soares de Mello, J.C.C.B., Machado, T.B. & Pereira, C.R. 2014. Efficiency assessment for a group of agroecological family farmers using data envelopment analysis. *Horticultura Brasileira* **32**(3), 336–341 (in Portuguese). https://doi.org/10.1590/S0102-05362014000300016

Rocha, J.R., 2021. *Environmental reforestation planning with the inclusion of local society in a peri-urban area*. Trabalho de conclusão de Curso, Universidade Federal Fluminense, Escola de Engenharia. 88 pp. (in Portuguese).

Rowell, A.L.K., Thomas, D.S.G., Bailey, R.M. & Holmes, P.J. 2018. Sand ramps as paleoenvironmental archives: Integrating general principles and regional contexts through reanalysis of the Klipkraal Sands, South Africa. *Geomorphology* **311**, 103–113. https://doi.org/10.1016/j.geomorph.2018.03.021

Sales, A., Silva, A.R., Veloso, C.A.C., Carvalho, E.J.M. & Miranda, B. M. 2018. Organic carbon and physical attributes of soil under management sustainable agricultural in the Legal Amazon. *Colloquium Agrariae* **14**(1) (in Portuguese). ttps://doi.org/10.5747/ca.2018.v14.n1.a185

Sarvade, S., Gupta. B. & Singh, M., 2016. Soil carbon storage potential of different land use systems in upstream catchment area of Gobind Sagar reservoir, Himachal Pradesh. *Indian Journal of Soil Conservation* **44**(2), 112–119.

Taiz, L., Zeiger, E., Moller, I.M. & Murphy, A. 2017. *Physiology and Plant Development*. chapter 5, sixth ed. Artimed. 888 pp. (in Portuguese).

Várallyay, G. 2010. The impact of climate change on soils and on their water management. *Agronomy Research* **8**(Special Issue II), 385–396.

Wang, J., Zhao, X., Deuss, K.E., Cohen, D.R. & Triantafilis, J., 2022. Proximal and remote sensor data fusion for 3D imaging of infertile and acidic soil. *Geoderma* **424**. https://doi.org/10.1016/j.geoderma.2022.115972

WRB - World Reference Base for Soil Resources. 2022. International soil classification system for naming soils and creating legends for soil maps. 4th edition. International Union of Soil Sciences (IUSS), Vienna, Austria. https://www.isric.org/sites/default/files/WRB_fourth_edition_2022-12-18.pdf (accessed 26 October 2023).

Xiao, Y., Huang, M., Xie, G. & Zhen, L. 2022. Evaluating the impacts of land use change on ecosystem service values under multiple scenarios in the Hunshandake region of China. *Science of the Total Environment* **850**. https://doi.org/10.1016/j.scitotenv.2022.158067

Agronomy Research **21**(S3), 1464–1472, 2023
https://doi.org/10.15159/AR.23.104

Yield and morphology of *Nopalea cochenillifera* under N fertilization and biological inoculation

E.R.T. Cruz*, F.A. Teixeira, D.D. Fries, R.R. Jardim, N.T. Cruz*, F. Rossa, A.P.S. Santos, E.M.V. Porto and H.S. Silva

State University of Southwest of Bahia, BR45700-000, Itapetinga, Bahia, Brazil
*Correspondence: elitonrtdacruz@hotmail.com; teles.nc@gmail.com

Received: August 15th, 2023; Accepted: October 30th, 2023; Published: November 9th, 2023

Abstract. The objective was to evaluate the effect of inoculation with *Azospirillum brasilense* and levels of nitrogen fertilization on the productive aspects of the spineless cactus (*Nopalea cochenillifera*). The experiment was carried in Ribeirão do Largo, Southwest region of the state of Bahia, from April 2019 to April 2020. The experiment was carried out in a 2×4 factorial, in a randomized block design with eight treatments and four replications. The treatments consisted of the absence or inoculation with *Azospirillum brasilense* and nitrogen fertilization levels 0, 50, 100 and 150 kg^{-1} of N ha^{-1}. There was a positive effect for the use of the bacteria on cladode area index, height, number of secondary, tertiary and total cladodes, total weight for cladodes of all orders and also for final weight per ha^{-1}. There was a significant effect of the use of the inoculant for the levels of total soluble sugars and starch, where there was a decrease in the values for the treatments submitted to the use of the bacteria. There was a quadratic effect for the weight of the tertiary cladodes, number of tertiary cladodes and total of spineless cactus when submitted to nitrogen fertilization levels. There was a linear test for cladodes area index when nitrogen fertilization was used. The use of *Azospirillum brasilense* is positive for the cultivation of spineless cactus, improving development and increasing crop productivity.

Key words: *Azospirillum brasilense*, cladodes, microorganisms, morphometric characteristics, spineless forage cactus.

INTRODUCTION

Pasture growth in the Brazilian semiarid region is limited by the low water availability in the region, which means that pasture production does not meet the needs of the herd during the drought, directly impacting zootechnical indexes, requiring an alternative to meet this demand for food.

The spineless cactus is an alternative for cultivation in drier regions, because the plant can produce even water restriction situation, besides having a high roughness and the ability to produce forage (Silva et al., 2014). Higher spineless cactus productivity can be achieved when the crop is subjected to nitrogen fertilization, a fact that can be justified by the increase in the emission of cladodes, which in turn reflects directly on the production (Souza & Fernandes, 2006; Cunha et al., 2012).

With the growing demand for nitrogen fertilizers, an alternative has been sought to reduce costs and meet the nitrogen demands of plants, which can be achieved with the use of growth-promoting bacteria, which biologically fix atmospheric nitrogen, making it available for the culture with which it is associated. In addition to biological nitrogen fixation, these bacteria can stimulate plant growth by releasing phytohormones (Hungria, 2011).

Among the growth promoting bacteria we have *Azospirillum brasilense*, which has been bringing positive results in the agricultural scenario, being used in the cultivation of corn, wheat and pastures, increasing productivity and reducing production costs of these crops (Guimarães et al., 2022).

In order to characterize bacterial isolates in giant and spineless cactus (*Opundia* spp. and *Nopalea* spp.), using a partial gene, Silva et al. (2015), managed to isolate twelve types of batteries, among them the *Azospirillum* genus. Bacteria of the genus *Azospirillum* are free living organisms, considered as growth promoters of plants, capable of fixing atmospheric nitrogen in a usable form for plants, these organisms can live in a way associated with the rhizosphere of plants internally or externally (Okon & Lacerda Gonzales, 1994).

The mode of action of the bacterium is associated with nitrogen fixation and also the secretion of phytohormones, which interfere with the development of the plant, acting mainly on the root system, making it have a greater capacity for absorbing nutrients, the result being better development of the plant, the combination of factors (Bashan &Levanony, 1990; Okon & Itzigsohn, 1995).

The nitrogen fixing diazotrophic bacteria, a group to which the *genus Azospirillum spp.* belongs, can perform biological nitrogen fixation, fixing N2 in NH3, with FBN being the main form of entry of atmospheric nitrogen into natural systems (Hungria, 2011; Freitas et al., 2015). These bacteria can be used as an alternative to supply nitrogen to the spineless cactus and provide for its growth, however, no work has addressed this subject.

These bacteria can be used as an alternative to supply nitrogen to the spineless cactus and provide for its growth Almeida et al. (2012), report that the practice of nitrogen fertilization in palm guarantees a significant increase in productivity, regardless of the cultivar, showing positive responses to nitrogen fertilization in conjunction with other nutrients.

The objective of this work was to evaluate the effect of inoculation with *Azospirillum brasilense* and levels of nitrogen fertilization on the productive aspects of the spineless cactus.

MATERIALS AND METHODS

The experiment was conducted on a farm in the district of Rio do Curral, Encruzilhada, BA, the geographical coordinates in which the experimental area is located are 15° 33'35" south latitude, 40° 43'39" west longitude, and with an approximate altitude of 890 m. The region is characterized by a tropical climate, with an average annual rainfall of 777 mm, an average annual temperature of 22.2 °C according to the Köppen classification.

The treatments were carried out in a randomized block design, composed of 8 treatments arranged in a 2×4 factorial scheme, with four replications, totaling thirty-two experimental units. The first factor was constituted by the presence or absence of the bacteria (*Azospirillum brasilense*) in the dosage of 1 L ha^{-1}, with the administration of the amount divided in two moments, the second factor was constituted in levels of nitrogen fertilization (0, 50, 100 e 150 kg ha^{-1} of N) so that it can be verified whether there will be a linear increase in productivity. The experimental plot had its stipulated dimensions of 8 m × 4 m, and a useful area of 6 m × 3 m.

With the defined area, 5 soil samples were collected at a depth of 0 to 20 cm, which after being mixed were sent for analysis at the Laboratory of the Department of Agricultural and Soil Engineering at UESB, Vitória da Conquista Campus, the chemical analysis of the soil revealed the following characteristics: pH (water) = 4.8; p = 1.0 mg dm^{-3}; K^+ = 0.10 cmolc dm^{-3}; Ca^{2+} = 1.3 cmolc dm^{-3}; Mg^{2+} = 1.0 cmolc dm^{-3}; Al^{3+} = 0.7cmolc dm^{-3}; H^+ = 6.5 cmolc dm^{-3}; and organic matter (OM) = 18.0 g dm^{-3}. The recommendation for fertilizing and liming was carried out according to Ribeiro et al. (1999), with a calculated dose of 4.09 ton ha^{-1} of limestone, after ninety days of the application of the limestone, phosphorus was applied in the amount of 181,8 kg ha^{-1} of P_2O_5, using the simple superphosphate as the source of the nutrient, and potassium in the amount of 282,48 kg ha^{-1} of K_2O using potassium chloride as the nutrient source. The planting furrows were made, with the aid of a furrower, for planting spineless cactus. The seedlings obtained were removed from the mother plants, selected in the field, and after this process, they were left to rest in the shade for a period of fifteen days for the wilt and healing of the wounds arising from the harvest and selection process.

The crop was implanted at 0.10 m × 2 m spacing, aiming at a population of 50,000 plants ha^{-1}. The cladodes were deposited in the planting furrows on April 29, 2019, burying them to a depth of up to one-third the length of the cladode. The first application of the bacteria (*Azospirillum brasilense*) was carried out shortly after planting the cladodes, on April 29, at a dose of 500 mL ha^{-1}, or 1.6 mL per plot, the strains used come from selection research carried out in Brazil by Embrapa (Brazilian Agricultural Research Corporation), with strains AbV5 (CNPSo 2083) and AbV6 (CNPSo 2084) which are currently used as inoculants for agricultural crops such as corn (*Zea mays L.*) for pastures planted with Urochloa spp. (*Brachiaria spp.*) and can also be used in coinoculation of soybean (*Glycine max L.*) (Hungria et al., 2010; Hungria et al., 2013; Hungria et al., 2016). At the beginning of the water season, on October 29, the second dose of the bacteria (500 mL ha^{-1}, or 1.6 mL in each experimental unit) was applied. The microorganism was applied to the plant cladodes in a sprayed manner, diluting 1.6 mL of the solution with *A. brasilense* in 500 mL of distilled water. At the beginning of the water period, the treatments submitted to nitrogen fertilization received the first fertilization dose, which was divided into 50 kg ha^{-1} of N or 355 g of urea per experimental unit, for each month, during the months of October, November and December, respecting the pre-established quantities for each treatment, which were applied in installments. Nitrogen fertilization in cover was carried out by hand. Weed control was performed through manual weeding, without using phytosanitary products.

In April 2020, quarterly collections of morphometric data were carried out as a monthly increase in the width and length of the cladodes of the plants. The final data collection took place on April 29, 2020, where morphological data were collected, such as width, length and thickness of all cladodes of spineless cactus plants, with the aid of

a caliper and an invar basimeter, also the height and number of cladodes data. In possession of these values, the cladodes area indices were calculated according to the methodology proposed by Pinheiro et al. (2015). The cladodes collected from the plots were weighed in the field, with a precision scale to determine the production of green mass. The cladode samples were pre-dried in a forced ventilation oven at 55 °C for 72 hours, then they were weighed again to determine the dry mass production. Total soluble sugars and starch were quantified using the Antrona method (Dische, 1962).

The results were subjected to analysis of variance and, when significant, determined whether the regression to nitrogen levels and the F Test to compare the means of treatment without and with inoculation T adopted the 5% level of probability and used the statistical software SAS.

RESULTS AND DISCUSSION

The variables enlargement rate of secondary cladodes, elongation rate of primary cladodes and elongation rate of secondary cladodes (Enlar C2, Elong C1 and Elong C2), were influenced by inoculation ($P < 0.05$), with higher rates being demonstrated when use of bacteria, showing that inoculated plants have a higher rate of increase in the dimensions of cladodes (Table 1). It can also be observed the quadratic behavior for the Elong C2 variable, with maximum value 138.9 kg ha^{-1} of N.

Table 1. Enlargement and elongation rate of cladode the spineless cactus (cm month^{-1}) depending on the application of *Azospirillum brasilense* and nitrogen fertilization

Items	BAC		Nitrogen (kg ha^{-1})				CV	*P*-Value		
	With	Without	0	50	100	150		BAC	N	BACxN
Enlar C1	0.77A	0.76A	0.73	0.74	0.81	0.79	10.57	0.671	0.173	0.347
Enlar C2	0.77A	0.72B	0.71	0.72	0.76	0.79	7.43	0.010	0.055	0.068
Elong C1	2.04A	1.86B	1.96	1.87	2.00	1.98	10.38	0.027	0.562	0.424
Elong C2	2.11A	2.04B	$\hat{Y}$ =1.96 + 0.002x -0.000009x²; R^2=0.99				3.66	0.022	< 0.001	0.714

Enlar C1: Primary cladode enlargement rate; Enlar C2: secondary cladode enlargement rate; Elong C1: primary cladode elongation rate; Elong C2: secondary cladode elongation rate; BAC: bacteria; N: nitrogen. Means followed by the same capital letter, for bacteria, do not differ by the *F* test ($P > 0.05$).

For the total soluble sugars and starch, the effect of inoculation was verified ($P < 0.05$), with lower levels for the inoculated plants (Table 2). Such behavior is related to productivity, in the situation that plants in constant growth accumulate less reserve and sugars, because they are in constant use, as can be seen, inoculated plants obtained greater growth and presented lower levels of total soluble sugars and starch.

Table 2. Total soluble sugars and starch of the spineless cactus cladodes (mg g^{-1}) depending on the application of *Azospirillum brasilense* and nitrogen fertilization

Items	BAC		Nitrogen (kg ha^{-1})				CV5	*P*-Value		
	With	Without	0	50	100	150		BAC	N	BACxN
TSS	80.09B	103.74A	85.16	85.70	93.38	103.41	23.02	0.004	0.300	0.952
STARCH	13.47B	17.29A	13.86	15.58	15.55	16.54	25.23	0.011	0.588	0.658

TSS: Total soluble sugars; STARCH: Starch Content; BAC: bacteria; N: nitrogen; Means followed by the same capital letter, for bacteria, do not differ by the *F* test ($P > 0.05$).

Low levels of TSS and starch in plants with higher growth are justified, because plants in full vegetative growth, constantly consume soluble sugars for their development, and only store these carbohydrates when they slow their growth (Watt et al., 2013).

The inoculation factor had a significant influence ($P < 0.05$) for the variables of primary, secondary cladodes and average total length (LPC, LSC and LTTC) and also for the variables of secondary and tertiary cladodes, average total width (WSC, WTC, WTTC) (Table 3), where there were higher values for the variables when the inoculation was used. For the variable mean total thickness of cladodes, there was no difference between the factors studied ($P > 0.05$).

Table 3. Dimensions of the spineless cactus cladodes (cm) depending on the application of *Azospirillum brasilense* and nitrogen fertilization.

Items	BAC		Nitrogen (kg ha^{-1})				CV	*P*-Value		
	With	Without	0	50	100	150		BAC	N	BACxN
LPC	24.55A	22.43B	23.62	22.45	24.08	23.81	10.38	0.022	0.562	0.424
LSC	25.32A	24.52B	$\hat{Y} = 23.64 + 0.029x - 0.0001x^2$; R^2=0.99				3.66	0.020	< 0.001	0.710
LTC	23.32A	20.45A	19.29	23.22	21.26	23.76	23.53	0.129	0.317	0.659
LTTC	24.42A	23.11B	23.24	23.43	23.91	24.96	6.01	0.017	0.346	0.324
WPC	9.35A	9.20A	8.87	8.89	9.57	9.78	10.57	0.671	0.173	0.347
WSC	9.30A	8.64B	8.58	8.64	9.49	9.18	7.43	0.010	0.055	0.068
WTC	8.61A	7.25B	7.37	8.34	7.82	8.20	20.00	0.024	0.624	0.803
WTTC	9.05A	8.56B	8.53	8.49	9.23	8.98	6.34	0.020	0.051	0.506
TTC	1.68	1.43	1.63	1.41	1.66	1.52	30.71	0.165	0.707	0.351
PHEI	65.97A	60.04B	58.77	62.91	63.84	66.49	12.71	0.049	0.310	0.528

SPC: Length of primary cladodes; LSC: length of secondary cladodes; LTC: length of tertiary cladodes; LTTC: length of total cladodes; WPC: width of primary cladodes; WSC: width of secondary cladodes; WTC: width of tertiary cladodes; WTTC: width of total cladodes; TTC: thickness of total cladodes; PHEI: plant height; BAC: bacteria; N: nitrogen. Means followed by the same capital letter, for bacteria, do not differ by the F test ($P > 0.05$).

The length of secondary cladodes variable showed quadratic behavior when the nitrogen fertilization levels were evaluated, presenting the highest length cladode (25.8 cm) when the plot was subjected to application of 147 kg ha^{-1} of N. The width of primary cladodes variable did not show any difference for no factor.

The relationships between the morphological characteristics of the plant, such as width, length and height, are closely linked to the area index of cladodes, and consequently to the yield of the plant (Neder et al., 2013; Pinheiro et al., 2014).

Factors such as cladodes area index and height indicate the quality of fertilizer management on the crop, as they will directly correspond to productivity, in addition to estimates of forage accumulation (Costa et al., 2012; Litke et al., 2018; Hourani, 2023).

The interaction between inoculation with the bacterium *Azospirillum brasilense* and nitrogen fertilization was not significant ($P > 0.05$) for the cladodes area index (CAI), however, there was an isolated effect of the factors studied (Fig. 1) for CAI, obtaining higher values when they were inoculated with the bacteria.

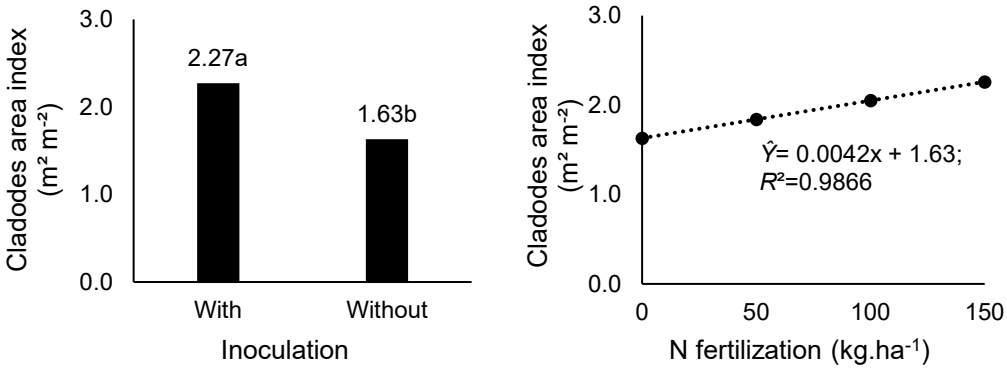

Figure 1. Cladodes area index of spineless cactus depending on the application of *Azospirillum brasilense* and nitrogen fertilization.

Averages followed by the same capital letter, for bacteria, do not differ by the *F* test ($P > 0.05$).

The variable CAI showed an increasing linear response to nitrogen fertilization levels, and it can be observed that as the nitrogen fertilization dose increases, the cladode area index has a positive response, presenting 2.29 when submitted to a dose of 150 kg ha^{-1} of N. Dubeux Júnior & Santos (2005) present in their work results that the spineless cactus extracts 9 kg of nitrogen for each ton of dry matter produced, emphasizing the importance of nitrogen fertilization for culture.

Lemaire & Chapman (1996), show that the appearance and development of leaves has a fundamental role in morphogenesis, and directly influences the structure of the pasture. As with the monthly increment values, the elongation and enlargement rates had significant increases when the plants were subjected to inoculation, which directly reflected in the height and CAI variables, also showing higher values with the inoculation, making the use of the same be beneficial for the development and growth of the spineless cactus.

Significant increments ($P < 0.05$) were obtained for the variables total average weight of primary cladodes, total average weight of secondary cladodes, total average weight of tertiary cladodes, total weight of green mass of cladodes and production of matter dry (TWPC, TWSC, TWTC, TWE and DMP). The plants that did not receive inoculation with the bacteria were the least productive (Table 4).

Table 4. Total weight of spineless cactus (kg ha^{-1}) depending on the application of *Azospirillum brasilense* and nitrogen fertilization

Items	BAC	Nitrogen (kg ha^{-1})					CV	*P*-Value		
	With	Without	0	50	100	150		BAC	N	BACxN
TWPC	108,638A	85,572B	93,154	94,133	96,752	104,379	21.47	0.005	0.702	0.103
TWSC	131,087A	85,626B	90,656	109,027	113,294	120,450	20.86	0.001	0.085	0.576
TWTC	50,3800A	28,103B	$\hat{Y} = 32{,}58 - 66.06x + 1.32x^2$; R^2=0.99				34.74	0.001	0.025	0.303
TW	292,480A	200,453B	217,960	237,067	251,437	279,402	18.01	0.001	0.070	0.181
DMP	23,813A	16,695B	18,537	19,301	20,971	22,203	18.97	0.001	0.249	0.229

TWPC: Total weight of primary cladodes; TWSC: total weight of secondary cladodes; TWTC: total weight of tertiary cladodes; TW: total weight of cladodes; DMP: dry matter production; Averages followed by the same capital letter, for bacteria, do not differ by the F test ($P > 0.05$).

For the variable total weight of tertiary cladodes (TWTC), when submitted to nitrogen fertilization levels, it presented a quadratic behavior, where the lowest weight of cladodes, 32,585 kg, can be identified, when nitrogen fertilization with values of 24.9 kg ha^{-1} of N was used.

Plants inoculated with *Azospirillum brasilense*, show greater development and production, as this bacterium can fix atmospheric nitrogen and produce phytohormones, inhabiting the rhizosphere of the plants, favoring the development of the same (Okon & Labandera Gonzalez, 1994; Bashan et al., 2004; Fiori et al., 2011).

Phytohormones such as cytokinin and auxin act directly on the growth and development of the plant, being transported to all parts of the plants through the xylem (Hungria et al., 2011). Cytokinin stimulates cell division, which can be called cytokinesis and, together with the auxin that regulates growth, providing greater vegetative development (Radwan et al., 2004; Moreira et al., 2010; Taiz & Zeiger, 2017).

Such development may be justified by the direct link with the production of phytohormones and biological nitrogen fixation, since they are growth promoters and act in different physiological processes, both in the root system and in the aerial part of the plant, therefore, justifying the largest length and width of the spineless cactus for treatments submitted to inoculation with *Azospirillum brasilense* (Dobbelaere et al., 2002; Hungria, 2011).

The auxins (indolacetic acid, indolbutyric acid and naphthalene acetic acid) and cytokinins (benzylaminopurine, isopentenyladenine and zeatin), will act on organs and tissues, being transported in the plant, where it is possible to identify the cytokinin in greater quantity, as the main responsible for favor the development of the aerial part of plants, which together with auxins will regulate plant growth (Moubayidin et al., 2009; Hungria et al., 2011; Nakhooda et al., 2012).

Greater development, production and vegetative growth were observed in inoculated plants, as can be seen by the value of total weight of cladodes (TWE), which reflect the result of the variables that indicate a better growth and development of spineless cactus plants that received the application of *Azospirillum brasilense*, attributing the bacterium the results.

CONCLUSIONS

The use of *Azospirillum brasilense* contributes positively to the development and productivity of the spineless cactus.

The use of nitrogen fertilization did not promote significant effects on crop productivity in the doses used.

ACKNOWLEDGEMENTS. To Coordination for the Improvement of Higher Education Personnel – CAPES, for the doctoral scholarship. Thanks to the State University of Southwest Bahia (UESB) for the support during the research development.

REFERENCES

Almeida, J., Peixoto, C.P. & Ledo, C.A.S. 2012. Vegetative and productive performance of forage palma. *Enciclopédia biosfera* **8**, 571–581 (in Portuguese).

Bashan, Y. & Levanony, H. 1990. Current status of *Azospirillum* inoculation technology: Azospirillum as a challenge for agriculture. *Canadian Journal of Microbiology* **36**, 591–608. doi: 10.1139/m90-105

Bashan, Y., Holguin, G. & Bashan, L.E. 2004. *Azospirillum*-plant relationships: physiological, molecular, agricultural, and environmental advances (1997-2003). *Canadian Journal of Microbiology* **50**, 521–577. doi: https://doi.org/10.1139/w04-035

Costa, N.D.L., Gianluppiu, V.D.L. & Moraes, A.D.L. 2012. Forage yields and morphogenesis of Trachypogon vestitus, during dryseason, in the savannas Roraima, Brazil. *Revista Trópica: Ciências Agrárias e Biológicas* **6**, 93–103. doi: 10.0000/rtcab.v6i1.363 (in Portuguese)

Cunha, D.N.F.V., Gomes, E.D.S., Martuscello, J.A., Amorim, P.L.D., Silva, R.C. & Ferreira, P.S. 2012. Forage yields and morphogenesis of Trachypogon vestitus, during dryseason, in the savannas Roraima, Brazil. *Revista brasileira de saúde e produção animal* **13**, 1156–1165. doi: http://dx.doi.org/10.1590/S1519-9940 2012000400005 (in Portuguese)

Dische, Z. 1962. General color reactions. In: Whistler, R.L. & Wolfram, M.L. (eds). *Carbohydrate chemistry*. New York: Academic Press, 477–512.

Dobbelaere, S., Croonenborghs, A., Thys, A., Ptacek, D., Okon, Y. & Vanderleyden, J. 2002. Effect of inoculation with wild type *Azospirillum brasilense* and *A. irakense* strains on development and nitrogen uptake of spring wheat and grain maize. *Biology and Fertility of Soils* **36**, 284–297. doi: 10.1007/s00374-002-0534-9

Dubeux Júnior, J.C.B. & Santos, M.V.F. 2005. Nutritional requirements of forage cactus. In: Menezes, R.S.C., Simões, D.A. & Sampaio, E.V.SB. (Eds.). *A palma no Nordeste do Brasil: conhecimento atual e novas perspectivas de uso.* Recife: Editora Universitária da UFPE, 105–127 (in Portuguese).

Fiori, C.C.L., Bartchechen, A., Watanabi, S.H., Guarido, R.C. 2011. Effect of inoculation of Azospirillum brasiliense in productivity the maize (Zea mays). *Revista Campo Digital* **5**, 56–59 (in Portuguese).

Freitas, A.D.S., Sampaio, E.V.S.B., Santos, C.E.R.S., Silva, A.F. & Souza, R.J.C. 2015. Biological nitrogen fixation in the Brazilian Semiarid. *Revista Brasileira de Geografia Física* **8**, 585–597. doi: 10.26848/rbgf.v8.0.p585-597 (in Portuguese).

Guimarães, G.S., Rondina, A.B.L., Santos, M.S., Nogueira, M.A. & Hungria, M. 2022. Pointing out Opportunities to Increase Grassland Pastures Productivity via Microbial Inoculants: Attending the Society's Demands for Meat Production with Sustainability. *Agronomy* **12**, 1748. doi: 10.3390/agronomy12081748

Hungria, M. 2011. Inoculation with Azospirillum brasilense: innovation in yield at low cost. *Circular Técnica* **325**, Embrapa Soja, Londrina (in Portuguese).

Hungria, M. 2016. Azospirillum: An old new ally. In: Proc. *FertBio: Towards new challenges*. Goiânia, Brazil, 2016.

Hungria, M., Campo, R.J., Souza, E.M. & Pedrosa, F.O. 2010. Inoculation with selected strains of Azospirillum brasilense and A. lipoferum improves yields of maize and wheat in Brazil. *Plant Soil* **331**, 413–425.

Hungria, M., Mendes, I.C., Mercante, F.M. 2013. Biological Nitrogen Fixation Technology with Bean Plant: Feasibility in Small Family Properties and Technified Properties; Embrapa Soy: Londrina, Brazil, pp. 32, (Embrapa Soja. Documentos, **338**).

Hourani, W. 2023. Effect of fertilizers on growth and productivity of saffron: a review. *Agronomy Research* **21**(1), 87–105.

Lemaire, G. & Chapman, D. 1996. Tissue flows in grazed plant communities. In: Hodgson, J. & Illius, A.W. (eds). *The Ecology and Management of Grazing Systems*. CAB International, Wallingford, 3–36.

Litke, L., Gaile, Z. & Ruza, A. 2018. Effect of nitrogen fertilization on winter wheat yield and yield quality. *Agronomy Research* **16**(2), 500–509.

Moreira, F.M.S., Silva, K., Nóbrega, R.S.A. & Carvalho, F. 2010. Diazotrophic associative bacteria: diversity, ecology and potential applications. *Comunicata Scientiae* **1**, 74–99. doi: 10.14295/cs.v1i2.45

Moubayidin, L., Di Mambro, R. & Sabatini, S. 2009. Cytokinin–auxin crosstalk. *Trends in plant science* **14**, 557–562. doi: 10.1016/j.tplants.2009.06.010.

Nakhooda, M., Watt, M.P. & Mycock, D. 2012. The properties and interaction of auxins and cytokinins influence rooting of shoot cultures of Eucalyptus. *African Journal of Biotechnology* **11**, 16568–16578. doi: 10.5897/AJB12.1523

Neder, D.G., Costa, F.R.D., Edvan, R.L. & Souto Filho, L.T. 2013. Correlations and path analysis of morphological and yield traits of cactus pear accessions. *Crop Breeding and Applied Biotechnology* **13**, 203–207. doi: 10.1590/S1984-70332013000300009

Okon, Y. & Itzigsohn, R. 1995. The development of *Azospirillum* as a commercial inoculant for improving crop yields. *Biotechnology advances* **13**, 415–424. doi: 10.1016/0734-9750(95)02004-M

Okon, Y. & Labandera-Gonzalez, C.A. 1994. Agronomic applications of Azospirillum: an evaluation of inoculation in the world field for 20 years. *Soil Biology and Biochemistry* **26**, 1591–1601. doi: 10.1016/0038-0717(94)90311-5

Pinheiro, K.M., Silva, T.G.F., Carvalho, H.F.S., Santos, J.E.O., Morais, J.E.F., Zolnier, S. & Santos, D.C. 2014. Correlations of the cladode area index with morphogenetic and yield traits of cactus forage. *Pesquisa Agropecuária Brasileira* **49**, 939–947. doi: 10.1590/S0100-204X2014 001200004 (in Portuguese).

Pinheiro, K.M., Silva, T.G.F., Diniz, W.J.S., Carvalho, H.F.S. & Moura, M.S.B. 2015. Indirect methods for determining the area index of forage cactus cladodes. *Pesquisa Agropecuária Tropical* **45**, 163–171. doi: 10.1590/1983-4063 2015v4530617

Radwan, T.E.E., Mohamed, Z.K. & Reis, V.M. 2004. Effect of inoculation with Azospirillum and Herbaspirillum on production of indolic compounds and growth of wheat and rice seedlings. *Pesquisa Agropecuária Brasileira* **39**, 987–994. doi: https://doi.org/10.1590/S0100-204X2004001000006

Ribeiro, A.C., Guimarães, P.T.G. & Alvarez, V.H. 1999. *Recommendations for the use of correctives and fertilizers in Minas Gerais: 5th approximation,* Viçosa, MG, CFSEMG, 1999. 359 pp.

Silva, L.M.D., Fagundes, J.L., Viegas, P.A.A., Muniz, E.N., Rangel, J.H.A., Moreira, A.L. & Backes, A.A. 2014. Produtividade da palma forrageira cultivada em diferentes densidades de plantio. *Ciência Rural* **44**, 2064–2071. doi: 10.1590/0103-8478cr20131305

Silva, M.L.R.B., Figueirôa, C.S. & Mergulhão, A.C.E.S. 2015. Identification of diazotrophs isolated from palm cultivars (Opuntia and Nopalea) using the recA gene. *Bioscience Journal* **31**, 577–583. doi: 10.14393/BJ-v31n2a2015-18244 (in Portuguese)

Souza, S.R. & Fernandes, M.S. Nitrogen. 2006. In: F*ERNANDES*, M.S. (ed.) *Mineral nutrition of plants.* Viçosa: Sociedade Brasileira de Ciência do Solo, pp. 215–252.

Taiz, L. & Zeiger, E. 2017. *Fisiologia Vegetal*, 6.ed. Artmed, 888 pp.

Watt, D.A., McCormick, A.J. & Cramer, M.D. 2013. Source and sink physiology. In: Moore, P.H. & Botha, F.C. (eds.) *Sugarcane: physiology biochemistry and functional biology.* Wiley, Hoboken, p.483–520. doi: 10.1002/9781118771280.ch18

Agronomy Research **21**(S3), 1473–1486, 2023
https://doi.org/10.15159/AR.23.102

Adaptation of Syrah wine grape cultivar to changing climatic conditions of the Bekaa valley, Lebanon

G. Ghantous[1,2], K. Popov[1], Z. El Sebaaly[2] and Y.N. Sassine[2,*]

[1]University of Forestry, Faculty of Agronomy, Department of Agronomy, 10 Kliment Ohridsky Blvd., BG1797 Sofia, Bulgaria
[2]Lebanese University, Faculty of Agronomy, Department of Plant Production, Gallery Matta Street, Dekwaneh, Beirut, Lebanon
[*]Correspondence: youssef.sassine@ul.edu.lb

Received: February 7th, 2023; Accepted: October 25th, 2023; Published: November 6th, 2023

Abstract. Climatic factors play a key role in determining the suitability of a given region for specific cultivars and wine types and the responses of individual grapevine cultivars to climate are of utmost importance for activity planning and decision making in viticulture. The study investigated the effect of climate conditions from 2006 till 2018 on the performance of cv. Syrah cultivated in two vineyards in Lebanon; Kanafar (at 1,020 m.a.s.l) and Mansoura (at 850 m.a.s.l). Cluster analysis based on climate indicators divided years into two clusters; in Kanafar (cluster 1: 2006–2015, cluster 2: 2016–2018) and in Mansoura (cluster 1: 2006 to 2008, cluster 2: 2009 to 2018). Solar radiation (May-June) and average wind speed (July-August-September) were the most influential predictors in Kanafar and Mansoura, respectively. In Kanafar, average yield and weight of 200 berries decreased by 21% and 22.7 g respectively in cluster 2, but in Mansoura only average yield increased by 3.7% in cluster 2. Total soluble solids and titratable acidity were not significantly affected by the shift in climate conditions at both vineyards, however total anthocyanin potential was significantly lower in Kanafar (by 114.2 mg kg^{-1}) and higher in Mansoura (by 353.4 mg kg^{-1}) in cluster 2. Total polyphenolic richness was only affected in Kanafar (reduction by 42 mg GAE g^{-1} in cluster 2). Syrah performance was more negatively affected by the changing climate conditions at Kanafar rather than Mansoura vineyards and it seems to better adapt to climate conditions of Mansoura overcoming the shift in climate that occurred after 2008 there.

Key words: climate change, winegrapes, production, quality, years.

INTRODUCTION

Lebanon is characterized by a natural complex diversity offering a great opportunity for a wide range of wine grape cultivars to adapt and grow in different terroirs at different altitudes (Moukarzel, 2013). Grape growing and wine making is a traditional heritage in Lebanon due to its climatic and geographical conditions. The last decades marked an important growth of the wine sector, ranking Lebanon as 45th largest wine producer in the world with 0.05% of global supply (Blominvest, 2013). Lebanon's climate is Mediterranean by excellence; it is characterized by hot, dry summers with low

precipitation levels (June-Sept) and cool, rainy winters (Dec-mid-March) (USAID, 2016). The maximum amounts of rainfall occur in January and the highest temperatures occur in July, during which maximum daily temperatures may exceed 35 °C, mainly in the Bekaa Valley (Karam, 2002). In general, geographic, climatic, demographic, and economic characteristics of the Bekaa valley play a key role in the development of wine production in Lebanon. With a mixed soil of limestone and clay, a gap of 15 °C between day and night, the Bekaa valleys ensures good climate conditions for the development of vines (Bou Antoun, 2014). In particular, the region of West-Bekaa is the main producing area for wine grapes holding the highest concentration of vineyards (56%), and diversity of wine grape cultivars. It is followed by North Bekaa (26%), Central Bekaa (11%), Mount Lebanon (3%), North Lebanon (3%), South Lebanon (1%), and East Bekaa (1%) in terms of vineyards concentration (Mohasseb et al., 2020).

Wine grape cultivars adapt differently to various climate conditions; their sunlight, heat, and water demands vary throughout the different stages of development (Fraga et al., 2014). Eventually, climatic factors are known as the main drivers of grapevine development and physiology (El Masri et al., 2018; Yu et al., 2022). As such, solar radiation, rainfall, and temperature could greatly influence the phenology, yields, and grape berry quality (Andreoli et al., 2019). Climatic factors play a key role in determining the suitability of a given region for specific cultivars and wine types (Jones et al., 2005; Fraga et al., 2014) and the responses of individual grapevine cultivars to climate are of utmost importance for activity planning and decision making in viticulture (Malheiro et al., 2013). Therefore, studying the phenology of different winegrapes cultivars under changing climate conditions would help viticulturists better adapt to climate change (Merrill et al., 2020).

With the climate change posing problems to the viticulture sector worldwide, Lebanon is not an exception. Eventually, average precipitation for the period 1986–2005 to 2081–2100 will likely to decrease between 20% and 30% coupled with an increase in temperature of 2 °C to 3 °C in the Middle East region (IPCC, 2013), and in Lebanon drought periods are expected to be 9 days longer by 2040, and 18 days longer by 2090. Indeed, changes in climate conditions over years may have direct impacts on vine yield, and wine production, therefore on winegrower's income (Santos, 2020). As grapevine cultivation is a part of the agricultural, economic, and cultural heritage of Lebanon, changes in the wine production chain as affected by changes of prevailing climate conditions may heavily affect socioeconomic aspects, unless adaptation measures are taken. Therefore, the present study investigated whether ther was a shift in climate conditions at the vineyards of Chateau KSARA, located at the Bekaa valley from 2006 until 2018, whether such a shift had an effect on the production and quality of Syrah cultivar, widely cultivated there, and whether such a cultivar had an adaptational behavior to the changing in climate conditions during the studied years. To our knowledge, this is the first attempt to examine temporal trends in vines' phenology and corresponding climate links in Lebanese vineyards, which highlights the importance of this study on the agricultural sector and its future implications for the country's economy.

MATERIALS AND METHODS

Vineyards description

To investigate the effect of climate factors on the performance of Syrah, data two vineyards located in the Bekaa valley, Lebanon were selected; 'Mansoura' (West Bekaa, at 850 m.a.s.l, latitude of 33,6794 and longitude of 35,8150) and Kanafar' (West Bekaa, at 1,020 m.a.s.l, latitude of 33,6406 and longitude of 35,7169). Both vineyards were managed by a local winery 'Chateau Ksara'. Experimental plantations were established in 2003 in Mansoura vineyards and in 2001 in Kanafar vineyards. In both vineyards, Syrah was planted at a 2.5 m × 1.25 m distance between plants, grafted on Ru140 rootstock, and pruned using the Royal Cordon technique leaving 10 buds per vine. Vines rows were oriented North-South at Mansoura, and South-East at Kanafar vineyards. Soil was clay at Kanafar vineyards and calcareous at Mansoura vineyards.

Climate data

Climate data for 2006 till 2018 was sourced from meteorological stations (Kanafar, Haouch Ammiq, and Tal-Amara stations) of the Lebanese Agricultural Research Institute (LARI). To interpret the effect of climate factors on the different phenological events of the vines, climate data was used either as yearly mean values of temperature, relative humidity, precipitation, wind speed (average and maximum), and solar radiation, or average values of same climate factors at specific intervals of the growing season for a more accurate determination of these climate factors' effects on tested indicators.

Studied indicators

Every season, at fruit set, defoliation was done to improve canopy microclimate, maintain berry health, and improve its composition. Only leaves covering the berries were removed to allow enough sunlight to reach the berries allowing berry veraison. Studied indicators included both quantitative and qualitative variables. Harvested yield (kg ha^{-1}) was recorded per plant and then expressed as kg ha^{-1}. The weight of 200 berries (W200B) was also measured in grams. For conducting analytical tests of quality, a sample of two hundred berries was collected randomly from vines in a way to cover the whole planted area; by walking in a W shaped pattern accross the field.

The Total Soluble Solids (TSS) content was determined in degree Brix at 20 °C using a digital refractometer (PR101, Atago, Bellevue, WA, USA) according to the ITV database (Blouin & Guimberteau, 2000). TSS was assessed in triplicates. The acid/base titration was used to measure the titratable acidity (TA), using NaOH 0.1 N and bromothymol blue (4g L^{-1}) as an indicator dye.

The ITV (Institut Technique de la Vigne et du Vin) method was used to measure anthocyanins and total phenolic compound contents of grapes after harvest (Lamadon, 1995). The concentration of anthocyanins (Ant) and the total anthocyanin potential (TAP) were estimated as follows: Anthocyanins (mg L^{-1}) = $OD_{520} \times 22.75 \times 20$.

Total anthocyanins potential (mg kg^{-1}) = Anthocyanins (mg L^{-1}) × 100 × (weight of grape juice (mg) + 100) / (weight of grape juice (mg)).

To estimate total phenolic richness (TPR) in the extracts macerated at pH 3.2, a dilution to 1/100 was performed and the optical density was measured at 280 nm against distilled water. Then total phenolic richness was calculated: $TPR = 2 \times OD_{280} \times 100$.

Statistical analysis

Cluster analysis was performed dividing years (2006 till 2018) into two distinct clusters based on climatic data for the determination of possible variability in climatic conditions in the two selected vineyards during the thirteen years of study. Each cluster included a separate set of years showing more or less comparable means of the predetermined climatic factors. The contribution of each climatic factor in the cluster analysis was determined using the factor analysis option provided by SPSS program. Also, *ANOVA* test was performed to investigate the separate and combined effects of year and vineyards on studied indicators. *t-test* was performed for mean comparison of indicators among two distinct groups of years at each vineyard. Principal Component Analysis (*PCA*) was performed over the thirteen years of study separately in each vineyard to investigate the correlations between Syrah indicators and climate predictors assessed as the most contributing to the results of cluster analysis. Tests were performed at a 95% confidence level using SPSS program.

RESULTS AND DISCUSSION

Climate variability at Syrah vineyards

Results of cluster analysis (Table 1) showed that in both vineyards, the level of importance of studied climate indicators (predictors) divided years (between 2006 and 2018) into two separate clusters. In vineyards of Kanafar, the first cluster enclosed years between 2006 till 2015, while cluster 2 enclosed years from 2016 till 2018. In the vineyards of Mansourah, the first cluster of years consisted of years from 2006 till 2008, and the second clusterincluded years from 2009 till 2018.

Table 1. Cluster analysis of climate predictors at the vineyards of Kanafar and Mansoura

Clusters	Kanafar		Clusters	Mansoura	
	year	frequency		year	frequency
One	2006	1	One	2006	1
	2007	1		2007	1
	2008	1		2008	1
	2009	1		Total	3
	2010	1	Two	2009	1
	2011	1		2010	1
	2012	1		2011	1
	2013	1		2012	1
	2014	1		2013	1
	2015	1		2014	1
	Total	10		2015	1
Two	2016	1		2016	1
	2017	1		2017	1
	2018	1		2018	1
	Total	3		Total	10

Influence of climate predictors

In the vineyards of Kanafar, solar radiation was the most influential predictor (Table 2), precisely solar radiation during May-June, followed by annual solar radiation, solar radiation during March-April, and solar radiation during March- September in respective decreasing order. Average wind speed during July-August-September was the most influencing predictor in Mansoura vineyards (Table 2).

Table 2. Contribution levels of climate predictors to results of cluster analysis

Predictor	Importance
Kanafar	
Solar radiation (May-June) (W.m-²)	1
Yearly solar radiation (W.m-²)	0.91
Solar radiation (March-April) (W.m-²)	0.89
Solar radiation (March-September) (W.m-²)	0.88
Maximum wind speed (March-April) (m.sec^{-1})	0.83
Solar radiation (August-September) (W.m-²)	0.82
Average wind speed (July-August) (m.sec$^{-1)}$	0.73
Temperature (March-September) (°C)	0.67
Average wind speed (March-April) (m.sec^{-1})	0.65
Maximum wind speed (July-August) (m.sec^{-1})	0.62
Mansoura	
Average wind speed (July-August-September) (m.sec^{-1})	1
Maximum wind speed (July-August-September) (m.sec^{-1})	0.72
Solar radiation (August-September) (W m-²)	0.47
Average Humidity (March-September) (%)	0.40
Solar radiation (May-June) (W m-²)	0.35
Average Humidity (September-August) (%)	0.35
Average Humidity (May-June) (%)	0.32
Annual solar radiation (W.m-²)	0.31
Precipitation (September-August) (mm)	0.26
Solar radiation (March-September) (W.m-²)	0.24

Vineyards and year's effects on Syrah

Results of ANOVA test (Table 3) showed that the separate effects of the factors vineyard and years were significant ($P_{value} < 0.05$) on all studied indicators, except for the separate effect of vineyard on sugar content in berries. The combined effects of both factors were also significant on all tested indicators, except on titratable acidity.

Table 3. Separate and combined effects of vineyard and year on Syrah production and quality ($P_{value} < 0.05$)

	P_{value} Yield	P_{value} W200B	P_{value} TSS	P_{value} TA	P_{value} TAP	P_{value} TPR
Vineyard	0.00	0.00	0.61	0.00	0.00	0.00
Years	0.00	0.00	0.00	0.00	0.00	0.00
Vineyard*year	0.00	0.00	0.00	0.40	0.00	0.00

W200b: weight of 200 berries; TSS: total soluble solids; TA: titratable acidity; TAP: total anthocyanin potential; TPR: total polyphenolic richness.

The analysis of tested productive and qualitative indicators in the two sets of years of clusters 1 and 2 (Tables 4 and 5) showed that average yield was significantly lower in cluster 2 compared to cluster 1 in Kanafar (reduction by 21.4%), but it was significantly higher in cluster 2 in Mansoura (increase by 3.7%).

Syrah yields recorded during 2008 and 2009 in Mansoura (15.2 and 15.1 t ha^{-1}, respectively) were significantly higher than all values recorded at both vineyards during the thirteen years of study. Overall, average yield ranged between 1,253.0 and 13.2 t ha^{-1} in Kanafar, and between 4.3 and 15.3 t ha^{-1} in Mansoura vineyards. At both vieyards

average yield recorded was higher than that reported by Favero et al. (2011) on the same cultivar cultivated in the Brazilian Southeast. Variability in yield observed even within the same vineyard may be associated with stable physical features, like soil and topography, that interact with seasonal biotic and abiotic factors, such as water and nitrogen availability, the presence of diseases, and climate (Pereyra et al., 2023). It also could be due to changing agronomic management strategies with years at the vineyard adopted to continously improve crop production. The current study deals with the factor climate and its impact on yield in time.

Table 4. Variation of Syrah production and quality as affected by year

Years	Yield (t. ha^{-1})	W200B (g)	TSS (° Brix)	TA (g. L^{-1})	TAP (mg kg^{-1})	TPR (mg GAE.g^{-1})
Kan2006	13.1 n	293.7 de	13.2 abcde	3.4 abcd	1,351.6 p	94.4 q
Kan2007	13.2 no	319.6 fg	12.8 ab	3.4 abc	1,368.3 p	158.7 s
Kan2008	1.2 a	277.0 c	13.0 abcd	3.3 ab	578.3 b	41.7 gh
Kan2009	12.7 lm	320.9 fg	12.9 abc	4.1 efghijkl	741.6 d	76.4 o
Kan2010	7.6 g	336.6 gh	13.8 defg	4.2 ghijkl	891.4 j	32.5 cd
Kan2011	9.6 k	339.0 ghi	12.9 abc	3.6 abcdefg	1,024.6 l	78.0 o
Kan2012	8.5 h	280.8 cde	14.1 fg	3.5 abcde	1,077.5 m	64.0 mn
Kan2013	8.9 ij	299.6 ef	13.5 bcdef	3.9 bcdefghi	1,214.9 n	83.2 p
Kan2014	7.11 f	299.8 ef	13.3 abcdef	4.5 jkl	1,215.2 n	56.0 j
Kan2015	4.8 c	202.3 a	13.5 bcdef	3.2 a	825.4 h	29.3 bc
Kan2016	6.0 d	274.1 cd	13.8 defg	3.9 bcdefghi	792.85 g	24.7 a
Kan2017	8.2 h	236.6 b	14.1 fg	3.8 abefghi	746.08 de	26.3 ab
Kan2018	6.2 de	292.2 de	15.5 h	4.2 hijkl	1,205.1 n	35.2 de
Man2006	7.1 f	326.6 g	13.0 abcd	3.9 cdefghijk	709.4 c	49.2 i
Man2007	9.2 j	388.4 k	12.9 abc	3.3 ab	768.8 f	63.4 lm
Man2008	15.2 p	227.9 b	13.8 cdefg	4.2 hijkl	338.9 a	57.3 jk
Man2009	15.0 p	330.0 g	12.9 abc	4.1 fghijkl	774.9 fg	67.3 n
Man2010	15.6 q	301.6 ef	14.1 efg	4.4 ijkl	699.2 c	44.1 h
Man2011	13.2 no	383.8 k	12.5 a	3.6 abcdefgh	877.7 ij	60.4 kl
Man2012	12.9 mn	373.4 jk	13.8 cdefg	3.5 abcdef	965.0 k	66.8 n
Man2013	13.4 o	359.8 ij	13.6 bcdef	3.9 bcdefghi	1,369.9 p	130.0 r
Man2014	8.8 i	240.8 b	13.9 defg	4.6 l	1,290.1 o	67.4 n
Man2015	4.3 b	353.2 hij	14.6 g	3.4 abcd	861.8 i	30.0 c
Man2016	6.9f	286.7 cde	13.9 defg	4.5 jkl	764.2 ef	39.2 fg
Man2017	6.5e	236.4 b	13.7 bcdef	4.0 defghijkl	1,042.0 l	40.0 fg
Man2018	12.6l	301.5 ef	13.3 abcdef	4.6 kl	946.32k	38.0 ef

Kan: Kanafar vineyards; Man: Mansoura vineyards; W200b: weight of 200 berries; TSS: total soluble solids; TA: titratable acidity; TAP: total anthocyanin potential; TPR: total polyphenolic richness.

Average weight of 200 berries was significantly lower in cluster 2 compared to cluster 1 in Kanafar (reduction by 22.7 g), but it did not significantly differ in Mansoura considering the two clusters of years. In Kanafar, AW200B ranged between 202.3 g in 2015 and 339.05 in 2011, while in Mansoura, this indicator recorded the lowest and highest values in 2008 and 2007, respectively (227.8 and 388.4 g).

Total soluble solids content and titratable acidity were not significantly affected by the shift in climate conditions at both vineyards, however total anthocyanin potential was significantly lower in Kanafar (by 114.2 mg kg^{-1}) and higher in Mansoura

(by 353.4 mg kg^{-1}) in cluster 2 years. TSS content ranged between 12.7 and 13.8 Brix recorded in 2007 and 2010, respectively in Kanafar vineyards, and between 12.47 and 14.6 ° Brix recorded in 2011 and 2015, respectively in Mansoura vineyards. Total polyphenolic richness was only affected in Kanafar (reduction in average by 42 mg GAE g^{-1} in cluster 2 compared to cluster 1). Ranges of TA, TAP, and TPR were as follows: 3.23–4.23 g L^{-1}, 578.3–1,368.3 mg kg^{-1}, and 24.7–158.7 mg GAE g^{-1}, respectively in Kanafar and 3.30–4.60 g L^{-1}, 338.91–1,369.9 mg kg^{-1}, and 30.0–130.03 mg GAE g^{-1} in Mansoura vineyards.

Table 5. *t-test* results comparing productive and qualitative indicators in two clusters of years in Kanafar and Mansoura vineyards

	Yield (t ha^{-1})	W200B (g)	TSS (° Brix)	TA (g L^{-1})	TAP (mg kg^{-1})	TPR (mg GAE g^{-1})
Kanafar cluster 1	8.7a	290.0a	13.3 a	3.7a	1,028.9a	71.4a
Kanafar cluster 2	6.8b	267.3b	14.5a	4.0a	914.7b	28.8b
P value	0.00	0.00	0.18	0.07	0.00	0.00
Mansoura cluster 1	10.5a	314.3a	13.2a	3.77a	605.7a	56.6a
Mansoura cluster 2	10.9b	316.7a	13.58a	4.10a	959.1b	58.3a
P value	0.00	0.55	0.20	0.28	0.00	0.45

Kanafar cluster 1: years from 2006 till 2015; Kanafar cluster 2: years from 2016 till 2018; Mansoura cluster 1: years from 2006 till 2008; Mansoura cluster 2: years from 2009 till 2018; W200B: weight of 200 berries; TSS: total soluble solids; TA: titratable acidity; TAP: total anthocyanin potential; TPR: total polyphenolic richness.

It is noteworhy that in particular years, values of TAP recorded in Mansoura vineyards were higher than those in Kanafar (2009, 2013, 2014, 2015, and 2017). Such findings contradict those of de Oliveira et al. (2019) who recorded higher anthocyanins concentrations in Syrah grapes cultivated at vineyards of higher altitudes in northeast Brazil. Considering that the optimal temperature range for anthocyanin accumulation is 17–26 °C, and that low night temperatures favor coloration in red grapes (Azuma et al., 2019), the higher TAP values recorded in Mansoura during the particular years of cluster 2 may be due to more suitable temperatures for berry coloration at such altitude compared to those at higher altitude. Assumably, temperature during these years did not overcome 35 °C, a temperature which generally inhibits anthocyanin synthesis (Liang et al., 2012). Consequently, the climate shift occuring in 2009 at Mansoura did not negatively impact on this indicator.

Correlation of climate with Syrah quantity and quality

Correlations were established between productive and qualitative indicators of Syrah and climate factors which were found to be main predictors influencing the variations of tested indicators among the two obtained clusters of years at relative vineyards.

Results of PCA analysis concerning Kanafar vineyards (Fig. 1), over the thirteen years of study, showed that there was a strong negative correlation between Syrah average yield and solar radiation at the vineyards of Kanafar, mostly with solar radiation during May to June (SRMayJun) and March to April (SRMarApr), and a weak negative correlation between this indicator and average temperature during March to September (TemMarSep). However, average yield was strongly positively correlated with

maximum wind speed from March to April (MWSMarApr). In Kanafar, average solar radiation during May-June (SR MayJun) and March-April (SR MarApr), and average temperature during March-September (tem MarSep) were lower in cluster 1 compared to cluster 2 (234.35 and 268.07 W m^{-2}, 172.2 and 188.7 W m^{-2}, and 19.8 and 20.8 °C, respectively) (Table 6). On the contrary, maximum wind speed during March-April (MWSMarApr) was higher in cluster 1 compared to cluster 2 (3.19 and 2.57 m.sec^{-1}, respectively) (Table 6). Comparing climate factors and Syrah yields at both vineyards, it was evident that lower solar radiation during spring and early summer months and lower temperatures from spring to late summer correlated to higher Syrah yields in cluster 1 years and higher values of these climate predictors correlated to the reduction in Syrah yields occurring in cluster 2. Besides, stronger winds during early spring correlated to higher Syrah yields in cluster 1 compared to cluster 2. Average weight of 200 berries was weakly negatively correlated to average values of solar radiation recorded annually (ASR), at different intervals of the growing season (SR MayJun, SRMarApr, SRMarSep, and SRAugSep), which were higher in cluster 2, causing a reduction in W200B compared to cluster 1. Assumably, lower yields in cluster 2 were caused by a lower weight of berries. Temperature is an important factor regulating berry growth and metabolism (Rienth et al., 2021). In particular, high heat during berry development is known to dramatically reduce berry growth by affecting berry size (Gouot et al., 2019). Besides, light and temperature may also have a synergistic effect on bud fruitfulness, anthesis, fruit set and berry growth (Vasconcelos et al., 2009). An increase in temperature of 1 °C during the growing season of the years 2016, 2017, and 2018 in Kanafar caused a reduction in yield and W200B of 21.4% and 22.2 g.

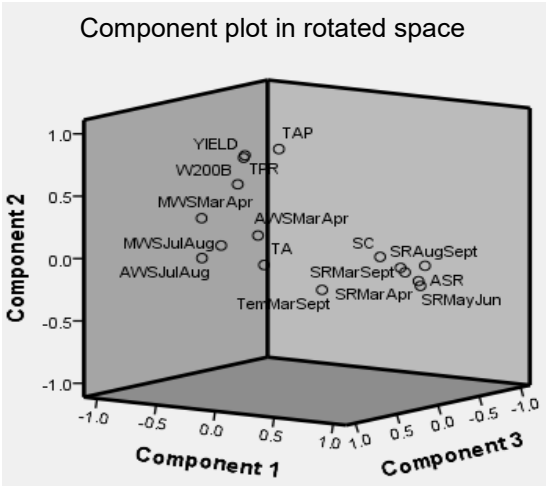

Figure 1. Correlations of Syrah quantitative and qualitative indicators to influencing climate predictors (average seasonal/annual values) from 2006 till 2018 at Kanafar vineyards.

(TAP: total anthocyanin potential; TPR: total polyphenolic richness; W200B: weight of 200 berries; TA: titratable acidity; SC: sugar content (TSS); AWS: average windspeed, MWS: Maximum windspeed; SR: solar radiation, Temp: temperature).

Winds occuring in spring season may have reduced the negative impact of high temperature on berry growth, by avoiding extra-heating of bunches, and causing better yields in years of cluster 1 at Kanafar vineyards. While Sadras & Soar (2009) found that increasing temperature in different timings of the growing season did not affect Syrah yield or yield components, Pagay & Collins (2017) reported negative impacts of an increase in the average growing season temperature on crop yield. Further, de Souza et al. (2019) reported that the sunlight and heating effects on leaves and grapes are directly influenced by row orientation in vineyards. However, in their study they observed no

significant effect of varying sunlight intensities caused by different vineyards' orientation on Syrah yield and cluster weight per vine.

Table 6. Mean/annual values of climate predictors found as main influencers on tested indicators in Kanafar and Mansoura vineyards during clusters 1 and 2 years

	Clusters	Kanafar			Mansoura	
		Mean	SD		Mean	SD
SR MayJun	One	234.35	5.97	AWS JulAugSep	3.85	0.40
	Two	268.07	4.94		0.67	0.07
ASR	One	53.65	1.93	MWS JulAugSep	0.75	0.01
	Two	162.15	4.43		3.04	0.40
SR MarApr	One	172.19	3.55	SR AugSep	194.22	8.75
	Two	188.69	2.56		238.26	11.92
SR MarSep	One	213.97	9.48	Hum MarSep	46.40	1.54
	Two	254.89	4.72		55.37	3.05
MWS MarApr	One	3.19	0.11	SR MayJun	231.39	8.40
	Two	2.57	0.17		258.55	9.48
SR AugSep	One	209.65	10.10	Hum SeptAug	49.85	2.17
	Two	255.75	9.83		55.56	4.16
AWS JulAug	One	0.78	0.03	Hum MayJun	42.95	2.89
	Two	0.65	0.04		53.72	4.39
Tem MarSep	One	19.85	0.19	ASR	157.99	8.27
	Two	20.82	0.36		173.99	4.23
AWS MarApr	One	0.77	0.03	Prec SepAug	1.83	4.49
	Two	0.67	0.03		3.11	4.41
MWS JulAug	One	3.43	0.20	SR MarSep	206.39	5.82
	Two	2.88	0.06		235.24	16.66

Kanafar cluster 1: years from 2006 till 2015; Kanafar cluster 2: years from 2016 till 2018; Mansoura cluster 1: years from 2006 till 2008; Mansoura cluster 2: years from 2009 till 2018; SR: solar radiation; ASR: annual solar radiation; MWS: maximum wind speed; Tem: temperature; AWS: average wind speed; Hum: Relative humidity; Prec: precipitation.

Total soluble solids content was strongly positively correlated to ASR and SR at different intervals of the growing season (SR MayJun, SRMarApr, SRMarSep, and SRAugSep), and to average temperature recorded during March-September (temp MarSep) of every year. Such correlations reflected a slightly higher sugar content in berries recorded in 2016, 2017, and 2018 compared to earlier years.

TAP and TPR were negatively correlated with average temperature during March-September (temp MarSep). Higher temperature recorded during the growing season of the years 2016, 2017, and 2018 caused a reduction in TAP and TPR compared to earlier years of study. Besides, in these three years, lower MWS values during early spring and higher SR values during late spring caused lower values of TPR at Kanafar. Eventually, TPR values were strongly positively correlated with MWS during March-April (MWSMarApr) and negatively correlated to SR during May-June (SRMayJun).

Climate and microclimate exert a good influence on berry composition (de Orduña, 2010). Eventually, in the last three years of study, the increase in temperature coupled with high solar radiation and low windspeed at Kanafar, had not only exerted a negative influence on berry growth, but also on its composition, which may consequently alter the quality of wine produced from Syrah at these vineyards. High berry temperature in

sun-exposed clusters can increase anthocyanin content, but extreme temperatures may alter the anthocyanin production in grapes (Haselgrove et al., 2000). Also, in warmer climates, winds can have a cooling effect, helping to slow down the ripening process and giving grapes more time to develop flavors (Tonietto et al., 2012). Using a long-time of biochemical data in field conditions for various berry quality aspects over a period of 6–19 years, Costa et al. (2020) also concluded that at maturity, high temperatures tend to decrease berry weight, titratable acidity, anthocyanins, and total phenols index and increase pH and potential alcohol.

Sugars have a fundamental role in the composition of the wines (Jordão et al., 2001) and the phenolic compounds present in the skin and seed of the grape are particularly important in enology (Andres et al., 2007). Anthocyanins are accumulated in grape skins after veraison. They are responsible fro grape berry and wine color because of their interactions with other phenolic compounds, proteins, and polysaccharides (Torres et al., 2021). Therefore, changes in the biosynthesis, translocation, degradation and accumulation of substances in the berry because of climate will directly impact on wine quality, defining its color, aroma, and flavor (Lima et al., 2011). The level of sugars and anthocyanins in grapes depends also on microclimatic conditions around the cluster zone (Barreiro et al., 2015).

With respect to correlations established relatively to Mansoura vineyards (Fig. 2), results showed that annual solar radiation (ASR) was slightly positively correlated with TSS, TA, TAP, TPR, and yield. At these vineyards, ASR was higher in cluster 2 than cluster 1 years (157.9 and 173.9 W m^{-2}, respectively) (Table 6) which might have correlated with a slight increase in TSS, TA, and TPR, a strong increase in yield and TAP during the years from 2009 till 2018, compared to earlier years. Furthermore, solar radiation during Mid-spring (SR MayJun) and late summer (SR AugSep) showed a slight negative correlation with W200B.

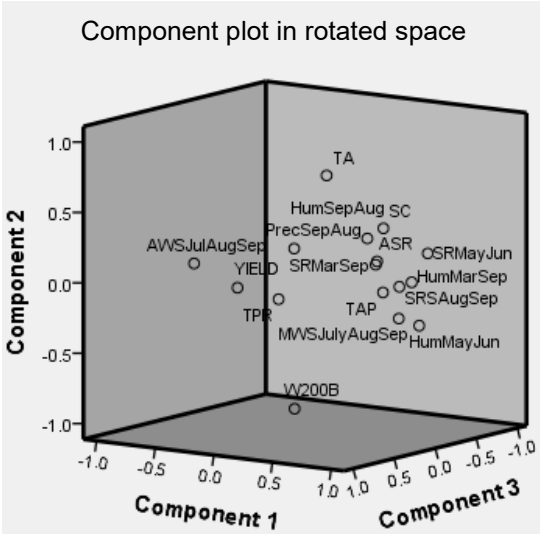

Figure 2. Correlations of Syrah quantitative and qualitative indicators to influencing climate predictors (average seasonal/annual values) from 2006 till 2018 at Mansoura vineyards.

((TAP: total anthocyanin potential; TPR: total polyphenolic richness; W200B: weight of 200 berries; TA: titratable acidity, SC: sugar content (TSS); AWS: average windspeed; MWS: Maximum windspeed; SR: solar radiation; Temp: temperature, Hum: humidity; Prec: precipitations).

Furthermore, solar radiation during May-June (SR MayJun) and August-September (SR AugSep), which were higher in average in cluster 2 (Table 6), showed a slight negative correlation with W200B. Thus, the increase in average yield occurring in cluster 2 could have been caused by higher average number of clusters produced in these years compared to earlier ones.

Average wind speed during July-August-September (AWS JulAugSep) showed a strong negative correlation with TAP and AW200B, and slightly negative correlation with TSS, TA, yield, and TPR. AWS decreased strongly in years of cluster 2 compared to cluster 1 (0.67 and 3.85 and m sec^{-1}, respectively) (Table 6) causing an increase, whether low or high, in yield as well as accumulation of sugars, anthocyanins, and polyphenols. Wind activity influences on fruit transpiration, and according to Pascual et al. (2022) fruit transpiration acts as one of the driving forces for sugar accumulation. Also, Further, Rebucci et al. (1997) postulated that water loss through transpiration leads to a lower turgor within the berry and maintains the gradient of water potential between the fruit and the stem, thus promoting the importing of assimilates into the berry. Zhang et al. (2017) reported that forced reduction in transpiration caused a lower solute accumulation rate in grape berries of Syrah, contradicting results of the current study.

Relative humidity during September-August (Hum SepAug) had a slight positive correlation with the majority of studied indicators, except W200B. Eventually, average value of this climate indicator was lower in cluster 1 compared to cluster 2 (49.8 and 55.6%, respectively) (Table 6) and correlated with slightly lower values of all indicators in the years 2006, 2007, and 2008 compared to later years. Temperature and relative humidity are other external factors determining berry transpiration, thus affecting solute accumulation in berries, though such a phenomenon is also influenced by cultivar-specific internal factors, such as primarily berry surface area and cuticular conductance (Zhang & Keller, 2015).

Precipitation during September-August (Pre SepAug), which were lower in cluster 1 (2006–2008) compared to cluster 2 (2009–2018) (1.83 and 3.1 mm, respectively) (Table 6) were slightly negatively correlated with all indicators. However, yield, W200B, TAP, and TPR were not negatively affected by an increase in precipitation of around 1.3 mm in average occurring during the years 2009 till 2018 in Mansoura. Camps & Ramos (2011) observed a decrease in grape yield coupled with lower precipitation during 1996–2009 in Penedès region, Spain.

CONCLUSIONS

There was a shift in climate conditions occurring after 2015 in Kanafar vineyards and after 2008 in Mansoura. The most influential predictors to such as shift were solar radiation during mid-late spring in Kanafar vineyards and average windspeed during mid-late summer at Mansoura vineyards. Changes in climate conditions had a varying effect on Syrah performance depending on the vineyard's location. In Kanafar, lower yields were recorded coupled with lower anthocyanins and polyphenols accumulation in berries, while in Mansoura there was a significant improvement in yield with no negative impact on berry composition. Conclusively, the quality of wine produced from Syrah cultivated at Mansoura may be preserved despite the changing climate occurring at these vineyards.

ACKNOWLEDGEMENTS. Authors would like to acknowledge Chateau KSARA for cooperating in data collection at their vineyards.

REFERENCES

Andreoli, V., Cassardo, C., Iacona, T. & Spanna, F. 2019. Description and preliminary simulations with the italian vineyard integrated numerical model for estimating physiological values (IVINE). *Agronomy* **9**(2), 94. doi: 10.3390/agronomy9020094

Andres, D.P.R., Yuste-Rojas, M., Sort, X., Andres-Lacueva, C., Torres, M. & Lamuela-Raventos, R.M. 2007. Effect of soil type on wines produced from Vitis vinifera L. Cv. Grenache in commercial vineyards. *Journal of Agricultural and Food Chemistry* **55**, 770–786. doi:10.1021/jf062446q

Azuma, A., Yakushiji, H. & Sato, A. 2019. Postharvest light irradiation and appropriate temperature treatment increase anthocyanin accumulation in grape berry skin. *Postharvest Biology and Technology* **147**, 89–99. doi:10.1016/j.postharvbio.2018.09.008

Barreiro, C.G., Rial-Otero, R.R., Cancho-Grande, B.C. & Simal-Gándara, J.S. 2015. Wine aroma compounds in grapes: A critical review. *Crit. Rev. Food Sci. Nutr.*, **55**(2), 202–218. doi: 10.1080/10408398.2011.650336

Blominvest, 2013. Exploring the Lebanese Wine Industry, Research Department, BLOMBANK.http://www.blominvestbank.com/Library/Files/BLOM%20Invest/Spot2013/2013-07-Exploring%20the%20Lebanese%20Wine%20Industry.pdf

Blouin, J. & Guimberteau, G. 2000. Ripening and maturity of grapes. Féret, Bordeaux (in French).

Bou Antoun, L. 2014. Food-processing industry as a basis for community dynamics and local socio-economic development: Wine industry in the Bekaa valley, Lebanon – a case study. *First Mediterranean Interdisciplinary Forum* (MIFS), Beirut, Lebanon, **2**, 18.

Camps, J.O. & Ramos, M.C. 2011. Grape harvest and yield responses to inter-annual changes in temperature and precipitation in an area of north-east Spain with a Mediterranean climate. *International Journal of Biometeorology* **56**(5), 853–64. doi:10.1007/s00484-011-0489-3

Costa, C., Graça, A., Fontes, N., Teixeira, M., Gerós, H. & Santos, J.A. 2020. The interplay between atmospheric conditions and grape berry quality parameters in Portugal. *Appl. Sci.,* **10**, 4943. doi:10.3390/app10144943

de Oliveira, J.B., Egiptoa, R., Laureanoa, O., de Castroa, R., Pereira, G.E., Ricardo-da-Silva, J.M. 2019. Climate effects on physicochemical composition of Syrah grapes at low and high altitude sites from tropical grown regions of Brazil. *Food Research International* **121**, 870–879. doi: 10.1016/j.foodres.2019.01.011

de Orduña, R.M. 2010. Climate change associated effects on grape and wine quality and production. *Food Research International* **43(**7), 1844–1855. doi: 10.1016/j.foodres.2010.05.00

de Souza, C.R., da Mota, R.V., Carvalho Silva, C.P., Paulino Raimundo, R.H., de Paula Fernandes, F. & Peregrino, I. 2019. Row orientation effects on Syrah grapevine performance during winter growing season. *Crop Production Rev. Ceres* **66(**3). doi:10.1590/0034-737X201966030004

El Masri, I.Y., Rizkallah, J. & Sassine, Y.N. 2018. Effects of Dormex (Hydrogen Cyanamide) on the performance of three seedless table grape cultivars grown under greenhouse or open-field conditions. *Agronomy Research* **16**(5), 2026–2036. doi:10.15159/AR.18.191

Favero, A.C., Angelucci de Amorim, D., Vieira da Mota, R., Soares, A.M., de Souza, C.R. & De Albuquerque Regina, M. 2011. Double-pruning of 'Syrah' grapevines: a management strategy to harvest wine grapes during the winter in the Brazilian Southeast. *Vitis* **50**(4), 151–158.

Fraga, H., Malheiro, A.C., Moutinho-Pereira, J., Cardoso, R.M., Soares, P.M.M., Cancela, J.J., Pinto, J.G. & Santos, J.A. 2014. Integrated analysis of climate, soil, topography and vegetative growth in iberian viticultural regions. *PLoS One* **9**(9), e108078. doi:10.1371/journal.pone.0108078

Gouot, J.C., Smith, J.P., Holzapfel, B.P. & Barril, C. 2019. Impact of short temperature exposure of Vitis vinifera L. cv. Shiraz grapevine bunches on berry development, primary metabolism and tannin accumulation. *Environmental and Experimental Botany* **168,** 103866. doi:10.1016/j.envexpbot.2019.103866

Haselgrove, L., Botting, D., Heeswijck, R.V., Hoj, P.B., Dry, P.R., Ford, C. and Land, P.G.I. 2000. Canopy microclimate and berry composition: The effect of bunch exposure on the phenolic composition of *Vitis vinifera* L. Cv. Shiraz grape berries. *Aust. J. Grape Wine Res*. **6**, 141–149. doi:10.1111/j.1755-0238.2000.tb00173.x

IPCC, 2013. Landmark United in Science Report Informs Climate Action Summit. IPCC Landmark United in Science Report Informs Climate Action Summit Comments.

Jones, G.V., White, M.A., Cooper, O.A. & Storchmann, K. 2005. Climatic change and global wine quality. *Clim. Change* **73**(3), 319–343. doi:10.1007/s10584-005-4704-2

Jordão, A.M., Ricardo-da-Silva, J.M. & Laureano, A. 2001. Evolution of catechins and oligomerics procyanidins during grape maturation of Castelão and Touriga Francesa. *American Journal of Enology and Viticulture* **52**, 230–234. doi:10.5344/ajev.2001.52.3.230

Karam, F. 2002. Climate Change and Variability in Lebanon: Impact on Land Use and Sustainable Agriculture Development, Lebanon: National Agriculture Research Institute.

Lamadon, F. 1995. Protocol for evaluating the polyphenolic richness of grapes. *Revue des œnologues et des techniques vitivinicoles et œnologique : Magazine trimestriel d'information professionnelle* **21**, 37–38 (in French).

Liang, N.N., He, F., Bi, H.Q., Duan, C.Q., Reeves, M.J. & Wang, J. 2012. Evolution of flavonols in berry skins of different grape cultivars during ripening and a comparison of two vintages. *European Food Research and Technology* **235**, 1187–1197. doi:10.1007/s00217-012-1850-4

Lima, L.L.A., Pereira, G.A. & Guerra, N.B. 2011. Physicochemical characterization of tropical wines produced in the Northeast of Brazil. *Acta Horticulturae* **910**, 131–134. doi:10.17660/ActaHortic.2011.910.10

Malheiro, A.C., Campos, R., Fraga, H., Eiras-Dias, J., Silvestre, J. & Santos, J.A. 2013. Winegrape phenology and temperature relationships in the Lisbon wine region, Portugal. *OENO One* **47**(4), 287–299. doi:10.20870/oeno-one.2013.47.4.1558

Merrill, N.K., García de Cortázar-Atauri, I., Parker, A.K., Walker, M.A. & Wolkovich, E.M. 2020. Exploring grapevine phenology and high temperatures response under controlled conditions. *Frontiers in Environmental Science* **8**(516527), 1–10. doi:10.3389/fenvs.2020.516527

Mohasseb, R., Sassine, Y.N., Sebaaly, Z., Kfoury, L. & Kattar, S. 2020. Survey study on the state of viniculture and wine production in Lebanon. *Acta Hortic.* **1276**, 15–22 doi:10.17660/ActaHortic.2020.1276.3

Moukarzel, J. 2013. *The Lebanese wine landscape, part of an exceptionnel terroir*. Master thesis, Université Libanaise, Beirut, Lebanon, 102 pp. (in French).

Pagay, V. & Collins, C. 2017. Effects of timing and intensity of elevated temperatures on reproductive development of field-grown Shiraz grapevines. *OENO One*, **51**(4). doi:10.20870/oeno one.2017.51.4.1066

Pascual, I., Antolín, M.C., Goicoechea, N., Irigoyen, J.J. & Morales, F. 2022. Grape berry transpiration influences ripening and must composition in cv. Tempranillo (*Vitis vinifera* L.). *Physiol Plant* **174**(4), e13741. doi:10.1111/ppl.13741

Pereyra, G., Pellegrino, A., Ferrer, M. & Gaudin, R. 2023. How soil and climate variability within a vineyard can affect the heterogeneity of grapevine vigour and production. *OENO One* **57**(3), 297–313. doi:10.20870/oeno-one.2023.57.3.7498

Rebucci, B., Poni, S., Intrieri, C., Magnanini, E. & Lakso, A. 1997. Effects of manipulated grape berry transpiration on post-veraison sugar accumulation. *Aust. J. Grape Wine Res*. **3**, 57–65. doi:10.1111/j.1755-0238.1997.tb00116.x

Rienth, M., Vigneron, N., Darriet, P., Sweetman, C., Burbidge, C., Bonghi, C., Walker, R.P., Famiani, F. & Castellarin, S.D. 2021. Grape berry secondary metabolites and their modulation by abiotic factors in a climate change scenario-a review. *Front Plant Sci.* **12**, 643258. doi: 10.3389/fpls.2021.643258

Sadras, V.O & Soar, C.J. 2009. Shiraz vines maintain yield in response to a 2–4 °C increase in maximum temperature using an open-top heating system at key phenostages. *European Journal of Agronomy* **31**(4), 250–258. doi: 10.1016/j.eja.2009.09.004

Santos, J.A., Fraga, H., Malheiro, A.C., Moutinho-Pereira, J., Dinis, L-T, Correia, C., Moriondo, M., Luisa, L., Dibari, C., Costafreda-Aumedes, S., Kartschall, T., Christoph, M., Molitor, D., Junk, J., Beyer, M. & Schultz, H.R. 2020. A review of the potential climate change impacts and adaptation options for european viticulture. *Appl. Sci*. **10**, 3092. doi:10.3390/app10093092

Tonietto, J., Ruiz, V.S. & Gómez-Miguel, V.D. 2012. Climate, zoning and typicity of wine in Iberoamerican wine regions. Madrid: CYTED35.

Torres, N., Martínez-Lüscher, J., Porte, E., Yu, R. & Kaan Kurtural, S. 2021. Impacts of leaf removal and shoot thinning on cumulative daily light intensity and thermal time and their cascading effects of grapevine (*Vitis vinifera* l.) berry and wine chemistry in warm climates. *Food Chem* **343,** 128447. doi: 10.1016/j.foodchem.2020.128447

USAID, 2016. Climate risk profile- Lebanon https://www.climatelinks.org/sites/default/files/asset/document/2016_USAID_Climate%20Risk%20Profile_Lebanon_2.pdf

Vasconcelos, M.C., Greven, M., Winefield, C.S., Trought, M.C. & Raw, V. 2009. The flowering process of Vitis *vinifera*: a review. *American Journal of Enology and Viticulture* **60**, 411–434. doi:0.5344/ajev.2009.60.4.411

Yu, R., Torres, N., Tanner, J.D., Kacur, S.M., Marigliano, L.E., Zumkeller, M., Gilmer, J.C., Gambetta, G.A. & Kurtural, S.K. 2022. Adapting wine grape production to climate change through canopy architecture manipulation and irrigation in warm climates. *Front. Plant Sci*. **13**. doi:10.3389/fpls.2022.1015574

Zhang, Y., Perez, J. & Keller, M. 2017. Grape berry transpiration: determinant factors, developmental changes, and influences on berry ripening. *Acta Horticulturae* **1188**, 51–56. doi:10.17660/ActaHortic.2017.1188.7

Zhang, Y. & Keller, M. 2015. Grape berry transpiration is determined by vapor pressure deficit, cuticular conductance, and berry size. *American Journal of Enology and Viticulture* **66**(4), 454–462. doi:10.5344/ajev.2015.15038

Agronomy Research **21**(S3), 1487–1498, 2023
https://doi.org/10.15159/AR.23.100

Unveiling the factors influencing groundwater resources in a coastal environment – a review

A.M. Nair[1], G. Yesodharan[2], K. Arun[2] and G. Prasad[3,*]

[1]Amrita School for Sustainable Futures, Amrita Vishwa Vidyapeetham, Amritapuri, India
[2]Department of Commerce & Management, Amrita Vishwa Vidyapeetham, 690525 Amritapuri, India
[3]Department of Mechanical Engineering, Amrita Vishwa Vidyapeetham, Amritapuri, India
[*]Correspondence: geena@am.amrita.edu

Received: July 27th, 2023; Accepted: October 25th, 2023; Published: November 5th, 2023

Abstract. The coastal environment is a dynamic and complex system where the interaction between land and sea gives rise to many challenges and opportunities. Among the critical resources in these regions, groundwater resources in a coastal environment play a vital role in sustaining human communities, ecosystems, and diverse economic endeavors. However, these resources encounter unique challenges due to the complex interaction between freshwater and saltwater interfaces, and the sustainability of coastal groundwater resources is increasingly threatened by various factors. This review highlights the factors that influence these resources to ensure their sustainable management, which sheds light on the intricate dynamics of coastal groundwater systems and for developing effective strategies to safeguard long-term availability.

Key words: coastal groundwater, groundwater resources, islands.

INTRODUCTION

Water is a dynamic resource essential to sustain life on Earth. As an integral part of the hydrological cycle, water intrudes into the soil and is retained in underground reservoirs. The main source of natural recharge of these aquifers is through the infiltration of precipitation into the ground (Roumasset & Wada, 2015). Almost 30% of the freshwater available on the earth is groundwater (Shamsudduha & Panda, 2019). Rising population, urbanization, and industrialization have increased stress on both surface water and groundwater resources (Vo, 2007; Zheng et al., 2020). Large groundwater resources or aquifers are used as additional water sources to meet the water demand. In 2010, a study by Margot and Gun reported that about 982 km^3 $year^{-1}$ of groundwater has been abstracted worldwide for drinking water supply, irrigation, and industrial water supply (Margat & Gun, 2013).

Despite covering just 20% of the Earth's surface, the coastal region is home to 41% of the global population (Martínez et al., 2007). The global average coastal population density is around 80 people per square kilometre (Dugan et al., 2011). Consequently, the water demand in these regions is increasing not only due to the rising population but also due to the increasing standards of living (Dugan et al., 2011; Abarna et al., 2023). Coastal environments are dynamic and captivating terrains where the convergence of land and sea creates a plethora of geological formations and hydrological phenomena, presenting unique challenges and opportunities. Groundwater serves as the primary source of water for rural and coastal water supply systems, often utilized without limitations to meet the growing demand in households, farms, and factories (Foster et al., 2000; Hamed et al., 2018; Prusty & Farooq, 2020).

These resources are significant in coastal environments due to their unique interrelationship between seawater and fresh groundwater. Discharge from coastal aquifers to sea may transport nutrients to support the ecosystem and influence the salinity of the coastal groundwater. Most nutrients, like phosphorus and nitrates, are carried by groundwater to the ocean surfaces (Cabral et al., 2023).

Megacities, which include large population densities, fast urbanization, and intensive human activity, are often found in coastal locations. Factors like transportation and trade options, historical or cultural value, closeness to ports and harbours for commerce, and proximity to other economic and social centres, contribute to the advantageous positioning of many coastal cities. Sufficient water supply is also essential for the effective operation of cities to fulfill their water requirements. Therefore, coastal groundwater resources are crucial to the water supply of coastal cities. However, in big coastal cities, the influence of urban growth on aquifers may be substantial, leading to the depletion of groundwater supplies, the infiltration of saline water, and a decline in water quality (Nlend et al., 2018; Prasad et al., 2021). The coastal aquifer also contributes to tourism activities in the area which help in the socio-economic development of the area. Coastal megacities exert significant pressure on the local groundwater reserves. Researching coastal regions is vital due to the resources and ecological services they offer, along with their crucial role in societal and economic development.

High islands, primarily of rugged volcanic mountains, have water from both surface water as springs and groundwater, whereas in low islands, groundwater is the main source of water (Grover, 2007). In most coastal areas, access to surface water is limited. Therefore, the main source of fresh water to support the needs of the coastal community is groundwater resources. The extent of availability of this source depends on various factors, including geology, climate, and size and shape of the area. Climate change, pollution, and overconsumption affected the groundwater quantity and quality, creating stress in most countries. These have a higher impact on the coastal community, which is already socio-economically and environmentally sensitive (Mastrocicco & Colombani, 2021).

The major reason for the degradation of groundwater is saltwater intrusion due to natural and anthropogenic activities. As sea level rise due to climate change, the water table of coastal aquifers also rises (Chang et al., 2011). This will result in the movement of the mixing zone to the inland and the tidal surges that cause the mixing of saltwater in aquifers. Whereas anthropogenic activities like over-pumping and the adoption of impermeable pavement restricted the percolation of water for the replenishment of the aquifers and degraded the quantity and quality of the aquifers (Chang et al., 2011).

Various factors affect the quality and quantity of the coastal groundwater resources aquifers. Because of the proximity to the ocean and the increase in human habitation in this fragile area, fresh groundwater is more likely to be degraded in coastal regions. Sustainable groundwater extraction is possible because, unlike other natural resources, groundwater is often a renewable resource in some parts of the globe. Identifying groundwater contamination sources and understanding the mechanisms that influence the development of groundwater quality are prerequisites for developing effective management methods whose goal is to conserve groundwater quality. To secure the long-term viability of these resources, insight into the complex dynamics and factors causing these variations in coastal groundwater systems is required (Venkatesh et al., 2021). To guarantee the sustainable availability and management of this unique resource in coastal areas, a comprehensive review of these factors is essential.

GROUNDWATER RESOURCES IN THE COASTAL ENVIRONMENT

The study of coastal groundwater has gained significant attention from researchers due to its vital role in sustaining ecosystems and supporting human activities in these regions. Understanding various formations of groundwater resources in these regions is imperative for several reasons, including sustainable water management, ecosystem preservation, and water supply systems; such understanding will help in developing effective strategies and policies to ensure the long-term availability and resilience of groundwater resources in these dynamic and valuable ecosystems.

In the subsequent session, we will delve into the vital fresh groundwater resources present in the coastal region. These sources play a key role in supplying communities with clean and accessible water by supporting the fragile ecosystems and biodiversity in the coastal areas.

Coastal Aquifer

An aquifer that extends under both land and sea is said to be a coastal aquifer. Specifically, it is in the coastal zone, which stretches between the mainland and the water. Rainfall and ocean water are the two main sources that replenish coastal aquifers, which may be confined or unconfined. Seawater is the primary distinction between coastal and inland aquifers. The composition of the aquifer medium in a region is significantly influenced by the geological formations present. The continual supply of sand from the sea, rivers (especially in river mouth locations), and wind cause most of the world's coastal aquifers to be formed of sedimentary formations (Jayasingha et al., 2014).

The coastal sandy aquifer is a specific type of coastal aquifer. It has distinct ecosystems due to the mixing of terrestrial fresh groundwater with salty groundwater from the sea, resulting in high chemical and physical gradients. Many important ecological functions, such as filtration and purification, nutrient mineralization, storage and outflow of subsurface groundwater, and functional connectivity between land and sea, are provided by sandy beaches. The groundwater in the beach aquifer is divided into three regions: an intertidal saltwater cell, where seawater is pushed through the beach under the influence of waves and tides; a zone of terrestrial freshwater; and a deep saltwater wedge. Subterranean estuaries, like those on the surface, are characterized by steep physical and chemical gradients at the interface between different water types.

Submarine groundwater discharge refers to water outflow from the beach aquifer into the coastal ocean (Archana et al., 2021).

Perched Aquifer

An isolated water body held by an impermeable barrier located above the local water table is referred to as a perched aquifer. Perched aquifers are frequently associated with impermeable strata that serve as a barrier, preventing water from passing below them and retaining it above. In areas with deep regional water tables, they are easily separated. They are mostly found in the vadose zone, the region between the surface earth to the top of the main water table. They are susceptible to contamination, changes in land use, and climatic conditions because of their shallow depth (Hamutoko et al., 2019; Prasad & Ramesh., 2019).

Dyke Impounded Aquifer

Like in the islands of Hawaii, dyke impounded aquifer is the main water source. Dykes are often found in the late phases of the volcanic cycle and are characterized by being almost vertical intrusions. Volcanic dykes have been variously characterized as draining structures or flow barriers, depending on the underlying geology. Low permeability and hard rock conditions are characteristic of where draining features are found. The high degree of dyke weathering, host rock fractures during emplacement, volcanic material contraction, and internal fractures during cooling all contribute to the unusually high permeability in these situations. In contrast, for unweathered dykes implanted in greater permeability and/or weakly consolidated host rocks, barrier features have been identified (Comte et al., 2017). When surrounded by less permeable host rock, dykes may function as preferred flow pathways. Due to their poor permeability, such dykes or dyke swarms may play a significant role in subsurface flow dynamics. Groundwater may be impounded by dykes, resulting in elevated levels like more than 600 m above sea level on the island of Hawaii and limited separation of the aquifer (Houben et al., 2018).

Freshwater Lens or Basal Aquifers

The density of fresh groundwater is typically about 1,000 kg m^{-3}, whereas the density of seawater is between 1,022 kg m^{-3} and 1,028 kg m^{-3} (Holzbecher, 1998). Due to the density differences between freshwater and saltwater, their inability to blend together results in the formation of freshwater lenses above typically saline aquifers in specific regions. These lenses play a crucial role in sustaining both human and environmental activities. Rainfall infiltration forms freshwater lenses above the salty groundwater that originates from the ocean, which may be found in coastal aquifers and on marine islands (Laattoe et al., 2017).

Coastal Karst Aquifer

One kind of coastal aquifer is the karst aquifer, which may be recognized by its location in karst landscapes, commonly in the Mediterranean basin (Bakalowicz, 2018). In many coastal areas, coastal karst aquifers are the primary or sole supply of drinking water. Karst topography is distinguished by the dissolved rocks like limestone and dolomite. Consequently, a subterranean system of caverns, channels, and fissures is formed, facilitating the smooth passage of water through the rock. Limestone has a high

porosity, which facilitates the infiltration of precipitation into the underlying subsurface (González-Herrera et al., 2022). Coastal karst aquifers are key water sources, valued for their ability to naturally prevent saltwater intrusion and discharge freshwater to the communities and ecosystems, particularly in the Mediterranean basin and its surrounding regions (Larson & Mylroie, 2018a).

FACTORS INFLUENCING THE COASTAL GROUNDWATER

Understanding the factors that influence the groundwater is essential for effectively managing and conserving this valuable resource. Various factors, ranging from natural to anthropogenic as shown in Fig 1, can significantly impact groundwater behaviour and availability.

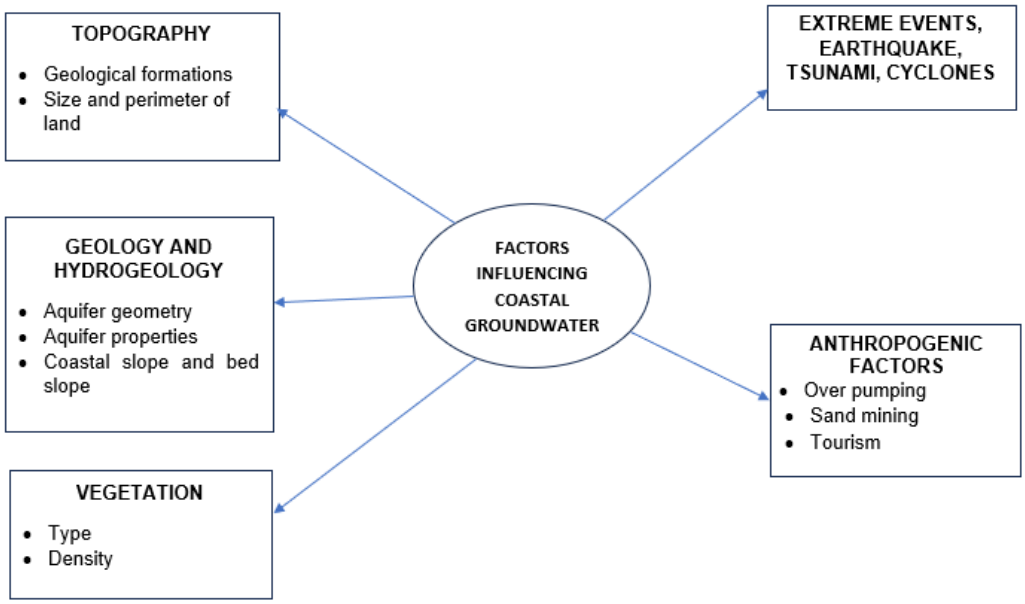

Figure 1. Factors influencing coastal groundwater.

Topography

Topography plays an important role in groundwater dynamics. In coastal areas, topography has significance in groundwater recharge, groundwater flow, and salinity. The geological formations of coastal areas determine the topographical features which helps in the groundwater flow and storage. Coastal formations like sand dunes, barriers, and karstic formations influence the groundwater storage, recharge as well as flow in a coastal aquifer.

Because of climate change-induced sea level rise, low-lying coastal communities face an increased risk of flooding. Saltwater may seep into groundwater reserves when the water table rises due to rising sea levels (Abd-Elhamid et al., 2023). There is a potential for damage to coastal groundwater resources from lateral saltwater intrusion and vertical infiltration during high tides and ocean surge inundation. The quantity of

infiltrating seawater is greatly increased by depressions with ponded saltwater, and the time taken to flush the area is significantly lengthened (Yu et al., 2016).

The configuration of the flow system that forms within a freshwater lens is significantly influenced by the size of the islands present. Diffuse flow easily transports caught meteoric water from the freshwater lens to the sea if the island is small and the underlying geology contains carbonates. The area of the island responsible for meteoric catchment expands exponentially, whereas the perimeter responsible for discharging the lens expands only in a linear manner, as predicted by Mylroie and Vacher (Larson & Mylroie, 2018b).

Geology and Hydrogeology

The movement, quality, and sustainability of coastal groundwater are significantly impacted by the geological composition of the area. This can be volcanic, limestone, sedimentary, or various other types of rock in nature. Water movement along the beach and the interactions between saltwater and groundwater may be affected by the complicated groundwater flow patterns caused by geologic variability in coastal aquifers (Zamrsky et al., 2020). Submarine groundwater discharge is influenced by geology and may alter coastal water quality and geochemical cycles via passing heat, nutrients, and pollutants.

The chemical constituents of coastal groundwater are affected by both natural and anthropogenic chemical inputs, as well as the composition of the aquifer media at the time of formation and subsequent geochemical processes. The geological formation of a region largely dictates the components of the aquifer medium. The continual supply of sand from the sea, rivers, and wind causes the vast majority of the world's coastal aquifers to be formed of sedimentary formations, which tend to be shallow and unconfined (Jayasingha et al., 2014). Aquifer geometry is directly related to the aquifer width, the distance from the circle centre to the no-flow boundary, and the aquifer shape, i.e., whether the aquifer is convergent or divergent, and thus impacts the freshwater-seawater interface and water table elevation. Aquifers with a convergent shape have the least amount of seawater intrusion, while those with a divergent shape are the most susceptible. Correspondingly, the water table elevation is the lowest in divergent aquifers and highest in convergent aquifers (Luo et al., 2021).

The aquifer's permeability and storage capacity affect groundwater near the coast. The permeability and percolation of water in the system depend on the pore size of the soil. Several forms of pollutants may impair groundwater if they make their way into the surrounding aquifer from the water table or the land surface above. Because of frictional losses associated with the aquifer's permeability and poroelastic storage capacity, the pressure signal of groundwater flow is often reduced (Oberle et al., 2017). Thus, the aquifer's permeability and storage affect groundwater's response to climate and sea-level changes. Slope also affects the groundwater quality, saltwater intrusion rises with increasing coastal slope, and the length of saltwater intrusion decreases with increasing bed slope towards the land (Abd-Elhamid et al., 2019; Abd-Elaty & Polemio, 2023). Precipitation and groundwater are interconnected as rainfall is the major source for the recharge of the groundwater in coastal areas. The supply of freshwater for coastal populations is threatened by changes in precipitation patterns brought on by climate change, which may lead to extended periods of droughts and floods. In addition to

seawater intrusion, rising sea levels may also push the freshwater/saltwater boundary closer to land (Bar et al., 2021).

Vegetation

The interaction between vegetation and groundwater is complex and has a significant impact on the overall health and stability of the environment. One way in which plants influence groundwater is through evapotranspiration. Evapotranspiration is the combined process of water vapour loss from the soil and transpiration from the plants. This process can reduce the amount of water available for the recharge of the aquifer. Studies have shown that evapotranspiration accounts for about 50% of water loss in coastal environments (Fahle & Dietrich, 2014).

However, vegetation can also help to maintain groundwater levels by acting as a sponge for absorbing the rainfall. It decelerates water flow towards water bodies, extending the duration of water within the soil and facilitating water percolation for recharging groundwater. Plant roots aid in stabilizing the soil, contributing to the prevention of soil erosion and supporting infiltration. The type and density of vegetation also affect the groundwater level. Coastal wetlands and mangroves help in coastal zone protection as well as in water purification (Kayalvizhi & Kathiresan, 2019). Protecting and retaining sediments from erosive processes like tides, waves, and storms, coastal vegetation, including mangroves, salt marshes, seagrasses, macroalgae, and coastal strands and dunes, are essential. These ecosystems perform vital environmental roles by filtering water and absorbing nutrients (Dugan et al., 2011).

Extreme Events

Extreme events, earthquakes, cyclones, and tsunamis affect the coastal groundwater system. These events have a long-term effect on the groundwater and need a larger recovery time to reach the before-event condition. Variations in groundwater levels can occur due to earthquakes and the ground displacements caused by the seismic activity can produce fissures in the aquifer. This may result in water entering or leaving the aquifer via such fissures. When an earthquake occurs, it may induce a pressure difference between the freshwater aquifer and the saltwater ocean below. As a result of the pressure difference, saltwater may seep into the freshwater aquifer. A study conducted in Korea by Lee reported the rise in water level and change in physical and chemical characteristics in Seacheon, due to the M5.8 earthquake and aftershock in Gyeongju, which is 241 km away (Lee et al., 2020).

Similar to earthquake, tsunami changes the aquifer characteristics. Changes in the groundwater level primarily stem from the post-event flash flood, which results in the intrusion of saltwater into the groundwater aquifer and changes the characteristics by introducing contaminants and saltwater. Following the Tohoku earthquake in March 2011 in Japan, more than 400 square kilometres of land were flooded, and both groundwater and river water were tainted by the tsunami. Although the tsunami did not cause any significant shifts in the groundwater table, but there was an increase in Cl, Na, Ca, Mg, and electric conductivity in the months after the disaster. However, the levels of Cl^- and electric conductivity experienced a sharp decline after June 2011. Additionally in June 2011, elevated concentration of Pb and Cu were detected in the regions' wells, likely transported from the seafloor of the Pacific Ocean by tsunami waves (Kaihotsu et al., 2017). While some preliminary research has been conducted on the topic of tsunami-

caused groundwater contamination, no comprehensive scientific and dynamic studies spanning long periods have yet to be conducted.

Cyclones and storm surges threaten coastal groundwater resources because the precipitation and high tides they bring may cause flooding, pollution from surface runoff, and vertical saltwater intrusion (Van Biersel et al., 2007). The frequency, intensity, and duration of surges affect the groundwater. The movement of groundwater can be impacted by floods triggered by storm surges. Medium-intensity storm surges, for instance, might disrupt groundwater dynamics, hindering complete restoration even after the surge has receded. It takes time for the soil to drain and recover to its initial state after a storm. The drainage process can vary from one to ten days in the absence of such incidents. Similar to the effects of stronger tropical cyclones, moderate and more common storm surges may devastate coastal ecosystems. Plants and animals that depend on groundwater may not thrive or survive if the salinity and water table are altered (Nordio et al., 2023).

Anthropogenic factors

The rise in human settlement in the coastal region, influences the coastal aquifer, with changes in the surface and increased pumping rates. The over-pumping of coastal aquifers for agriculture, industrial use, and drinking water supply can lead to saltwater intrusion, which lowers the water table resulting in infiltration of saltwater from the ocean to the aquifer, thereby deteriorating water quality. Excessive pumping can occasionally lead to the subsidence of coastal land, allowing seawater to infiltrate the aquifer, mainly depending on the aquifer's properties such as permeability. Northern China's Yang-Dai River plain is a vital agricultural area that depends significantly on groundwater. According to studies undertaken in this area, excessive groundwater pumping has caused saltwater to seep underground, contaminating coastal groundwater and rendering it unfit for human use. Anthropogenic activities like the intensive usage of fertilizers and the construction of an anti-tide dam were found to be the primary causes of the coastal groundwater salinization in the Yang-Dai River plain (He et al., 2020; Prasad et al., 2022).

Another anthropogenic activity is coastal sand mining for heavy minerals sand comprising ores like ilmenite and iron that serves as sources of metals such as titanium, zircon, iron, monazite, and garnet. These metals find application in our day-to-day products like ceramics, paint, etc (Bisht & Martinez-Alier, 2023). Loss of land due to coastal erosion, lower water levels, and reduced sediment supply are some of the negative effects of the current rate of sand extraction, which is having a ripple effect on economic and social development in coastal and marine areas (Leal Filho et al., 2021).

Many coastal regions rely heavily on tourism, which may have serious consequences for groundwater supplies. Overexploitation of groundwater resources due to tourism-related water consumption has resulted in a drop in the water table, land subsidence, decline in groundwater quality, and potential intrusion of saltwater (Gössling, 2001). Soil subsidence and saline intrusion, caused by the overuse of water resources, pose threats to the health of coastal ecosystems and the livelihoods of both coastal residents and tourists.

The effects of tourism on coastal groundwater resources have been the subject of several studies, which have offered suggestions for more environmentally friendly approaches to industry. Land use change, global warming, rising sea levels, and

abundant tourist infrastructure are all problems that demand attention. The sustainable preservation of coastal groundwater resources necessitates the adoption of practices like water preservation, efficient wastewater management, and the utilization of alternative water sources (Gössling, 2001; Pérez et al., 2020; Prasad et al., 2020).

CONCLUSIONS

In coastal areas, groundwater is a vital asset for human well-being and environmental health. However, both natural and anthropogenic activities pose significant threats to these resources, including saltwater intrusion and over-exploitation. The factors that govern the groundwater are interconnected, for instance, reduced vegetation and steeper slopes lead to increased runoff, and reduced infiltration of precipitation, thereby reducing the recharge of the aquifer followed by inland movement of saltwater.

To prevent the pressure on the groundwater resources, suitable sustainable management practices need to be adopted, and proper documentation is also needed. Significant temporal variability in water quality parameters has been observed in recent decades, especially in coastal settings; therefore, documenting the dominant scales of variation of these parameters and identifying the underlying factors causing these variations is essential for ensuring sustainable management. The ideas like coastal reservoirs also help in the beneficial use of these resources. The man-made wetlands may operate as a pollution barrier, charge aquifers, conserve water, and provide a home for species when flood water flows through them on its way to coastal reservoirs. This can aid in purifying and storing freshwater, mitigating flooding, replenishing groundwater tables, provision of nurseries for freshwater and marine fish, safeguarding coastlines, retention of sediment, establishing harbours, preserving ecological diversity, and reduction of the impacts of climate change. Lack of data, limited accessibility, and outdated information are the few factors that make the groundwater monitoring and development policy difficult. A single model governance is unfeasible, whereas various levels of operating from local to international governance are needed for successfully implementing policies. The development of new methods with more accuracy, simplicity, and less cost is needed to assess the challenges faced by groundwater resources and should be able to predict the future as the climate is changing abruptly. Suitable policies and sustainable management practices are needed to monitor and reduce the stress on these vulnerable resources ensuing their conservation for the future generations.

ACKNOWLEDGEMENTS. ‘This project has been funded by the E4LIFE International Ph.D. Fellowship Program offered by Amrita Vishwa Vidyapeetham. We extend our gratitude to the Amrita Live-in-Labs® academic program for providing all the support’.

REFERENCES

Abarna, R., Leo George, S., Balasubramani, K., Yuvaraj, S., Shekhar, S., Gnanappazham, L. & Prasad, K.A. 2023. Estimating built-up risk from multi-natural hazards: A case study of Northern coastal plains of Tamil Nadu. *Natural Hazards Research* **3**(1), 49–65. https://doi.org/10.1016/j.nhres.2023.01.001

Abd-Elaty, I. & Polemio, M. 2023. Saltwater intrusion management at different coastal aquifers bed slopes considering sea level rise and reduction in fresh groundwater storage. *Stochastic Environmental Research and Risk Assessment* **37**(6), 2083–2098. https://doi.org/10.1007/s00477-023-02381-9

Abd-Elhamid, H. F., Abd-Elaty, I. & Sherif, M.M. 2019. Effects of Aquifer Bed Slope and Sea Level on Saltwater Intrusion in Coastal Aquifers. *Hydrology* **7**(1), 5. https://doi.org/10.3390/hydrology7010005

Abd-Elhamid, H.F., Zeleňáková, M., Javadi, A.A. & Qahman, K. 2023. *Assessment and Management of Seawater Intrusion in Gaza Aquifer Due to Over Pumping and Sea Level Rise*, 153–165. https://doi.org/10.1007/978-3-031-24506-0_11

Archana, A., Francis, C.A. & Boehm, A.B. 2021. The Beach Aquifer Microbiome: Research Gaps and Data Needs. *Frontiers in Environmental Science* **9**. https://doi.org/10.3389/fenvs.2021.653568

Bakalowicz, M. 2018. Coastal Karst Groundwater in the Mediterranean: A Resource to Be Preferably Exploited Onshore, Not from Karst Submarine Springs.*Geosciences* **8**(7), 258. https://doi.org/10.3390/geosciences8070258

Bar, S., Kumari, B. & Gupta, S.K. 2021. Salinization of Coastal Groundwater Resource in the Perspective of Climate Change. *Fate and Transport of Subsurface Pollutants*, pp. 315–326. https://doi.org/10.1007/978-981-15-6564-9_17

Bisht, A. & Martinez-Alier, J. 2023. Coastal sand mining of heavy mineral sands: Contestations, resistance, and ecological distribution conflicts at HMS extraction frontiers across the world. *Journal of Industrial Ecology* **27**(1), 238–253. https://doi.org/10.1111/jiec.13358

Cabral, A., Sugimoto, R., Taniguchi, M., Tait, D., Nakajima, T., Honda, H. & Santos, I.R. 2023. Fresh and saline submarine groundwater discharge as sources of carbon and nutrients to the Japan Sea. *Marine Chemistry* **249**, 104209. https://doi.org/10.1016/j.marchem.2023.104209

Chang, S.W., Clement, T.P., Simpson, M.J. & Lee, K.-K. 2011. Does sea-level rise have an impact on saltwater intrusion?, *Advances in Water Resources* **34**(10),1283–1291. https://doi.org/10.1016/j.advwatres.2011.06.006

Comte, J.-C., Wilson, C., Ofterdinger, U. & González-Quirós, A. 2017. Effect of volcanic dykes on coastal groundwater flow and saltwater intrusion: A field-scale multiphysics approach and parameter evaluation. *Water Resources Research* **53**(3), 2171–2198. https://doi.org/10.1002/2016WR019480

Dugan, J.E., Airoldi, L., Chapman, M.G., Walker, S.J. & Schlacher, T. 2011. Estuarine and Coastal Structures: Environmental Effects, A Focus on Shore and Nearshore Structures. *Treatise on Estuarine and Coastal Science* **8**, 17–41. Elsevier. https://doi.org/10.1016/B978-0-12-374711-2.00802-0

Fahle, M. & Dietrich, O. 2014. Estimation of evapotranspiration using diurnal groundwater level fluctuations: Comparison of different approaches with groundwater lysimeter data. *Water Resources Research* **50**(1), 273–286. https://doi.org/10.1002/2013WR014472

Foster, S., Chilton, J., Moencg, M., Cardy, F. & Schiffler, M. 2000. Groundwater in rural development. The World Bank. https://doi.org/10.1596/0-8213-4703-9

González-Herrera, R., Cortazar-Cepeda, M., Sánchez-Pinto, I. & Canto-Rios, J. 2022. A homogeneous approach in modeling a coastal karst aquifer. *Earth Science Informatics* **15**(3), 1825–1840. https://doi.org/10.1007/s12145-022-00841-4

Gössling, S. 2001. The consequences of tourism for sustainable water use on a tropical island: Zanzibar, Tanzania. *Journal of Environmental Management* **61**(2), 179–191. https://doi.org/10.1006/jema.2000.0403

Grover, V.I., 2007. *Water: A source of conflict or cooperation?*. Science Publishers, Inc. https://doi.org/10.1201/9780367803650

Hamed, Y., Hadji, R., Redhaounia, B., Zighmi, K., Bâali, F. & El Gayar, A. 2018. Climate impact on surface and groundwater in North Africa: a global synthesis of findings and recommendations. *Euro-Mediterranean Journal for Environmental Integration* **3**(1), 25. https://doi.org/10.1007/s41207-018-0067-8

Hamutoko, J.T., Post, V.E.A., Wanke, H., Beyer, M., Houben, G. & Mapani, B. 2019. The role of local perched aquifers in regional groundwater recharge in semi-arid environments: evidence from the Cuvelai-Etosha Basin, Namibia. *Hydrogeology Journal* **27**(7), 2399–2413. https://doi.org/10.1007/s10040-019-02008-w

He, Z., Han, D., Song, X. & Yang, S. 2020. Impact of human activities on coastal groundwater pollution in the Yang-Dai River plain, northern China. *Environmental Science and Pollution Research* **27**(30), 37592–37613. https://doi.org/10.1007/s11356-020-09760-7

Holzbecher, E.O. & Holzbecher, E.O. 1998. Density and other water properties. *Modeling Density-Driven Flow in Porous Media: Principles, Numerics, Software*, pp. 11–23.

Houben, G.J., Stoeckl, L., Mariner, K.E. & Choudhury, A.S. 2018. The influence of heterogeneity on coastal groundwater flow - physical and numerical modeling of fringing reefs, dykes and structured conductivity fields. *Advances in Water Resources* **113**, 155–166. https://doi.org/10.1016/j.advwatres.2017.11.024

Jayasingha, P., Pitawala, A. & Dharmagunawardhane, H.A. 2014. Evolution of coastal sandy aquifer system in Kalpitiya peninsula, Sri Lanka: sedimentological and geochemical approach. *Environmental Earth Sciences* **71**(11), 4925–4937. https://doi.org/10.1007/s12665-013-2885-y

Kaihotsu, I., Onodera, S., Shimada, J. & Nakagawa, K. 2017. Recovery of groundwater in the Sanriku region contaminated by the tsunami inundation from the 2011 Tohoku earthquake. *Environmental Earth Sciences* **76**(6), 250. https://doi.org/10.1007/s12665-017-6569-x

Kayalvizhi, K. & Kathiresan, K. 2019. Microbes from wastewater treated mangrove soil and their heavy metal accumulation and Zn solubilization. *Biocatalysis and Agricultural Biotechnology* **22**, 101379. https://doi.org/10.1016/j.bcab.2019.101379

Laattoe, T., Werner, A.D., Woods, J.A. & Cartwright, I. 2017. Terrestrial freshwater lenses: Unexplored subterranean oases. *Journal of Hydrology* **553**, 501–507. https://doi.org/10.1016/j.jhydrol.2017.08.014

Larson, E. & Mylroie, J. 2018a. Diffuse Versus Conduit Flow in Coastal Karst Aquifers: The Consequences of Island Area and Perimeter Relationships. *Geosciences* **8**(7), 268. https://doi.org/10.3390/geosciences8070268

Larson, E. & Mylroie, J. 2018b. Diffuse Versus Conduit Flow in Coastal Karst Aquifers: The Consequences of Island Area and Perimeter Relationships. *Geosciences* **8**(7), 268. https://doi.org/10.3390/geosciences8070268

Leal Filho, W., Hunt, J., Lingos, A., Platje, J., Vieira, L., Will, M. & Gavriletea, M. 2021. The Unsustainable Use of Sand: Reporting on a Global Problem. *Sustainability* **13**(6), 3356. https://doi.org/10.3390/su13063356

Lee, S., Lee, J.M., Yoon, H., Kim, Y., Hwang, S., Ha, K. & Kim, Y. 2020. Groundwater Impacts from the M5.8 Earthquake in Korea as Determined by Integrated Monitoring Systems. *Groundwater* **58**(6), 951–961. https://doi.org/10.1111/gwat.12993

Luo, Z., Kong, J., Shen, C., Xin, P., Lu, C., Li, L. & Barry, D. A. 2021. Effects of aquifer geometry on seawater intrusion in annulus segment island aquifers. *Hydrology and Earth System Sciences* **25**(12), 6591–6602. https://doi.org/10.5194/hess-25-6591-2021

Margat, J. & Gun, J. van der. 2013. *Groundwater around the World*. CRC Press. https://doi.org/10.1201/b13977

Martínez, M.L., Intralawan, A., Vázquez, G., Pérez-Maqueo, O., Sutton, P. & Landgrave, R. 2007. The coasts of our world: Ecological, economic and social importance. *Ecological Economics* **63**(2–3), 254–272. https://doi.org/10.1016/j.ecolecon.2006.10.022

Mastrocicco, M. & Colombani, N. 2021. The Issue of Groundwater Salinization in Coastal Areas of the Mediterranean Region: A Review. *Water* **13**(1), 90. https://doi.org/10.3390/w13010090

Nlend, B., Celle-Jeanton, H., Huneau, F., Ketchemen-Tandia, B., Fantong, W.Y., Boum-Nkot, S.N. & Etame, J. 2018. The impact of urban development on aquifers in large coastal cities of West Africa: Present status and future challenges. *Land Use Policy* **75**, 352–363. https://doi.org/10.1016/j.landusepol.2018.03.007

Nordio, G., Frederiks, R., Hingst, M., Carr, J., Kirwan, M., Gedan, K., Michael, H. & Fagherazzi, S. 2023. Frequent Storm Surges Affect the Groundwater of Coastal Ecosystems. *Geophysical Research Letters* **50**(1). https://doi.org/10.1029/2022GL100191

Oberle, F., Swarzenski, P. & Storlazzi, C. 2017. Atoll Groundwater Movement and Its Response to Climatic and Sea-Level Fluctuations. *Water* **9**(9), 650. https://doi.org/10.3390/w9090650

Pérez, D.M.G., Martín, J.M.M., Martínez, J.M.G. & Sáez-Fernández, F.J. 2020. An Analysis of the Cost of Water Supply Linked to the Tourism Industry. An Application to the Case of the Island of Ibiza in Spain. *Water* **12**(7), 2006. https://doi.org/10.3390/w12072006

Prasad, G., Mamane, H. & Ramesh, M.V. 2022. Geogenic and anthropogenic contamination of groundwater in a fragile eco-friendly region of southern Kerala, India. *Agronomy Research* **20**(S1), 1072–1089. https://doi.org/10.15159/AR.22.010

Prasad, G. & Ramesh, M.V. 2019. Spatio-temporal analysis of land use/land cover changes in an ecologically fragile area - Alappuzha District, Southern Kerala, India. *Natural Resources Research* **28**(1), 31–42. https://doi.org/10.1007/s11053-018- 9419-y

Prasad, G., Reshma, A.S. & Ramesh, M.V., 2021. Assessment of drinking water quality on public health at Alappuzha district, southern Kerala, India. *Materials Today: Proceedings* **46**, 3030–3036.

Prasad, G., Rajesh, R. & Arun, K., 2020. Land use pattern as an indicator of sustainability: a case study. In *10th Annual International Conference on Industrial Engineering and Operations Management. IEOM Society International. ISSN*. 2169–8767.

Prusty, P., & Farooq, S. H. (2020). Seawater intrusion in the coastal aquifers of India - A review. HydroResearch, 3, 61–74. https://doi.org/10.1016/j.hydres.2020.06.001

Roumasset, J.A. & Wada, C.A. 2015. Integrated Groundwater Resource Management. In *Sustainable Economic Development,* 77–89. Elsevier. https://doi.org/10.1016/B978-0-12-800347-3.00005-4

Shamsudduha, M. & Panda, D.K. 2019. Spatio-temporal changes in terrestrial water storage in the Himalayan river basins and risks to water security in the region: A review. *International Journal of Disaster Risk Reduction* **35**, 101068. https://doi.org/10.1016/j.ijdrr.2019.101068

Van Biersel, T.P., Carlson, D.A. & Milner, L.R. 2007. Impact of hurricanes storm surges on the groundwater resources. *Environmental Geology* **53**(4), 813–826. https://doi.org/10.1007/s00254-007-0694-x

Vo, P. Le. 2007. Urbanization and water management in Ho Chi Minh City, Vietnam-issues, challenges and perspectives. *GeoJournal* **70**(1), 75–89. https://doi.org/10.1007/s10708-008-9115-2

Yu, X., Yang, J., Graf, T., Koneshloo, M., O'Neal, M.A. & Michael, H.A. 2016. Impact of topography on groundwater salinization due to ocean surge inundation. *Water Resources Research* **52**(8), 5794–5812. https://doi.org/10.1002/2016WR018814

Zamrsky, D., Karssenberg, M.E., Cohen, K.M., Bierkens, M.F.P. & Oude Essink, G.H.P. 2020. Geological Heterogeneity of Coastal Unconsolidated Groundwater Systems Worldwide and Its Influence on Offshore Fresh Groundwater Occurrence. *Frontiers in Earth Science*, **7**. https://doi.org/10.3389/feart.2019.00339

Zheng, X., Huang, G., Liu, L., Zheng, B. & Zhang, X. 2020. A multi-source virtual water metabolism model for urban systems. *Journal of Cleaner Production* **275**, 124107. https://doi.org/10.1016/j.jclepro.2020.124107

Agronomy Research **21**(S3), 1499–1518, 2023
https://doi.org/10.15159/AR.23.076

Morphological, molecular, and pathogenic characterization of *Colletotrichum gloeosporioides* sensu stricto associated with imported citrus fruits

Nurholis[1], S.H. Hidayat[1], K.H. Mutaqin[1], S. Widodo[2] and Widodo[1,*]

[1]IPB University, Faculty of Agriculture, Department of Plant Protection, Jl. Kamper Babakan Dramaga, Kabupaten Bogor, ID16680 Jawa Barat, Indonesia
[2]IPB University, Faculty of Agricultural Technology, Department of Agricultural Engineering and Biosystem, Jl. Kamper Babakan Dramaga, Kabupaten Bogor, ID16680 Jawa Barat, Indonesia
[*]Correspondence: widodo@apps.ipb.ac.id

Received: March 19th, 2023; Accepted: August 5th, 2023; Published: August 24th, 2023

Abstract. *Colletotrichum gloeosporioides* is a fungal pathogen that causes anthracnose disease in citrus fruits. *C. gloeosporioides* has the potential to be carried by imported citrus fruits. The aim of this study was to detect, isolate, identify, and test the pathogenicity of *C. gloeosporioides* associated with imported citrus fruits. The detection method was carried out by freezing imported citrus fruits at -20 °C for 15 hours. *C. gloeosporioides* was identified morphologically and molecularly. The morphological identification method was done by observing mycelial colonies and conidia. The molecular identification method was done by the Polymerase Chain Reaction technique using 3 locus of ITS, GAPDH, and TUB2. The pathogenicity was tested by attaching 1 culture circle of *C. gloeosporioides* to the surface of the citrus fruit and injecting 100 µl of conidia suspension at a density of 10^5 conidia mL^{-1} into the inside of the citrus fruit. The main results showed that *C. gloeosporioides* was successfully detected at 4 days after incubation by the emergence of mycelia on the surface of citrus fruits. Morphological and molecular identification proved that the species of fungus was *C. gloeosporioides* sensu stricto which was a pathogenic fungus on imported and local citrus fruits with a disease incidence value of 100%, and a disease severity value of 97.78% and 98.89%, respectively.

Key words: anthracnose, disease incidence, disease severity, identification, pathogenicity.

INTRODUCTION

Colletotrichum gloeosporioides (Penz.) Penz. & Sacc. is a pathogenic fungus that causes anthracnose disease in citrus fruits (Patricia et al., 2021). Anthracnose is an important disease on citrus fruits because it can cause economic losses from the field to storage. Yield losses caused by *C. gloeosporioides* infection can reach 80% (Silva-Junior et al., 2014). Therefore, Dean et al. (2012) categorized *C. gloeosporioides* into the 10 most important of plant pathogenic fungi in the world. Symptoms of anthracnose include light brown to black necrotic lesions on almost the entire

surface and blackish brown rot on the inside of citrus fruits (Cruz-Lagunas et al., 2020; Khamsaw et al., 2022).

Anthracnose disease is spread in almost all citrus plantations in the world (Perez-Mora et al., 2020). *C. gloeosporioides* was also reported to attack citrus plantations in several areas in Indonesia. Suryaningsih et al. (2015) isolated *C. gloeosporioides* from citrus fruits with anthracnose symptoms in citrus plantations in Bali. The most recent report was submitted by Wiyanna et al. (2022) who have characterized *C. gloeosporioides* from citrus plantations in Singkawang, West Kalimantan. The geographic distribution of plant pathogens influences the level of pathogen virulence (Shaw & Osborne, 2011). This means that *C. gloeosporioides* species from various countries are thought to have different characters and levels of virulence. Sacristan & Garcia-Arenal (2008) stated that the differences in character were caused by differences in pathogen strains.

Indonesia is still importing citrus fruits from various countries, such as Pakistan, Australia, China, and Argentina. Lichtenberg & Olson (2018) stated that imported citrus fruits have the potential to carry pathogens that cause plant diseases. This potential is based on the ability of the pathogen to latently infect citrus fruits without expressing disease symptoms on the surface of the fruit (Johnston et al., 2005). Infected fruits with a latent fungus look as healthy and normal as uninfected fruits. Latent infectious fungi were difficult to be detected and isolated (Schaad et al., 2003). This detection difficulty raises concerns that latent infectious fungi on imported citrus fruits will be brought and spread to local citrus fruit plantations. *C. gloeosporioides* is a fungus that is known to be able to latently infect postharvest fruits (Agrios, 2005). *C. gloeosporioides* infects latently by forming an inactive structure in the fruit when the physical condition of the fruit is not yet possible to be infected (Prusky & Lichter, 2007). Droby & Wisniewski (2018) explained that the fungus starts the infection when the postharvest fruits have undergone a senescence process. Michailides et al. (2010) added that the physicality of fruits is weakened during the senescence process.

C. gloeosporioides infects latently in citrus fruits and being difficult to be detected. Latent infection in fruits can be physically detected. Michailides et al. (2010) reported that *Monilinia fructicola* and *M. laxa* causing brown rot in fruits, *Botrytis cinerea* causing rot in grapes and *Alternaria* causing blight in nuts, can be physically detected within 5 to 7 days using the Overnight Freezing Incubation Technique (ONFIT). *C. gloeosporioides* is also difficult to be identified accurately. According to Cai et al. (2009), the difficulty in identifying *C. gloeosporioides* is caused by the number of morphological characters as biological markers are few and varied, and has a wide host range with varying levels of pathogenicity. Therefore, identification of *C. gloeosporioides* through morphological characters is not enough, but needs further identification through a polyphasic approach by combining identification using genetic and physiological characters. Species of a pathogen is essential to be identified to understand the epidemiology and to develop effective controls. Therefore, even though *C. gloeosporioides* is already an endemic fungal pathogen in Indonesia, but its presence in imported citrus fruits must still be characterized because it comes from a different geographical area. Moendeg et al. (2017) explained the difference in geographical areas can cause different strains of pathogens.

This study aims to detect, isolate, identify, and test the pathogenicity of *C. gloeosporioides* carried by imported citrus fruits. The research results are expected to be used as guidance for consideration in mitigating the risk of the spread of *C. gloeosporioides*.

MATERIALS AND METHODS

Research Locations, time, and citrus fruits

The research was conducted at the Plant Mycology Laboratory, Department of Plant Protection, IPB University, Bogor Regency and Biotechnology Laboratory, Applied Research Institute of Agricultural Quarantine, Bekasi Regency from December 2021 to October 2022. Citrus fruits come from imported commodities obtained from Tanjung Priok Port, Jakarta, Indonesia. The variety of citrus fruit is mandarin (*Citrus reticulata*). Citrus fruits used in the study met the criteria of being healthy without showing disease symptoms and were uniform in shape, size, and color.

Detection and isolation of *C. gloeosporioides*

C. gloeosporioides was detected using the Overnight Freezing Incubation Technique (ONFIT). Citrus fruits were washed using tap water to clean all material attached to the surface of the fruit and rinsed 2 times using sterile water. Citrus fruits were dried and placed on a rack in a 35×27×10 cm plastic container (Fig. 1). Sterile water was added to the plastic container to maintain moisture. The plastic container was tightly closed and stored in the freezer at -20 °C for 15 hours. Citrus fruits in plastic containers were incubated at room temperature. The mycelia of *C. gloeosporioides* that appeared on the surface of citrus fruits were isolated and grown on PDA media.

Identification of *C. gloeosporioides* morphologically and molecularly was carried out using pure cultures to ensure that the identification process was conducted only on 1 individual species not mixed with other species (contaminants). Pure cultures were prepared by the conidial serial dilution technique. A total of 5 mycelial circles of *C. gloeosporioides* culture on PDA media were taken using a cork borer (4.5 mm in diameter). The culture circle was put into 10 mL of sterile distilled water and shaken. A total of 1 mL of sterile distilled water mixed with mycelia and conidia of *C. gloeosporioides* was taken and transferred to 9 mL of sterile distilled water (10^{-1}). Dilution was continued until the mixture between the mycelia and the conidia of *C. gloeosporioides* did not look thick. A total of 0.1 mL of each dilution was taken and spread on PDA media. The mycelia that grew from 1 conidium were removed, transferred, and re-grown onto new PDA media as a pure culture.

Morphological identification of *C. gloeosporioides*

C. gloeosporioides was identified morphologically from a pure culture based on the characteristics of the fungi's identifying organs, such as mycelia and conidia. Identification of mycelia was carried out by observing the growth pattern of mycelial colonies on PDA media which included texture and color. Conidia were identified morphometrically by observing the shape and measuring 50 conidia randomly. The decision of morphological identification is based on the similarity between the obtained morphological character data and the identification key from several available references.

DNA extraction of *C. gloeosporioides*

The DNA of *C. gloeosporioides* was extracted using 2 conventional methods by Abd-Elsalam et al. (2003) with some modifications and Ausubel et al. (2003) with some modifications. The pure culture of the *C. gloeosporioides* used in the DNA extraction process was 7 days old.

1) Abd-Elsalam et al. (2003) with some modifications.

The mycelia of the *C. gloeosporioides* were taken from the pure culture and inoculated into 500 µl of Potato Dextrose Broth (PDB) medium in a 1.5 mL tube. Fungal mycelia in PDB was shaken at 150 rpm at room temperature for 72 hours. The growing mycelia were pelleted using a centrifugation technique at 13,000 rpm for 5 minutes at room temperature. The liquid phase (supernatant) was discarded and the pellet was washed with 500 µl of Tris-EDTA solution (pH 8.0). The pellet was again centrifuged at 13,000 rpm for 5 minutes. The supernatant was removed and the pellet was crushed using a pistil. 300 µl of extraction solution (200 mm Tris-HCl [pH 8.5], 250 mm NaCl, 25 mm EDTA, and 0.5% sodium dodecyl sulfate) was added to the pellet and homogenized with a pistil for 5 minutes. 150 µl of 3M sodium acetate (pH 5.2) was added and cooled at -20 °C for 10 minutes. The pellet was centrifuged at 13,000 rpm for 5 minutes. The resulting liquid (supernatant) was measured and transferred to a new 1.5 mL tube. An equal volume of isopropanol with supernatant was added and centrifuged at 13,000 rpm for 5 minutes. DNA was washed by adding 500 µl 70% ethanol and centrifuged at 13,000 rpm for 5 minutes. The supernatant was discarded and the DNA was dried. DNA was suspended in 100 µl Tris-EDTA solution (10 mm Tris-HCl [pH 8.0], 1 mm EDTA). The DNA suspension was stored at -20 °C.

2) Ausubel et al. (2003) with some modifications.

A total of 10 mycelial circles from a pure culture of *C. gloeosporioides* were taken using a 4.5 mm diameter of cork borer. The mycelial circles were put into a sterile aluminum foil container with a tight cover and stored in the freezer -80 °C for 3 hours. The frozen mycelial circles were crushed until smooth using a mortar and dissolved by adding 600 µl of a mixed solution of CTAB extraction and 2% mercaptoethanol which had been previously heated in a water bath at 65 °C. The mycelial suspension was put into a 1.5 mL tube and heated in a water bath at 65 °C for 60 minutes with occasional homogenization by hand. 600 µl CI (24:1) was added, homogenized, and centrifuged at 10,000 rpm at 4°C for 5 minutes. The supernatant was taken, measured, and transferred to a new 1.5 mL tube. The CTAB/NaCl solution that had been preheated in a 65 °C water bath was taken as much as 1 10^{-1} of the volume of the supernatant and stirred until evenly distributed. CI (24:1) with the same volume was added, shaken, and centrifuged at 10,000 rpm at 4 °C for 5 minutes. The supernatant was taken, measured, and transferred to a new 1.5 mL tube. CTAB precipitation solution of as much as 1 volume of supernatant was added, stirred evenly, and centrifuged at 2,700 rpm at 4 °C for 5 minutes. 150 µl of TE solution with high salt content was added and shaken evenly. DNA was precipitated by adding isopropanol as much as 0.6 volume of the total solution and centrifuged at 10,000 rpm at 4 °C for 20 minutes. The supernatant was discarded, and the DNA pellet was washed by adding 500 µl 80% ethanol and centrifuged at 8,000 rpm for 5 minutes at room temperature. The remaining ethanol was discarded and the DNA pellet was dried. DNA was suspended by adding 100 µl of TE solution. The DNA suspension was stored at -20 °C.

The concentration of extracted *C. gloeosporioides* DNA was measured using Nanodrop One with serial number AZY2125665. DNA measurement aims to assess the quantity of obtained DNA from the two extraction methods used.

Molecular identification of *C. gloeosporioides*

ITS, GAPDH, and TUB2 genes were amplified using primers pair of ITS1 and ITS4, GDF1 and GDR1, Btub2Fd and Btub4Rd through PCR technique. Amplicon nucleotide bases were sequenced. The DNA sequence was identified using the Basic Local Alignment Search Tool program (BLAST) on the website https://www.ncbi.nlm.nih.gov/.

DNA Amplification of the ITS, GAPDH, and TUB2 locus of *C. gloeosporioides*

The *C. gloeosporioides* DNA was amplified using primer pairs of ITS with an amplicon size of around 600 bp, GAPDH with an amplicon size of around 200 bp, and TUB2 with an amplicon size of around 600 bp. The sequences of all primers were shown in Table 1. The amplification process was carried out by PCR technique using the 'Applied Biosystems type Veriti' thermal cycler. The PCR reaction was conducted in a 50 µl volume containing 20 µl PCR master mix, 2 µl ITS1F primer, 2 µl ITS4 primer, 4 µl extracted DNA, and 22 µl ddH2O. ITS and GAPDH amplification was carried out for 35 cycles with the steps of DNA double-strand denaturation at 94 °C for 35 seconds, primer attachment to the ITS DNA locus at 51 °C for 1 minute, and DNA elongation at 72 °C for 2 minutes (White et al., 1990; Gardes & Bruns, 1993; Guerber et al., 2003). TUB2 amplification was carried out for 35 cycles with the steps of DNA double-strand denaturation at 94 °C for 30 seconds, primer attachment to the ITS DNA locus at 52 °C for 30 seconds, and DNA elongation at 72 °C for 30 seconds (Woudenberg et al., 2009). The results of DNA amplification were visualized on 1% agarose gel.

Table 1. List of primers used in this study

Locus	Primer name	Sequence (5'-to-3')	References
ITS	ITS1F	CTTGGTCATTTAGAGGAAGTAA	Gardes & Bruns (1993)
	ITS4	CCTCCGCTTATTGATATGC	White et al. (1990)
GAPDH	GDF1	GCCGTCAACGACCCCTTCATTGA	Guerber et al. (2003)
	GDR1	GGGTGGAGTCGTACTTGAGCATGT	Guerber et al. (2003)
TUB2	Btub2Fd	GTBCACCTYCARACCGGYCARTG	Woudenberg et al. (2009)
	Btub4Rd	CCRGAYTGRCCRAARACRAAGTTGTC	Woudenberg et al. (2009)

The ITS, GAPDH, and TUB2 locus sequencing of the *C. gloeosporioides* DNA

The PCR product containing the ITS, GAPDH, and TUB2 amplicon of *C. gloeosporioides* DNA was sequenced at First Base, Malaysia. The DNA nucleotide sequences of *C. gloeosporioides* were analyzed by BLAST on the NCBI website. The BLAST process was carried out to identify DNA sequences based on species that have the highest DNA sequence similarities in NCBI GenBank.

Phylogenetic tree

The genetic relationship between *C. gloeosporioides* from local and imported citrus fruits, and other countries was determined by constructing a phylogenetic tree. The phylogenetic tree was built using Mega software version 10, through a neighbor-joining approach with a bootstrap value of 1,000 times.

Pathogenicity Test

Pathogenicity test of *C. gloeosporioides* used imported and local healthy mandarin citrus fruits without showing disease symptoms. The pathogenicity test was carried out using the attachment technique of *C. gloeosporioides* culture to the surface of citrus fruits and the injection technique of *C. gloeosporioides* conidia suspension into citrus fruits. Citrus fruits were surface sterilized before being used. Citrus fruits were immersed in a 5.26% sodium hypochlorite solution for 4 minutes to disinfect surface pathogens. Citrus fruits were rinsed 2 times using sterile water and dried on sterile tissue paper. Ten citrus fruits were arranged on a rack in a sterile plastic container of 35×27×10 cm and tightly closed. Sterile water was added to the plastic container to make suitable humidity for *C. gloeosporioides* growth.

1) The attachment technique of *C. gloeosporioides* culture to the surface of citrus fruits.

The *C. gloeosporioides* culture was taken using a 4.5 mm of cork borer. One side of the upper surface of the citrus fruit was injured using a sterile syringe from the outer surface to the deepest skin. One circle of culture was attached to the surface of the citrus fruit that has been injured. Injury treatment and culture attachment were carried out on 10 citrus fruits which had been arranged on a rack in a plastic container. The control treatment was wounded by a sterile syringe and followed by the attachment of 1 circle of blank PDA media without *C. gloeosporioides* culture to 10 citrus fruits. Citrus fruits were incubated at room temperature for 21 days. The treatment of culture attachment and control was conducted with 3 replications.

2) The injection technique of *C. gloeosporioides* conidia suspension into citrus fruits.

Ten citrus fruits in a plastic container were injected using a sterile syringe containing 100 µl of *C. gloeosporioides* conidia suspension at a density of 10^5 conidia mL^{-1} into the columella of the citrus fruit through the base of the calyx. Citrus fruits were injected with 100 µl of sterile water in the control treatment. Citrus fruits were incubated at room temperature for 21 days. The injection treatment of conidial suspension and control was repeated 3 times (Camiletii et al., 2022).

Citrus fruits were observed by assessing the broad scale of anthracnose symptoms caused by *C. gloeosporioides*. Symptoms were observed from the outside and inside of citrus fruits. Observation of internal symptoms was carried out by splitting citrus fruits. Scale 0 = no visible symptoms; 1 = 1–30% symptom; 2 = 30–60% symptom; and 3 = ≥ 60% symptoms (Mojerlou & Safaie, 2012). The pathogenicity of *C. gloeosporioides* was determined by assessing the incidence and severity of the disease based on the appearance and scale of anthracnose symptoms on citrus fruits. The incidence and severity of the disease were calculated using the following formula:

$$\mathrm{DI} = \frac{\text{Number of rotten fruit}}{\text{Total number of fruits observed}} \text{ x } 100\%$$

$$\mathrm{DS} = \sum \frac{(\mathrm{n \text{ x } V})}{\mathrm{Z \text{ x } N}} \text{ x } 100\%$$

where DI – Disease Incidence; DS – Disease Severity; n – number of fruits showing the same scale; V – symptom scale; Z – the highest scale; N – total number of fruits observed.

Pathogenicity test used a Completely Randomized Design (CRD). Data were analyzed by Analysis of Variance (ANOVA). If the results of the analysis show a *P*-value < $\alpha = 0.05$, then proceed with the Tukey test at level $\alpha = 0.05$ to determine differences in disease severity between the pathogenicity treatments of

C. gloeosporioides and control (Kasiamdari & Sangadah, 2015). Analysis was performed using SAS software version 9.4.

RESULTS AND DISCUSSION

Results

Detection and isolation of *C. gloeosporioides*

C. gloeosporioides was successfully detected at 4 Days After Incubation (DAI) using the ONFIT method through the emergence of mycelia on the surface of imported citrus fruits. Fig. 1 shows grayish-white mycelia on the surface of citrus fruits, like coarse cotton with a flat and spreading growth pattern. The ONFIT treatment caused skin discoloration of the citrus fruit from orange to dark brown and the skin texture became dry. Meanwhile, citrus fruits in the control treatment still look fresh and orange in color (Fig. 1). Table 2 shows 37% of the imported citrus fruits carried *C. gloeosporioides*. Citrus fruits were not covered by mycelia at all in the control treatment without the ONFIT method.

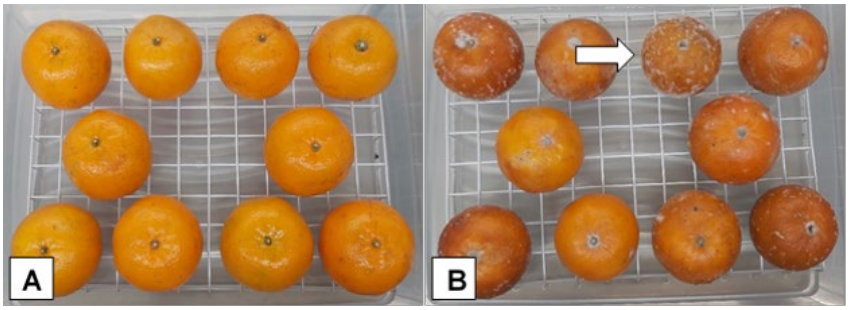

Figure 1. The emergence of *C. gloeosporioides* mycelia on the surface of imported citrus fruits at 4 DAI. A – Control treatment; B – ONFIT treatment.

Table 2. The emergence percentage of *C. gloeosporioides* mycelia on the surface of imported citrus fruits at 4 DAI

Treatment	Characterization of mycelia on the surface of citrus fruits	Amount	Percentage of emergence (%)[1]
Control	No mycelia found	0	0
ONFIT	Mycelial colonies are grayish-white, like coarse cotton, and grow flat	37	37

[1] Percentage of emergence was obtained from the number of mycelial emergences in 100 citrus fruits. The emergence of the same mycelia in more than one of the same citrus fruit was counted as 1.

Morphological identification of *C. gloeosporioides*

Colonies of *C. gloeosporioides* mycelia that grew from a single conidium on PDA media had a diameter of 6.74–7.01 (mean 6.82, $n = 5$) cm at 7 DAI (Table 3). Characteristics of mycelia were aerial types, such as coarse cotton, and grayish-white. Conidia size were 8.20–21.20×3.80–5.50 (mean 15.28×4.59, $n = 50$) µm, hyaline, cylindrical, non-septate, broadly rounded at one end, and tapered at the other (Fig. 2).

Table 3. Morphological characterization of *C. gloeosporioides* from imported citrus fruits

Morphological characterization	Description
Macroscopic characteristics	
Colonies on the surface of citrus fruits[1]	
Color	Grayish-white
Texture of mycelia	Like coarse cotton
Colonies on PDA media[2]	
Color	Grayish-white
Form	Circular
Elevation	Flat
Margin	Undulate
Pigmentation[3]	No pigmentation
Growth rate (cm)[4]	6.82 ± 0.13
Microscopic characteristics	
Conidia morphology	Cylindrical and slender
Apical cell morphology	Broadly rounded
Basal cell morphology	Tapered
Mean length of conidia (µm)[5]	15.28 ± 2.08
Mean width of conidia (µm)[6]	4.59 ± 0.40
Septation	Non-septate

[1]Colonies were observed at the surface of the citrus fruits; [2]Colonies were observed at the top of the culture of *C. gloeosporioides*; [3]Pigmentation was observed on the bottom of the culture of *C. gloeosporioides*; [4]The mycelial growth rate of *C. gloeosporioides* was observed at 7 DAI; [5,6]The mean length and width of conidia, were observed from 50 randomly selected conidia ± standard deviation.

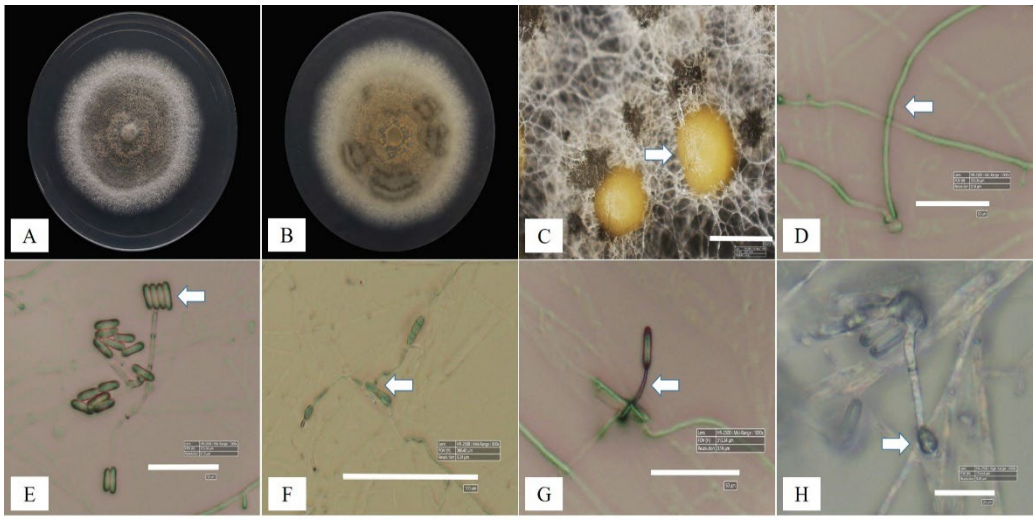

Figure 2. Morphological characteristics of *C. gloeosporioides* from imported citrus fruits. A – Fungal colonies 7 days old on upper PDA media; B – Bottom part of fungal culture; C – Conidiomata on PDA, scale bar = 500 µm; D – Hyphae, scale bar = 50 µm; E – Conidia, scale bar = 50 µm; F – Hyphae formed from a conidium, scale bar = 100 µm; G – Conidiophore, scale bar = 50 µm; H – Appressorium developed from a conidium with a long germ tube, scale bar = 20 µm.

DNA extraction of *C. gloeosporioides*

Both DNA extraction methods succeeded in obtaining the DNA of *C. gloeosporioides*. However, DNA measurements using nanodrop of the two extraction methods yielded different concentrations. Table 4 informs that the DNA extraction method from Abd-Elsalam et al. (2003) produced the highest DNA concentration of 487.806 ng μl^{-1} compared to the Ausubel et al. (2003) method of 56.868 ng μl^{-1}. Abd-Elsalam et al. (2003) method also had a higher A260/A280 value of 2.175 compared to the Ausubel et al. (2003) method of 1.620. However, the extraction time of the Abd-Elsalam et al. (2003) method was about 3 days and 2 hours longer than the Ausubel et al. (2003) method about 6 hours.

Table 4. DNA quantification using nanodrop

DNA extraction methods	Concentration (ng μl^{-1})	A260/A280	Extraction time
Abd-Elsalam et al. (2003)	487.806 ± 35.350	2.175 ± 0.016	± 3 days and 2 hours
Ausubel et al. (2003)	56.868 ± 8.307	1.620 ± 0.014	± 6 hours

Molecular identification of *C. gloeosporioides*

DNA Amplification of the *C. gloeosporioides* ITS, GAPDH, and TUB2 locus

The extracted DNA from both methods was successfully amplified by ITS1 and ITS4 primers at the ITS locus, GDR1 and GDF1 at the GAPDH locus, Btub2Fd and Btub4Rd at the TUB2 locus. Visualization of DNA bands on 1% agarose gel can be seen in both extraction methods according to the ITS target size of ± 600 bp. Fig. 3 shows the total DNA concentration correlated with the visualization of the DNA bands. Abd-Elsalam et al. (2003) method which has the highest DNA concentration shows the DNA bands thicker than the Ausubel et al. (2003).

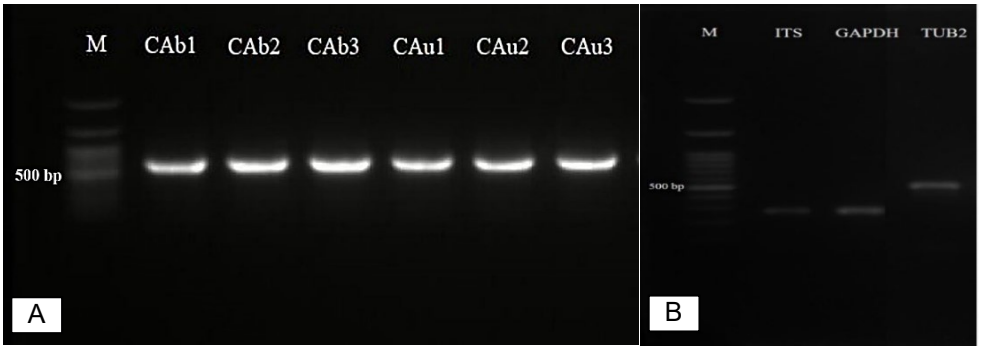

Figure 3. Visualization of DNA bands. A – DNA bands from all DNA extraction methods using universal primer pairs ITS1 and ITS4. CAb1–CAb3 are Abd-Elsalam et al. (2003) method with 3 replications and CAu1–CAu3 are Ausubel et al. (2003) method with 3 replications. B – DNA bands from locus ITS, GAPDH, and TUB2.

DNA sequencing of the *C. gloeosporioides* ITS, GAPDH, TUB2 locus

DNA amplicon that has been sequenced was subjected to the BLAST process on the NCBI website. BLAST results showed that the ITS locus amplicon of *C. gloeosporioides* DNA from imported citrus fruits had the highest DNA sequence similarity with isolate *Colletotrichum gloeosporioides* COL5 from Pakistan with

accession number MH645072.1. The GAPDH locus amplicon of *C. gloeosporioides* DNA had the highest DNA sequence similarity with isolate *Colletotrichum gloeosporioides* WT-Y4 from China with accession number MK940674.1. The TUB2 locus amplicon of *C. gloeosporioides* DNA had the highest DNA sequence similarity with isolate *Colletotrichum gloeosporioides* strain 8 from Italy with accession number JN121296.1. Table 5 presents the top 5 of BLAST results of *C. gloeosporioides* from imported citrus fruits with various isolates showing the highest similarity.

Table 5. The similarity of *C. gloeosporioides* isolate from imported citrus fruit with other isolates in GenBank

Isolate identity from imported citrus fruits	Locus	Isolate identity in *GenBank*	Accession number	Query cover (%)	Similarity (%)	Origin
Colletotrichum gloeosporioides isolate CGJIPKN1	ITS	*Colletotrichum gloeosporioides* COL5	MH645072.1	100	98.55	Pakistan
		Colletotrichum gloeosporioides	MH520670.1	100	98.39	Pakistan
		Colletotrichum gloeosporioides strain AGMy0229a	KX578796.1	100	98.07	Brazil
		Colletotrichum siamense SY71	OM967145.1	100	97.91	China
		Colletotrichum fructicola C09320	MW368667.1	100	97.59	South Korea
	GAPDH	*Colletotrichum gloeosporioides* WT-Y4	MK940674.1	100	100	China
		Colletotrichum gloeosporioides	MH321225.1	100	100	China
		Colletotrichum gloeosporioides strain AGMy0075	KX578776.1	100	100	South Africa
		Colletotrichum gloeosporioides	KU612891.1	100	100	Australia
		Colletotrichum gloeosporioides	ON050981.1	100	100	Colombia
	TUB2	*Colletotrichum gloeosporioides* Strain 8	JN121296.1	99	99.62	Italy
		Colletotrichum gloeosporioides	MT409132.1	98	99.62	Italy
		Colletotrichum gloeosporioides Strain HNHJ-73	MN908602.1	98	99.62	China
		Colletotrichum gloeosporioides Strain FMB 0137	MN339477.1	98	99.62	Pakistan
		Colletotrichum gloeosporioides Strain BRIP 66213	MK390653.1	98	99.62	Australia

Phylogenetic tree

Several strains of the *C. gloeosporioides* species complex listed in Table 6 have been determined for their genetic relationship through a phylogenetic tree. Fig. 4 shows that *C. gloeosporioides* from imported citrus fruits has a close genetic relationship with *C. gloeosporioides* isolates from Italy, Australia, Banyuwangi and Malang, Indonesia. These findings prove that *C. gloeosporioides* from imported citrus fruits is the same species as *C. gloeosporioides* from Banyuwangi and Malang, Indonesia.

Table 6. A list of *C. gloeosporioides* species complex strains used in this study

Species	Host	Country	GenBank Accession Number		
			ITS	GAPDH	TUB2
C. aenigma	*Persea americana*	Israel	JX010244	JX010044	JX010389
	Pyrus pyrifolia	Japan	JX010243	JX009913	JX010390
C. aeschynomenes	Aeschynomene virginica	USA	JX010176	JX009930	JX010392
C. alatae	*Dioscorea alata*	India	JX010190	JX009990	JX010383
	Dioscorea alata	Nigeria	JX010191	JX010011	JX010449
C. alienum	*Persea americana*	Australia	JX010217	JX010018	JX010385
	Malus domestica	New Zealand	JX010251	JX010028	JX010411
C. aotearoa	*Vitex lucens*	New Zealand	JX010220	JX009906	JX010421
	Kunzea ericoides	New Zealand	JX010198	JX009991	JX010418
C. asianum	*Mangifera indica*	Australia	JX010192	JX009915	JX010384
	Coffea arabica	Thailand	FJ972612	JX010053	JX010406
C. clidemiae	*Vitis sp.*	USA	JX010274	JX009909	JX010439
	Clidemia hirta	USA	JX010265	JX009989	JX010438
C. cordylinicola	*Cordyline fruticosa*	Thailand	JX010226	JX009975	JX010440
C. fructicola	*Coffea arabica*	Thailand	JX010165	JX010033	JX010405
	Fragaria x ananassa	USA	JX010179	JX010035	JX010394
C. gloeosporioides	*Citrus sinensis*	Italy	JX010152	JX010056	JX010445
	Citrus reticulata	Australia	MG572144	MG572133	MG572155
C. horii	*Diospyros kaki*	New Zealand	GQ329687	GQ329685	JX010375
	Diospyros kaki	China	JX010212	GQ329682	JX010378
C. kahawae subsp. ciggaro	*Olea europaea*	Australia	JX010230	JX009966	JX010434
	Kunzea ericoides	New Zealand	JX010227	JX009904	JX010427
C. kahawae subsp. kahawae	*Coffea arabica*	Angola	JX010234	JX010040	JX010435
	Coffea arabica	Cameroon	JX010232	JX010046	JX010431
C. musae	*Musa sapientum*	Kenya	JX010142	JX010015	JX010395
	Musa sp.	USA	JX010146	JX010050	HQ596280
C. nupharicola	*Nuphar lutea subsp. polysepala*	USA	JX010189	JX009936	JX010397
C. psidii	*Psidium sp.*	Italy	JX010219	JX009967	JX010443
C. queenslandicum	*Carica papaya*	Australia	JX010276	JX009934	JX010414
	Coffea sp.	Fiji	JX010185	JX010036	JX010412
C. salsolae	*Salsola tragus*	Hungary	JX010242	JX009916	JX010403
C. siamense	*Persea americana*	Australia	JX010250	JX009940	JX010387
	Coffea arabica	Thailand	JX010171	JX009924	JX010404
C. theobromicola	*Stylosanthes guianensis*	Australia	JX010291	JX009948	JX010381
	Theobroma cacao	Panama	JX010294	JX010006	JX010447
C. ti	*Cordyline australis*	New Zealand	JX010267	JX009910	JX010441
C. tropicale	*Litchi chinensis*	Japan	JX010275	JX010020	JX010396
	Theobroma cacao	Panama	JX010264	JX010007	JX010407
C. xanthorrhoeae	*Xanthorrhoea preissii*	Australia	JX010261	JX009927	JX010448

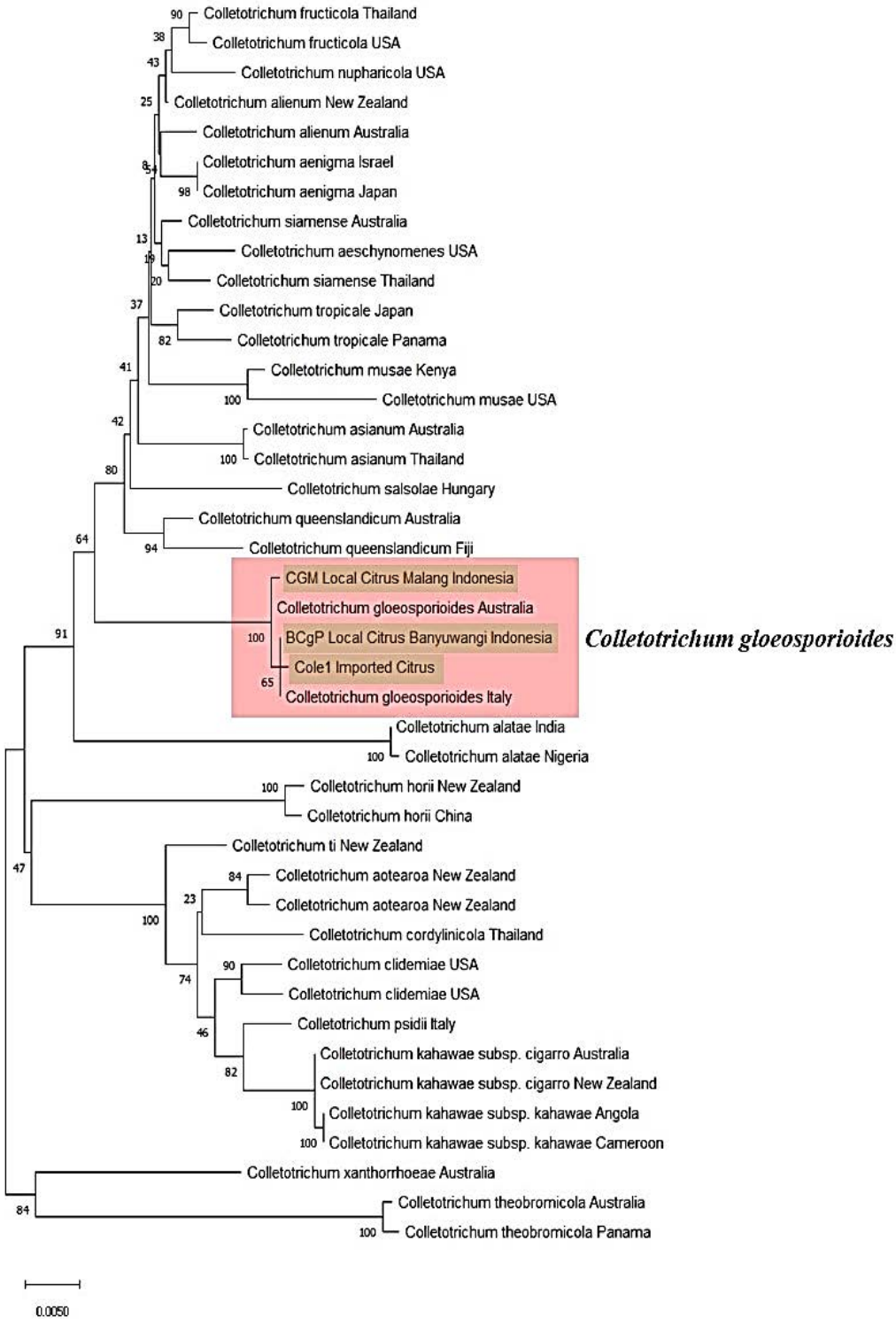

Figure 4. Phylogenetic tree of *C. gloeosporioides* strains using DNA multi locus (ITS, GAPDH, TUB2) from imported and local citrus fruits, and other countries.

Pathogenicity Test

The pathogenicity test showed that *C. gloeosporioides* from imported citrus fruits can cause anthracnose rot disease in imported and local healthy citrus fruits, either through the culture attachment method or the conidial suspension injection method. These results proved that *C. gloeosporioides* carried by imported citrus fruits was a fungal pathogen. *C. gloeosporioides* caused a disease incidence of 100% in imported (Table 7) and local citrus fruits (Table 8). This means that all the tested citrus fruits were rotten. However, the percentage of disease severity showed a different value between the culture attachment method and the conidial suspension injection method. The culture attachment method had a lower disease severity value compared to the conidial suspension injection method. Rot symptoms were seen in 0.25 part of the culture attachment method. Fig. 5 showed that the disease with rot symptoms occurred in almost all citrus fruits by the conidial suspension injection method. *C. gloesporioides* isolated from imported citrus fruits caused high disease severity in both imported and local citrus fruits of 97.78 ± 1.92 and 98.89 ± 1.92, respectively. In addition, *C. gloeosporioides* isolated from local citrus fruits caused a disease severity of 96.67 ± 3.33 (Table 8). Meanwhile, citrus fruits still looked healthy without rotting symptoms at 21 DAI in the control treatment using PDA media attachment without *C. gloeosporioides* and the sterile water injection method.

Table 7. Incidence and severity of anthracnose rot disease in imported citrus fruits

Treatment	Disease incidence (%)	Disease severity (%)
The attachment of blank PDA media without *C. gloeosporioides* (Control)	0 ± 0.00 a	0 ± 0.00 a
The attachment of *C. gloeosporioides* culture isolated from imported citrus fruits	100 ± 0.00 b	38.89 ± 3.85 b
The injection of sterile water without *C. gloeosporioides* (Control)	0 ± 0.00 a	0 ± 0.00 a
The injection of conidial suspension of *C. gloeosporioides* isolated from imported citrus fruits	100 ± 0.00 b	97.78 ± 1.92 c

Values are stated as mean ± SD. Mean values in the same column followed by different letters indicate a significant difference according to Tukey's test at $P < 0.05$.

Table 8. Incidence and severity of anthracnose rot disease in local citrus fruits

Treatment	Disease incidence (%)	Disease severity (%)
The injection of sterile water without *C. gloeosporioides* (Control)	0 ± 0.00 a	0 ± 0.00 a
The injection of conidial suspension of *C. gloeosporioides* isolated from imported citrus fruits	100 ± 0.00 b	98.89 ± 1.92 b
The injection of conidial suspension of *C. gloeosporioides* isolated from local citrus fruits	100 ± 0.00 b	96.67 ± 3.33 b

Values are stated as mean ± SD. Mean values in the same column followed by different letters indicate a significant difference according to Tukey's test at $P < 0.05$.

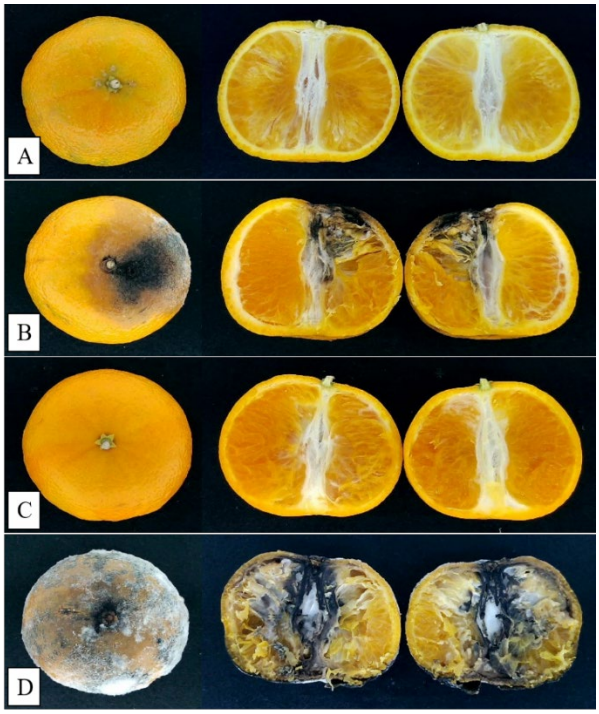

Figure 5. Severity of anthracnose rot disease in imported citrus fruits. A – Healthy citrus fruit in the control treatment of the attachment of blank PDA media without *C. gloeosporioides*; B – Citrus fruit with anthracnose rot disease in the treatment of the attachment of *C. gloeosporioides* culture isolated from imported citrus fruits; C – Healthy citrus fruit in the control treatment of the injection of sterile water without *C. gloeosporioides*; D – Citrus fruit with anthracnose rot disease in the treatment of the injection of conidial suspension of *C. gloeosporioides* isolated from imported citrus fruits.

Figure 6. Severity of anthracnose rot disease in local citrus fruits. A – Healthy citrus fruit in the control treatment of the injection of sterile water without *C. gloeosporioides*; B – Citrus fruit with anthracnose rot disease in the treatment of the injection of conidial suspension of *C. gloeosporioides* isolated from imported citrus fruits; C – Citrus fruit with anthracnose rot disease in the treatment of the injection of conidial suspension of *C. gloeosporioides* isolated from local citrus fruits.

Discussion

The ONFIT method was successful in detecting the presence of *C. gloeosporioides* by emerging mycelia on the surface of imported citrus fruits at 4 DAI (Fig. 1). The emergence of mycelia proved that *C. gloeosporioides* was already inside healthy citrus fruit when being imported from the country of origin into Indonesia. According to Michailides & Elmer (2000), *C. gloeosporioides* existed in citrus fruits since the plants

entered the flowering and fruiting phases in the field. The condition of the imported citrus fruits containing *C. gloeosporioides* still looked healthy and fresh without showing symptoms of anthracnose when being arrived at the port of Tanjung Priok, Jakarta. This was due to the status of *C. gloeosporioides* as a latent pathogen with inactive structures or as a non-pathogenic endophyte in citrus fruit tissues (Sinclair, 1991). *C. gloeosporioides* can actively infect when the structure of citrus fruit begins to weaken, either due to senescence or other physical processes (Paramasivan et al., 2009). Faisal et al. (2011) stated that the cause of *C. gloeosporioides* being in a latent position was due to the unripe citrus fruits during harvest and low-temperature storage during the transportation process. Mehrota (2001) explained that unripe fruit is difficult to be infected because the potentially important enzymes possessed by *C. gloeosporioides* are not sufficient to destroy the structural strength of the fruit. Prusky & Lichter (2007) added that unripe fruit cannot provide nutrients that can be directly absorbed by *C. gloeosporioides*. In addition, secondary metabolites in unripe fruit are toxic which can inhibit *C. gloeosporioides* infection.

The ONFIT method worked by destroying the physical and chemical structure of citrus fruits. Agrios (2005) mentions that physical structure is an important factor for plants that can act as a means of host defense against pathogen attack. The plant cell wall is one of the physical defenses. Pathogens generally must first penetrate the plant cell wall to be able to carry out the infection process. The ONFIT method can damage plant cell walls, making it easier for *C. gloeosporioides* to infect and grow on citrus fruits. Ginzberg & Stern (2016) reported the structure of the cell wall of citrus fruits is composed of epidermal and cuticle cells which make the fruit difficult to be infected by pathogens. However, the ONFIT method resulted in the death of epidermal and cuticle cells, making it easy for *C. gloeosporioides* to penetrate. In addition, the ONFIT method is thought to be able to break down the macromolecular structure of complex sugars into a micromolecular structure of simple sugars that can be absorbed directly by *C. gloeosporioides* as a source of nutrition.

Table 2 shows none of the *C gloeosporioides* mycelia growing on 100 citrus fruits in the control treatment. All citrus fruits still looked healthy, fresh, and orange in color (Fig. 1). Health and freshness indicate that citrus fruits are still actively carrying out metabolic processes even though they have been harvested. Brizzolara et al. (2020) explained that citrus fruits still carry out metabolic processes even though they have been separated from the plant. The ONFIT method can destroy fruit cells, so that metabolic processes are no longer produced. Cell death was indicated by a change in colour from orange to dark brown on the surface of the fruit (Fig. 1). Cells that have died are no longer able to carry out metabolism to produce toxic secondary metabolites. Therefore, *C. gloeosporioides* will become active and easily infect. The mycelia of *C. gloeosporioides* became clearly visible at 4 DAI (Fig. 1). However, the mycelial activation of *C. gloeosporioides* in citrus fruits is strongly suspected to have started before the 4th day. The emergence of mycelia also confirms that the ONFIT method only kills fruit tissue but does not kill *C. gloeosporioides* which infects latent in imported citrus fruits.

The technique of dilution and spreading of conidia on PDA media succeeded in obtaining pure cultures that grew from a single conidium. Choi et al. (1999) stated that the use of pure cultures derived from single spore isolation is the basis for the identification process of fungi. In addition, Goh & Hanlin (1997) also stated that fungal

cultures derived from single spores are important in identifying species through a phylogenetic concept approach based on morphological and molecular characters. Characterization of mycelia and conidia identified the species growing on the surface of imported citrus fruits as *C. gloeosporioides*. The characteristics of the conidia were imperfectly cylindrical in shape with two distinct ends. One end of the conidia had a slender or tapered end and the other end was broadly rounded (Fig. 2). Wang et al. (2021) also explained that the conidia of *C. gloeosporioides* were subcylindrical in shape with uneven sizes. The conidia of *C. gloeosporioides* varied in length and width. The conidia of *C. gloeosporioides* isolated from imported citrus fruits in Table 3 had an average length and width of 15.28 ± 2.08 µm × 4.59 ± 0.40 µm almost the same as the conidia of *C. gloeosporioides* from citrus fruits in Florida isolated by Agostini et al. (1992) with a size of 15.5 ± 0.5 µm × 4.5 ± 0.9 µm. In addition, the yellow conidiomata on PDA media were the same as the conidiomata of *C. gloeosporioides* from citrus fruit in Australia isolated by Wang et al. (2021). Several morphological character similarities that were found simultaneously identified that the fungus mycelia isolated from the surface of imported citrus fruits were indeed *C. gloeosporioides*.

DNA concentration, A260/A280 ratio and extraction time were different between both extraction methods (Table 4). Motkova & Vytrasova (2011) explained that the amount of concentration and purity of DNA is the main criterion in evaluating the quality of DNA. The total concentration of DNA produced by the method of Abd-Elsalam et al. (2003) was the highest compared to the method of Ausubel et al. (2003) (Table 3). According to Desloire et al. (2006), the difference in the chemical composition of the extraction buffer from each method was the main cause of the difference of the DNA concentration. In addition, Cermakova et al. (2021) explained that differences in chemical concentrations amount of extraction buffers also produced differences in DNA concentration. The PCR process succeeded in amplifying the target DNA in both extraction methods even though the concentrations were different. Sikdar et al. (2014) explained that the minimum limit for the concentration of fungal DNA used in the PCR process is 5 ng per PCR reaction. Therefore, both DNA extraction methods can be used in PCR reactions because having concentrations > 5 ng. DNA purity was analyzed from the value of the ratio A260/A280 (Motkova & Vytrasova, 2011). Each extraction method produced a different ratio of A260/A280. According to Sambrook et al. (1989), DNA purity was in the range of A260/A280 ratio between 1.8–2. An A260/A280 ratio below 1.8 indicated too much RNA and an A260/A280 ratio above 2 indicated too much protein contamination. Table 4 shows the method of Abd-Elsalam et al. (2003) had an A260/A280 ratio above 2. This means that the method produced quite a lot of protein contaminants. Meanwhile, Ausubel et al. (2003) produced a lot of RNA because it had an A260/A280 ratio below 1.8. Fig. 3 shows that differences in DNA concentrations affect the visualization of DNA bands produced on 1% agarose gel. DNA band in the extraction method Abd-Elsalam et al. (2003) was thicker compared to Ausubel et al. (2003). The intact DNA produced by both methods was of good quality which was characterized by visualization of a single amplicon of target DNA in each well of the agarose gel without any DNA fragments (smearing). Sambrook et al. (1989) explained that DNA bands that were clearly visible as a single band without DNA fragments (smearing) indicated DNA integrity. Lorenz (2012) explained that smears occur due to differences in the size of the DNA in the agarose gel.

BLAST results showed that *C. gloeosporioides* from imported citrus fruits had the highest DNA sequence similarity with *C. gloeosporioides* in all locus. This DNA similarity identified that *C. gloeosporioides* found in imported citrus fruits was *C. gloeosporioides*. Table 4 presents a list of the top five of GenBank isolates that have the highest DNA similarity with *C. gloeosporioides* isolated from imported citrus fruits. Most of the isolates are *C. gloeosporioides*. However, there are several other isolates in ITS locus identified as *C. siamense*, and *C. fructicola*. Referring to the report of Liu et al. (2013) that the other two identities are still in the *C. gloeosporioides* complex group. Thus, the two isolates will definitely have high DNA similarities with *C. gloeosporioides* because they are in the same group as *C. gloeosporioides* species complex.

The phylogenetic tree in Fig. 4 informs that *C. gloeosporioides* from imported citrus fruits places in the same clade with *C. gloeosporioides* from Italy and Banyuwangi, Indonesia. According to Hassan et al. (2002), the position of species within the same clades indicates the same species. *C. gloeosporioides* from imported citrus fruits is different position with *C. gloeosporioides* from Australia and Malang, Indonesia. Hossain et al. (2021) said species of fungi that are in different clades in the phylogenetic tree show genetic variation between fungal species. A genetic relationship that is different clades indicates differences in strains (Das et al., 2020). Thus, *C. gloeosporioides* carried in imported citrus fruits was the same strain with *C. gloeosporioides* from Italy and Banyuwangi, Indonesia. *C. gloeosporioides* carried in imported citrus fruits had an intraspecific variation with *C. gloeosporioides* from Australia and Malang, Indonesia.

C. gloeosporioides carried by imported citrus fruits was a pathogen. Agrios (2005) describes the pathogenic character based on the ability of the fungus to infect and cause the host to become sick. Table 7 informs that *C. gloeosporioides* was able to make 100% of the tested citrus fruits sick. Diseased citrus fruits were characterized by the appearance of black dry rot symptoms on the outside and inside of the citrus fruit (Fig. 5; Fig. 6). Symptoms are expressions of disease caused by the activity of a virulent pathogen (Ciofini et al., 2022). Pathogen virulence can be determined from the severity of the disease (Mojerlou & Safaie, 2012). This study recorded that *C. gloeosporioides* carried by imported citrus fruits was highly virulent on citrus fruits causing disease severity of up to 97.78% in the conidia suspension injection method. Meanwhile, the severity of the disease in the culture attachment method was 38.89%. The severity of the disease was high in the injection method because a large number of conidia were in sterile water in the fruit, so they could spread with the flow of the liquid into the intercellular spaces in the citrus fruit tissue. The movement of water helps in the process of spreading pathogens (Agrios, 2005). Disease severity in the culture attachment method was lower because the pathogen must move without the aid of water movement to a source of nutrition through the activity of mycelia growth and elongation in citrus fruits. *C. gloeosporioides* isolated from imported citrus fruits was also pathogenic to local citrus fruits. As a result, *C. gloeosporioides* could hazard local citrus fruit production (Fig. 6). Disease severity caused by *C. gloeosporioides* isolated from imported citrus fruits was higher than local strain. Therefore, *C. gloeosporioides* from imported citrus fruits was more virulent than the local. The pathogenicity test used a predetermined concentration of 10^5 conidia mL^{-1} to assess the virulence of *C. gloeosporioides* isolated from imported citrus fruits against imported and local citrus fruits. However, the concentration of conidia certainly varies in citrus fruit under in vivo conditions or in storage.

CONCLUSIONS

C. gloeosporioides has been found on imported citrus fruits. *C. gloeosporioides* sensu stricto was successfully detected using the overnight freezing incubation method and identified morphologically and molecularly. *C. gloeosporioides* from imported citrus fruits was the same strain with *C. gloeosporioides* from Banyuwangi, Indonesia, but it has a genetic variation with *C. gloeosporioides* from Malang, Indonesia. *C. gloeosporioides* from imported citrus fruits was pathogenic to imported and local citrus fruits with a disease incidence value of 100%, and a disease severity value of 97.78% and 98.89%, respectively.

ACKNOWLEDGEMENTS. The authors highly appreciate to the Agricultural Quarantine of Tanjung Priok, Jakarta for the samples of imported citrus fruits and the Indonesian Agency of Agricultural Extention and Human Resources Development (IAAEHRD), Ministry of Agriculture, Indonesia for funding this research.

REFERENCES

Abd-Elsalam, K.A., Aly, I.N., Abdel-Satar, M.A., Khalil, M.S. & Verreet, J.A. 2003. PCR identification of *Fusarium* genus based on nuclear ribosomal-DNA sequence data. *African Journal of Biotechnology* **2**, 82–85.

Agostini, J.P., Timmer, L.W. & Mitchell, D.J. 1992. Morphological and Pathological Characteristics of strains of *Colletotrichum gloeosporioides* from citrus. *Phytopathology* **82**, 1377–1382.

Agrios, G.N. 2005. Plant Pathology, 5th ed. California: Elsevier Academic Press.

Ausubel, F.M., Brent, R., Kingston, R.E., Moore, D.D., Seidman, J.G., Smith, J.A. & Struhl, K. 2003. Current protocols in molecular biology. *John Wiley & Sons*, Inc. 4648 p.

Brizzolara, S., Manganaris, G.A., Fotopoulos, V., Watkins, C.B. & Tonutti, P. 2020. Primary metabolism in fresh fruits during storage. *Front Plant Science* **11**, 1–17.

Cai, L, Hyde, K.D., Taylor, P.W.J., Weir, B.S., Waller, J., Abang, M.M., Zhang, J.Z., Yang, Y.L., Phoulivong, S., Liu, Z.Y., Prihastuti, H., Shivas, R.G., McKenzie, E.H.C. & Johnston, PR. 2009. A polyphasic approach for studying *Colletotrichum*. *Fungal Diversity* **39**, 183–204.

Camiletti, B.X., Lichternberg, P.S.F., Paredes, J.A., Carraro, T.A., Velascos, J. & Michailides, T.J. 2022. Characterization, pathogenicity, and fungicide sensitivity of *Alternaria* isolates associated with preharvest fruit drop in California citrus. *Fungal Biology* **126**, 277–289.

Cermakova, E., Zdenkova, K., Demnerova, K. & Ovesna, J. 2021. Comparison of methods to extract PCR-amplifiable DNA from fruit, herbal and black teas. *Czech Journal of Food Sciences* **39**, 410–417.

Choi, Y.W., Hyde, K.D. & Ho, W.H. 1999. Single spore isolation of fungi. *Fungal Diversity* **3**, 29–38.

Ciofini, A., Negrini, F., Baroncelli, R. & Baraldi, E. 2022. Management of post-harvest anthracnose: current approaches and future perspectives. *Plants* **11**, 1–20.

Cruz-Lagunas, B., Ortega-Acosta, S.A., Reyes-Garcia, G., Toribio-Jimenez, J., Juarez-Lopez, P., Guillen-Sanchez, D., Damian-Nava, A., Romero-Ramirez, Y. & Palemon-Alberto, F. 2020. *Colletotrichum gloeosporioides* causes anthracnose on grapefruit (*Citrus paradisi*) in Mexico. *Australasian Plant Disease Notes* **15**, 1–4.

Das, A., Roy, B., Jangra, S., Chowdhury, A., Kamil, D. & Devi, T.P. 2020. Analysis of genetic diversity of *Colletotrichum* population causing anthracnose in fruit crops using ISSR markers. *Indian Phytopathology* 1–15.

Dean, R., Van Kan, J.A.L., Pretorius, Z.A., Hammond-Kosack, K.E., Di Pietro, A., Spanu, P.D., Rudd, J.J., Dickman, M., Kahmann, R., Ellis, J. & Foster, G.D. 2012. The top 10 fungal pathogens in molecular plant pathology. *Molecular Plant Pathology* **13**, 414–430.

Desloire, S., Moro, C.V., Chauve, C. & Zenner, L. 2006. Comparison of four methods of extracting DNA from *D. gallinae* (Acari: Dermanyssidae). *Veterinary Research* **37**, 725–732.

Droby, S. & Wisniewski, M. 2018. The fruit microbiome: a new frontier for postharvest biocontrol and postharvest biology. *Postharvest Biologi and Technology* **140**, 107–112.

Faisal, P.M., Nagendran, K. & Ranjitham, P. 2011. Specific detection of *Colletotrichum musae* inciting anthracnose disease in Banana. *Libyan Agriculture Research Center Journal International* **2**, 279–286.

Gardes, M. & Bruns, T.D. 1993. ITS primers with enhanced specificity for basidiomycetes-application to the identification of mycorrhizae and rusts. *Molecular Ecology* **2**, 113–118.

Ginzberg, I. & Stern, R.A. 2016. Strengthening fruit-skin resistance to growth strain by application of plant growth regulators. *Scientia Horticulturae* **198**, 150–153.

Goh, T.K & Hanlin, R.T. 1997. Nuclear divisions in the ascus and ascospores of *Mefanospora zamiae. Mycological Research* **101**, 1511–1514.

Guerber, J.C., Liu, B., Correll, J.C. & Johnston, P.R. 2003. Characterization of diversity in *Colletotrichum acutatum sensu lato* by sequence analysis of two gene introns, Mtdna and Intron Rflps, and mating compatibility. *Mycologia* **95**, 872.

Hassan, O., Kim, J.S., Romain, B.B.N.D. & Chang, T. 2022. An account of *Colletotrichum* species associated with anthracnose of *Atractylodes ovata* in South Korea based on morphology and molecular data. *PLoS ONE* **17**, 1–24.

Hossain, M.I., Ahmad, K., Vadamalai, G., Siddiqui, Y,, Saad, N., Ahmed, O.H. & Hata, E.M. 2021. Phylogenetic analysis and genetic diversity of *Colletotrichum falcatum* isolates causing sugarcane red rot disease in Bangladesh. *Biology* **10**, 1–25.

Johnston, P.R., Pennycook, S.R. & Manning, M.A. 2005. Taxonomy of fruit-rotting fungal pathogens : What"s really out there ?. *New Zealand Plant Protection* **58**, 42–46.

Kasiamdari, R.S. & Sangadah, U. 2015. Identification of anthrachnose disease on strawberry fruit (*Fragraria vesca* L.) and its control by betel (*Piper betle* L.) leaf extract. *The 3rd International Conference on Biological Science* **2**, 458–465.

Khamsaw, P., Sangta, J., Chaiwan, P., Rachtanapun, P., Sirilun, S., Sringarm, K., Thanakkasaranee, S. & Sommano, S.R. 2022. Bio-circular perspective of citrus fruit loss caused by pathogens: occurrences, active ingredient recovery and applications. *Horticulturae* **8**, 1–21.

Lichtenberg, E. & Olson, L.J. 2018. The fruit and vegetable import pathway for potential invasive pest arrivals. *PLoS ONE* **13**, 1–16.

Liu, F., Damm, U., Cai, L. & Crous, P.W. 2013. Species of the *Colletotrichum gloeosporioides* complex associated with anthracnose diseases of *Proteaceae*. *Fungal Diversity* **61**, 89–105.

Lorenz, T.C. 2012. Polymerase Chain Reaction: basic protocol plus troubleshooting and optimization strategies. *Journal of Viss Expiration* **63**, 1–15.

Mehrota, R.S. 2001. Plant Pathology, 1st ed. New York: Tata Mc Graw Hill Publishing Company, pp. 572–584.

Michailides, T.J. & Elmer, P.A.G. 2000. *Botrytis* grey mold of kiwi fruit caused by *Botrytis cinerea* in the United States and New Zealand. *Plant Disease* **84**, 208–223.

Michailides, T.J., Morgan, D.P. & Luo, Y. 2010. Epidemiological assesments and postharvest disease incidence. In: Prusky D, Gullino mL, editor. Postharvest Pathology, Plant Pathology in the 21st Century. 2nd ed. California.

Moendeg, K.J., Angeles, J.M.M., Nakao, R., Leonardo, L.R., Fontanilla, I.K.C., Goto, Y., Kirinoki, M., Villacorte, E.A., Rivera, P.T., Inoue, N., Chigusa, Y. & Kawazu, S. 2017. Geographic strain differentiation of *Schistosoma japonicum* in the Philippines using microsatellite markers. *PLoS Negl Trop Dis* **11**, 1–14.

Mojerlou, S. & Safaie, N. 2012. Phylogenetic analysis of *Alternaria* species associated with citrus black rot in Iran. *Journal of Plant Pathology* **3**, 1–4.

Motkova, P. & Vytrasova, J. 2011. Comparison of methods for isolating fungal DNA. *Czech Journal of Food Science* **29**, 76–85.

Paramasivan, M., Mohan, S., Ali, G.S., Mathiyazhagan, S. & Muthukrishanan, N. 2009. Detection of latent infections in mango fruit with herbicides. *Archives of Phytopathology and Plant Protection* **42**, 318–326.

Patricia, L.C.C., Maria del Socorro, R.G., Ivan, R.H., Erika, D.C.A., Carolina, D.S., Keiko, S. & Alberto, N.Z.J. 2021. Occurrence and infective potential of *Colletotrichum gloeosporioides* isolates associated to *Citrus limon* var Eureka. *Biotechnology Reports* **31**, 1–12.

Perez-Mora, J.L, Mora-Romero, G.A., Beltran-Pena, H., Garcia-Leon, E., Lima, N.B., Camacho-Tapia, M. & Tovar-Pedraza, J.M. 2020. First report of *Colletotrichum siamense* and *C. gloeosporioides* causing anthracnose of *Citrus* spp. in Mexico. *Plant Disease* **105**, 1.

Prusky, D. & Lichter, A. 2007. Activation of quiescent infections by postharvestpathogens during transition from the biotrophic to the necrotrophic stage.*FEMS Microbiology Letters* **268**, 1–8.

Sacristan, S. & Garcia-Arenal, F. 2008. The evolution of virulence and pathogenicity in plant pathogen populations. *Molecular Plant Pathology* **9**, 369–384.

Sambrook, J., Fritsch, F. & Miniatis, T. 1989. Molecular Cloning Laboratory Manual, 3rd ed. New York: Cold Spring Harbor Laboratory Pr.

Schaad, N.W., Frederick, R.D., Shaw, J., Schneider, W.L., Hickson, R., Petrillo, M.D. & Luster, D.G. 2003. Advances in molecular based diagnostics in meeting crop biosecurity and phytosanitary issues. *Annual Review of Phytopathology* **41**, 305–324.

Shaw, M.W. & Osborne, T.M. 2011. Geographic distribution of plant pathogens in response to climate change. *Plant Pathology* **60**, 31–43.

Sikdar, P., Okubara, P., Mazzola, M. & Xiao, C.L. 2014. Development of PCR assays for diagnosis and detection of the pathogens *Phacidiopycnis washingtonensis* and *Sphaeropsis pyriputrescens* in apple fruit. *Plant Disease* **98**, 241–246.

Silva-Junior, G.J., Sposito, M.B., Marin, D.R. & Amorim, L. 2014. Efficacy and timing of application of fungicides for control of citrus postbloom fruit drop. *Crop Protection* **59**, 51–56.

Sinclair, J.B. 1991. Latent infection of soybean plants and seeds by fungi. *American Phytopathological Society* **75**, 220–224.

Suryaningsih, K.I., Sudana, I.M. & Suada, I.K. 2015. The control of anthracnose disease (*Colletotrichum gloeosporioides* Penz) on citrus fruits *(Citrus nobilis* var. *microcarpa)* by using clove and lemon grass essential oils. *E-Jurnal Agroekoteknologi Tropika* **4**, 16–24 (in Indonesian).

Wang, W., de Silva, D.D., Moslemi, A., Edwards, J., Ades, P.K., Crous, P.W. & Taylor, P.W.J. 2021. *Colletotrichum* species causing anthracnose of citrus in Australia. *Journal of Fungi* **7**, 1–24.

White, T.J., Bruns, T., Lee, S. & Taylor, J. 1990. Amplification and direct sequencing of fungal ribosomal RNA genes for phylogenetics. In: Innis MA, Gelfand, Sninsky JJ, White TJ, editor. PCR Protocols: A Guide to Methods and Application. London: Academic Press, 315–322.

Wiyanna, S., Rahmawati & Mukarlina. 2022. Morphological characteristics of *Aspergillus* and *Colletotrichum* from Siamese orange leaves (*Citrus nobilis* var. *microcarpa*) diseased in citrus plantations in Singkawang city. *Jurnal Mikologi Indonesia* **1**, 9–14 (in Indonesian).

Woudenberg, J.H.C., Aveskamp, M.M., de Gruyter, J., Spiers, A.G. & Crous, P.W. 2009. Multiple *Didymella* Teleomorphs are linked to the *Phoma clematidina* morphotype. *Persoonia Molecular Phylogeny Evolution of Fungi* **22**, 56–62.

Agronomy Research **21**(S3), 1519–1540, 2023
https://doi.org/10.15159/AR.23.099

Optimization of NPK levels of Clementine Sidi Aissa (*Citrus reticulata* Blanco) trees grafted on different citrus rootstocks

F.E. Omari[1], L. Beniken[1], A. Zouahri[2], R. Mrabet[3], H. Benaouda[1], R. Benkirane[4] and H. Benyahia[1]

[1]Regional Center of Agricultural Research of Kenitra, National Institute of Agricultural Research (INRA), N°14, Ave. Abou Temmam mailbox: 257 Kenitra, Morocco
[2]Regional Center of Agricultural Research of Rabat, National Institute of Agricultural Research (INRA), Ave. Mohamed Belarbi Alaoui mailbox: 6356 – Institutes, Rabat Morocco
[3]National Institute of Agricultural Research (INRA), Rabat- Morocco. Ave. Ennasr mailbox: 415 RP Rabat Morocco
[4]Plant Productions, Animal and Agro-Industry Laboratory, Ibn Tofail University, Faculty of Science of Kenitra, University Campus, mailbox 133 Kenitra, Morocoo
*Correspondence: fatimaezahra.omari@inra.ma

Received: August 15th, 2023; Accepted: October 18th, 2023; Published: November 5th, 2023

Abstract. The present study aims to investigate the impact of various nitrogen concentrations on young Clementine Sidi Aissa citrus trees (*Citrus reticulata* Blanco), grafted on five citrus rootstocks namely Moroccan Carrizo citrange, French Carrizo citrange, Troyer citrange, *Citrus macrophylla*, and sour orange *(Citrus aurantium* L.). The experiment took place in greenhouses at the Experimental station of El Menzeh INRA-Morocco, with the young trees grown in containers. We applied five different nitrogen treatments (expressed as mg L^{-1} of N-P_2O_5-K_2O): (0–0–0), (0–25–50), (25–25–50), (50–25–50), and (100–25–50). The split-plot experimental design was used with three replications.

The findings demonstrate that the nitrogen enrichment resulted in enhanced plant growth, marked by increased plant height, rootstock and scion stem diameters, diameter and shoot length, relative water content (RWC), as well as leaf chlorophyll and proline content. Optimal growth of the Clementine Sidi Aissa trees was observed under the 100–25–50 (mg L^{-1} of N-P_2O_5-K_2O) treatment.

The study also found that leaf nitrogen concentration increased in line with the quantity of nitrogen added, whereas the percentages of phosphorous and potassium in the leaves decreased. The most significant growth increase across the majority of the studied parameters was noted in Clementine Sidi Aissa trees grafted on Moroccan Carrizo citrange and Troyer citrange rootstocks.

Key words: citrus, rootstock, mineral nutrition, leaf nutrient, vegetative growth.

INTRODUCTION

Agricultural methods employed in the cultivation of citrus have undergone significant transformations over time. The focus has increasingly shifted towards enhancing the yield and quality of fruit using several strategies including the adoption of improved rootstocks, grafting techniques, and nutrient management (Alva et al., 2006a, 2006b, 2006c; Hawkesford et al., 2012). In citrus farming, the overall performance is largely dependent on the combination of rootstock and scion, which form the root and aerial parts of the plant, respectively. The rootstock exerts an influence on the scion's growth, impacting parameters such as photosynthesis (González-Mas et al., 2009), flowering, fruit quality (internal and external), canopy size, yield, and resistance to various factors (Forner-Giner et al., 2003; Castle et al., 2009; Kucukyumuk & Erdal, 2011; Parameshwar et al., 2018). It also affects an effective interaction between the rootstock and scion which is critical for the efficient translocation of water and minerals, promoting biomass production and resilience against biotic and abiotic stress, such as nutrient deficiency (Martínez-Ballesta et al., 2010; Schwarz et al., 2010).

Parameshwar et al. (2018) highlighted that the choice of rootstock significantly influences citrus growth, development, and crop yield. Different citrus rootstocks exhibit varying degrees of compatibility with different soil types, root dispersion patterns, and interactions with mycorrhizal fungi. Consequently, this variability leads to differences in content of the mineral elements in leaves of budded cultivars, ultimately impacting vegetative growth, fruit yield and quality. Within a budded tree, the type of rootstock also exerts an influence on various scion characteristics, including plant height, spread, and overall volume.

Enhanced vigor in citrus rootstocks' root systems leads to improved uptake of soil nutrients and water (Taylor & Dimsey, 1993; Lu et al., 2019). Thus, rootstocks influence on the photosynthetic capacity of the scion can play a crucial role in the overall performance of citrus plants, including vigor, crop load, and fruit characteristics (Jover, 2012). The type of rootstock used in a grafted tree significantly influences numerous features including leaf mineral components (Mattos Jr. et al., 2003; Toplu et al., 2008). Rootstocks play a vital role in the plant's capacity to absorb water and nutrients from the soil. Nutrient concentrations in grafted varieties can show variation even when cultivated under the same conditions. Therefore, understanding the influence of rootstocks on plant nutrient levels is essential for optimizing citrus fertilization programs.

Citrus cultivation today relies on composite trees that combine a rootstock and a scion. The scion draws water and mineral nutrients from the rootstock, which in turn relies on the scion for photosynthetic assimilation (Kocsis et al., 2012). Scions are selected based on fruit production-related criteria, such as size, yield, and quality parameters in grafted plants (Davis et al., 2008). Rootstocks are chosen for their disease and pest resistance, adaptability to pedoclimatic conditions, and agronomic performance when combined with the grafted variety. Iqbal et al. (1999) reported that the rootstock selection has a noteworthy impact on the mineral components found in the leaves of the kinnow mandarin grafted variety. Pestana et al. (2005) observed a significant variation in iron absorption based on the type of citrus rootstock.

Among various factors that impact citrus growth, including environmental conditions, management practices, and genetics, nutrient management, particularly nitrogen (N), is crucial for optimizing citrus production (Huang et al., 2021). Fertilization, particularly with Macronutrients encompassing elements of NPK, which plants necessitate in abundant amounts, serves as a significant procedural function for plant development and is essential for enhancing the fruit yield and quality (Hawkesford et al., 2012). The mineral status of citrus leaves markedly affects tree growth, fruit yield, and quality (Esteves et al., 2021). A balanced NPK amount plays a crucial role in tree structure and metabolic processes (Sinha & Tandon, 2020).

Nitrogen is vital for plant growth and development, involved in several physiological processes (Marschner, 2012; Sarvade et al., 2014). It plays a significant role in citrus trees' growth, canopy, fruit production, and quality, having a greater impact compared to other elements (Zekri & Obreza, 2003a, 2003b; Obreza et al., 2008). In cotton, Karydogianni et al. (2020) have shown that the combination of Urea, Nitrification Inhibitor (NI) and Urease Inhibitor (UI) led to the highest seed cotton yield and have a positively influenced the overall nitrogen uptake of the plant and notably enhanced the quality of the fiber.

Previous research has thoroughly examined diverse factors affecting the development of citrus fruits, encompassing environmental conditions, cultivation techniques, and genetic aspect (Davies & Albrigo, 1994). It has been shown that in young trees, nitrogen level could improve vegetative growth while reducing floral induction (Menino et al., 2003). Overabundance of nitrogen can promote excessive tree growth (Schumann et al., 2003; Alva et al., 2005a, 2005b), leading to the risk of groundwater contamination due to nitrate leaching from excess irrigation (Alva et al., 1998; He et al., 2000; Alva et al., 2006a, 2006b, 2008).

Nitrogen requirements for citrus have been found to vary widely, depending on factors such as tree age, rootstock, graft variety, and environmental conditions (Marschner, 2012; Mesquita et al., 2016; Carranca et al., 2018, Omari et al., 2020a). However, the optimal nutritional management of citrus seedlings have not yet fully understood, and there is a lack of recommendations on application of fertilizers in nursery conditions.

Most research on nitrogen management in citrus has focused on trees grown in fields (Nguyen & Tai, 2020; Omari et al., 2020b; Wassel et al., 2022); but studies on the production of citrus seedling under greenhouses conditions (nurseries) remain insufficient. It is imperative to understand the specific nutrient requirement of young citrus seedlings under such controlled environmental conditions.

Despite the agricultural importance of Clementine Sidi Aissa, research addressing the specific NPK requirements for trees grafted onto various citrus rootstocks remains notably scarce. While existing studies have focused on the general nutritional requirements of citrus trees, they often overlook to study the interaction scion/rootstock that arise from grafting scion on varying rootstocks. Indeed, prior studies have explored the impact of various rootstocks on citrus growth and nutrient uptake (Rameeh et al., 2019), but very few have aimed to identify the most suitable NPK doses for specific graft combinations. However, information regarding the optimal nutritional management of

young citrus trees is lacking, leading to an inadequacy of precise fertilizer recommendations for nursery conditions. Consequently, the existing gap in knowledge significantly impedes the efforts to develop precise fertilization approaches aimed at optimizing the growth, yield, and fruit quality of citrus crop.

In light of the aforementioned research gap, this study hypothesizes that the optimization of NPK levels for Clementine Sidi Aissa plants will exhibit significant variations depending on the type of citrus rootstock employed. We propose that adopting a sustainable nutrient management strategy to meet crop needs throughout a growing season, considering the interactions between the scion and rootstock will result in superior vegetative growth, increased fruit yield, and elevated fruit quality compared to conventional fertilization methods.

This study aims to address this gap by investigating the effects of different nitrogen doses on the vegetative growth and nutritional status of young citrus trees grafted on selected rootstocks in greenhouse conditions. The objective is to determine the optimal nitrogen doses that result in optimal plant growth and adequate foliar nutrient concentrations. This will help in determining the most appropriate NPK doses for each grafting combination for young Clementine Sidi Aissa seedlings. Such information can assist citrus farmers in fine-tuning their nutrient management strategies to suit specific grafting combinations and achieve optimal growth and yield results.

MATERIAL AND METHODS

Plant material and growth conditions

The experiment was conducted in a greenhouse at the Experimental station El Menzeh (CRRA-Kenitra, INRA-Morocco), located 10 km north of Kenitra at an altitude of 25m and at a latitude of 34°64N.

The study was carried out on 3-year-old seedlings of the clementine variety Sidi Aissa grafted on five citrus rootstocks: Carrizo citrange B2 28608 (French), Troyer citrange B2 31655, *Citrus macrophylla*, Carrizo citrange (Morocco) and Sour orange (*Citrus aurantium* L.). The studied rootstocks come from the collection of germplasm and from the citrus seed park of the El Menzeh experimental station of the National Institute of Agricultural Research (INRA) of Kenitra in Morocco. These rootstocks were chosen for their importance in new citrus plantations and the Sidi Aissa variety was used as a reference for small fruits.

These grafted plants were grown in 10L plastic containers containing a substrate composed of a mixture of peat and sand at 1:2 ratio. This substrate have a pH of 7.09 and containing 2.25% organic matter, 267.57 mg of P_2O_5 kg^{-1} and 268.11 mg of $K_2O kg^{-1}$.

The doses of fertilizer elements are provided from the nutrient solution (Maust & Williamson, 1994) which contains (in mg L^{-1}) (120 of Ca ($CaSO_4.2H_2O$); 40 Mg of ($MgSO_4.7H_2O$); 0.5 Mn ($MnCl_2.4H_2O$); 0.02 Mo ($NaMoO_4.2H_2O$); 0.02 Cu ($CuSO_4.5H_2O$); 0.05 Zn of ($ZnSO_4.7H_2O$); 0.5 B of (BO_3) and 5 Fe of (NaFeEDTA)). The source products used for NPK fertilizing elements are NH_4NO_3 for nitrogen, H_3PO_4 for phosphorus and K_2SO_4 for potassium. Five treatments of NPK fertilization, measured in milligrams per liter of Nitrogen-Phosphorus-Potassium (N-P_2O_5-K_2O), were evaluated: Treatment 0 (T_0) with 0–0–0, Treatment 1 (T_1) with 0–25–50, Treatment 2 (T_2) with 25–25–50, Treatment 3 (T_3) with 50–25–50, and Treatment 4 (T_4) with 100–25–50.

The plants were irrigated twice a week with the nutrient solution at the rate of 500 mL per containers throughout the study period.

The experiment was carried out using a split-plot design with three blocs replications, including the dose of NPK fertilizing elements as the main plot and the rootstock the subplot. Factor 1 (the main plot): N-P_2O_5-K_2O doses at five levels (T_0, T_1, T_2, T_3 and T_4). Factor 2 (the subplot): Five-level of rootstock (*Citrus macrophylla*, Carrizo citrange (Morocco), Troyer citrange B2 31655, Carrizo citrange B2 28608 (French), Sour orange (*Citrus aurantium* L.).

Measured parameters

Morphological parameters

Plant Height was periodically measured with a measuring tape graduated in 1mm precision. The measurement were taken from the base of the stem to the shoot apical. Rootstock stem diameter at 5 cm below the grafting point and diameter of scion stem at 5 cm above the grafting point were measured by a digital caliper at 0.001 mm precision. Diameter and length of the four shoots (young shoots) marked per containers were measured using a caliper to 0.001 mm precision and a tape measure graduated to 1 mm accuracy at every 15 days throughout the trial period. Number of leaves of the four marked shoots per containers was counted biweekly throughout the trial period.

Physiological parameters

The relative water content (RWC %): One leaf per rootstock and per treatment was cut with petiole and weighed immediately to determine the fresh weight (P_f). These leaves are put in test tubes filled with distilled water (submerged petiole), the tubes are placed in the dark for 24 hours, then weighed again to obtain the weight at saturation (Psat). Then, the samples are put in an oven for 24 hours at 80°C, the dry weight (Psec) is thus obtained. The relative water content is calculated according to the following formula (1):

$$RWC\ (\%) = 100*(P_f - P_{sec}) / (P_{sat} - P_{sec}) \quad (1)$$

Biochemical parameters

Concentration of total chlorophyll in the leaves: To determine the concentration leaf in chlorophyll, we used the method of Arnon (1949) described by Esposti et al. (2003). Thus, the chlorophyll content is calculated using the following Eq. 2:

$$Ch\ total\ (mg\ L^{-1}) = 8.02\ (D.O_{663}) + 20.20\ (D.O_{645}) \quad (2)$$

Proline content: Proline determination was performed following the method described by Bates et al. (1973) based on the reaction of proline with ninhydrin. The values obtained are converted into proline content (mg g^{-1} MF) from a standard curve, the relation of which is as follows (3):

$$Y = 0.1043*X \quad (3)$$

With: Y – represents the absorbance; X – represents the sodium concentration (mg g^{-1} MF).

Content of the mineral elements in leaves: Once collected, the leaves are washed with distilled water, dried in an oven at a temperature of 60 to 65 °C for 3 days and then ground using a grinder. The shredded leaves thus obtained were analyzed at the soil chemical and physical analysis Laboratory of the Research Unit on the Environment and the Conservation of Natural Resources (INRA-Rabat). The mineral analyzes focused on N, P, K mineral elements.

Statistical analysis

Values are presented as mean ± SE (standard error). Data were subjected to analysis of variance (ANOVA) using the GLM procedure SAS statistical software (SAS Institute Inc., NC, USA, version 9). Two classification factors were used, the nitrogen dose factor and the rootstock factor. We utilized Duncan's multiple-range test to compare the differences in averages between treatments and rootstocks, with a significance level set at $P \leq 0.05$.

RESULTS AND DISCUSSION

Effect of NPK nutrient doses and rootstocks on citrus plant growth

Statistical evaluation demonstrated a very highly significant effect of fertilizer treatment on plants height of the Sidi Aissa variety ($P < 0.0001$). The highest average height of the plants is recorded under T_3 (50–25–50) mg L^{-1} with an average value of 109.73cm, on the other hand the lowest value was observed under control with an average value of 80.03cm (Fig. 1).

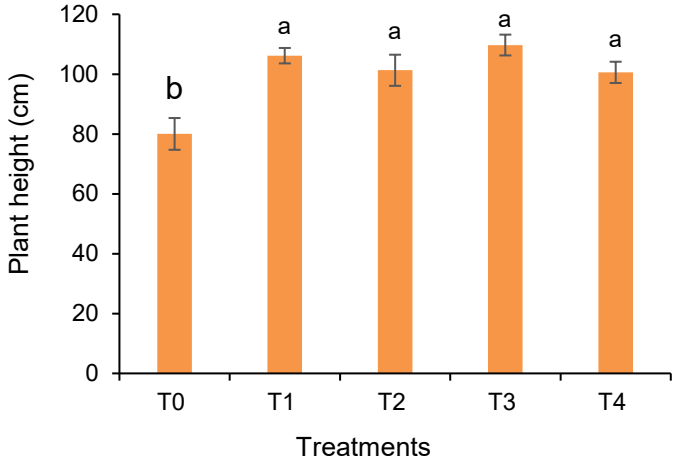

Figure 1. Effect of NPK doses of fertilizer elements on plant height of Sidi Aissa variety.
[*Values with the same letter are not significantly different (Duncan test, $p \leq 0.05$). Error bars represent standard errors of the mean (±SE)].

Statistical analysis revealed a significant impact of NPK doses ($P = 0.0105$) and rootstock ($P = 0.0002$) on the rootstock stem diameter of Sidi Aissa trees. The highest rootstock stem diameter was noted in the plants under T_4 (100N- 25P_2O_5- 50K_2O) mg L^{-1}

(18, 12 mm) (Fig. 2). The highest rootstock stem diameter is observed in Troyer citrange B2 31655 (18.83 mm), while the lowest value is recorded in sour orange (*Citrus aurantium L.*) (16.77 mm) (Fig. 2).

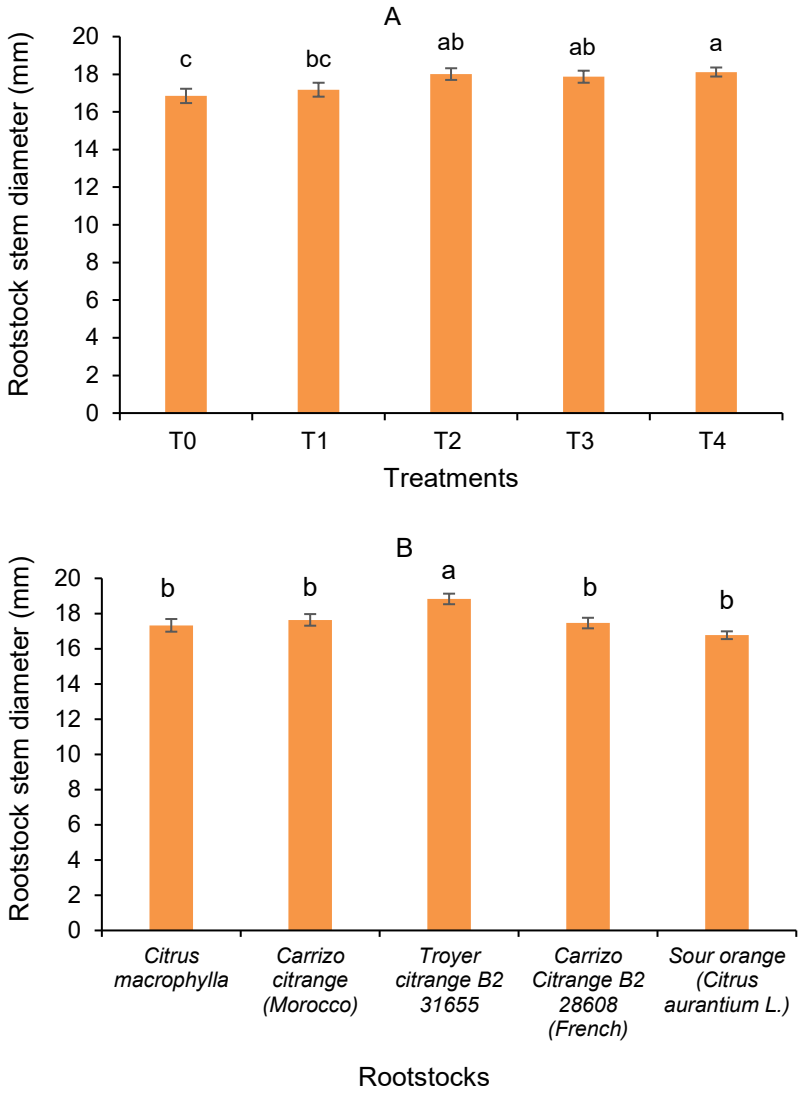

Figure 2. Effect of NPK doses (A) and citrus rootstocks (B) on rootstock stem diameter of Sidi Aissa variety.

[*Values with the same letter are not significantly different (Duncan test, $p \leq 0.05$). Error bars represent standard errors of the mean (±SE)].

Statistical analysis revealed a significant impact of the rootstock on the scion stem diameter ($P = 0.0239$) of Sidi Aissa trees. The largest main scion stem diameter was observed in the rootstocks *Citrus macrophylla* (13.88 mm) and Troyer citrange B2 31655 (13.60 mm) (Fig. 3).

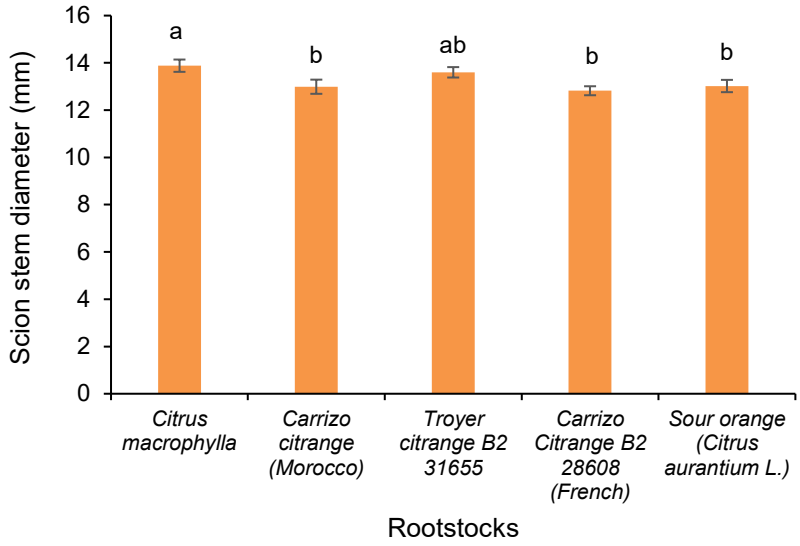

Figure 3. Effect of citrus rootstocks on scion stem diameter of Sidi Aissa.

[*Values with the same letter are not significantly different (Duncan test, $p \leq 0.05$). Error bars represent standard errors of the mean (±SE)].

Statistical analysis revealed a significant impact of fertilizer treatments ($P = 0.0048$) and rootstock ($P < 0.0001$) on shoot diameter. The highest shoot diameter is noted in plants at T_4 (100N-25P_2O_5-50K_2O) (2.26 mm) (Fig. 4). The highest average shoot diameter was observed in sour orange (*Citrus aurantium* L.) and Carrizo citrange (Morocco) (2.27 mm) (Fig. 4).

A significant impact of NPK doses ($P < 0.0001$) and the rootstock ($P < 0.0001$) was showed on an average length of the young shoot, and a significant effect of the interaction fertilizer Treatments x Rootstock ($P = 0.0109$). Carrizo citrange (Morocco) showed the highest average length of the young shoot of Sidi Aissa (17.00 cm) in T_4 (100N- 25P_2O_5- 50K_2O), while the lowest value was noted in Carrizo citrange B2 28608 (French) (7.39 cm) under T_0 (Table 1).

Table 1. Effect of NPK doses and rootstocks on the average length of young shoot (cm) of clementine Sidi Aissa

Rootstocks	Treatments N-P_2O_5-K_2O (mg L^{-1})				
	T0	T1	T_2	T_3	T_4
Citrus macrophylla	8.82 ± 1.19b*	9.54 ± 0.57b	9.93 ± 0.74b	10.17 ± 0.99b	14.17 ± 1.96a
Carrizo Citrange (Morocco)	10.11 ± 0.76b	9.25 ± 0.66 b	11.08 ± 0.83b	13.69 ± 0.92a	17.00 ± 1.46a
Troyer Citrange B2 31655	8.56 ± 0.73b	11.73 ± 0.65a	10.63 ± 0.68b	10.00 ± 1.08b	14.25 ± 1.05a
Carrizo Citrange B2 28608 (French)	7.39 ± 0.58b	10.92 ± 0.67ab	10.54 ± 1.00b	12.54 ± 0.96a	13.75 ± 1.51a
Sour orange (*Citrus aurantium* L.)	13.26 ± 1.22a	11.57 ± 0.69a	15.71 ± 1.19a	14.29 ± 0.83a	16.79 ± 1.12a

[*The means of the same column assigned by the same letter do not differ significantly at the 5% level according to Duncan's test. Each value is the mean ±Standard Error].

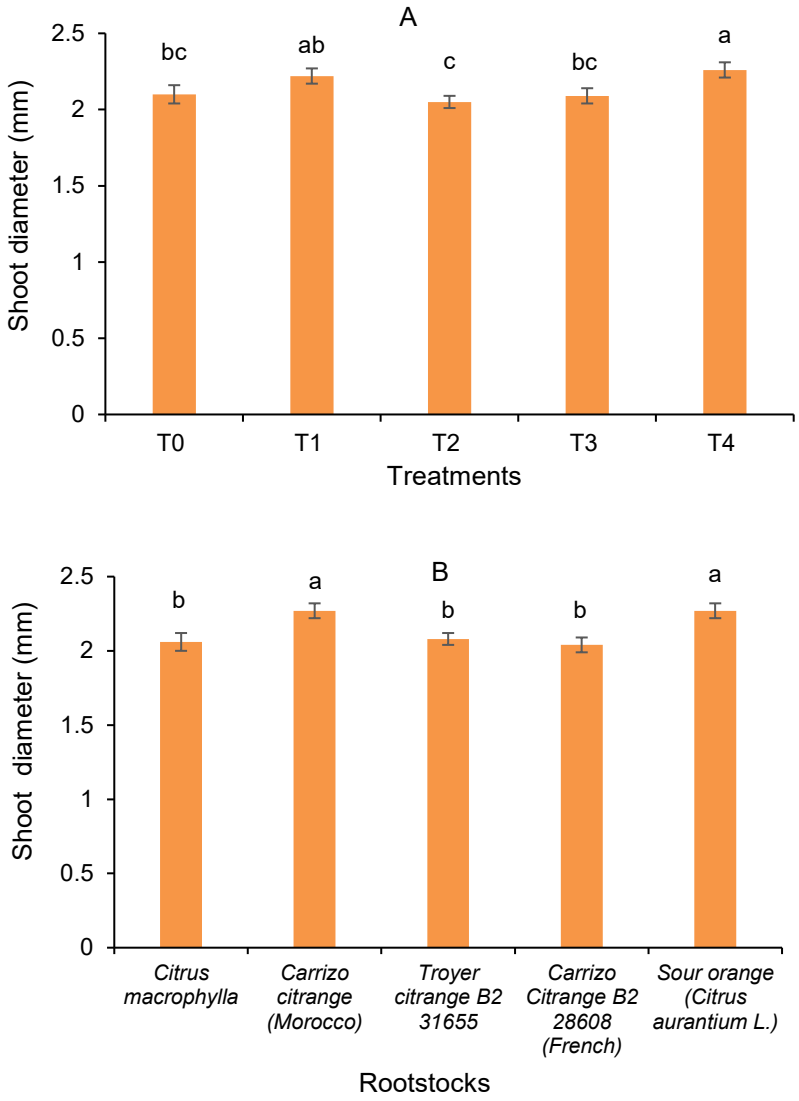

Figure 4. Effect of NPK doses (A) and citrus rootstocks (B) on young shoot diameter of Sidi Aissa variety.

[*Values with the same letter are not significantly different (Duncan test, $p \leq 0.05$). Error bars represent standard errors of the mean (±SE)].

A significant impact of the fertilizer treatments ($P < 0.0001$), the rootstock ($P = 0.0061$) and the interaction Fertilizer Treatments x Rootstocks ($P = 0.0051$) was shown on the average number of leaves per young shoot of Sidi Aissa variety. Under T_4 ($100N\text{-}25P_2O_5\text{-}50K_2O$) the highest average number of leaves per young shoot was recorded for Carrizo citrange B2 28608 (French) and Sour orange (*Citrus aurantium* L.) which is 20 leaves, whereas the lowest value was noted in the Troyer citrange B2 31655 (6 leaves) under the control treatment T_0 (Table 2).

Table 2. Effect of NPK doses and rootstocks on the average number of leaves per young shoot of plants of Sidi Aissa clementine

Rootstocks	Treatments N-P_2O_5-K_2O (mg L^{-1})				
	T_0	T_1	T_2	T_3	T_4
Citrus macrophylla	9 ± 1.58ab*	8 ± 0.87a	11 ± 1.33a	8 ± 0.78b	13 ± 2.07b
Carrizo Citrange (Morocco)	11 ± 1.38a	10 ± 1.41a	9 ± 1.50ab	9 ± 0.98ab	13 ± 1.31b
Troyer Citrange B2 31655	6 ± 0.57b	9 ± 1.15a	8 ± 1.06b	9 ± 1.17ab	15 ± 1.67ab
Carrizo Citrange B2 28608 (France)	8 ± 1.05ab	10 ± 0.94a	10 ± 1.18ab	9 ± 0.86ab	20 ± 1.85a
Bigaradier (*Citrus aurantium* L.)	12 ± 2.25a	9 ± 0.94a	9 ± 0.87ab	11 ± 1.17a	20 ± 2.29a

[*The means of the same column assigned by the same letter do not differ significantly at the 5% level according to Duncan's test. Each value is the mean ±Standard Error].

NPK doses has a significant impact on plants height of Sidi Aissa variety. Omari et al. (2012) showed that the nitrogen dose significantly affects the height growth of citrus rootstock plants. The height of the plant increases with the increase in dose of nitrogen applied from 0 to 5 mM. The highest values were noted in the plants having received the dose 5mM of nitrogen (*Citrus macrophylla* with 30.68 cm, *Citrus volkameriana* B2 28613 with 29.58 cm and Citrumelo 4475 AB6 A4 with 28.79 cm). Ouma (2006) demonstrated that the nitrogen dose has a highly significant effect on the height growth of citrus plants (Rough lemon). Thus, this author showed that citrus plants responded positively to increasing nitrogen doses. The height of the stem increased from 44 to 65cm by increasing the dose of nitrogen from 6 to 24g. The positive effect of nitrogen on growth parameters has also been reported in orange plants under nursery conditions (Maust & Williamson, 1994; Guazzelli et al., 1996; De Campos Bernardi et al., 2000). Kakabouk et al. (2020) have been reported that varying Nitrogen treatments significantly influenced the root density, surface area, and volume of camelina plants, and the highest impact was seen at 100 days post-treatment with 90 ppm Nitrogen, affecting plant leaf area, growth, yield, and 1,000 seed weight. Al-Jilihawi & Merza (2020) reported that treating lemon saplings with mineral NPK at a concentration of 2.0 g L^{-1} significantly boosted stem diameter, total leaf area, shoot and root dry weight.

The highest rootstock stem diameter of the plant was noted under T_4 (100N-$25P_2O_5$- $50K_2O$) mg L^{-1} in Troyer citrange B2 31655. The largest main scion stem diameter of the variety was observed in *Citrus macrophylla* and Troyer citrange B2 31655. This result agrees with what was found in the work of Esposti et al. (2003) conducted on seedlings of two citrus varieties grafted onto different rootstocks, which reported that increasing the nitrogen dose significantly affected growth (expressed in stem height, collar diameter, leaf, stem and root dry biomass, number of leaves per plant and leaf area) and leaf chlorophyll content.

The highest shoot diameter is noted in plants at T_4 (100N-$25P_2O_5$-$50K_2O$) in sour orange (*Citrus aurantium* L.) and Carrizo citrange (Morocco). Carrizo citrange (Morocco) showed the highest average length of the young shoot of Sidi Aissa in T_4 (100N- $25P_2O_5$- $50K_2O$). Our results are in line with Lu et al. (2004) who showed that young shoot length of citrus seedlings decreased by 21.3% in the absence of nitrogen in the nutrient solution and that by just 0–6.1% when the seedlings were been treated without the application of potassium and phosphorus, respectively. On the other hand,

these researchers reported that the growth of citrus plants increases accordingly with rising N dose. Also, Maust & Williamson (1991) showed that Nitrogen dose applied to citrus plants in the nursery has a highly significant effect on shoot length. The shoot length of 'Hamline' variety grafted on two rootstocks (Cleopatra mandarin and Carrizo citrange) responded significantly to the increase in the nitrogen dose. The maximum shoot length recorded on Cleopatra mandarin and Carrizo citrange rootstock (96.30 cm and 78.46 cm, respectively) under 100 ppm and 50 ppm, respectively. Alkhafaji & Khalil (2019) reported that lemon trees grafted on *Citrus aurantium* L. exhibited greater plant height, whereas trees grafted on *Citrus volkameriana* demonstrated higher rates in rootstock, scion diameter, and shoot number.

A significant effect of fertilizer treatments and rootstock on the average number of leaves per young shoot of Sidi Aissa variety has demonstrated. Our results are in agreement with those reported by Ouma (2006) who showed that the dose of nitrogen has a highly significant effect on the growth of citrus plants (Rough lemon) and the number of leaves per plant increased from 155 to 167 from 6 to 24 g of N/container.

Shaban & Mohsen (2009) revealed that the rootstock has a highly significant effect on the number of leaves per plant, growth (stem height), leaf area, root length, fresh and dry biomass, chlorophyll content and NPK leaf concentration. Thus, the maximum values of these parameters were observed in *Citrus volkameriana* compared to Sour orange which they recorded the minimum values for these parameters.

Chaudhry & Naveed (1992) studied the effect of rate of nitrogen application and their application date on leaf formation and yield of sweet lemon (*Citrus limettioides*). The nitrogen dose has a highly significant effect on number of leaves per shoot. Increasing the dose of nitrogen from 0.5 to 1.5 kg of N tree^{-1} significantly improved the number of leaves per shoot from 8.2 to 10.

Another experiment conducted by Hafez (2006) highlighted the effect of different rootstocks on growth parameters in citrus. Thus, he compared the vegetative parameters of six citrus rootstocks. Troyer citrange has the highest stem height (31.1cm) and the lowest is observed in *Citrus volkameriana* (13.2cm). Lime rangpur had the highest number of leaves per plant (45.4), while *Citrus volkameriana* and Sour orange had the lowest number of leaves (14.8). The maximum leaf area is recorded in Troyer citrange (8.2 cm²) and the lowest is observed in Sour orange and *Citrus volkameriana* (4.6 cm²).

Effect of NPK doses and rootstocks on Relative Water Content (RWC), total chlorophyll concentration and total proline content in the leaves

Statistical analysis revealed a significant impact of the fertilizer treatments ($P = 0.0183$) on Relative Water Content of Sidi Aissa clementine leaves. The highest Relative Water Content value was recorded in the plants treated with T_4 (100N-25P_2O_5-50K_2O) treatment with a percentage of 86.07%. On the other hand, the lowest value was noted in the control T_0 with a percentage of (66.27%) (Fig. 5).

Statistical analysis revealed a significant impact of fertilizer treatments on leaf chlorophyll content ($P < 0.0001$). The Sidi Aissa clementine plants treated with T_4 (100N-25P_2O_5-50K_2O) represent the highest value of the total chlorophyll content (14.70 mg L^{-1}). Whereas, the lowest value (6.57 mg L^{-1}) was observed under control (Fig. 6).

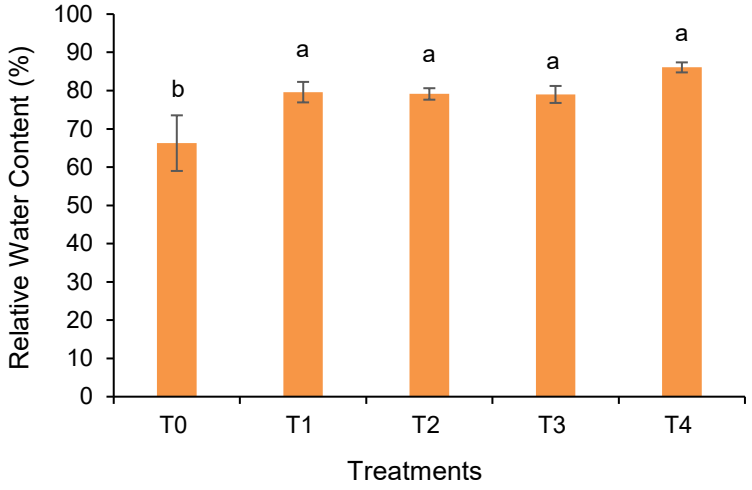

Figure 5. Effect of NPK doses on average Relative Water Content (RWC) of Sidi Aissa variety. [*Values with the same letter are not significantly different (Duncan test, $p \leq 0.05$). Error bars represent standard errors of the mean (±SE)].

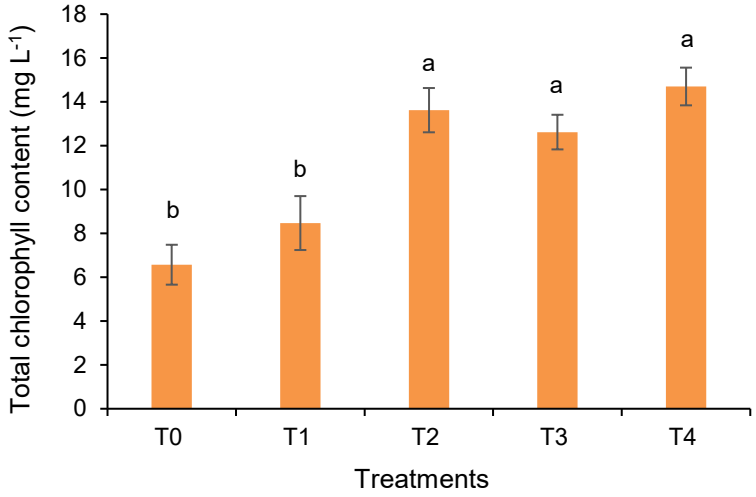

Figure 6. Effect of NPK doses on leaf total chlorophyll concentration of Sidi Aissa variety. [*Values with the same letter are not significantly different (Duncan test, $p \leq 0.05$). Error bars represent standard errors of the mean (±SE)].

A significant effect of the fertilizer treatments ($P < 0.0001$), the rootstock ($P < 0.0001$) and the interaction of fertilizer doses x Rootstock ($P < 0.0001$) on the leaf content in proline. The highest proline content was recorded in *Citrus macrophylla* (0.10 mg L^{-1}) under the T_3 (50 N-25P_2O_5-50K_2O), while the lowest value was noted in Troyer citrange B2 31655 (0 mg L^{-1}) under the control T_0 (Table 3).

Table 3. Effect of NPK doses and rootstocks on the total proline content (mg g^{-1}) in the leaves of Sidi Aissa plants

Rootstocks	Treatments N-P_2O_5-K_2O (mg L^{-1})				
	T_0	T_1	T_2	T_3	T_4
Citrus macrophylla	0.02 a*	0.02 a	0.04 a	0.10 a	0.07 b
Carrizo citrange (Morocco)	0.01 bc	0.02 a	0.05 a	0.04 c	0.06 b
Troyer citrange B231655	0.00 c	0.03 a	0.04 b	0.05 b	0.07 b
Carrizo citrange B2 28608 (French)	0.01 b	0.02 a	0.03 d	0.05 b	0.04 c
Sour orange (*Citrus aurantium* L.)	0.01 b	0.01 a	0.04 c	0.04 c	0.07 a

[*The means of the same column affected by the same letter does not differ significantly at the 5% level according to Duncan's test. Each value is the mean ±Standard Error].

NPK dose showed significant impact on Relative Water Content of Sidi Aissa clementine leaves. The highest Relative Water Content was recorded in the plants treated with 100N-25P_2O_5-50K_2O. Omari et al. (2012) reported that the application of nitrogen doses significantly affects the relative water content (RWC). The RWC values increase with increasing of nitrogen dose from 0 to 5 mM and that the rootstocks *Citrus volkameriana* B2 28613 (90.48%), sour orange (*Citrus aurantium* L.) (91.76%), and *Citrus macrophylla* (91.80%) showed the highest percentages of relative water content under treatments T_1 (0Mm of N), T_2 (1mM of N) and T_3 (5 mM of N), respectively.

Sidi Aissa clementine plants treated with T_4 (100N-25P_2O_5-50K_2O) represent the highest value of total chlorophyll leaf content (14.70 mg L^{-1}). Omari et al. (2012) reported that the application of nitrogen doses and rootstock significantly affects the concentration of total chlorophyll in the leaves of citrus rootstocks and that the 5 mM dose of N constitutes the treatment which recorded the highest value (11.06 mg L^{-1}) in *Citrus macrophylla* rootstock. Bondada & Syvertsen (2003) reported that the nitrogen dose significantly affects the concentration of chlorophyll in the leaves of the Cleopatra mandarin. The increase of nitrogen dose induced an increase in the concentration of chlorophyll in the leaf tissues of this rootstock. A positive and highly significant correlation was established between the applied nitrogen fertilizer and the total chlorophyll concentration of the leaves of Cleopatra mandarin plants. The increase of nitrogen dose induced a significant rise of the concentration of total chlorophyll in the leaves of 'Hamlin' variety grafted on the citrumelo Swingle. The change from 0 to 218 g of nitrogen per tree caused an increase in chlorophyll of 0.05 to 0.65 mmol m^{-2} in the leaves of 'Hamlin' variety (Bondada & Syvertsen, 2005).

The highest proline content was recorded in *Citrus macrophylla* rootstock under the T_3 (50N-25P_2O_5-50K_2O). Omari et al. (2012) reported that the proline content of leaves of citrus rootstocks in total soluble sugars was markedly affected by the nitrogen dose. The latter increases in parallel with the increase in the nitrogen dose from 0 to 5 mM and that Carrizo citrange recorded the highest value of the sugar content under the dose of 5 mM of nitrogen.

Effect of NPK doses and rootstocks on content of the mineral elements in leaves

Statistical analysis revealed a significant impact of the fertilizer treatments and the rootstock on the leaf nitrogen content of Sidi Aissa variety ($P < 0.0001$) and a highly significant effect of the interaction between rootstocks and treatments ($P = 0.0049$). The

nitrogen content of Sidi Aissa clementine leaves is clearly influenced by the nitrogen dose. Indeed, the leaf nitrogen concentration increases progressively and linearly with the increase in the nitrogen dose from 0 to 100 mg L^{-1} in all the rootstocks studied (Table 4). Under the T_3 (50N-25P_2O_5-50K_2O) treatment, the concentration of the leaves of Sidi Aissa variety in nitrogen in all studied citrus rootstocks were in the optimal range according to the standards interpreting of leaf analysis of Hanlon et al. (1995). However, under the T_1 (0N-25P_2O_5-50K_2O) treatment the nitrogen content of the leaves is considered to be at deficient levels in the different Sidi Aissa/rootstock associations (Table 4). This decrease in leaf nitrogen concentration in T_2 **(**25N-25P_2O_5-50K_2O**)** may be related to the high phosphorus fertilization application.

The nitrogen concentration of Sidi Aissa clementine leaves is also influenced by the rootstock. In fact, a variability in leaf nitrogen concentration is clearly observed within the different rootstocks with respect to the same nitrogen dose (Table 4). *Citrus macrophylla* rootstock recorded the lowest leaf nitrogen concentration under the control, which is around 1.157%. While, sour orange (*Citrus aurantium* L.) with 3.487%,Carrizo citrange B2 28608 (French) with 3.303% and Carrizo citrange (Morocco) with 3.3% showed the highest nitrogen content of Sidi Aissa clementine leaves under the treatment T_4(100N-25P_2O_5-50K_2O) (Table 4).

Table 4. Effect of NPK doses and rootstocks on leaf N content of Sidi Aissa

Rootstocks	Leaf N content (%)				
	T_0	T_1	T_2	T_3	T_4
Citrus macrophylla	1,157 ± 0.022c*	1,307 ± 0.112b	2,200 ± 0.231ab	2,520 ± 0.127cd	2,993 ± 0.118bc
Carrizo citrange (Morocco)	1,470 ± 0.023b	1,507 ± 0.118ab	2,347 ± 0.089a	2,910 ± 0.104ab	3,300 ± 0.057ab
Troyer citrange B2 31655	1,160 ± 0.115c	1,530 ± 0.017ab	1,793 ± 0.003c	2,713 ± 0.008bc	2,843 ± 0.026c
Carrizo citrange B2 28608 (French)	1,683 ± 0.003a	1,877 ± 0.003a	2,397 ± 0.118a	3,113 ± 0.014a	3,303 ± 0.003ab
Sour Orange (*Citrus aurantium* L.)	1,393 ± 0.003b	1,473 ± 0.274ab	1,880 ± 0.069bc	2,343 ± 0.014d	3,487 ± 0.245a

[*The means of the same column affected by the same letter does not differ significantly at the 5% level according to Duncan's test. Each value is the mean ±Standard Error].

A significant effect of the fertilizer treatments showed on the leaf phosphorus content ($P < 0.0001$). The phosphorus concentration of Sidi Aissa clementine leaves is clearly influenced by the nitrogen dose. A negative relationship and antagonism has been demonstrated between the phosphorus concentration of the leaves and the nitrogen dose applied and it is clearly noted that the phosphorus content of the leaves decreases with the increase in the nitrogen dose of T_1 (0N-25P_2O_5-50K_2O) to T_4 (100N-25P_2O_5-50K_2O) in all the rootstocks studied while remaining at optimal levels (Fig. 7).

The Sidi Aissa clementine plants treated with T_1 (0N-25P_2O_5-50K_2O) and T_2 (25N-25P_2O_5 - 50K_2O) represent the highest value of the phosphorus content of the leaves (0.185% and 0.179%, respectively). Whereas, the lowest value was observed in the control plants T_0 with 0.126% of leaf phosphorus content (Fig. 7).

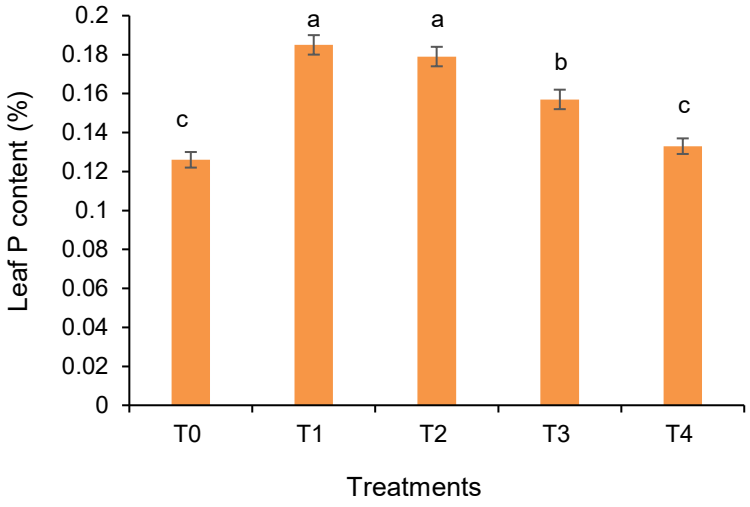

Figure 7. Effect of NPK doses and rootstocks on leaf P content of Sidi Aissa.

[*Values with the same letter are not significantly different (Duncan test, $p \leq 0.05$). Error bars represent standard errors of the mean (±SE)].

Statistical analysis revealed a significant impact of the fertilizer treatments ($P < 0.0001$), the rootstock ($P < 0.0001$) and the interaction of Fertilizer treatments x Rootstock ($P < 0.0001$). The leaf potassium content of Sidi Aissa is clearly influenced by the nitrogen dose. The leaf potassium concentration varies according to the interaction between the applied of N and K nutrients. A negative correlation was demonstrated between the dose of nitrogen applied and the leaf potassium concentration in Sidi Aissa plants. It is clearly noted that the leaf potassium content decreases with the increase in the dose of nitrogen from T_1 (0N-25P_2O_5-50K_2O) to T_4 (100N-25P_2O_5-50K_2O) in all the rootstocks studied while remaining at optimal levels sufficient for the proper development of young citrus plants (Table 5).

Table 5. Effect of NPK doses and rootstocks on leaf K content of Sidi Aissa

Rootstocks	Leaf K content (%)				
	T_0	T_1	T_2	T_3	T_4
Citrus macrophylla	1,167 ± 0.01a*	2,333 ± 0.193b	1,820 ± 0.104b	1,710 ± 0.000b	1,657 ± 0.078 a
Carrizo citrange (Morocco)	1,000 ± 0.115b	2,943 ± 0.003a	2,270 ± 0.219a	1,867 ± 0.014a	1,543 ± 0.009ab
Troyer citrange B2 31655	1,160 ± 0.023a	1,980 ± 0.011b	1,787 ± 0.003b	1,600 ± 0.058c	1,217 ± 0.061c
Carrizo citrange B2 28608 (French)	1,240 ± 0.023a	2,860 ± 0.052a	1,957 ± 0.020ab	1,733 ± 0.037b	1,363 ± 0.101bc
Sour Orange (*Citrus aurantium* L.)	1,203 ± 0.02a	2,733 ± 0.147a	1,947 ± 0.032ab	1,690 ± 0.058bc	1,383 ± 0.049bc

[*The means of the same column affected by the same letter does not differ significantly at the 5% level according to Duncan's test. Each value is the mean ±Standard Error].

Under the treatments T_1(0N-25P_2O_5-50K_2O) and T_2(25N-25P_2O_5-50K_2O) the leaf potassium concentration of Sidi Aissa in all citrus rootstocks studied was higher according to the interpretation standards of leaf analysis by Hanlon et al. (1995). However, under the T_4 treatment (100N-25P_2O_5-50K_2O) the leaf potassium content decreased significantly but remained within the optimal range in the Sidi Aissa plants/different rootstocks (Table 5).Carrizo citrange rootstock (Morocco) recorded the lowest leaf potassium concentration under the control treatment T_0(1%). Sour orange (*Citrus aurantium* L.) (2.733%), Carrizo citrange B2 28608 (French) (2.860%) and Carrizo citrange (Morocco) (2.943%) showed a higher leaf potassium content of Sidi Aissa clementine under T_1 (0N-25P_2O_5-50K_2O) (Table 5).

The leaf nitrogen content of Sidi Aissa clementine is clearly influenced by the nitrogen doses. The leaf nitrogen concentration increases linearly with the increase in the nitrogen dose from 0 to 100 mg L^{-1} in all the rootstocks studied. These results are in agreement with those obtained by many researchers. Thompson & White (2004) reported that leaf nitrogen content of citrus trees was positively correlated with increasing applied nitrogen rate.

The nitrogen concentration of Sidi Aissa clementine leaves is also influenced by the rootstock. In fact, a variability in leaf nitrogen concentration is clearly observed within the different rootstocks with respect to the same nitrogen dose. Our results are in agreement with those reported by Jahromi et al. (2012) who reported that the type of rootstock has a significant influence on the total nitrogen concentration in the leaves of citrus varieties (Sweet lime, Mexican lime, Valencia and orange Washington navel, Kinnow mandarin and Orlando tangelos). The maximum total N concentration (2.12% dry matter) was in Sour orange and the lowest (1.77% dry matter) in Mexican lime and *C. volkameriana* rootstocks.

The type of rootstocks affects more than twenty horticultural properties, among these properties is the leaf mineral element concentration of citrus varieties and each particular scion receives a varying amount of the mineral elements from a special rootstock (Waqar et al., 2007). Rootstocks directly influence the capacity of the grafted plant to absorb water and nutrients from the soil (Richardson et al., 2003).

Sorgona et al. (2006) reported that the highest absorption and total nitrogen concentration is observed in Sour orange and weakest in sweet orange (Sweet orange). Thus, sour orange is very suitable for soils with a low nitrogen dose. On the contrary, Toplu et al. (2008) reported that the highest leaf nitrogen concentration is observed in Carrizo citrange and the lowest in sour orange.

Iqbal et al.(1999) evaluated the effect of rootstock type on the total N concentration of Kinnow Mandarin leaves, they found that the highest total N concentration was in the leaves of varieties grafted on the Citrumelo 4475 and Citrumelo 1452 rootstocks and the weakest in the Rough lemon and Yuma citrange rootstocks. Satsuma grafted on Carrizo citrange rootstock had a higher total N concentration in the leaves than on sour orange (Creste, 1995).

Leaf phosphorus concentration of Sidi Aissa clementine is clearly influenced by the nitrogen dose. A negative relationship and antagonism has been demonstrated between the phosphorus concentration of the leaves and the nitrogen dose applied and it is clearly noted that the phosphorus content of the leaves decreases with the increase in the nitrogen doses in all the rootstocks studied while remaining at optimal levels. Mattos et al. (2006) reported that there is an antagonism between N and P when the applied

nitrogen fertilization is very high in young citrus trees. On the other hand, Sabbah et al. (1997) reported that leaf phosphorus content was not significantly affected by the amount of nitrogen applied to citrus plants. Tu et al. (2018) reported that the application of phosphorus (P) induced elevated levels of N, P, K and Mg in various parts of citrus plants, leading to a significant increase in the dry weight of roots, branches and leaves.

The leaf potassium content of Sidi Aissa is clearly influenced by the nitrogen dose. The leaf potassium concentration varies according to the interaction between the applied of N and K nutrients. A negative correlation was demonstrated between the dose of nitrogen applied and the leaf potassium concentration in Sidi Aissa plants. This decrease in foliar potassium concentration with increasing N fertilizer doses can be considered as an effect caused by vigorous plant growth induced by nitrogen application. Similar results were obtained by Sabbah et al. (1997) and Wassel et al. (2007) on citrus trees. Similarly, Robert et al. (1999) reported that as the N/K_2O fertilizer ratio increases leaf potassium concentration decreases. De Campos Bernardi et al. (2000) reported that 4 months after transplanting the seedlings to the nursery, the maximum leaf potassium concentration was produced with the application of the nitrogen dose of 0.47 g $plant^{-1}$ and a dose of potassium of 4.67 g $plant^{-1}$. Toplu et al. (2012) observed notable variations in nutrient concentrations within the leaves of three Mandarin varieties (Okitsu, Clausellina, and Silverhill) when grafted on three different citrus rootstocks (Sour Orange, Troyer Citrange, and Carrizo Citrange). Specifically, varieties grafted on Carrizo Citrange demonstrated elevated levels of nitrogen and potassium in the leaves. Whereas those grafted on Troyer Citrange revealed higher leaves phosphorus and iron content. Yilmaz et al. (2018) reported that the rootstocks significantly affects the physiological properties and yield of Rio Red grapefruit. Specifically, the study found that all examined rootstocks (Carrizo citrange, citremon, sour orange, Swingle citrumelo, Troyer citrange and *Citrus volkameriana*) influenced the leaf chlorophyll concentrations. Moreover, notable rootstock effects were observed on the concentrations of several leaf minerals, with *C. volkameriana* having the highest leaf Zn concentration. However, there were no significant rootstock effects on leaf N, P, K, and Fe concentrations.

CONCLUSION

The study investigated the impact of various fertilizer treatments on Sidi Aissa citrus plants. The increase in the nitrogen dose significantly affects the morphological, physiological and biochemical parameters of Sidi Aissa plants grafted on five citrus rootstocks. The optimal growth on plants height, rootstock stem diameter, number of leaves, shoot length and shoot diameter of the young plants of Sidi Aissa clementine was recorded under the treatment of $100N\text{-}25P_2O_5\text{-}50K_2O$ in mg L^{-1}. Plants treated with $100N\text{-}25P_2O_5\text{-}50K_2O$ mg L^{-1} showed the highest Relative Water Content and total chlorophyll content. In addition, we have shown that there is variability within Sidi Aissa associations on different rootstocks with respect to the response to the dose of NPK nutrients. Sidi Aissa clementine plants grafted on Carrizo citrange (Morocco) and Troyer citrange B231655 rootstocks showed significant improvements in all studied parameters. Nitrogen leaf content of Sidi Aissa clementine increases proportionally with the increase in nitrogen dose from 0 to 100 mg L^{-1} while the foliar content of phosphorus and potassium were reduced in Sidi Aissa plants on all the rootstocks studied. In the absence of mineral element deficiency or toxicity, it is advised to utilize a nutrition solution with

a composition of 100 N-25 P_2O_5-50 K_2O mg L^{-1} to ensure optimal growth of citrus plants in the nursery.

REFERENCES

Al-Jilihawi, D.A.H. & Merza, T.K. 2020. Effect of soil fertilization and foliar nano-NPK on growth of key lemon *Citrus aurantifolia* rootstock saplings. *Plant Archives* **20**(2), 3955–3958.

Alkhafaji, A.R. & Khalil, N.H. 2019. Effect of fertilization, rootstocks and growth stimulant on growth of *Citrus limon* L. sapling. *Iraqi Journal of Agricultural Sciences* **50**(4), 990–1000.

Alva, A.K., Paramasivam, S. & Graham, W.D. 1998. Impact of nitrogen management practices on nutritional status and yield of Valencia orange trees and groundwater nitrate. *J. Environ. Qual.* **27**, 904–910. http://dx.doi.org/10.2134/jeq1998.00472425002700040026x

Alva, A.K., Mattos, D. Jr. & Quaggio, J.A. 2008. Advances in nitrogen fertigation of citrus. *J. Crop Improv.* **22**, 121–146.

Alva, A.K., Mattos, Jr. D., Paramasivan, S., Patil, B., Dou, H. & Sajwan, K.S. 2006a. Potassium management for optimizing citrus production and quality. *International Journal of Fruit Science* **6**, 3–43.

Alva, A.K., Paramasivam, S., Fares, A., Delgado, J.A., Mattos, Jr. D. & Sajwan, K. 2005a. Nitrogen and irrigation management practices to improve nitrogen uptake efficiency and minimize leaching losses. *Crop Improvement* **15**, 369–420.

Alva, A.K., Paramasivam, S., Obreza, T.A. & Schumann, A.W. 2005b. Nitrogen best management practice for citrus trees: I. Fruit yield, quality and leaf nutritional status. *Sci. Hortic.* **107**, 233–244.

Alva, A.K., Paramasivam, S., Obreza, T.A. & Schumann, A.W. 2006b. Nitrogen best management practice for citrus trees I. Fuit yield, quality and leaf nutritional status. *Scientia Hort.* **107**, 233–244.

Alva, A.K., Paramasivam, S., Fares, A., Obreza, T.A. & Schumann, A.W. 2006c. Nitrogen best management practice for citrus trees II. Nitrogen fate, transport and components of N budget. *Scientia Horticulture* **109**, 223–233.

Arnon, D. 1949. Copper enzymes isolated chloroplasts, polyphenoloxidase in Beta vulgaris. *Plant Physiology* **24**, 1–15

Bates, L, Waldren, R.P., Teare, I.D. 1973. Rapid determination of free proline for water-stress studies. *Plant and Soil*. **39**, 205–207.

Bondada, B.R. & Syvertsen, J.P. 2003. Leaf chlorophyll, net gas exchange and chloroplst ultrastructure in citrus leaves of different nitogen status. *Tree Physiologie* **23**, 553–559.

Bondada, B.R. & Syvertsen, J.P. 2005. Concurent changes in net CO_2 assimilation and chloloroplast ultrastructure in nitrogen deficient citrus leaves. *Environemental and experimental Botany* **54**, 41–48.

Carranca, C., Brunetto, G. & Tagliavini, M.2018. Nitrogen Nutrition of Fruit Trees to Reconcile Productivity and Environmental Concerns. *Plants* **7**(4), 1–12.doi:10.3390/plants7010004

Castle, W.S., Nunnallee, J. & Manthey, J.A. 2009. Screening Citrus Rootstocks and Related Selections in Soil and Solution Culture for Tolerance to Low-iron Stress. *HortScience* **44**(3), 638–645.

Chaudhry, M.I. & Naveed, F. 1992. Effect of time of nitrogen application on growth and productivity of sweet lime (*Citrus limettioides* TANAK*). Pak. J. Agri. Sci.* **29**(2), 151–155.

Creste, J.E. 1995.Effect of different rootstocks on the mineral composition of leaves on fruiting stem of Satsuma. *Centifica.* **23**(1), 9–16.

Davies, F.S. & Albrigo, L.G. 1994. *Citrus*. Crop Protection Science in Horticulture. No: 2. – CAB International, Redwood Books, Trowbridge, Wiltshire, UK, 254 pp.

Davis, A.R., Perkins-Veazie, P., Hassell, R., Levi, A., King, S.R. & Zhang, X. 2008. Grafting effects on vegetable quality. *HortScience.* **43**, 1670–1672.

De Campos Bernardi, A.C., de Camargo Carmello, Q.A. & de Carvalho, S.A. 2000. Development of citrus nursery trees grown in pots in response to NPK fertilization. *Sci. Agric.* **57**, 733–738.

Esposti, M.D.D., Siqueira, D.L., Pereira, P.R.G., Venegas, V.H.A., Salomao, L.C.C. & Filho, J.A.M. 2003. Assessment of nitogenized nutrition of citrus rootstocks using chlorophyll concentration in the leaf. *Journal of Plant nutrition* **26**(6), 1287–1299.

Esteves, E., Maltais-Landry, G., Zambon, F., Ferrarezi, R.S. & Kadyampakeni, D.M. 2021. Nitrogen, calcium, and magnesium in consistently affect tree growth, fruit yield, and juice quality of huanglongbing-affected orange trees. *Hort. Science* **56**(10), 1269–1277.

Forner-Giner, M.A., Alcaide, A., Primo-Millo, E. & Forner, J.B. 2003. Performance of 'Navelina' orange on 14 rootstocks in Northern Valencia (Spain). *Scientia Horticulturae* **98**(3), 223–232.

González-Mas, M.C., Llosa, M.J., Quijano, A. & Forner-Giner, M.A. 2009. Rootstock Effects on Leaf Photosynthesis in 'Navelina' Trees Grown in Calcareous Soil. *HortScience* **44**(2), 280–283.

Guazzelli, L., Ferguson, J.J. & Davies, F.S., 1996. Preplant leaf nitrogen effects on growth of young Hamlin orange trees. *Proc. Fla. State Hortic. Soc.* **109**, 72–76.

Hafez, O.M. 2006. Evaluation of growth characteristic of some citrus rootstocks using protein finger print technique. *American-Eurasian J. Agricol Environ. Sci.* **1**(3), 243–248.

Hanlon, E.A., Obreza, T.A. & Alva, A.K. 1995. Tissue and soil analysis. In: Nutrition of Florida Citrus Trees, Tucker, D.P.H., A.K. Alva, L.K. Jackson and T.A. Wheaton (Eds.). University of Florida, Gainesville: 13–20.

Hawkesford, M., Horst, W., Kichey, T., Lambers, H., Schjoerring, J., Moller, I.S. & White, P. 2012. Functions of Macronutrients. In: Mineral Nutrition of Higher Plants. P. Marschner (eds), 3rd ed. *Elsevier*. U.S.A. 135–157.

He, Z.L., Calvert, D.V., Alva, A.K. & Li, Y.C.2000. Management of nutrients in citrus production systems in Florida: An overview. *Soil Crop Sci. Fla. Proc*. **59**, 2–10.

Huang, W.-T., Xie, Y.-Z., Chen, X.-F., Zhang, J., Chen, H.-H., Ye, X., Guo, J., Yang, L.-T., Chen, L.-S. 2021. Growth, mineral nutrients, photosynthesis and related physiological parameters of Citrus in response to nitrogen deficiency. *Agronomy* **11**, 1859.

Iqbal, S., Chandhary, M.I. & Anjum, M.A. 1999. Effect of various rootstocks on leaf mineral composition and productivity of Kinnow mandarine. *International Journal of Agriculture and biology* **1**(3), 91–93.

Jahromi, A.A., Hasanzada, H. & Farahi, M.H. 2012. Effect of Rootstock Type and Scion Cultivar on Citrus Leaf Total Nitrogen. *World Applied Sciences Journal* **19**(1), 140–143.

Jover, S., Martíne -Alcantra, B., Rodrígue -Gamir, J., Legaz, F., Primo-Millo, E., Forner, J. & Forner-Giner, M.A. 2012: Influence of rootstocks on photosynthesis in navel orange leaves: Effects on growth, yield, and Carbohydrate distribution. *Crop Science* **52**, 863–848.

Kakabouki, I., Folina, A., Karydogianni, S., Zisi, Ch. & Efthimiadou, A. 2020. The effect of nitrogen fertilization on root characteristics of Camelina sativa L. in greenhouse pots. *Agronomy Research* **18**(3), 2060–2068. https://doi.org/10.15159/AR.20.178

Karydogianni, S., Darawsheh, M.K., Kakabouki, I., Zisi, Ch., Folina, A.E., Roussis, I., Tselia, Z. & Bilalis, D. 2020. Effect of nitrogen fertilizations, with and without inhibitors, on cotton growth and fiber quality. *Agronomy Research* **18**(2), 432–449. https://doi.org/10.15159/AR.20.148

Kocsis, L., Tarczal, E. & Kállay, M. 2012. The effect of rootstocks on the productivity and fruit composition of Vitis vinifera L. Cabernet Sauvignon Kékfrankos *Acta Hortic*. **931**, 403–411.

Kucukyumuk, Z. & Erdal, I. 2011. Rootstock and cultivar effect on mineral nutrition, seasonal nutrient variation and correlations among leaf, flower and fruit nutrient concentrations in apple trees. Bulg. *J. Agric. Sci*. **17**, 633–641.

Lu, J.W., Chen, F., Wang, Y.H., Liu, D.B., Wan, Y.F. & Yu, C.B. 2004. Effect of N, P, K fertilization on young citrus growth, fruit yield and quality in area of red soil. *Plant Nut. Fert. Sci.,* **10**, 413–418.

Lu, Z.-J., Yu, H.-Z., Mi, L.-F., Liu, Y.-X., Huang, Y.-L., Xie, Y.-X., Li, N.-Y., Zhong, B.-L. 2019. The effects of inarching Citrus reticulata Blanco var. tangerine on the tree vigor, nutrient status and fruit quality of Citrus sinensis Osbeck Newhall'trees that have Poncirus trifoliate (L.) Raf. as rootstocks. *Sci. Hortic*. **256**, 108600.

Marschner, H. 2012. *Marschner's mineral nutrition of higher plants* (3rd ed.). Cambridge, MA : Academic Press, 651 pp.

Martínez-Ballesta, M.C., Alcaraz-López, C., Muries, B., Mota-Cadenas, C. & Carvajal, M. 2010. Physiological aspects of rootstock–scion interactions. *Sci. Hortic.* **127**, 112–118.

Mattos, Jr. D., Quaggio, J.A., Cantarella, H. & Alva, A.K. 2003. Nutrient content of biomass components of Hamlin sweet orange trees. *Sci.Agric.* **60**(1), 155–160, doi: 10.1590/S0103-901620030001 00023.

Mattos, Jr.D., Quaggio, J.A., Cantarella, H., Alva, A.K. & Graetz, D.A. 2006. Response of young citrus trees on selected rootstoks to nitrogen, phosphorus and potassium fertilization. *J. Plant Nutr.* **29**, 1371–1385.

Maust, B.E. & Williamson, J.G. 1991. Nitrogen rate effect on growth of containerized citrus nursery plants. *Proc. Fla. State. Hort. Sci.* **104**, 191–195.

Maust, B.E. & Williamson, J.G. 1994. Nitrogen nutrition of containerized citrus nursery plants. *J.Am. Soc. Hortic. Sci.,* **119**, 195–201.

Menino, M.R., Carranca, C., de Varennes, A., d'Almeida, V.V. & Baeta, J. 2003.Tree size and flowering intensity as affected by nitrogen fertilization in non-bearing orange trees grown under Mediterranean conditions. *J. Plant Physiol.* **160,** 1435–1440.

Mesquita, G.L., Zambrosi, F.C.B., Tanaka, F.A.O., Boaretto, R.M., Quaggio, J.A., Ribeiro, R.V. & Mattos-Jr., D. 2016. Anatomical and Physiological Responses of Citrus Trees to Varying Boron Availability Are Dependent on Rootstock. *Front. Plant Sci.* **7**, 224. doi: 10.3389/fpls.2016.00224

Nguyen, H.H. & Tai, T.N. 2020. Effects of combination between nitrogen and potassium fertilization on yield and quality of valencia orange fruits. *Journal of Agricultural Science.* **12**(1), 38–45. doi:10.5539/jas.v12n1p38

Obreza, T.A., Kelly, T. & Morgan. 2008. *Nutrition of Florida Citrus Trees*. SL 253. University of Florida Lake Alfred. FL., 96 pp.

Obreza, T.A., Zekri, M. & Hanlon, E.W. 2008. Soil and leaf tissue testing. In: Nutrition of Florida Citrus Trees, Obreza, T.A. and K.T. Morgan (Eds.). 2nd Edn. Florida Cooperative Extension Service, Institute of Food and Agricultural Sciences, University of Florida, pp. 24–32.

Omari, F.E., Beniken, L., Gaboune, F., Zouahri, A., Benkirane, R. & Benyahia, H. 2012. Effet de la nutrition azotée sur les paramètres morphologiques et physiologiques de quelques porte-greffes d'agrumes. *Journal of Applied Biosciences.* **53**, 3773–3786.

Omari, F.E., Beniken, L., Zouahri, A., Douaik, A., Mrabet, R., Benkirane, R., Benyahia, H. 2020b. Effet de la fertilisation N, P et K sur la production et la qualité des fruits de la clémentine Sidi Aissa. *AFRIMED AJ –Al Awamia.* **129**, 76–91.

Omari, F.E., Beniken, L., Zouahri, A., Talha, A., Benkirane, R. & Benyahia, H. 2020a. Effect of nitrogen level application on yield and fruit quality of Navel orange variety in a sandy soil. *African & Mediterranean Agricultural Journal –Al Awamia.* **129**, 92–107.

Ouma, G.B. 2006. Growth responses of Rough Lemon (citrus limon L.) rootstock seedlings to different container sizes and nitrogen levels. *Agricultura Tropica et subtropica* **39**(3), 183–189.

Parameshwar, P., Joshi, P.S. & Nagre, P.K. 2018. Effect of Rootstock on Plant Growth and Fruit Quality of Sweet Orange (*Citrus sinensis* var. Valencia late). *Int. J. Curr. Microbiol. App. Sci.* **7**(04), 1685–1689. doi: https://doi.org/10.20546/ijcmas.2018.704.190

Pestana, M., de Varennes, A., Abadía, J. & Faria, E.A. 2005. Differential tolerance to iron deficiency of citrus rootstocks grown in nutrient solution. *Sci.Hortic* **104**, 25–36. doi: 10.10 16/j.scienta.2004.07.007

Rameeh, V., Ramzanpour, M.R. & Matani, R. 2019. Effects of citrus rootstocks on some plant nutrient elements absorption of grafted cultivars. *Cercetări Agronomice în Moldova.* Vol. LII, **4**(180), 379–387. doi: 10.46909/cerce-2019-0036.

Richardson, A., Mooney, P., Anderson, P., Dawson, T. & Watson, M. 2003. How do rootstocks affect canopy development? Hort. Research, Kerikeri Research center. NewZeland. http://www. hortnet. co.nz/publications/science/r/richardso/rootcan.htm.

Robert, E.R., Obreza, T.A. & Sherrod, J.B. 1999. Yield and relative cost of controlled-release fertilizer on young bearing citrus trees. *Proc. Fla. State Hortic. Soc.* **112**, 46–50.

Sabbah, S.M., Bacha, M.A. & El Hamady, M.A. 1997. Effect of source and rate of nitrogen fertilization on yield, fruit quality and leaf mineral composition of Valencia orange trees grown in Riyadh, Saudi Arabia. *J. King Saud. Univ. Agrisci.* **9**(1), 141–152.

Sarvade, S., Mishra, H.S., Kaushal, R., Chaturvedi, S., Tewari, S. & Jadhav, T.A. 2014. Performance of wheat (*Triticum aestivum* L.) crop under different spacings of trees and fertility levels. *African Journal of Agricultural Research* **9**(9), 866–873.

Schumann, A.W., Fares, A., Alva, A.K. & Paramasjvam, S. 2003. Response of 'Hamlin'orange to fertilizer source, annual rate and irrigated area. *Proc. Fla. State Hort. Soc*. **116**, 256–260.

Schwarz, D., Rouphael, Y., Colla, G. & Venema, J.H. 2010. Grafting as a tool to improve tolerance of vegetables to abiotic stresses: Thermal stress, water stress and organic pollutants. *Sci. Hortic.* **127**, 162–171.

Shaban, A.E.A. & Mohsen, A.T. 2009. Respons of citrus rootstocks and transplants to biofertilizers. *Journal of Horticultural Science and Ornomental plant* **1**(2), 39–48.

Sinha, D. & Tandon, P.K. 2020. An Overview of Nitrogen, Phosphorus and Potassium: Key Players of Nutrition Process in Plants. In: Mishra, K., Tandon, P.K., Srivastava, S. (eds) Sustainable Solutions for Elemental Deficiency and Excess in Crop Plants. Springer, Singapore. https://doi.org/10.1007/978-981-15-8636-1_5

Sorgona, A., Abenavoli, M.R., Gringeri, P.G. & Cacco, G. 2006. A comparison of nitrogen use efficiency definitions in Citrus rootstocks. *Scientia Horticulturae* **109**, 389–393.

Taylor, B.K. & Dimsey, R.T. 1993. Rootstock and scion effects on the leaf nutrient composition of citrus trees. *Aust. J. Exp. Agric.* **33**, 363–371.

Thompson, T.L. & White, S.A. 2004. Nitrogen and phosphorus fertilizer requirements for young, bearing microsprinkler-irrigated citrus, 2004 report. http://www.azda.gov/CDP/NewCBC/ACRC/ACRC2003Research/2003-02.pdf.

Toplu, C., Kaplankiran, M., Demirkeser, T. H. & Yildiz, E. 2008. The effects of citrus rootstocks on Valencia late and Rohde Red Valencia oranges for some plant nutrient elements. *African Journal of Biotechnology* **7**(24), 4441–4445.

Toplu, C., Uygur, V., Kaplankıran, M., Demirkeser, T.H. & Yıldız, E. 2012. Effect of citrus rootstocks on leaf mineral composition of 'Okitsu', 'Clausellina', and 'Silverhill' mandarin cultivars. *J. Plant Nutr*. **35**, 1329–1340.

Tu, P.F., Deng, L. S., Li, J., Zhang, C. L., He, S.X., Chen, J.Z., Cheng, F.X. & Ji, J.H. 2018. Effect of phosphorus on N, P, K, Mg accumulation and plant growth of different citrus rootstocks. *Applied Ecology and Environmental Research* **16**(1), 819–836. doi: http://dx.doi.org/10.15666/aeer/1601_819836

Waqar Ahmed, M., Azher Navaz, M., Azhar Iqbal, M. & Khan, M.M. 2007. Effect of different rootstocks on plant nutrient status and yield in Kinnow mandarin (*citrus reticulate* Blanco). *Pak. J. Bot.* **39**(5), 1779–1786.

Wassel, A.H., Ahmed, F.F., Ragab, M.A. & Ragab, M.M. 2007. Response of balady mandarin trees to drip irrigation and nitrogen fertigation, I-Effect of nitrogen fertigation and drip irrigation on the vegetative growth and the yield of balady mandarin trees (*Citrus reticulata*). *Afr. Crop Sci. Conf. Proc.* **8**, 503–511.

Wassel, A.M.M., Abdel –Aziz, F.H., Ismaiel, H.M.H & Abdel–Rahman, S.E.A. 2022. Effect of soil nitrogen fertilizer on fruit set, the yield and fruit quality of Valencia orange trees. *Minia J. of Agric. Res. & Develop.***42**(1), 59–66.

Yilmaz, B., Cimen, B., Incesu, M., Uysal Kamiloglu, M. & Yesiloglu, T. 2018. Rootstock influences on seasonal changes in leaf physiology and fruit quality of Rio Red grapefruit variety. *Applied Ecology and Environmental Research* **16**(4), 4065–4080. doi: http://dx.doi.org/10.15666/aeer/1604_40654080

Zekri, M. & Obreza, T.A. 2003a. Plant nutrients for citrus trees. Extension service fact sheet SL 200. Florida Cooperative Extension Service, Institute of Food and Agricultural Sciences, University of Florida, Gainesville.

Zekri, M. & Obreza, T.A. 2003b. Macronutrient Deficiencies in citrus: Calcium, Magnesium, and Sulfur. Institute of Food and Agricultural Sciences, University of Florida. http://edis.ifas.ufl.edu.

Agronomy Research **21**(S3), 1541–1554, 2023
https://doi.org/10.15159/AR.23.106

Growth and yield response of sweet potato (*Ipomoea batatas* var. batatas) under acid sandy soil, northeast of Thailand

N. Ruangsuriya and K. Sungthongwises*

Agronomy section, Faculty of Agriculture, Khon Kaen University, TH40002 Khon Kaen, Thailand
*Correspondence: skiriy@kku.ac.th

Received: May 28th, 2023; Accepted: August 16th, 2023; Published: November 15th, 2023

Abstract. Sweet potato is one of the major crops grown for food, animal feed and industrial products. The yield obtained in the Northeast of Thailand is far below its genetic potential due to soil degradation, erosion, acidification, loss of organic matter, waterlogging and salinization causing nutrient deficiency. The objectives of this research are to investigate yield components, accumulation of nutrients and food nutrition of different sweet potato species under acidic sandy soil. The experiment with four replications was laid out in a farmer's field at Phu Wiang and Nong Ruea District, Khon Kaen Province, where young smart farmers are interested to grow sweet potato. Trials were planted for 2 years using four species of sweet potato: (A) Honey Sweet, (B) Okinawan Orange, (C) Okinawan Purple and (D) Purple Sweet Lord. All plots were treated with a basal application of 1.56 t ha^{-1} of cow and poultry manure with 0.03 t ha^{-1} of chemical fertilizer formula (N12-P4-K4). An addition of 0.15 t ha^{-1} of chemical fertilizer formula (N12-P4-K20) was made at 15 and 30 days after growing. The results show that Okinawan Orange and Purple Sweet Lord were higher growth in Phu Wiang district than Nong Ruea district. If the cost and unit price are the same, Okinawan Orange will give farmers a higher return than Purple Sweet Lord. Regarding the leaf residues of Okinawan Orange and Purple Sweet Lord are suitable to be used for fish farming, because they contain the highest protein and carbohydrates.

Key words: acid soil, decision, growth, sweet potato, yield components.

INTRODUCTION

Since there is a trend towards healthy food, sweet potato is grown throughout all regions of Thailand with different colors. Thailand consumers mostly prefer dessert types and salad. Dessert types of sweet potato generally have orange flesh and are served with coconut milk, with 70% consists of starch from dry matter (Karan & Şanli, 2021). Sweet potato is a good source of phytochemicals, which have beneficial health effects, while roots and leaves contain β-carotene (provitamin A), ascorbicacid (vitamin C), vitamin B complex and phenolic compounds such as anthocyanins (Teow et al., 2007; Ji et al., 2015). Teow et al. (2007) reported that β-carotene content significantly to the sweet potato genotypes, orange potato roots are rich sources of β-carotene while yellow potato roots provide moderate amounts of β-carotene. Nowadays, the consumption demand for sweet potatoes in various countries has also increased. Thailand has higher potential

production and export compared to Japan, republic of China (Taiwan) and the republic of Korea. These producers have limited agricultural areas and high labor costs for production compared to Thailand. Therefore, when starting to produce sweet potatoes suitable for available planting areas, it is necessary to help farmers select sweet potato varieties that meet the highest growth potential and market demand. Sweet potatoes for fresh consumption come in a variety of flesh colors, including white, yellow, orange and purple, depending on the species. For the processing industry, white-fleshed sweet potato varieties are needed with a high starch percentage. While eating for health by steaming or grilling, it is popular to consume sweet potatoes with yellow, orange and purple flesh.

Sweet potato has a wide tolerance to soil conditions, allowing extended cultivation in previously marginal areas. It produces yield earlier (average 140 days) and the high edible proportion of the harvested product contributes to a very high edible energy yield compared to potato, banana, maize, cassava, wheat, rice and sorghum. In Ethiopia, average sweet potato yield is 33.74 t ha^{-1} (CSA, 2014) which is very low as compared to the crop potential which rises to 50 t ha^{-1} (Gurmu & Mekonen, 2017). Amede et al. (2006) submitted that most soils in southern Nigeria are acidic due to the nature of parent materials, leaching and intense weathering. In addition, high acidity induces nutrient deficiency. The yield obtained in Nigeria is far below its genetic potential due to soil degradation, erosion, acidification, and loss of organic matter, waterlogging and salinization (FAO, 2008). Popradit (2021) reported that the yield of sweet potato (Okinawan) was significantly lower than that of sweet potato (Native sweet potato). The maximum yield weight of native sweet potato in plot 3 (0.96 kg $tree^{-1}$, using 150 kg of compost fertilizer and the yield weight of Okinawan show the lowest yield in the plot 4 (0.27 kg $tree^{-1}$, which was the control plot with natural conditions. The chemical fertilizer formula (N13-P13-K21) used in the sweet potato cultivation by Hmong hill tribe farmers had lower quantities of K and P, while the amount of N in such a formula was suitable to the growing needs. However, the studies have also shown that sweet potato is unsuitable for upstream cultivation due to its high uptake of soil nutrients, which could cause soil deterioration. Many of these factors play a role in many countries which have adopted sweet potato as a subsistence crop.

Moreover, sweet potato crops take up large amounts of nutrients from the soil (Troncoso & Pedreschi, 2009). Considering that the uptake and removal of nutrients by the sweet potato are relatively high (Fernandes et al., 2020), nutrient supplementation in an appropriate and balanced way becomes necessary to attain the full production potential of sweet potato (Dawit & Habte 2023). For maximum benefit to producers, planting sweet potato for suitable cultivars under acid sandy soil in Northeast Thailand need to be explored. As a result of the above problems, various cultivars of sweet potato efficacy were tested, in order to obtain suitable quantity and quality of sweet potato yield, macronutrients content and this study's results could guide decision making on sweet potato production by new farmers in the future.

MATERIALS AND METHODS

Experimental site

The study was conducted at the beginning of the rainy season in 2021–2022, on farmer fields in Phu Wiang and Nong Ruea District, Khon Kaen Province, Northeast Thailand. The site is located within Latitudes 16° 22.65′ N and 16° 57.6′ N and Longitudes

102° 43.42′ E and 102° 48.5′ E in a dry area at an elevation of 210 and 192 m respectively. The rainy season is characterized from May to October following the winter and the dry season. Total rainfall of 864 and 850 mm occurred during the crop growth period of 6 months in Phu Wiang and Nong Ruea District, respectively. The maximum and minimum temperatures were recorded as 31.67 and 25 °C in Phu Wiang District and 32 and 25 °C in Nong Ruea District. The dominant soil order in the studied area is acid sandy soil. Prior to field experimentation, a composite soil sample was obtained from the experimental site and was analyzed for its chemical properties. The results of the soil analysis are given in Table 1.

Experimental design and treatments

The trial was established as a randomized complete block design with four replications of across sites. The treatments involved four varieties (Okinawan Orange, Okinawan Purple, Purple Sweet Lord and Honey Sweet) of sweet potato. Each plot measured 1×50 m with a spacing of 1 m between plots and 2.00 m between blocks.

Cultural practices

Sweet potatoes were planted in farmers' fields at the end of March, 2021–2022. For both fields, cured poultry and cow manure was incorporated into the soil at a rate of 6.25 t ha^{-1} two weeks prior to planting. At planting, vines of 25–30 cm length with 5–7 nodes were collected from the apical meristem and planted at a spacing of 1 m between ridges and 0.50 m within rows, during the early hours of the day. The vines were planted at an angle of 45° and a planting depth of 5 cm with 3–4 nodes in the soil. The plots were irrigated by drip irrigation system immediately after planting. Weeding was done manually using hoes two weeks after planting and subsequently as was necessary. Harvesting was done at 12–14 weeks after planting when fresh tubers were fully grown, depending on varieties, and when the leaves and vines had turned brown and dried up. Harvesting was done by removing the dried vines using a machete and uprooting the tubers using spades and hoes.

Data collection

During the growing phase, data were taken for survival percentage, vine length, nodes length, SPAD, leaf area, leaf and stem fresh weight, leaf and stem dry weight, N, P and K content in leaf and stem at 1 and 2 months after planting. Sweet potato leaf area (LA) was estimated using a leaf area meter LI-Cor 3100, LI-COR Inc., Lincoln, NE, USA. At harvest, data were collected on the number of tubers per plant, tuber length, tuber diameter, tuber weight, tuber yield, leaf and stem fresh weight, leaf and stem dry weight, nutrition in tuber, leaf and stem of sweet potato such as fresh moisture percentage, ash, protein, fat, fiber and carbohydrate. Tuber weight was determined by weighing all harvested tubers within each net plot of 1×10 m in kg and dividing by the number of plants within the net plot. Tuber yield was estimated thus:

Tuber yield = kg tuber weight within each net plot of (10 m^2×1,600 m^2)/10 m^2.

Data analysis

Collected data were subjected to analysis of variance using Statistix 10 software. Significantly different treatment means were separated and compared using Fisher's least significant different (LSD) at the 0.05 level of probability.

RESULTS

Chemical properties of soil prior to cropping

The results of the pre-cropping soil properties of the experimental site are presented in Table 1. The soil was sandy loam, with a strongly acidic condition in the Nong Ruea district field. Organic matter, total nitrogen, available phosphorus, exchangeable potassium, calcium, magnesium, iron, manganese, copper and zinc, total chromium and lead were significantly different between the fields. The Nong Ruea district field tended to have soil chemical properties such as organic matter, total nitrogen, exchangeable calcium, magnesium, iron, manganese, copper and zinc, total chromium and also heavy metal like lead more than the Phu Wiang district field. However available phosphorus and exchangeable potassium were higher in the soil at the Phu Wiang district field. Simson et al. (2016) point out of the effect of tuber variety, location and specific interactions among ions must be considered. Nitrogen element may mainly results in delayed maturity, K deficiency reduces partitioning of dry matter and P aids to alleviate adverse NK interaction in terms of dry matter content.

Table 1. Soil chemical properties before growing sweet potato (*Ipomoea batatas* L.)

Soil chemical properties	Phu Wiang district	Nong Ruea district
pH** (1:1 H_2O)	5.75^{a}	4.71^{b}
OM** (%)	0.38^{b}	0.62^{a}
EC (mS cm^{-1})	0.02	0.02
Total N** (%)	0.02b	0.06^{a}
Available P** (mg kg^{-1})	406.25^{a}	204.17^{b}
Exchangeable K** (mg kg^{-1})	53.77^{a}	49.14^{b}
Exchangeable Ca** (mg kg^{-1})	109.83^{b}	222.44^{a}
Exchangeable Mg** (mg kg^{-1})	17.24^{b}	60.58^{a}
Exchangeable Fe** (mg kg^{-1})	54.99^{b}	263.41^{a}
Exchangeable Mn** (mg kg^{-1})	4.58^{b}	26.22^{a}
Exchangeable Cu** (mg kg^{-1})	0.12^{b}	0.46^{a}
Exchangeable Zn** (mg kg^{-1})	0.38^{b}	0.51^{a}
Total Cr** (mg kg^{-1})	8.39^{b}	12.45^{a}
Total As (mg kg^{-1})	1.76	1.80
Total Cd (mg kg^{-1})	0.55	0.53
Total Pb** (mg kg^{-1})	1.38^{b}	4.27^{a}

a Treatments at $p \leq 0.05$, derived from *LSD*. **: Represent significance at $p \leq 0.01$.

Growth of sweet potato

When sweet potatoes were planted for 1 month, it was found that Honey Sweet and Okinawan Orange varieties had the highest survival percentage in both fields (Table 2). Okinawan Purple and Purple Sweet Lord with such a low survival rate in both fields, according to the use of lack integrity and strength of the vines. Vegetative growth of Okinawan Orange and Purple grown in Phu Wiang district were highest according to the longest node lengths of 2.44 and 2.81 cm respectively. In particular Okinawan Orange has the highest leaf area for photosynthesis, therefore giving more biomass than Okinawan Purple, Purple Sweet Lord and Honey Sweet. Moreover, the leaf SPAD observation obtained from chlorophyll meter (Minolta SPAD502, Japan) by measuring mature leaves, had no statistical difference. It is positively correlated with leaf chlorophyll and N contents (Kandel, 2020). The chlorophyll content will increase in proportion to the amount of nitrogen present in the leaf. For a particular plant species, a higher SPAD value indicates a healthier plant. Similar to the research work of Novikova et al. (2021) biomass is consumed for the leaf surface formation at the beginning of vegetative growth and then the biomass produced was spent on tuberization.

Table 2. Variables of sweet potatoes at 1 month of growing

Field experiment	Sweet potato	Survival (%)	Vine Length (cm)	Nodes Length (cm)	SPAD	Leaf Area/ Plant (cm^2)	Leaf Fresh Weight/ Plant (g)	Stem Fresh Weight/ Plant (g)	Leaf Dry Weight/ Plant (g)	Stem Dry Weight/ Plant (g)
Phu Wiang District	Honey Sweet	100.00[a]	28.18[b]	1.21[b]	44.08	1,375.50[b]	11.25[b]	10.50[b]	2.75[b]	2.00[b]
	Okinawan Orange	98.00[a]	54.25[a]	2.44[a]	45.70	6,256.80[a]	57.00[a]	65.00[a]	10.75[a]	7.00[a]
	Okinawan Purple	47.00[c]	53.95[a]	2.81[a]	47.23	1,066.80[b]	17.75[b]	11.75[b]	3.00[b]	1.75[b]
	Purple Sweet Lord	59.25[b]	26.58[b]	2.26[a]	45.18	1,628.00[b]	17.50[b]	18.00[b]	2.25[b]	0.75[c]
Nong Ruea District	Honey Sweet	94.44[a]	19.83[b]	2.63	41.33[b]	479.30[b]	5.25[b]	5.25[b]	1.63[b]	0.88
	Okinawan Orange	89.00[a]	22.75[b]	1.96	46.93[a]	1,063.80[a]	12.50[ab]	8.00[ab]	2.50[ab]	1.13
	Okinawan Purple	68.50[b]	58.80[a]	4.23	41.08[b]	1,308.30[a]	19.75[a]	15.50[a]	4.00[a]	2.25
	Purple Sweet Lord	60.00[c]	30.83[b]	2.48	45.51[a]	1,066.50[a]	16.25[a]	11.00[ab]	3.50[ab]	1.25

a Treatments at $p \leq 0.05$, derived from *LSD*.

High tuber yields, sufficient leaf area is necessary to provide by the onset of tuberization. This is the basic information to assess performance and adaptation particularly in areas with short growing seasons before leaf senescence. Also, the vegetative growth of Okinawan Purple grown in Nong Ruea district had the longest vine length of 58.80 cm with leaves area per plant for photosynthesis higher than Honey Sweet, thus giving the most biomass. Sweet potato, like any other root crop, is a heavy feeder exploiting a greater volume of soil for nutrients and water. It was found that the leaf part of Purple Sweet Lord and Okinawan Purple accumulated nitrogen, phosphorus and potassium more than Okinawan Orange and Honey Sweet, respectively (Table 3) in Phu Wiang district. Also, nitrogen and potassium accumulated more in the stem part, while Okinawan Purple and Orange accumulated more nitrogen, phosphorus and potassium in Nong Ruea district.

Table 3. Macronutrients content of sweet potatoes at 1 month of growing

Field experiment	Sweet potato	Leaf			Stem		
		N (%)	P (%)	K (%)	N (%)	P (%)	K (%)
Phu Wiang district	Honey Sweet	2.92^{c}	0.16^{c}	3.24^{c}	1.28^{c}	0.25^{a}	4.71^{d}
	Okinawan Orange	3.48^{b}	0.17^{b}	3.01^{d}	1.20^{d}	0.18^{b}	4.90^{c}
	Okinawan Purple	4.02^{a}	0.20^{a}	3.43^{b}	1.82^{b}	0.17^{c}	5.52^{b}
	Purple Sweet Lord	4.10^{a}	0.20^{a}	3.87^{a}	2.27^{a}	0.16^{d}	6.13^{a}
Nong Ruea district	Honey Sweet	3.18^{b}	0.17^{b}	1.18^{d}	2.10^{b}	0.14^{a}	2.07^{d}
	Okinawan Orange	2.45^{c}	0.19^{a}	1.83^{b}	2.28^{a}	0.14^{a}	2.84^{a}
	Okinawan Purple	3.57^{a}	0.16^{c}	2.89^{a}	1.89^{c}	0.11^{b}	2.20^{c}
	Purple Sweet Lord	3.35^{b}	0.15^{d}	1.40^{c}	1.49^{d}	0.09^{c}	2.37^{b}

a Treatments at $p \leq 0.05$, derived from *LSD*.

After 2 months of transplanting, the vine lengths of all sweet potatoes in Phu Wiang and Nong Ruea districts increased due to the length of the node (Table 4), especially Purple Sweet Lord, followed by Okinawan Purple and Okinawan Orange. As a result, the biomass of leaf and stem increased at 1 month from transplanting, despite the decrease in leaf area for photosynthesis per plant in Phu Wiang district. But in Nong Ruea district, the leaf area for photosynthesis per plant increased in all sweet potatoes compared to 1 month from transplanting. Okinawan Orange in both fields still had the highest accumulation of nitrogen in the leaf and stem part (Table 5). Potassium accumulation of all sweet potatoes in Nong Ruea district increased compared to 1 month from transplanting, especially Purple Sweet Lord which accumulated 5.09% of potassium. Alternately, the potassium accumulation of all sweet potatoes in Phu Wiang district tended to decrease. This may be linked to the tuber formation of sweet potatoes in Phu Wiang district beginning before sweet potatoes in Nong Ruea district. Early bulking maturity implies an ability to produce a high yield of tubers and allows avoiding biotic and abiotic stresses (Novikova et al., 2021).

Table 4. Growth of sweet potatoes at 2 months of growing

Field experiment	Sweet potato	Vine Length (cm)	Nodes Length (cm)	SPAD	Leaf Area/ Plant (cm^2)	Leaf Fresh Weight/ Plant (g)	Stem Fresh Weight/ Plant (g)	Leaf Dry Weight/ Plant (g)	Stem Dry Weight/ Plant (g)
Phu Wiang district	Honey Sweet	31.28^{b}	1.55^{c}	41.43^{b}	448.39^{b}	31.75^{c}	33.50^{b}	22.65^{b}	19.77^{b}
	Okinawan Orange	65.68^{a}	3.30^{b}	39.43^{b}	527.86^{ab}	39.50^{bc}	66.75^{a}	21.65^{b}	24.40^{a}
	Okinawan Purple	98.25^{a}	4.73^{a}	39.73^{b}	546.65^{a}	44.75^{ab}	57.75^{a}	23.50^{b}	23.35^{a}
	Purple Sweet Lord	96.95^{a}	3.53^{ab}	47.42^{a}	608.32^{a}	51.50^{a}	64.50^{a}	25.63^{a}	23.73^{a}
Nong Ruea district	Honey Sweet	28.93^{c}	1.16^{b}	48.12^{ab}	667.60^{c}	31.75^{b}	34.25^{b}	20.33^{b}	19.32^{b}
	Okinawan Orange	89.75^{ab}	5.19^{a}	50.90^{a}	$1,268.50^{b}$	37.50^{ab}	55.50^{ab}	21.13^{ab}	21.75^{ab}
	Okinawan Purple	81.58^{b}	3.94^{a}	45.63^{b}	$1,566.10^{b}$	50.25^{a}	55.00^{ab}	24.20^{a}	21.88^{ab}
	Purple Sweet Lord	116.12^{a}	5.45^{a}	51.40^{a}	$2,141.90^{a}$	51.75^{a}	63.00^{a}	24.55^{a}	23.18^{a}

a Treatments at $p \leq 0.05$, derived from *LSD.*

Table 5. Macronutrients content of sweet potatoes at 2 months of growing

Field experiment	Sweet potato	Leaf			Stem		
		N (%)	P (%)	K (%)	N (%)	P (%)	K (%)
Phu Wiang district	Honey Sweet	2.57[c]	0.26[a]	2.87[a]	0.89[c]	0.40	3.51[d]
	Okinawan Orange	3.23[a]	0.18[b]	2.61[c]	0.85[c]	0.19	4.64[a]
	Okinawan Purple	2.56[c]	0.16[c]	2.18[d]	1.18[a]	0.16	3.64[c]
	Purple Sweet Lord	3.10[b]	0.18[b]	2.75[b]	0.99[b]	0.16	4.02[b]
Nong Ruea district	Honey Sweet	3.49[d]	0.14	2.31[d]	1.51[c]	0.10	4.90[b]
	Okinawan Orange	4.42[a]	0.18	2.86[a]	1.68[a]	0.07	3.34[d]
	Okinawan Purple	3.92[c]	0.17	2.43[c]	1.68[a]	0.08	4.17[c]
	Purple Sweet Lord	4.05[b]	0.17	2.63[b]	1.42[d]	0.07	5.09[a]

a Treatments at $p \leq 0.05$, derived from *LSD*.

To investigate planting of four sweet potato types in Phu Wiang and Nong Ruea district, Okinawan Orange gave the highest tuber yields at 15,515 and 8,080 kg ha^{-1} (Table 6), respectively, with the average number of tubers per plant being 3.75 and 4.50 tubers, respectively, and the average tuber length being between 12.90 and 17.52 cm. But Honey Sweet and Okinawan Purple grown in Nong Ruea district did not provide the tuber yield. Dimante & Gaile (2018) mention that under field conditions plant development was significantly affected by cultivar. The significantly different response of cultivars tested revealed the necessity for field performance after planting and more growing degree days required to emerge and tuberization, when compared to medium early and medium late cultivar. For the nutritional value after harvest, Okinawan Orange and Purple Sweet Lord in Phu Wiang district had the highest percentage of tuber moisture content at 74.98% and 74.64%, respectively, followed by Honey Sweet and Okinawan purple (Table 7). The highest percentage of tuber moisture content lowered the content of undissolved minerals (ash) than in sweet potatoes with a lower percentage of tuber moisture content. The Purple Sweet Lord has higher protein and carbohydrates followed by Okinawan Orange, Okinawan Purple and Honey Sweet. However, Okinawan Orange and Purple Sweet Lord had lower fiber in the tuber yield than Honey Sweet and Okinawan Purple; even Okinawan Orange is higher in fat than other varieties. In addition, the leaf biomass of Okinawan Orange and Purple Sweet Lord tend to produce more protein and carbohydrates (Table 8) while the stem biomass was higher in fiber than leaf biomass (Table 9).

Table 6. Yield components of sweet potatoes

Field experiment	Sweet potato	No. of Tubers/ Plant	Tuber Fresh Weight/ Hectare (kg)	Tuber Length (cm)	Tuber Diameter (cm)	Leaf Fresh Weight/ Hectare (kg)	Stem fresh weight/ Hectare (kg)	Leaf dry weight/ Hectare (kg)	Stem dry weight/ Hectare (kg)
Phu Wiang district	Honey Sweet	3.25	1,716.88^{c}	16.63^{a}	3.75	880.00^{c}	2,240.00^{c}	142.38^{c}	376.56^{b}
	Okinawan Orange	3.75	15,515.00^{a}	17.52^{a}	4.81	4,260.00^{b}	6,986.88^{bc}	468.81^{bc}	697.44^{b}
	Okinawan Purple	2.75	1,835.00^{c}	17.57^{a}	4.00	5,320.00^{b}	10,213.13^{ab}	829.38^{b}	1,697.13^{a}
	Purple Sweet Lord	4.25	10,260.00^{b}	11.19^{b}	4.48	8,506.88^{a}	14,946.88^{a}	1,363.25^{a}	1,932.25^{a}
Nong Ruea district	Honey Sweet	-	-	-	-	633.31^{b}	680.00^{b}	412.69	377.31
	Okinawan Orange	4.50^{a}	8,080.00^{a}	12.90	4.10	5,420.00^{a}	9,466.88^{a}	649.19	972.31
	Okinawan Purple	-	-	-	-	853.31^{b}	873.13^{b}	458.00	403.31
	Purple Sweet Lord	2.75^{b}	3,535.00^{b}	12.90	4.28	4,653.31^{a}	5,460.00^{ab}	690.13	630.94

a Treatments at $p \leq 0.05$, derived from *LSD*.

Table 7. Nutritional content of tuber sweet potatoes

Field experiment	Sweet potato	Fresh Moisture (%)	Ash (%)	Protein (%)	Fat (%)	Fiber (%)	Carbohydrate (%)
Phu Wiang district	Honey Sweet	72.91^{b}	4.07^{a}	2.35^{d}	0.39^{c}	7.77^{a}	82.03^{c}
	Okinawan Orange	74.98^{a}	3.59^{b}	3.50^{c}	1.69^{a}	3.62^{b}	86.43^{a}
	Okinawan Purple	70.47^{c}	4.01^{a}	3.87^{b}	0.69^{c}	8.11^{a}	80.47^{c}
	Purple Sweet Lord	74.64^{a}	3.15^{c}	5.33^{a}	1.28^{b}	3.15^{b}	84.46^{b}
Nong Ruea district	Honey Sweet	-	-	-	-	-	-
	Okinawan Orange	71.80	3.64^{a}	4.87^{b}	1.80^{a}	2.39^{b}	84.67^{b}
	Okinawan Purple	-	-	-	-	-	-
	Purple Sweet Lord	72.20	3.03^{b}	5.13^{a}	1.11^{b}	2.52^{a}	85.84^{a}

a Treatments at $p \leq 0.05$, derived from *LSD*.

Table 8. Nutritional content of leaf sweet potatoes

Field experiment	Sweet potato	Ash (%)	Protein (%)	Fat (%)	Fiber (%)	Carbohydrate (%)
Phu Wiang district	Honey Sweet	12.61^{c}	2.26^{c}	37.99^{a}	33.28^{d}	9.47^{b}
	Okinawan Orange	19.92^{a}	3.84^{a}	11.12^{c}	52.78^{b}	12.09^{a}
	Okinawan Purple	12.15^{d}	2.33^{c}	36.81^{b}	36.13^{c}	8.68^{c}
	Purple Sweet Lord	14.99^{b}	2.61^{b}	8.54^{d}	65.62^{a}	7.08^{d}
Nong Ruea district	Honey Sweet	-	-	-	-	-
	Okinawan Orange	24.76^{a}	3.52^{a}	10.17^{a}	49.41^{b}	11.45^{a}
	Okinawan Purple	-	-	-	-	-
	Purple Sweet Lord	23.36^{b}	3.16^{b}	8.77^{b}	56.55^{a}	7.48^{b}

a Treatments at $p \leq 0.05$, derived from *LSD*.

Table 9. Nutritional content of stem sweet potatoes

Field experiment	Sweet potato	Ash (%)	Protein (%)	Fat (%)	Fiber (%)	Carbohydrate (%)
Phu Wiang district	Honey Sweet	3.94^{b}	1.96^{c}	36.72^{a}	47.29^{d}	7.59^{b}
	Okinawan Orange	3.20^{d}	3.61^{a}	24.80^{d}	56.05^{b}	9.61^{a}
	Okinawan Purple	4.27^{a}	2.50^{b}	34.80^{b}	49.20^{c}	6.83^{c}
	Purple Sweet Lord	3.76^{c}	2.55^{b}	26.39^{c}	59.29^{a}	6.75^{c}
Nong Ruea district	Honey Sweet	-	-	-	-	-
	Okinawan Orange	7.48	2.29^{b}	21.15^{b}	55.48^{b}	10.71^{a}
	Okinawan Purple	-	-	-	-	-
	Purple Sweet Lord	7.41	3.27^{a}	22.42^{a}	57.43^{a}	8.02^{b}

a Treatments at $p \leq 0.05$, derived from *LSD*.

DISCUSSION

Present consumer preference for more nutritious foods, sweet potato has gradually improved as one of the most nutritious vegetables (Truong et al., 2018) with exciting colors and flavor profiles, for instance purple, cream and orange colors. The crop is now extended to northeast of Thailand with acid sandy soil and drought. However, sweet potato is recognized as adapted to cope to numerous types of soils and climates, especially warm-season with daily maximum air-temperatures between 29.7 °C and 35.3 °C for storage root production. Suitable soils texture for sweet potato production ranges from sand to loamy sand and low in salts. Recent studies have shown sweet potato can grow in heavy soils, but yield and quality can decrease (Duque et al., 2022). From the experiment, Okinawan Orange, Okinawan Purple and Purple Sweet Lord showed the longest vine length respectively. These differences in vine length might be attributed to

variation in the genotypes' genetic make-up and their interaction with the environment. Their performance varies from place to place due to genotype by environment interaction and this calls for specific area recommendation. Shamil (2021) discovered vine lengths ranging of sweet potato varieties could be from 135.2 cm to 175.1 cm. Similar to the study result of Nazrul (2018) also reported significant variation in sweet potato vine length which ranged from 119 cm to 192.3 cm among sweet potato varieties, this variability might be attributed to their growth traits. This indicates that it's could be used as a good vine source for vines sweet potato producing. While Honey Sweet had the lowest vine length in both fields. Moreover, the young vines and leaves of the crop can be eaten as vegetables for human consumption or given to animal due to proteins and minerals richness (Kebede et al., 2008).

Sweet potato canopy is the main source of photosynthetic material that will be distributed to tubers production (Rahmawati et al., 2020). In this study, variety with medium vine length (Okinawan Orange) produced maximum storage root yield. This might be due to the growth in vine length up to optimum stage may improve storage root yield up to some point through increased leaf number that photosynthesize and accumulate more dry matter. However, excess vine length growth may result in reduced storage root yield which could be attributed to most of the assimilates produced used in leaf and vine growth instead of tuber growth as a consequence of higher competition for assimilates. At the beginning of growth stage, Okinawan Orange produced the largest leaf area, followed by Purple Sweet Lord, its were also moderate vine length in the trials during establishment in the field for sunlight and carbohydrate synthesis than those with a small leaf area (Van den Berge et al., 2004; Ahmed et al., 2012; Kareem, 2013). This is an opportunity of the tubers crop for the highest yield and quality from weeds (Laurie & Niederwieser, 2004; Moyo et al., 2004; Ministry of Agriculture & Food Security, 2007; Workayehu et al., 2011). Usually, storage root formation started between the 30th and 60th DAP. Then vegetative growth and rapid storage root during 60th and 90th DAP refer to the different genetic potential to form tubers. The environment and technical culture also influenced on number of sweet potato tubers. Generally, Okinawan Purple and Purple Sweet Lord are well varieties on root growth, if farmers can't remove the vines in time, this sweet potato will provide a lot of roots with incomplete tubers. Moreover, fibrous roots formation was re-direct photosynthates towards than storage roots with temperatures greater than 28 °C (Eguchi et al., 2003). During the experimental run, the maximum and minimum temperatures were 31.67 and 25 °C in Phu Wiang District and 32 and 25 °C in Nong Ruea District. High temperatures increase of gibberellic acid (GA) and trigger Indoleacetic Acid (IAA) oxidase activity, these causes to promote vine growth and storage root formation decrease (Kelm et al., 2000).

Along with the growing period from April to June with high temperature and rainy before harvesting in both fields, provided some stress environment for storage root growth and productivity. The sweet potato cultivars were grown in Nong Ruea district tended to slowly for root yield formation and roots yield rarely reached full size even genetic constituents. While Honey Sweet was consistently the lowest tuber yielding variety according to its shortest vine length. Storage roots yield significantly different due to genotypes also reported in other sweet potato trials (Rahmawati et al., 2020; Dawit & Habte 2023). High acidity induces nutrient deficiency which causes yield potential of

different genotypes by tuber yield reduction. Phu Wiang district showed the highest tuber yield across genotypes under suitable soil pH for nutrients absorption and the suitable available P and exchangeable K, while the yield at Nong Ruea district was the lowest. Tuber yield was related to tuber size and tubers number which are affected by soil fertility conditions (Dawit & Habte 2023). Our results showed that Okinawan Orange produced significantly different average tuber fresh weights, starch content, fat content and tuber moisture content. The growing sites influences the yield and quality of tubers which causes a very significant decrease in the parameters of tuber weight, tuber length, protein content, starch content and tuber water content. Stated that the high production of Okinawan Orange is able to adapt to the environment. The genetic potential is very supportive in the success of farming, means Okinawan Orange converted more its photosynthetic products to roots carbohydrates stored. Tuber moisture content is a parameter influenced by the availability of water that can be absorbed by the roots to meet plant needs. Additionally, genotype and location had a substantial influence on sweet potatoes productivity in Khon Kaen province, northeast of Thailand. Our study clearly revealed that the farmer should select suitable sweet potato cultivars for the field, since all introduced cultivars were popular in market demand. Among the introduced genotypes, Okinawan Orange look interesting for farmer fields to increase an income as its higher total tuber root yield under the same investment. Despite its importance and suitability to the agro-ecology of the region including the presence of suitable soil type, temperature and rainfall for sweet potato production. However, further adaptation studies should be investigated in new areas for more acceptable, stability of yield production, β-carotene content, sweetness and flavor as potentially useful.

CONCLUSIONS

Yields of four sweet potato types under acid sandy soil in Phu Wiang and Nong Ruea district, Khon Kaen province, Northeast of Thailand were significantly lower than approximately 80–100 t ha^{-1}. Okinawan Orange provided the maximum yield weight of 15,515 kg ha^{-1} in Phu Wiang district and 8,080 kg ha^{-1} in Nong Ruea district. Okinawan Orange provided the highest tuber root yield and showed stability in the trial. For tuber production, Okinawan Orange seem to be beneficial to grow in the northeast Thailand. Some promising lines with the large leaf area and longer vines such as Okinawan Purple and Purple Sweet Lord, were benefit for vine production. However, studies have also shown that sweet potato have high uptake of soil nutrients, which could possibly cause soil deterioration. Then the farmer should manage fertilizer properly for sweet potato production.

ACKNOWLEDGEMENTS. This research operated as part of the Plant Genetic Conservation Project under The Royal Initiative of Her Royal Highness Princess Maha Chakri Sirindhorn, Khon Kaen University. This study was fully supported by Innovation and Enterprise Affairs, Khon Kaen University. We wish to express our sincere gratitude to the Northeast Agriculture Research and Development Centre in the Faculty of Agriculture at Khon Kaen University, Thailand.

REFERENCES

Ahmed, M., Nigussie-Dechassa, R. & Abebie, B. 2012. Effects of planting methods and vine harvesting on shoot and tuberous root yields of sweet potato (*Ipomoea batatas* (L.) Lam.) in the afar region of Ethiopia. *Afric. J. Agric. Res* **7**(7), 1129–1141.

Amede, T., German, L., Rao, C., Opondo, C. & Stroud, A. 2006. Integrated natural resource management in practice: enabling communities to improve mountain livelihoods and landscapes. In: Proceedings of the African Highland Initiative Conference, October, 2004, pp. 1215.

CSA (Central Statistical Agency). 2014. Crop production forecast sample survey, 2013/14. In: *Report on Area and Production for Major Crops* (for Private Peasant Holdings 'Meher' Season). Addis Ababa, Ethiopia.

Dawit, M. & Habte, A. 2023. Yield and profitability of sweet potato (*Ipomoea batatas* (L.) Lam) as a function of increasing levels of phosphorus and varieties in southern Ethiopia. *Applied and Environmental Soil Science*. https://doi.org/10.1155/2023/2716227

Dimante, I. & Gaile, Z. 2018. Assessment of potato plant development from Minitubers. *Agron. Res* **16**(4), 1630–1641.

Duque, L.O., Sánchez, E., Pecota, K. & Yencho, C. 2022. A win–win situation: performance and adaptability of petite sweetpotato production in a temperate region. *Horticulturae* **8**, 172. https://doi.org/10.3390/horticulturae8020172

Eguchi, T., Kitano, M., Yoshida, S. & Chikushi, J. 2003. Root temperature effects on tuberous root growth of sweet potato (*Ipomoea batatas* (L)). *Env. Cont. Biol.* **41**, 43–49.

FAO. 2008. Corporate Document Repository. The impact of HIV/AIDS on the agricultural sector. Retrieved 2015 February 28 from http://www.fao.org/docrep/005/Y4636E/y4636e05.htm

Fernandes, A.M., Natália, S.A., Nathalia, P.R., Bruno, G. & Rudieli Machado, S. 2020. Nutrient uptake and removal by sweet potato fertilized with green manure and nitrogen on sandy soil. *Rev. Bras. Cienc. Solo* **44**.

Gurmu, F. & Mekonen, S. 2017. Registration of a newly released sweet potato variety 'Hawassa-09' for production in Ethiopia. *Agrotechnology* **6**(2), 1–3.

Ji, H., Zhang, H., Li, H. & Li, Y. 2015. Analysis on the nutrition composition and antioxidant activity of different types of sweet potato cultivars. *Food Nutr Sci*. **6**, 161.

Kandel, B.P. 2020. Spad value varies with age and leaf of maize plant and its relationship with grain yield. *Kandel BMC Res Notes* **13**, 475. https://doi.org/10.1186/s13104-020-05324-7

Karan, Y.B. & Şanli, O.G. 2021. The assessment of yield and quality traits of sweet potato (*Ipomoea batatas* L.) genotypes in middle Black Sea region, Turkey. *PLoS ONE* **16**(9), e0257703. https://doi.org/10.1371/journal. pone.0257703

Kareem, I. 2013. Effects of phosphorus fertilizer treatments on vegetative growth, tuberous yield and phosphorus uptake of sweet potato (*Ipomoea batatas*). *Afri. J. Agric. Res* **8**(22), 2681–2684.

Kelm, M., Brück, H., Hermann, M. & Sattelmacher, B. 2000. Plant productivity and water use efficiency of sweet potato (*Ipomoea batatas* (L)) as affected by nitrogen supply. CIP program report, pp. 273.

Laurie, S.M. & Niederwieser, J.G. 2004. The sweet potato plant. In: Niederwieser JG (Ed). *Guide to sweet potato production in south africa*. ARC-Roodeplaat Vegetable and Ornamental Plant Institute, Pretoria, South Africa, pp. 7–14.

Ministry of Agriculture & Food Security (MoAFS). 2007. *Cassava and sweet potato production handbook*. Lilongwe, Malawi, pp. 23–39.

Moyo, C.C., Benesi, I.R.M., Chipungu, F.P., Mwale, C.H.L., Sandifolo, V.S. & Mahungu, N.M. 2004. Cassava and Sweet Potato Yield Assessment in Malawi. *Afric. Crop Sci. J.* **12**(3), 295–203.

Murdock, L, Jones, S, Bowely, C, Needham, P, James, J & Howe, P. 1997. *Using a chlorophyll meter to make nitrogen recommendations on wheat*. Cooperative Extension Service University of Kentucky-college of Agriculture. http://www2.ca.uky.edu/agcomm/pubs/agr/agr170/agr170.pdf

Nazrul, M.I. 2018. On-farm evaluation of orange fleshed sweet potato varieties under acidic soil of north-east region in Bangladesh. *Bangladesh Agron J.* **21**(2), 59–65.

Novikova, L. Yu., Chalaya, N.A., Sitnikov, M.N., Gorlova, L.M., Kiru, S.D. & Rogozina, E.V. 2021. Dynamics of tuber weight in early potato varieties in the contrasting weather conditions of the Northwestern Russia. *Agron. Res.* **19**(1), 185–198.

Popradit, A. 2021. Yield response and soil nutrient change of sweet potato varieties to different fertilization treatments. *Thai Environ. Eng. J.* **35**(2), 29–37.

Rahmawati, N., Lahay, R.R., Irmansyah, T. & Mawarni, L. 2020. Yield and tuber quality of orange-fleshed sweet potato cultivars under drought stress in greenhouse. *International Conference on Agriculture, Environment and Food Security* (AEFS) 2019. IOP Conf. Series: Earth and Environmental Science **454**. doi:10.1088/1755-1315/454/1/012159

Shamil, A.S. 2021. Evaluation of sweet potato (*Ipomoea batatas* (L) Lam) varieties at tepi, southwestern Ethiopia. *World J. Agric. Soil Sci.* **6**(4), 1–4.

Simson, R., Tartlan, L., Nugis, E. & Eremeev, V. 2016. The effect of fertilizer and growing season on tuber dry matter and nitrate content in potato. *Agron. Res.* **14**(4), 1486–1493.

Teow, C.C., Truong, V.D., McFeeters, R.F., Thompson, R.L., Pecota, K.V. & Yencho, G.C. 2007. Antioxidant Activities, Phenolic and B-carotene Contents of Sweet Potato Genotypes with varying Flesh Colours. *Food Chem* **103**, 829–838.

Troncoso, E. & Pedreschi, F. 2009. Modeling water Loss and oil uptake during vacuum frying of pre-treated potato slices. *LWT - Food Sci. Technol. J.* **42**(6), 1164–1173.

Truong, V.D., Avula, R.Y., Pecota, K.V. & Yencho, G.C. 2018. Sweetpotato production, processing, and nutritional Quality. In Handbook of Vegetables and Vegetable Processing; John Wiley and sons Ltd.: New York, NY, USA, pp. 811–838.

Van den Berge, A.A. & Laurie, S.M. 2004. Cultivation. In: niederwieser JG (Ed). Guide to sweet potato production in south africa, ARC-Roodeplaat vegetable and ornamental plant institute, Pretoria, South Africa, pp. 15–27.

Workayehu, T., Mangezia, W. & Hidoto, L. 2011. Growth habit, plant density and weed control on weed and root yield of sweet potato (*Ipomoea batatas* L.), Areka, Southern Ethiopia. *J. Hort. and For* **3**(8), 251–258.

Agronomy Research **21**(S3), 1555–1566, 2023
https://doi.org/10.15159/AR.23.084

Preliminary study on the potential use of RPA images to quantify the influence of the defoliation after coffee harvesting to its yield

L.M. dos Santos[1,*], G.A.S. Ferraz[1], M.A.F. Carvalho[2], M.S. Vilela[3] and P.H.O. Estima[1]

[1]Federal University of Lavras, Department of Agricultural Engineering, University Campus, BR37.200-000 Lavras-MG, Brazil
[2]Embrapa Café, Brasília BR70770-901, Distrito Federal, Brazil
[3]Federal University of Lavras, Department of Agronomy/ Phytotechnics, University Campus, BR37.200-000 Lavras-MG, Brazil
[*]Correspondence: luanna_mendess@yahoo.com.br

Received: January 24th, 2023; Accepted: May 22nd, 2023; Published: September 18th, 2023

Abstract. Coffee is an agricultural commodity with global commercial importance capable of impacting the production chain. The quantification of defoliation at harvest is important for monitoring crop yield because defoliation is one of the main types of damage caused by this agricultural operation in coffee crops. Thus, the objective of this study was to evaluate the relationship between yield and defoliation obtained in the field and obtained through remotely piloted aircraft (RPA) images. The experiment was conducted in a coffee plantation belonging to the Federal University of Lavras (UFLA), Lavras, Minas Gerais state, Brazil. An RPA with a rotary wing containing a multispectral camera was used in autonomous flight mode with a height of 30 m, an image overlap of 80%, and a speed of 3 m s^{-1}. The images were collected before and after the 2020 and 2021 harvest, defoliation data obtained in the field were measured in 2020 and 2021, and the yield was measured from 2019 to 2021. Image processing was performed in the software PhotoScan, postimage processing was performed in QGIS, and statistical analyses were performed using the software R. With the processing of the images in 2020, the crop showed reductions of 17.3% and 18.4% in leaf area and volume, respectively, after harvest. In 2021, the crop showed reductions of 12.8% and 9.8% in leaf area and volume, respectively, after harvest. The leaf area and leaf volume of the coffee plantation after harvest could be quantified by means of images obtained by RPA, which allowed the observation of the loss of area and volume of the coffee plantation. Furthermore, it was possible to analyse the interactions between field data and the yield of the same harvest year, which were directly proportional, and the interaction of image data from one year with the previous yield, which were inversely proportional. In the year 2020, there was a reduction of 17.3% in leaf area after harvest, and a reduction of 18.4% in leaf volume after harvest in the plots under study.In the processing carried out in 2021, there was a 12.8% reduction in leaf area after harvest, and a 9.8% decrease in leaf volume after harvest in the plots under study.

Key words: canopy volume, coffea arabica l., digital image processing, harvest, systems of unmanned aircraft.

INTRODUCTION

Coffee is an agricultural commodity of global importance with the ability to impact the production chain. The estimated global coffee production for the 2020/2021 harvest was 175.5 million bags (60 kg). Brazil significantly participates in this sector; it contributes the greatest proportion at approximately 38.6% of the world coffee production (USDA, 2021). This makes Brazil the largest producer and exporter of Coffea arabica and the second largest producer of Coffea canephora of the global production of this cultivar.

These data reflect the significant economic and social importance of this culture for Brazil. In addition, due to the growing global demand for specialty coffees, it is necessary to develop productive techniques and culture monitoring to differentiate Brazilian producers. However, this culture undergoes oscillations such as those cited by Silva et al. (2010), in which factors such as crop management can also cause spatial and temporal variations in the crop.

The quantification of defoliation at harvest is important for monitoring crop yield because it is one of the main types of damage caused by this agricultural operation in the coffee crop. Defoliation causes the plant to produce less in the following year because it uses its reserves to recompose its vegetation, which results in less fruit (Silva et al., 2010). Thus, frequent defoliation induces plant stress and reduces plant longevity (Bártholo & Guimarães, 1997; Oliveira et al., 2007).

Precision agriculture combined with computational tools has been studied and widely disseminated in terms of coffee crops. According to Amaral et al. (2020), sensors and applications in remote sensing (RS) at all levels (orbital, aerial and terrestrial) have significantly evolved; however, at the aerial level, remotely piloted aircraft (RPA) were one of the most developed tools in recent years. This tool captures images with high spatial resolution (with a spatial resolution on the order of mm, depending on the flight height) and high temporal resolution (it is possible to use RPA whenever there are good climatic conditions and sufficient battery life) that can be processed by using the Structure from Motion (SfM) algorithm.

SfM is based on the principles of traditional stereoscopic photogrammetry, using the overlapping of multiple images obtained by conventional cameras to obtain geometric characteristics and generating a 2D and 3D point cloud (Martínez-Carricondo et al., 2018; Santos et al., 2020a). The point cloud facilitates the generation of a digital surface model (DSM) and digital elevation model (DEM); these products can be used for the production of orthophoto mosaics, 3D modelling, and metric information such as area, volume, and height (Nex & Remondino, 2014; Santos et al., 2020a).

In this context, the use of RPA has enabled the collection of data for estimating morphological parameters (Santos et al., 2020a; Barbosa et al., 2021), crop coefficients (Kc) (Santos et al., 2020b), and leaf area indexes (Santos et al., 2020c), volume (Cunha et al., 2019) and for monitoring leaf nitrogen (Parreiras et al., 2020; MARIN et al., 2021b), frost damage (MARIN et al., 2021a), and fruit ripening (Martins et al., 2021).

Cunha et al. (2019) developed a methodology to determine the vegetation volume of coffee crops from RPA images and compared this approach with the traditional estimate of vegetation volume (the tree row volume (TRV) method). The authors studied this method under normal crop conditions to obtain the volume for defining pesticide application techniques. These authors concluded that the vegetation volume of coffee plants can be

determined in a practical and accurate manner by digital processing of the images captured by RPA because it is a fast method that allows the evaluation of large areas.

However, the quantification of the area and volume of coffee crops after harvest using images obtained by RPA to obtain defoliation have not been explored. Based on this, we hypothesize that it is possible to quantify the area and volume of coffee crops before and after harvest to obtain defoliation by using RPA; this would be useful for supporting studies on the biennial production and yield of crops that undergo this agricultural operation. In this sense, the objective was to evaluate the relationship between yield and defoliation obtained in the field and obtained through RPA images.

MATERIALS AND METHODS

Study area

We conducted the experiment in an area of 0.48 ha in an experimental coffee plantation (Coffea arabica L.) belonging to the Coffee Plant Sector of the Department of Agriculture (DAG, for its acronym in Portuguese) of the Federal University of Lavras (UFLA), in Lavras - MG. We used the cultivar 'Mundo Novo 379-19'; this cultivar was planted in January 2016, with a spacing of 3.6 metres between the planting rows and 0.75 metres between the plants, and its treatments are described by Castanheira et al. (2019) and Alecrim et al. (2020).

The geographic coordinates of the area are 21°13'36.47" South latitude and 44°57'40.35 West longitude, with a mean altitude of 975 metres, the terrain under study has a 2% slope (Fig. 1).

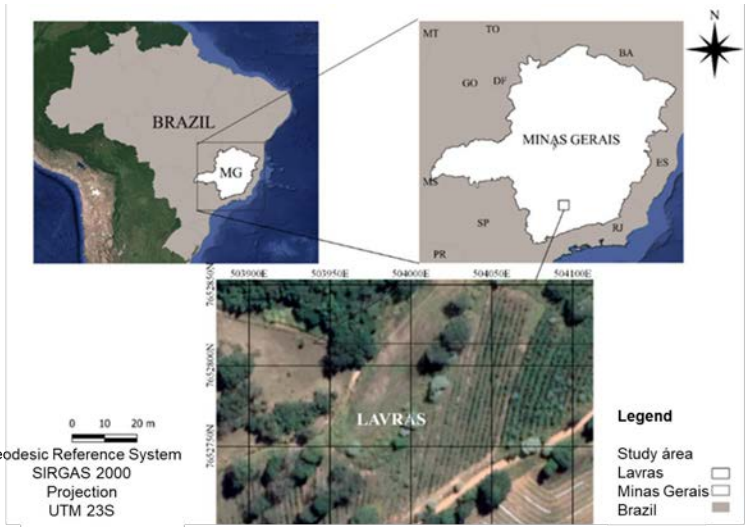

Figure 1. Delimitations of the state of Minas Gerais, the municipality of Lavras, and the study plot.

We used a total of 90 experimental plots, in which each experimental plot consisted of six plants, with four central plants being considered useful plants. We used a border row between the treatment rows to avoid interference. We georeferenced the study area, the sampled plots, and control points with the aid of a differential global positioning system (DGPS) (Trimble Navigation Limited, Sunnyvale, California, USA) with horizontal and vertical accuracy of 0.007 m.

Acquisition and processing of RPA images

In this study, we used a quadcopter (Matrice 100, DJI) equipped with a high spatial resolution multispectral camera (Parrot SEQUOIA) carrying a payload of 72 g as the RPA platform to capture images in the visible range of the RGB spectrum (red - R, green - G and blue - B) and images in nonvisible spectral ranges such as red edge (REG) and near infrared (NIR).

The RGB camera had a resolution of 16 megapixels with a lens focal length of 5 mm. In addition, the camera had another 1.2-megapixel sensor with a focal length of 4 mm and captured the four spectral bands of G (wavelength of 530–570 nm), R (wavelength of 640–680 nm), REG (wavelength of 730–740 nm), and NIR (wavelength of 770–810 nm), which were not used in the present study.

We collected images simultaneously from a flight altitude of 30 m above ground level, with 80% frontal and lateral overlap, at speeds of 3 m s^{-1}, according to the methodology of Santos et al. (2020a), and obtained a spatial resolution of 0.86 cm with the RGB camera.

Four flights were performed, the first before harvest on 1st of May 2020, the second after harvest on 8th of May 2020, the third before harvest on 1st of May 2021, and the fourth after harvest on 12th of May 2021. The images were collected around noon, with clear and sunny skies, to minimize the effects of clouds and the generation of shadows in the images.

The images were processed in PhotoScan Professional 1.4.0 software (Agisoft LLC, St. Petersburg, Russia) (Table 1), following the available processing workflow, in which the photos were geometrically aligned to build the point cloud, 3D model, digital terrain model (DTM), DSM, and orthomosaic.

Table 1. Data of RPA image processing

Information	Preharvest	Postharvest	Preharvest	Postharvest
Date (dd/mm/yy)	01/05/2020	08/05/2020	01/05/2021	12/05/2021
Time (duration)	8 min 52 s			
Number of images	120	121	119	120
Flight height (m)	30			
Data size (GB)	1.03	1.08	1.08	1.02
Processing time (h)	5.47	6.14	4.88	5.44
Software platform	Microsoft Windows 7 (64 -bit)			
Spatial resolution (cm/pixel)	1.03	1.13	1.04	1.01
Reprojection error (RMS) (pixel)	1.34	1.43	1.81	1.84

We georeferenced the orthomosaics using the second-order polynomial transformation with the nearest neighbour resampling method, using 6 control points (CPs) distributed in the area. We adopted the Geocentric Reference System for the Americas (SIRGAS 2000) and the Universal Transverse Mercator (UTM) projection (zone 23S). We used the software QGIS version 3.10 (Quantum GIs) for preprocessing and map preparation.

We determined the plant height by using a raster calculator in QGIS, in which we obtained a canopy height model (CHM) by subtracting the DTM from the DSM according to the methodology used by Santos et al. (2020a), Panagiotidis et al. (2017), and Iizuka et al. (2017).

We used the raster volume surface plugin in the QGIS to obtain the area and volume of the crop in each of the 90 experimental plots under study. This algorithm calculates the volume above the base level of the CHM surface. The algorithm generates the calculated volume, the total area, and the total number of pixels analysed. The plots of the area and the calculated volume depend on the coordinate reference system of the input raster file. Thus, as the projection system used was UTM (in metres), we present the CHM height (in metres) and the calculated values for the area and for the volume in m^2 and m^3, respectively.

We obtained the defoliation data of the aircraft in area (DAA) (m^2/plant) and the defoliation data of the aircraft in volume (DAV) (m^3/plant) by subtracting the data obtained for area and volume before and after harvest and dividing it by the number of useful plants in each experimental plot, using an Excel spreadsheet.

Field data collection

We collected coffee production data from each experimental plot (L/plot) in 2019 and 2020. We obtained these data by manual harvesting onto a canvas; after the removal of twigs and leaves, we performed shaking and collected the fruits in a container graduated in litres. With this measurement, we obtained the yield (L/plant) (Y-2019 and Y-2020) as the mean of the useful plants of each experimental plot.

When harvesting onto a canvas, we removed and weighed the leaves that fell on the canvas due to this process. We obtained the field defoliation based on the leaf fresh weight (FDW) (kg) after manual harvest using a portable scale up to 12 kg, following the methodology of Silva et al. (2010). With this measurement, we obtained the defoliation (kg/plant) as the mean defoliation of the useful plants of each experimental plot. We obtained the yield and defoliation samples on 7th of May 2020.

We obtained the coffee production of each experimental plot (L/plot) of the harvest performed in 2021 by semimechanized harvesting using portable harvesters. When harvesting onto the canvas, we removed and weighed the leaves and twigs that fell on the canvas due to this process. With this measurement, the yield of useful plants (L/plant) was obtained (Y-2021). We obtained field defoliation was obtained based on the fresh weight of leaves and twigs (FDW) (kg) using a portable scale up to 12 kg following the methodology of Bordin et al. (2019). We measured the field defoliation based on the volume of fresh leaves and twigs (FDV) (L) in a 14 L bucket. We adopted this methodology to evaluate the correlation between the defoliation data in the field and the data obtained from the RPA images. With these measurements, we obtained defoliation (kg/plant and L/plant). We obtained the yield and defoliation samples on 11th of May 2021.

The Pearson correlation was applied to all variables studied, Y-2019, DAA-2020, DAV-2020, FDW-2020, Y-2020, DAA-2021, DAV-2021, FDW-2021, FDV-2021, and Y-2021, to evaluate the relationships between them. To verify the significance, we adopted $\alpha = 5\%$ (correlation coefficient). We calculated the residuals as the difference between defoliation and yield and calculated the mean absolute error (MAE), as well as the root mean square error (RMSE). We performed descriptive statistical analyses using the statistical software R (R Core Team, Vienna, Austria).

RESULTS AND DISCUSSION

There were significant ($p \leq 0.05$) and insignificant ($p > 0.05$) variations between the variables studied. Given this result, this study considered only the analyses with positive and/or negative significant variations, which are highlighted in bold in Table 2.

Table 2. Pearson correlation coefficients of the study variables; the significant relationships are in bold

	Y-2019	DAA-2020	DAV-2020	FDW - 2020	Y-2020	DAA-2021	DAV-2021	FDW - 2021	FDV - 2021	Y-2021
Y-2019	- -									
DAA -2020	-0.25	- -								
DAV-2020	-0.10	0.63	- -							
FDW-2020	0.04	-0.13	0.00	- -						
Y-2020	0.15	-0.14	-0.06	0.56	- -					
DAA-2021	-0.11	0.17	0.13	-0.25	-0.17	- -				
DAV-2021	-0.15	0.16	0.15	-0.19	-0.19	0.87	- -			
FDW-2021	0.01	0.13	0.15	0.41	0.12	0.15	0.14	- -		
FDV-2021	0.13	0.09	0.19	0.34	0.15	0.20	0.18	0.70	- -	
Y-2021	0.14	-0.02	0.16	0.06	-0.25	0.28	0.21	0.54	0.72	- -

Defoliation data of the aircraft in area (DAA) (m^2/plant); defoliation data of the aircraft in volume (DAV) (m^3/plant); field defoliation obtained based on leaf fresh weight (FDW-2020) (kg/plant); field defoliation obtained based on the fresh weight of leaves and twigs (FDW-2021) (kg/plant); field defoliation obtained based on the volume of fresh leaves and twigs (FDV-2021) (L/plant), and Y-yield (L/plant).

Therefore, we analysed the relationships between Y-2020 and FDW-2020; Y-2021 and FDW-2021; and Y-2021 and FDV-2021, and these correlations were statistically adequate for analysing the relationships between field defoliation and yield. We used the relationships between Y-2019 and DAA-2020; Y-2020 and DAA-2021; and Y-2020 and DAV-2021 to analyse the defoliation obtained by the aircraft and yield. Notably, there were no significant correlations between the defoliation obtained in the field and the defoliation obtained by the aircraft, this result can be attributed to the fact that the field methodology is not ideal for quantifying defoliation, as recent RPA research shows the potential of this type of data collection capable of estimating the entire area and not just the sampled plants as in the field methodology.

The study developed by Cunha et al. (2019), in which the authors state that the use of manual methods in large areas becomes costly, time-consuming and may possibly generate inaccurate data. In addition to the samples being random, the number may not be representative, unlike the digital image processing method, the sample sizes can vary and the results are more accurate. In addition, the correlation between DAV-2020 and DAA-2020 showed strong and positive correlations ($R = 0.63$) and the relationships between DAV-2021 and DAA-2021 ($R = 0.87$) were expected as the methodology uses the CHM to obtain the area and volume of the processed images (Santos, et al., 2020a). The relationship between FDV-2021 and FDW-2021 ($R = 0.70$) was another expected result because these variables represent field data from the same year measured differently.

Analysis of field defoliation and yield

After manual harvesting, FDW-2020 showed values from 0 to 0.64 kg/plant, as shown in Table 3. The defoliation values observed in the present study were close to those found by Silva et al. (2000), approximately 0.64 kg/plant. Silva et al. (2010) found plant defoliation values caused by manual harvesting from 0 to 0.9 kg/plant.

After the semimechanized harvest, FDW-2021 showed values from 0 to 4 kg/plant, as shown in Table 3. Notably, FDW-2021 was higher than FDW-2020 due to the amount of twigs and leaves that fell on the canvas due to the harvesting process. However, these measurements cannot be compared because they were obtained at different time points and used different methodologies.

Table 3. Exploratory data analysis

	2020		2021	
Statistics	FDW (kg/plant)	Yield (L/plant)	FDW (kg/plant)	Yield (L/plant)
Minimum	0	0	0	0
1st Quartile	0.01	2.38	0.1	0.1
Median	0.06	4.67	0.38	1.71
Mean	**0.08**	**4.59**	**0.45**	**3.64**
3rd Quartile	0.13	6.71	0.72	5.67
Maximum	0.64	13	4	26

Field defoliation obtained based on leaf fresh weight (FDW-2020) (kg/plant); field defoliation obtained based on the fresh weight of leaves and twigs (FDW-2021).

Y-2020 showed values ranging from 0 to 13 L/plant, and Y-2021 showed values ranging from 0 to 26 L/plant (Table 3). When observing the two harvests, we noted that 2020 had a high crop yield, and the mean yield was higher than that in 2021. In 2021, the crop had a 20% lower yield than that of the previous year, and low crop yield was attributed to 2021.

The yield values found in this study were consistent with the study conducted by Ferraz et al. (2012), who studied a crop 2 years and seven months in age and found yield values from 0.025 to 3.95 L/plant. Conversely, the study by Silva et al. (2010) found yield values from 0 to 11.8 L/plant in a 16-year-old crop.

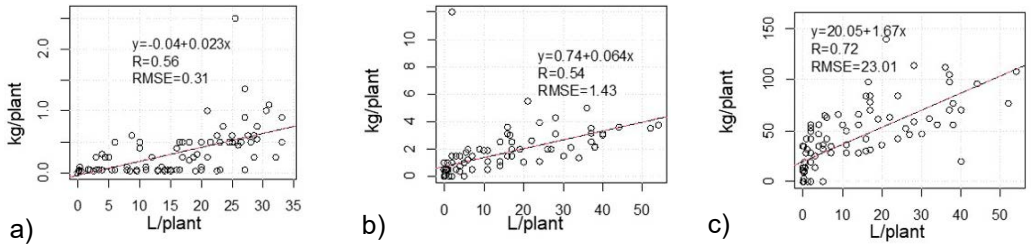

Figure 2. Regression and correlation: a) Y-2020 and FDW-2020; b) Y-2021 and FDW-2021, and c) Y-2021 and FDV-2021.

The interaction between Y-2020 and FDW-2020 was moderate and positive at 56% (Fig. 2, a), as well as the interaction between Y-2021 and FDW-2021 at 54% (Fig. 2, b) and the interaction between Y-2021 and FDV-2021 at 73% (Fig. 2, c). Such positive correlation results indicate that the yield is directly proportional to the defoliation of the

same year; thus, the higher the yield is, the greater the defoliation as a function of the harvest. These results corroborate the study conducted by Oliveira et al. (2007), in which the authors concluded that an increase in the volume of harvested grains was proportional to an increase in defoliation.

Defoliation is the main type of damage caused in coffee plants by the action of harvesting. With defoliation, the plant produces less in the following year since it uses its reserves for the restoration of vegetation and, consequently, produces less fruit (OLIVEIRA et al., 2007). Studies performed by Silva et al. (2010) found that manual harvesting resulted in more defoliation in places of higher yield and reduced yield in the subsequent year, as also observed in this study. This is due to the loss of leaf area and the reduction in the photosynthetically active area characteristic of the crop.

Analysis of defoliation obtained by aircraft and yield

We found significant correlations at the 5% significance level. The correlation between Y-2019 and DAA-2020 (Fig. 3, a) presented a weak and negative interaction of 25%. The results of the negative correlation indicate that the yield of one year is inversely proportional to the defoliation of the following year; thus, negative correlations imply that the higher the yield of one year is, the lower the defoliation of the following year, to which it is correlated because of the biennial characteristics of the coffee plant. We found a similar result for the correlation between Y-2020 and DAA-2021 of -17% (Fig. 3, b) and for Y-2020 and DAV-2021 of -19% (Fig. 3, c).

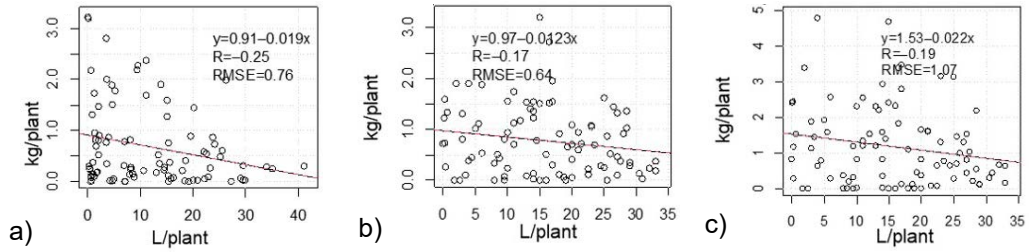

Figure 3. Regression and correlation. a) Y-2019 and DAA-2020; b) Y-2020 and DAA-2021, and c) Y-2020 and DAV-2021.

By comparing the data obtained from the crop images after the 2020 harvest with the data obtained from the crop images before the 2021 harvest, we could quantify the recovery of the crop from one year to the other, in which there was a 22.8% increase in leaf area and a 19.6% volume increase in the crop. This result expresses the physiological characteristics of coffee plants and their biennial nature, and it is possible to observe the losses caused by harvest.

This study reflects the importance of loss of leaf area. Any factor that reduces leaf area negatively influences the photosynthetic capacity of the plant (Magalhães, 1964). This loss of leaf area should be considered given the biennial nature of coffee plants, as the alternation of defoliation patterns tends to be reflected in yield. Similar to the study conducted by Magalhães (1964), the effect of the 25% reduction in leaf area resulted in a 32.6% delay in leaf development and a 10.5% decrease in the development of the plant shoots. In this study, this loss of leaf area was below 20%, and it was possible to observe

the recovery of the plant in the subsequent year. This further reinforces the need to perform samplings such as these so that actions can be taken quickly and accurately.

With the processing of images from 2020, the obtained crop areas were 354.6 m^2 (Fig. 4, a) and 293.1 m2 (Fig. 4, b) before and after harvest, respectively. This result demonstrates a reduction of 17.3% in leaf area after harvest. The crop volumes before and after harvest were 505.6 m^3 and 412.7 m^3, respectively, with an 18.4% reduction in leaf volume after harvest in the plots under study.

The crop area obtained in 2021 was 379.9 m^2 before harvest (Fig. 4, c) and 331.2 m^2 (Fig. 4, d) after harvest. This result reflects a 12.8% reduction in leaf area after harvest. The crop volumes were 524.9 m^3 and 473.4 m^3 before and after harvest, respectively, which resulted in a 9.8% decrease in leaf volume after harvest in the plots under study.

Figure 4. Leaf area of coffee plants a) before the 2020 harvest, b) after the 2020 harvest, c) before the 2021 harvest, and d) after the 2021 harvest.

The results of the analyses of the relationship between yield and defoliation obtained in the field and the relationship between yield and defoliation obtained through the RPA images were complementary. It is noteworthy that in 2020, the crop showed a greater reduction in leaf area after harvest obtained by the RPA and a higher yield than the year 2021. These results agree with the defoliation obtained in the field with the yield of 2020 and the lower yield in the following year and validate what was observed when using both methodologies. Thus, we observed that high yield combined with high defoliation in the same year is complementary to high yield in the year combined with the low defoliation in the following year (due to the lower yield of the following year). We recommend that these analyses be performed in a consecutive period of four years to obtain relevant and repeated data in a biennial coffee cycle for both methods.

Otsu et al. (2019) studied a combined random forest classification for the detection of defoliation in a forest area by means of histogram threshold analysis with four vegetation indices obtained from RPA images. The authors obtained good results; however, this methodology for obtaining defoliation of a given vegetation requires multispectral cameras to calculate vegetation indices that use spectral bands in the NIR range, and it is a more costly methodology than that of this study, which, although it uses a multispectral camera, does not use the nonvisible bands of the spectrum. Thus, it was not necessary to perform the calibration in the data processing, as in the studies performed by Cunha et al. (2019), in which the authors used an RGB camera to conduct their study. Thus, the proposed methodology is accessible to small coffee producers who want to obtain morphological parameters of their crop, such as height, crown diameter,

plant area, plant volume, and crop defoliation using an accessible camera that is easy to handle and process.

This study is relevant because it quantifies the areas and volume of coffee plants without the need for direct sampling in the field, where data are obtained remotely, which facilitates quicker and more accurate interventions in the crop. Cunha et al. (2019) developed a method to determine the vegetation volume of coffee crops from images obtained by RPA; however, the authors used a computational routine implemented in the software Pix4D that allows the volume of the target to be estimated. This difference in processing may lead to an underestimation or overestimation of the canopy volume because the authors did not individualize the plants.

The advantage of this study is that it considers the height of the plants obtained by the CHM and is an agile methodology for obtaining this information from the entire area under study without having to perform field measurements. In addition, it allows us to remotely obtain the morphological parameters of the crop, favouring the more efficient identification of anomalies in the crop and streamlining necessary crop treatment procedures in the field.

Some additional aspects should be considered for this methodology, such as the effect of the flight overlap parameters on the quality of the images, terrain topography, and ground control points (GCPs) with georeferencing obtained with a global navigation satellite system (GNSS) receiver, to improve the accuracy and processing of the images.

For future studies, we suggest testing the methodology on different terrains and developing plugins that automate and standardize this processing and technologies that allow obtaining this information in real time. In addition, the use of unmanned aerial vehicle laser scanning (UAV-LS) technology (Brede et al., 2019) in coffee crops has been suggested.

CONCLUSIONS

It was possible to analyse and correlate the relationship between yield and defoliation obtained in the field and obtained through RPA images.

The non-significance between the defoliation obtained in the field and the defoliation obtained by the aircraft should be highlighted, for this result reinforces the need for complementary studies and investigations longer than 2 years.

The interactions between the defoliation data obtained in the field and the yield of the same harvest year showed a directly proportional relationship, and the interaction of yield with the defoliation data obtained by the RPA in the subsequent year showed an inversely proportional relationship.

ACKNOWLEDGEMENTS. We acknowledge the Federal University of Lavras (UFLA) and the Graduate Program in Agricultural Engineering (PPGEA, for its acronym in Portuguese) for supporting the study, the Research Coffee Consortium (project approved in call no. 20/2018) - Embrapa Coffee for funding the research, the National Council for Scientific and Technological Development (CNPq), the Minas Gerais Research Foundation (FAPEMIG), and the Brazilian Federal Agency for the Support and Evaluation of Graduate Education (CAPES) for financial support, and the Coffee Sector of UFLA, Centre for Agricultural Systems Studies (NESA, for its acronym in Portuguese), and Centre for Coffee Culture Studies (NECAF, for its acronym in Portuguese) for the support and development of the research.

REFERENCES

Alecrim, A.O., Castanheira, D.T., Voltolini, G.B., Netto, P.M., Guimarães, R.J. & Gonçalves, A.H. 2020. Phytosociology of weeds in coffee plants with different soil management techniques. *Scientia Agraria Paranaensis* **19**(3), 270–279.

Amaral, L.R.D., Zerbato, C., Freitas, R.G.D., Barbosa Júnior, M.R. & Simões, I.O.P.D.S. 2020. UAV applications in Agriculture 4.0. *Revista Ciência Agronômica* **51**, e20207748. https://doi.org/10.5935/1806-6690.20200091

Barbosa, B.D.S., Ferraz, G.A.S., Santos, L.M.D., Santana, L.S., Marin, D.B., Rossi, G. & Conti,L. 2021. Application of RGB Images Obtained by UAV in Coffee Farming. *Remote Sensing* **13**, 2397, 2021.

Bártholo, G.F. & Guimarães, P.T.G. 1997. Care in harvesting and preparing coffee. *Informe Agropecuário* **18**(187), 33–42. (in Portuguese).

Bordin, B.C.D.M., Ronchi, C.P., Campos, A.A.V., Miranda, F.R., Batista, L.B., Ribeiro, A.J. & Mewes, W.L.C. 2019. Productive responses of first-crop crops to manual and mechanized harvesting. X Simpósio de Pesquisa dos Cafés do Brasil. (in Portuguese).

Brede, B., Calders, K., Lau, A., Raumonen, P., Bartholomeus, H.M., Herold, M. & Kooistra, L. 2019. Non-destructive tree volume estimation through quantitative structure modelling: Comparing UAV laser scanning with terrestrial LIDAR. *Remote Sensing of Environment* **233**, 111355. doi: 10.1016/j.rse.2019.111355

Castanheira, D.T., Barcelos, T.R., Guimarães, R.J., Carvalho, M.A.D.F., Rezende, T.T., Bastos, I.D.S. & Cruvinel, A.H. 2019. Agronomic techniques for mitigating the effects of water restriction on coffee crops. *Coffee Science* **14(**1), 104–115.

Cunha, J.P., Neto, M.A.S. & Hurtado, S. 2019. Estimating vegetation volume of coffee crops using images from unmanned aerial vehicles. *Engenharia Agrícola* **39**(SPE), 41–47.

Ferraz, G.A., Silva, F.M.D., Costa, P.A.N.D., Silva, A.C. & Carvalho, F.D.M. 2012. Precision agriculture to study soil chemical properties and the yield of a coffee field. *Coffee Science* **7**(1), 59–67 (in Portuguese).

Iizuka, K., Yonehara, T., Itoh, M. & Kosugi, Y. 2017. Estimating tree height and diameter at breast height (DBH) from digital surface models and orthophotos obtained with an unmanned aerial system for a Japanese cypress (Chamaecyparis obtusa) forest. *Remote Sensing* **10**(13), 1–14. doi: 10.3390/rs10010013

Magalhães, A.C.N. 1964. Effect of leaf surface reduction on coffee plant development. *Bragantia* **23**, 337–342 (in Portuguese).

Martins, R.N; Pinto, F. De A. De C., Queiroz, D.M. De, Valente, D.S.M. & Rosas, J.T.F. 2021. A Novel Vegetation Index for Coffee Ripeness Monitoring Using Aerial Imagery. *Remote Sensing* **13**(2), 263–273. doi: 10.3390/rs13020263

Martínez-Carricondo, P., Agüera-Vega, F., Carvajal-Ramírez, F., Mesas-Carrascosa, F.J., García-Ferrer, A. & Pérez-Porras, F.J. 2018. Assessment of UAV-photogrammetric mapping accuracy based on variation of ground control points. *International Journal of Applied Earth Observation and Geoinformation* **72**, 1–10.

Nex, F. & Remondino, F. 2014. UAV for 3D mapping applications: a review. *Applied Geomatics* **6**(1), 1–15.

Oliveira, E. De, Silva, F.M. Da, Salvador, N. & Figueiredo, C.A.P. 2007. The influence of the sticks vibration and the speed in the displacement of the harvester machine on mechanized coffee harvest process. *Engenharia Agrícola* **27**(3), 714–721 (in Portuguese).

Otsu, K., Pla, M., Duane, A., Cardil, A. & Brotons, L. 2019. Estimating the threshold of detection on tree crown defoliation using vegetation indices from UAS multispectral imagery. *Drones* **3**(4), 80–90.

Panagiotidis, D., Abdollahnejad, A., Surový, P. & Chiteculo, V. 2017. Determining tree height and crown diameter from high-resolution UAV imagery. *International Journal of Remote Sensing* **38**(8–10), 2392–2410.

Parreiras, T.C., Lense, G.H.E., Moreira, R.S., Santana, D.B. & Mincato, R.L. 2020. Using unmanned aerial vehicle and machine learning algorithm to monitor leaf nitrogen in coffee. *Coffee Science* **15**(1), 1–9.

Santos, L.M. Dos; Barbosa, B.D. De S., Diotto, A.V., Maciel, D.T. & Xavier, L.A.G. 2020a. Biophysical parameters of coffee crop estimated by UAV RGB images. *Precision Agriculture* **21**(6), 1227–1241.

Santos, L.M., Ferraz, G.A.S., Barbosa, B.D.S., Diotto, A.V., Andrade, M.T., Conti, L. & Rossi, G. 2020b. Determining the Leaf Area Index and Percentage of Area Covered by Coffee Crops Using UAV RGB Images. *IEEE Journal of Selected Topics in Applied Earth Observations and Remote Sensing* **13**(1), 6401–6409.

Santos, L.M, Ferraz, G.A.S., Diotto, A.V., Barbosa, B.D.S., Maciel, D.T., Andrade, M.T. & Rossi, G. 2020c. Coffee crop coefficient prediction as a function of biophysical variables identified from RGB UAS images. *Agronomy Research* **18(**2), 1463–1471.

Silva, F.M.D., Alves, M.D.C., Souza, J.C.S. & Oliveira, M.S.D. 2010. Effects of manual harvesting on coffee (Coffea arabica L.) crop biannuality in Ijaci, Minas Gerais. *Ciência e Agrotecnologia* **34**(3), 625–632 (in Portuguese).

Silva, F.M., Rodrigues, R.F., Salvador, N., Tourino, E.S. & Silva, S.S.S. 2000. Cost of mechanized coffee harvesting with self-propelled harvesters in Sul de Minas. *Engenharia na Agricultura* **8**(1), 54–60 (in Portuguese).

United States Department of Agriculture (USDA). Avaible in:< http://usda.mannlib.cornell.edu/MannUsda/viewDocumentInfo.do?documentID=1801> Access in: February 2023.

Agronomy Research **21**(S3), 1567–1580, 2023
https://doi.org/10.15159/AR.23.080

Spatial and temporal variability of productivity of coffee plants grown in an experimental field located in Três Pontas, Brazil

S.A. Santos[1,*], G.A.S. Ferraz[1], V.C. Figueiredo[2], M.M.L. Volpato[2], C.S.M. Matos[2], A.B. Pereira[2], L. Conti[3], G. Bambi[3] and D.B. Marin[3]

[1]Federal University of Lavras, Department of Agricultural Engineering, Trevo Rotatório Professor Edmir Sá Santos, BR37200-900, Lavras, Brazil
[2]Agricultural Research Company of Minas Gerais, Av. José Cândido da Silveira 1647, Bairro União Belo Horizonte, BR31170-495 Belo Horizonte, Brazil
[3]University of Florence, Department of Agricultural, Food and Forestry Science and Technology, Piazza S. Marco 4, IT055 27571, Florence, Italy
[*]Correspondence: sthefany.santos1@estudante.ufla.br

Received: January 31st, 2023; Accepted: April 25th, 2023; Published: September 5th, 2023

Abstract. The coffee grower seeks to increase productivity, as well as reduce the operating costs of his crop. Precision Agriculture (PA) is composed of a cycle of tools and technologies that can bring a good return to coffee growers, seeking to optimize production processes, bringing better yields and minimizing costs. Therefore, the objective of this research is to evaluate the space-time behavior of productivity in a coffee plantation, aiming to apply AP techniques. The study was carried out in a coffee plantation of the species *(Coffea arabica)*, cultivar Topázio MG1190, located in the municipality of Três Pontas, Brazil, with an area of 1.2 ha. With the aid of a GNSS RTK, 30 plants were georeferenced, from which their yields were later sampled in the years 2020, 2021 and 2022. The collected data were evaluated in two statistical processes in the RStudio software. The first stage consisted of a one-way analysis of variance with repeated measures, from the results it is concluded that there are differences between the production averages when buying the productivity of the years 2020, 2021 and 2022 and, in addition, the coefficient of variation for the three sets of samples was quite high (CV > 30%) indicating a heterogeneity between the data. The second stage consisted of a geostatistical analysis the data were fitted in a model and interpolated by ordinary kriging; the result was maps of spatial variability. Through these maps it was possible to evaluate the behavior of productivity spatially and temporally, as well as to quantify areas that had higher and lower levels of this attribute. It is concluded that productivity, even in the case of such a small productive area, can vary substantially in space and time, and the use of PA can help producers in decision making regarding management.

Key words: biennial, geoestatistics, precision agriculture in coffee trees.

INTRODUCTION

The coffee agro-industrial system is the focus of several studies due to its importance in the economic and social history of Brazil since the colonial period. This commodity

played an important role in the accumulation of foreign exchange that started the country's industrialization process (Cardozo et al., 2019).

Coffee cultivation in Brazil occurs in environments with great diversity (Alves et al., 2011) and this cultivation is very sensitive to climatic conditions (Aparecido et al., 2015). Climate variability has a strong impact on agricultural activities (Sá Junior et al., 2012), being the main factor responsible for fluctuations and oscillations in coffee bean productivity (Camargo, 2010).

According to Santana et al. (2022) the Precision Agriculture applied to coffee production still needs to be developed and implemented. But the same authors indicate that there is still a propensity to research, defunded, and adopted due to the benefits and adopted due to the benefits it can bring as efficiency, environmental and economic sustainability.

Productivity maps are one of the precision agriculture tools and are an excellent indicator of problems that may occur during the productive cycle of a crop. Failure to use tools like these leads the producer to consider mean values for decision-making in relation to management, which can lead to decisive errors. Even if the crop is treated (fertilizing, spraying, controlling pests and diseases, etc) throughout this cycle, productivity is a factor that will not be uniform, as this is an attribute that is influenced by factors such as: biennial (Camargo & Camargo, 2001), soil fertility and leaf nutrition (Wadt & Dias, 2012; Scalco et al., 2014) occurrence of pests, diseases and weeds (Fialho et al., 2010; Carvalho et al., 2012, Lopes et al., 2012), physical attributes of the plant (Carvalho et al., 2013; Burak et al., 2016; Santos et al., 2023) among other factors.

Taking into account that coffee production is strongly influenced by several factors which may lead to a high rate of spatial variability of this attribute, in this context, Precision Agriculture (PA) arises with the objective of evaluating and quantifying this spatial variability. PA when applied to coffee growing is called Precision Coffee Growing (Ferraz et al., 2012a). Precision Agriculture (PA) approaches seek to understand the spatial and temporal variability present in agricultural variables within a production field (Martello et al., 2022).

The need to modernize agricultural production has encouraged more and more producers to adopt agricultural practices within the PA context (Dong et al., 2013). A more up-to-date definition of precision coffee farming was described by Santana et al. (2022) who define it as updated techniques and technologies use that aim to maximize crop profitability, increase operations efficiency, search for business sustainability, environmentally sustainable production, and unceasing search for maximizing productivity and improving final product quality.

Ferraz et al. (2017) state that geostatistics is an important methodology for data analysis, being used as a tool within PA to analyze the factors involved in production systems (Carvalho et al., 2013). Through geostatistical analysis, it is possible to identify whether there is spatial dependence for the analyzed factors, enabling the creation of thematic maps that help in decision making (Carvalho et al., 2013). The use of the GIS environment has great potential for accurate and rapid research, bringing clear results (Piri et al., 2019) especially when it comes to assessing climate variability and its consequences on productivity.

It is important to mention that the application of PA techniques and technologies in coffee growing is recent, mainly when it comes to the evaluation of heterogeneity of factors related to soil and plants, and bearing in mind that few studies evaluate small-scale productive crops. In this context, this work aims to evaluate the spatial variability

of the productivity obtained for three consecutive years, 2020, 2021 and 2022 and, in this way, if the spatial dependence is proven, generate maps through interpolation by kriging, which will establish values of this attribute at unsampled locations within the study area.

MATERIALS AND METHODS

Workflow

The workflow of this research (Fig. 1) was defined in the following stages: construction of the sampling grid, georeferencing of points, productivity sampling and geostatistical analysis.

Figure 1. Work flowchart.

Description of the Study Area

The study was conducted in a coffee plantation of the Experimental Field of the Minas Gerais Agricultural Research Company (EPAMIG, as abbreviated in Portuguese), located in the municipality of Três Pontas in the southern region of the state of Minas Gerais, Brazil, at an altitude of 905 m and a Universal Transverse Mercator (UTM) coordinate system position of 7640030.4 S and 449531.5E, Zone 23K. This municipality has an mean annual temperature of 20.3 °C and an mean annual rainfall of 1,429 mm (Climate Data, 2023).

The soil in this area is classified as oxisol. The area of the experiment comprised 1.2 ha of a coffee plantation of the species *Coffea arabica* L. of the Topázio MG1190 cultivar (Fig. 2). This crop was established in 1998 with spacings between rows of 3.70 m and between plants of 0.70 m (EPAMIG, 2023).

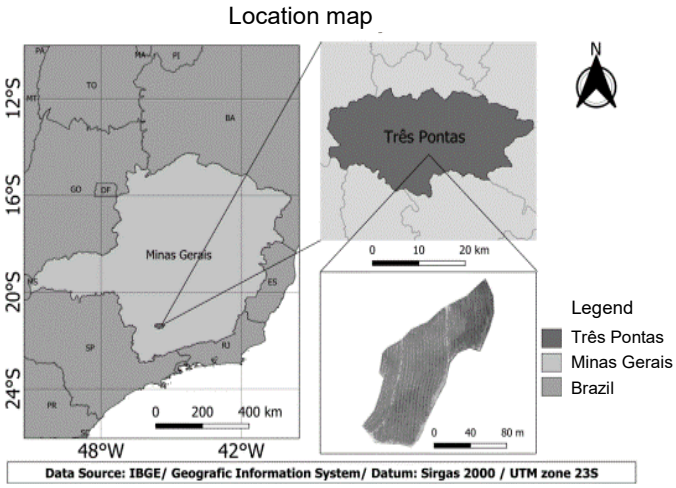

Figure 2. Location map.

Sampling grid

The sampling grid was prepared with QGIS software, version 3.4.8, and 30 sampling points representing a sampling density of 25 points per hectare were laid out (Fig. 3).

For the construction of the sampling mesh, the methodology of the equidistant sampling mesh proposed by Faria (2019) was used, this method consists of reducing the walking within the plot using walking routes. Within the sampling of 30 points, the smallest distance between them was 6m and the greatest distance was 175 m.

For this study, the productivity data of the 30 georeferenced plants were sampled on the following dates: 1st collection (30 June 2020), 2nd collection (08 June 2021) and 3rd collection (13 June 2022).

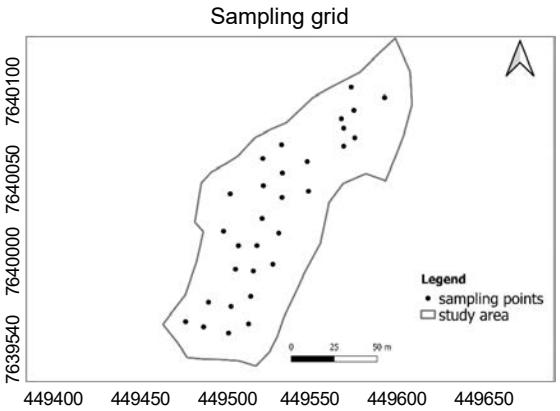

Figure 3. Equidistant sampling grid used for sampling the 30 georeferenced points in this study.

Productivity sampling

Productivity data were sampled at 30 georeferenced points within the study area. For each sampling point represented by 1 coffee plant, productivity was obtained through semi-mechanized harvesting using a derriçadora (Fig. 4, a). After harvesting each sampling point, the fruits that fell under the cloths were selected to separate them from leaves and branches (Fig. 4, b), and then they were deposited in a graduated container, which will indicate the productivity in liters per plant (L /plant) (Fig. 4, c).

Figure 4. Productivity sampling (a) semi-mechanized harvesting, (b) separation of leaves and branches and (c) productivity measurement in L/plant in graduated bucket.

Statistical analysis

Taking into account that during the three years of sampling, the same 30 plants were sampled, in this way, as the dataset represents a group of samples where repeated measurements of productivity were obtained during a time interval (2020, 2021 and 2022), The one-way analysis of variance (ANOVA) statistical test with repeated measures was used in order to evaluate the mean productivity of each group as a whole. For this

analysis, tests were first performed to verify outliers in the samples and then a Shapiro Wilk test to verify data normality.

Then, the analysis of variance model was built using the variables year (independent variable) and productivity (dependent variable), the result of this model is a table containing: degree of freedom of the evaluated variable, degree of freedom of error, sum of squares, F-value and *p*-value. For this F test to be valid, it is necessary to verify the sphericity of the data, and this will be done using the Mauchly test, this test considers the following hypotheses:

$H_{0Mauchly}$: data are spherical when $p > 0.05$;

$H_{1Mauchly}$: data are not spherical when $p \leq 0.05$.

If sphericity is verified and the null hypothesis is accepted, the following hypotheses for the F test performed in the analysis of variance of a repeated measures way must be considered:

H_{0ANOVA}: mean productivity 2020 = mean productivity 2021 = mean productivity in 2022; $p > 0.05$

H_{1ANOVA}: there is at least one difference between the means of productivity $p \leq 0.05$

If the null hypothesis of the Mauchly test ($H_{0Mauchly}$) is rejected and the alternative hypothesis ($H_{1Mauchly}$) is accepted, it is necessary to correct the degrees of freedom of the variance analysis using the Greenhouse-Geisser method for the lack of sphericity, and from there, obtain a new p value, and only then apply the hypothesis analysis of the one-way ANOVA method with repeated measures. After performing the F test by one-way ANOVA with repeated measures and if the null hypothesis (H_{0ANOVA}) of the test is rejected and the alternative hypothesis is accepted (H_{1ANOVA}), that is, that there is at least one difference between the measurements of productivity it is necessary to verify what this difference is, through a pair comparison test using the Bonferroni adjustment, which will result in a comparison matrix between the mean productivity, where the following hypotheses must be considered:

$H_{0\ Bonferroni}$: if $p > 0.05$ there is no difference between the productivity means;

$H_{1\ Bonferroni}$: if $p \leq 0.05$ there is a difference between the productivity means.

And finally, to close the statistical analysis of the data, a descriptive statistics table was generated containing: productivity mean for the three years, standard deviation and coefficient of variation. Gomes & Garcia (2002) state that the variability of an attribute can be classified according to the magnitude of its coefficient of variation (CV), according to the authors, the CV is low when it is less than 10%, moderate when it is in the range from 10 to 20%, high when it is between 20 and 30% and very high when it is above 30%. All statistical analysis of the data was performed using the RStudio software using the dplyr, ez, reshape and rstatix libraries.

Geostatistical analysis

Semivariograms were used to analyze the spatial dependence of the productivity. The semivariance is classically estimated by Eq. (1) according to Vieira (2000):

$$\hat{\gamma}(\mathrm{h}) = \frac{1}{2\,N(\mathrm{h})} \sum_{i=1}^{Ni=(\mathrm{h})} [Z\,(x_i) - Z\,(x_i + \mathrm{h}\,)]^2 \qquad (1)$$

where N (h) is the number of experimental pairs of observations $Z\,(x_i)$and $Z\,(x_i + \mathrm{h}\,)$, separated by a distance h. The semivariogram is represented by the graph $\hat{\gamma}(\mathrm{h})$ versus h. From the fitting of a mathematical model to the calculated values of $\hat{\gamma}(\mathrm{h})$, the coefficients

of the theoretical model are estimated for the semivariogram, called the nugget effect (C_0), sill ($C_0 + C_1$), and range (a), as described by Bachmaier & Backes (2008).

The semivariograms were adjusted using the Ordinary Least Squares (OLS) method. The adjusted semivariogram model was the spherical one, since this is the most used in geostatistics studies related to soil and coffee culture (Grego & Vieira, 2005; Silva et al., 2007) mainly evaluating coffee productivity (Ferraz et al., 2012a; Ferraz et al., 2012b; Carvalho et al., 2013, Carvalho et al., 2017; Ferraz et al., 2017).

To verify that this model fits the cross-validation requirements, the mean error (ME) was calculated as described by Isaaks & Srivastava (1989). ME should be as close to zero as possible.

With the adjustment of the semivariograms, after the identification of the spatial variability, the data were interpolated by ordinary kriging. Thus, the variable was estimated in places where it was not sampled, which allowed us to visualize its distribution in space in the form of thematic maps.

The calculation of the degree of spatial dependence (DSD) of the variables followed the classification proposed by Cambardella et al. (1994). In this classification, the authors point out that there is strong spatial dependence when the semivariogram shows a nugget effect equal to or less than 25% of the sill, moderate spatial dependence when this ratio is between 25% and 75%, and weak spatial dependence when it is greater than 75%.

The geoR package of the R software was used for geostatistical analysis and for the creation of the thematic maps (Ribeiro Junior & Diggle, 2001).

RESULTS AND DISCUSSION

Statistical analysis

Fig. 5 represents a column chart containing the productivity data sampled in the 30 georeferenced plants in the years 2020, 2021 and 2022. It is observed that the highest values of productivity in coffee trees were found in the year 2022 for plants 25 (39 L/plant) and 2 (34 L/plant) respectively. The lowest productivity values were found for plants 2 and 8 in the year 2021 and for plant 21 in the year 2022, both with zero productivity.

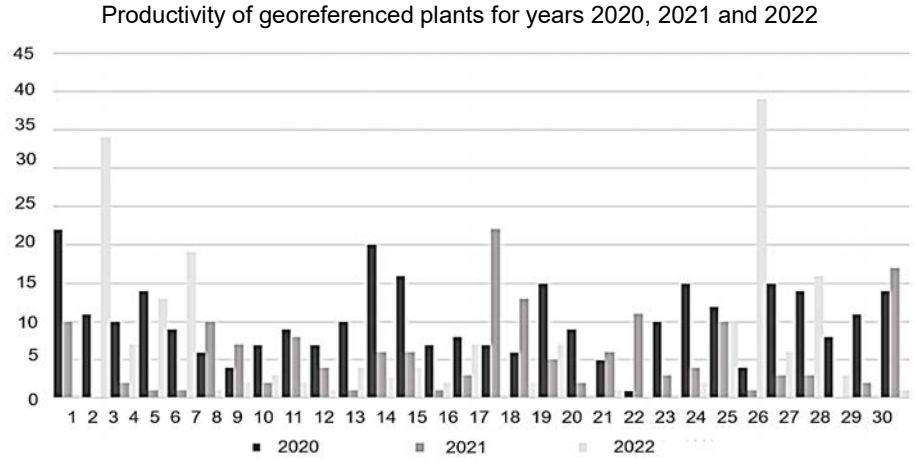

Figure 5. Productivity in liters per plant (L/plant) obtained for the 30 plants georeferenced and sampled in the years 2020, 2021 and 2022.

Table 1 represents the results generated by the one-way analysis of variance with repeated measures, including the F test of hypotheses, as well as the Mauchly test to verify the sphericity of the data.

Table 1. One-way analysis of variance with repeated measures and Mauchly test to verify sphericity

Analysis of variance							Mauchly's Test	
Variable	DFn	DFd	SSn	SSD	F	P_{ANOVA}	W	$P_{Mauchly}$
Year	2	58	650.2889	2459.0440	7.6690	0.0011*	0.9271	0.3466

DFn: sample degrees of freedom; DFd: error degrees of freedom; SSn: sample sum of squares; SSd: error sum of squares; F: value of F; pANOVA : probability of observation of the test F; W : statistics of the test; $p_{Mauchly}$: observation probability of the Mauchly test; *: significant at the 5% level of probability.

Through the analysis of variance modeling, it was observed that the $_{Mauchly}p$ value was greater than 0.05 (pMauchly > 0.05), that is, the Mauchly null hypothesis is accepted ($H_{0Mauchly}$) that the data are spherical, so the hypotheses of the F test can be evaluated without a sphericity correction using the Greenhouse-Geisser method. The F test performed by analysis of variance indicated an $_{ANOVA}$ p value = 0.0011 that is ($p_{ANOVA} \leq 0.05$), thus rejecting the null hypothesis of the analysis of variance (H_{0ANOVA}) and accepting the alternative hypothesis (H_{1ANOVA}) stating that there is at least one difference between the average productivity in the coffee tree between the years of 2020, 2021 and 2022. To quantify this difference, a comparison between pairs was performed using the Bonferroni test, which resulted in a matrix (Table 2) for comparing means by pairs.

Table 2. Bonferroni test for comparing means between pairs

Year	2020	2021
2021	0.2477	-
2022	0.0005*	0.1808

*: significant at the 5% probability level.

The results show that between the years 2021/2020 and 2022/2021 there were no differences between the productivity means ($p > 0.05$), while between the years 2022/2020 there was a difference between the productivity means, that is, the average productivity for the year 2022 differs significantly from the average productivity for the year 2020 ($p \leq 0.05$). After carrying out the analysis of variance of the set of data obtained in the field, the analysis of descriptive statistics was performed (Table 3).

Table 3. Data descriptive statistics

Year	mean	SD	CV (%)
2020	8.47	4.64	54.78
2021	11.30	7.29	64.51
2022	15.00	7.65	51.00

SD: standard deviation, CV: coefficient of variation.

After the variance analysis of the coffee productivity data, sampled in the years 2020, 2021 and 2022, the following hypotheses are concluded:

a) As much as the average productivity for the year 2022 is higher (15 L/plant), no it was necessarily the year that produced the most, and this was justified by the Bonferroni test, where the average productivity of the year 2022 differed significantly from the year 2020, the year in which most of the plants produced more compared to the years 2021 and 2022;

b) The difference in productivity between the productive cycles of the coffee tree can be justified by the bienniality, a phenomenon found in coffee plantations, where one year there is a lot of production and the next one less production.

c) The high productivity heterogeneity between plants during the same year can be explained by two factors: the first is the age of the coffee tree (25 years) and the second is the management adopted over all these years (conventional fertilization based on average fertility sampled in the field) which can generate a lack or excess of nutrients in the plants, which directly affects the individual production of each plant in this coffee tree.

Silva et al. (2007) evaluating the 2004 harvest of a 4.2 ha Mundo Novo coffee tree with 4m spacing between rows and 1m between plants, found in their study an average productivity of 4.81 (L/plant). Ferraz et al. (2012a) evaluating soil chemical attributes and productivity for the 2007–2008 season in a coffee plantation of 22 ha under the cultivation of coffee trees of the Topázio cultivar planted at spacing of 3.8 m between rows and 0.7 m between plants, found a productivity average of 1.45 (L/plant). With the aim of evaluating the spatial and temporal variability of productivity Ferraz et al. (2012b) the authors sampled this attribute in three harvests (2008, 2009 and 2010) in diferente sampling grids within the same coffee tree of 22ha. As a result, the authors obtained average productivity values of 1.45 (L/plant) for the 2008 season, 2.72 (L/plant) for the 2009 season and 4.93 (L/plant) for the 2009 season. 2010.

All the authors mentioned above found average productivity values much lower than those found in this study, and this is justified by several factors such as: coffee variety, spacing, climatic conditions, sampling mesh used in each study, management adopted in the field, etc.

Geostatistical Analysis

Table 4 represents the adjustment parameters of the semivariograms by the spherical model and by the ordinary least squares method. Figs 6 and 7 represent the semivariograms adjusted for the productivity variable and the thematic maps generated by kriging interpolation for the three years of collection, respectively.

Table 4. Parameters for fitting the spherical and exponential semivariogram models of the variables evaluated by the OLS method

	Year	C_0	C_1	$C_0 + C_1$	A	SDD		ME
Productivity	2020	0.10	24.00	24.01	25	0.41	strong	-0.01
	2021	0.50	20.00	20.5	30	2.43	strong	-0.02
	2022	0.01	80.00	80.01	12	0.01	strong	0.00

C_0 – Nugget effect; C_1 – Contribution; $C_0 + C_1$ – Sill; A – Range (m); SDD – Spatial dependence degree; ME – Mean error.

Through the geostatistical analysis of the productivity data obtained for the 2020, 2021 and 2022 harvests, it was possible to identify and quantify the spatial dependence of this variable. Camargo et al. (2004) states when an increase is observed between the absolute value of the difference between two samples and the increment of the separation distance between them until reaching a value in which there is no more spatial influence, thus causing the stabilization of the semivariogram the spatial dependence of the attribute is confirmed.

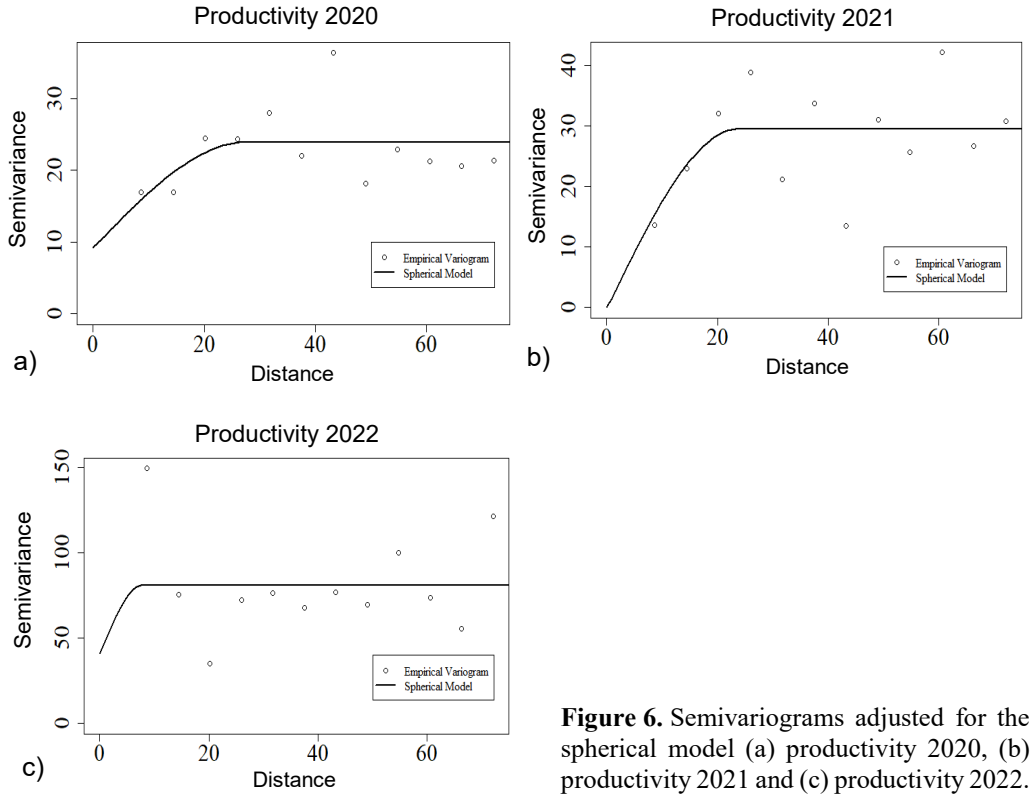

Figure 6. Semivariograms adjusted for the spherical model (a) productivity 2020, (b) productivity 2021 and (c) productivity 2022.

Regarding the adjustment parameters of the semivariograms, it is observed that the nugget effect was different from zero for all years of collection of the productivity attribute, it is an important parameter of the semivariograms as it indicates unexplained variability or even measurement errors, considering the sampling distance used (Carrasco, 2010). The nugget effect can be expressed as a percentage of the plateau, making it easier to compare the degree of spatial dependence.

All seasons (2020, 2021 and 2022) showed a strong degree of spatial dependence according to the criteria of Cambardella et al. (1994). Carvalho et al. (2017) state that the amplitude values relative to the semivariograms are of considerable importance in determining the limit of spatial dependence and can also be an indicator of the interval between the mapping units, important for optimizing future samplings. The highest range was for the 2021 productivity (25 m) and the lowest was for the 2022 productivity samples (12 m). The spherical model used in this study was efficient, as the mean error value calculated for all seasons was very close to zero, thus meeting the cross-validation criteria.

Geostatistics has been widely used in productivity mapping, as observed in the works Silva et al. (2007, 2008, 2010), Molin et al. (2010), by Ferraz et al. (2012a, 2012b), Carvalho et al. (2013), Carvalho et al. (2017), Ferraz et al. (2017) and Ferraz et al. (2019), all these authors confirmed the spatial dependence of productivity, but no research evaluates the spatial dependence in such a small crop. In relation to the semivariogram adjustment parameters, all these authors found different nugget and range effect values.

These differences can be justified, among other factors, by: crop management, crop age, chosen cultivar, soil management and type, climate.

As represented by figures 7, a, 7, b and 7, c, it can be seen that there was a wide variation in productivity for all the years evaluated. The highest values of this attribute are represented by the lighter color (light gray/white), while the lower concentrations of productivity are represented by dark colors (dark gray/black). Visually, the largest contractions in productivity were represented by the year 2020 and the lowest recorded in the year 2022.

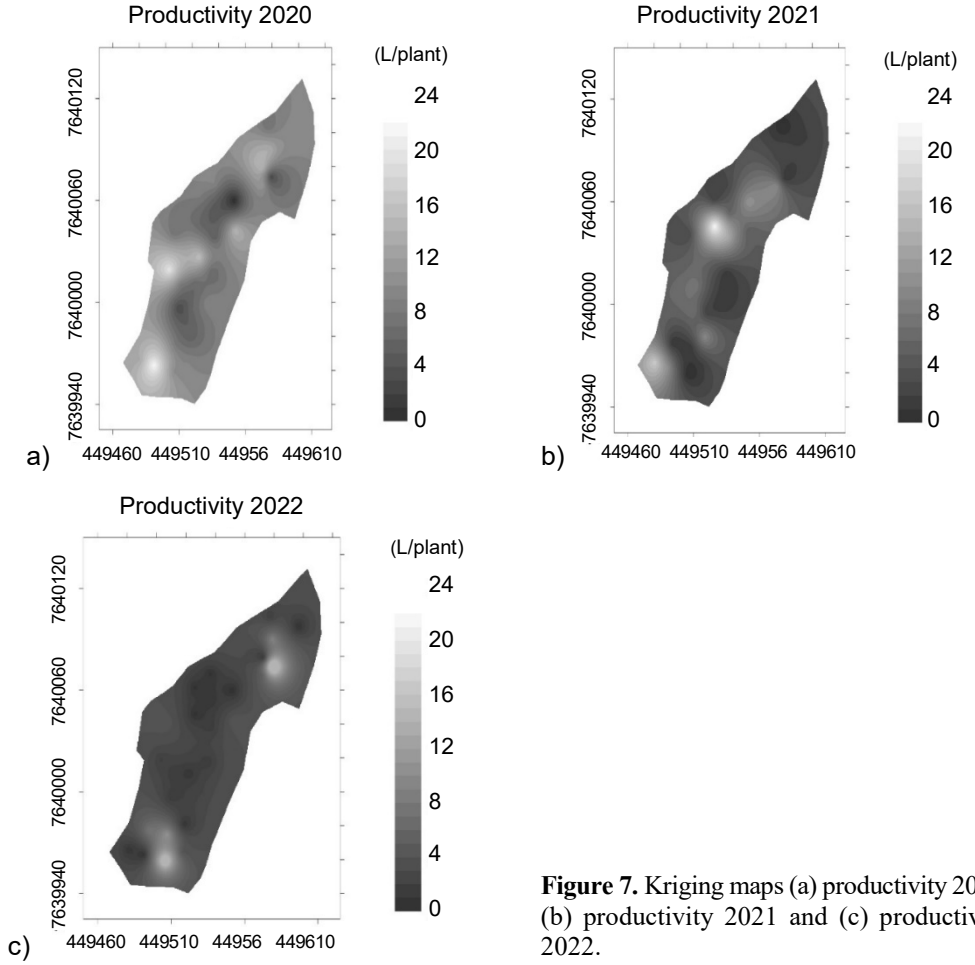

Figure 7. Kriging maps (a) productivity 2020, (b) productivity 2021 and (c) productivity 2022.

Ferraz et al. (2012a) state that productivity maps can be used in harvest management, be it manual, semi-mechanized or mechanized, that is, these maps are important for harvest logistics. In manual harvesting, in addition to estimating productivity, maps may be necessary to establish the number of workers to be hired. As for mechanized harvesting, in addition to the benefits mentioned above, the productivity maps helped in decision-making regarding the rent and/or purchase of machinery and equipment. And finally, in mechanized harvesting, they will be important for the construction of routes, especially when it comes to emptying the tractor support cart, avoiding unnecessary stops and maneuvers.

Fig. 7, a represents the spatial variability of the productivity evaluated in the year 2020, it is observed that a good part of the productivity was in the range of 7 to 13 L/plant and two points of high productivity were observed in the southwest of the area and two points of low productivity in the center of the area.

Fig. 7, b represents the map of spatial dependence of the productivity obtained in the year 2021, it was observed that in this year a good part of the productivity was concentrated in the low productivity interval (1 to 7 L/plant) and only a small point of high productivity was found in the center of the area.

The spatial variability of productivity for the year 2022 (Fig. 7, c) was also concentrated in the range of low productivity (1 to 7 L/plant) and unlike what happened in 2021, where there was a high concentration of productivity (center of the area for the 2021 harvest) in the year 2022, this point had low productivity.

The coffee tree, as a perennial plant with a biennial production cycle, also has different needs from one year to the next. In years of high load, the nutrient demand for fruit production, added to the demand for continuous plant growth, results in a greater need for fertilization (Mesquita et al., 2016). The biennial is a phenomenon considered to be a constant in the production of coffee trees. According to Mendonça et al. (2011) there is a high correlation between management and the biennial, that is, the inefficiency of the cultural management and the climatic adversities accentuate the biennial in the coffee tree, however the nature and magnitude of this influence still lack scientific clarification.

A visual comparison demonstrates the occurrence of biennial productivity, as the regions that in 2020 had the highest productivity had the lowest productivity for the years 2021 and 2022 in the following and consecutively. Plants that produced a lot in 2020 (regions with lighter coloring Fig. 7, a) used their reserves for fruiting, negatively influencing branch growth and, consequently, reducing productivity in 2021 and 2022 (regions with dark coloring). This can be confirmed by the difference between the evaluated harvests (Fig. 7, a, 7, b and 7, c), as these maps show that the areas with the greatest difference, positive or negative, coincide with areas with greater or lesser productivity respectively. Similar results are found in the work by Carvalho et al. (2017) where the authors evaluated two harvests (2012 and 2013) in a 22 ha field under the cultivation of *Coffea arabica* L, cultivar Topázio.

We can call this phenomenon internal variability, by definition the biennial is described as one year producing more and one year producing less, but taking into account that this crop is over 20 years old and the management system adopted is conventional, the needs The specific characteristics of each plant within that crop have not been met over the years, and thus, even with the biennial within coffee crops, for this specific crop the behavior was individual for each evaluated plant, that is, the highest productivitys are observed in the 2020 crop, then the 2021 crop is smaller than the 2020 crop and finally the 2022 crop is smaller than the previous two.

The results obtained by a map of spatial variability of productivity and together with maps of chemical and physical attributes of the soil can be useful to find the reasons for the occurrence of variability in productivity, mainly in the case of low productivity, which will enable the correction failures, allowing these problems to be minimized in the next harvest.

CONCLUSION

By using one-way analysis of variance with repeated measures, it was possible to verify and quantify the difference between productivity means. The descriptive statistics analysis proved the existence of high variability among the data, by calculating the coefficient of variation.

Through the geostatistical analysis of the productivity data collected in different seasons, it was possible to verify that this attribute has spatial dependence. By adjusting the semivariogram and kriging interpolation, it was possible to prove the magnitude of this spatial dependence. The final product generated by this study were thematic maps, where through them it was possible to identify areas that have the highest and lowest concentrations of productivity.

It is important to emphasize that due to the biennial phenomenon that occurs in coffee growing, productivity is an attribute that will always present a high rate of spatial variability within the same crop, this effect can be minimized with practices and techniques of precision agriculture, that is, the use of specific and localized management can be a great ally to minimize the impacts caused by this variation in productivity. Geostatistics has shown good results in estimating results in unsampled locations, which directly benefits the producer, avoiding intensive and expensive sampling and bringing a quick and reliable return to the producer.

REFERENCES

Alves, M.C., Da Silva, F.M., Moraes, J.C., Pozza, E.A., de Oliveira, M.S., Souza, J.C. & Alves, L.S. 2011. Geostatistical analysis of the spatial variation of the berry borer and leaf miner in a coffee agroecosystem. *Precision Agriculture* **12**, 18–31. doi: 10.1007/s11119-009-9151-z

Aparecido, L.E.O, de Souza Rolim, G. & de Souza, P.S. 2015. Sensitivity of newly transplanted coffee plants to climatic conditions at altitudes of Minas Gerais, Brazil. *Australian Journal of Crop Science* **9**(2), 160–167.

Bachmaier, M. & Backes, M. 2008. Variogram or semivariogram? Understanding the variances in a variogram. *Precision Agriculture* **9**, 173–175.

Burak, D.L., Santos, D.A. & Passos, R.R. 2016. Spatial variability of physical attributes: relief, organic matter and productivity in conilon coffee. *Coffee Science* **11**(4), 455–466 (in Portuguese).

Camargo, Â.P.D. & Camargo, M.B.P.D. 2001. Definition and layout of the phenological stages of Arabica coffee under tropical conditions in Brazil. *Bragantia* **60**, 65–68 (in Portuguese). doi: 10.1590/S0006-87052001000100008

Camargo, E.C.G., Fucks, S.D. & Câmara, G. 2004. Spatial analysis of surfaces. Spatial analysis of geographic data. *Planaltina: Embrapa Cerrados*, 79–122 (in Portuguese).

Camargo, M.B.P.D. 2010. The impact of climatic variability and climate change on arabic coffee crop in Brazil. *Bragantia* **69**, 239–247. doi: 10.1590/S0006-87052010000100030

Cambardella, C.A., Moorman, T.B., Novak, J.M., Parkin, T.B., Karlen, D.L., Turco, R.F. & Konopka, A.E. 1994. Field-scale variability of soil properties in central Iowa soils. *Soil science society of America journal* **58**(5), 1501–1511.

Carrasco, P.C. 2010. Nugget effect, artificial or natural? The *Journal of the Southern African Institute of Mining and Metallurgy* **110**, 299–306.

Cardozo, D.P., Las Schaab, L. & Parré, J.L. 2019. Spatial analysis of coffee productivity in the Southeast region of Brazil: 1990–2015. *Revista Economia Ensaios* **34**(1), 176–198 (in Portuguese). doi: 10.14393/REE-v34n1a2019-40853

Carvalho, A.M.D., Mendes, A.N.G., Botelho, C.E., Oliveira, A.C.B.D., Rezende, J.C.D. & Rezende, R.M. 2012. Agronomic performance of rust resistant coffee cultivars in the State of Minas Gerais, Brazil. *Bragantia* **71**, 481–487. doi: 10.1590/S0006-87052013005000007

Carvalho, L.C.C., Da Silva, F.M., Ferraz, G.A., da Silva, F.C. & Stracieri, J. 2013. Spatial variability of soil physical attributes and agronomic characteristics of coffee crop. *Coffee Science* **8**(3), 265–275.

Carvalho, L.C., Silva, F.M.D., Ferraz, G.A., Stracieri, J., Ferraz, P.F. & Ambrosano, L. 2017. Geostatistical analysis of Arabic coffee productivity in two crop seasons. *Revista Brasileira de Engenharia Agrícola e Ambiental* **21**, 410–414. doi: 10.1590/1807-1929/agriambi.v21n6p410-414

Climate Date 2023. Dados climáticos para cidades mundiais - Climate-Data.org. Accessed 20.11.2022.

Dong, X., Vuran, M.C. & Irmak, S. 2013. Autonomous precision agriculture through integration of wireless underground sensor networks with center pivot irrigation systems. *Ad Hoc Networks* **11**(7), 1975–1987. doi:10.1016/j.adhoc.2012.06.012

EPAMIG (Minas Gerais Agricultural Research Company). EPAMIG – Empresa de Pesquisa Agropecuária de Minas Gerais. Accessed 20.11.2022.

Ferraz, G.A.S., Silva, F.M.D., Carvalho, L.C., Alves, M.D.C. & Franco, B.C. 2012a. Spatial and temporal variability of phosphorus, potassium and productivity in a coffee crop. *Engenharia Agrícola* **32**, 140–150 (in Portuguese). doi: 10.1590/S0100-69162012000100015

Ferraz, G.A.S., Da Silva, F.M., de Carvalho Alves, M., de Lima Bueno, R. & da Costa, P.A.N. 2012b. Geostatistical analysis of fruit productivity and detachment force in coffee. *Precision Agriculture* **13**, 76–89. doi: 10.1007/s11119-011-9223-8

Ferraz, G.A., Silva, F.M.D., Oliveira, M.S.D., Custódio, A.A.P. & Ferraz, P.F.P. 2017. Spatial variability of plant attributes of a coffee crop. *Revista Ciência Agronômica* **48**, 81–91. doi: 10.5935/1806-6690.20170009

Ferraz, G.A.S., Ferraz, P.F.P., Martins, F.B., Silva, F.M., Damasceno, F.A. & Barbari, M. 2019. Principal components in the study of soil and plant properties in precision coffee farming. *Agronomy Research* **17**(2), 418–429. doi: 10.15159/ar.19.114

Fialho, C.M.T., Silva, G.R., Freitas, M.A.M., França, A.C., Melo, C.A.D. & Silva, A.A. 2010. Weed competition with the coffee crop in two infestation times. *Planta Daninha* **28**, 969–978 (in Portuguese). doi: 10.1590/S0100-83582010000500005

Gomes, F.P. & Garcia, C.H. 2002. Statistics applied to agronomic and forestry experiments: presentation with examples and guidelines for using applications. Piracicaba: FEALQ, v. **11**, p. 21.

Grego, C.R. & Vieira, S.R. 2005. Spatial variability of soil physical properties in an experimental plot *Revista Brasileira de Ciência do Solo* **29**, 169–177 (in Portuguese).

Isaaks, E.H. & Srivastava, R.M. 1989. *An introduction to applied geostatistics*. New York: Oxford Universit, 561 pp.

Lopes, P.R., Araújo, K.C.S., Ferraz, J.M.G., Lopes, I.M. & Fernandes, L.G. 2012. Agroecological coffee production in southern Minas Gerais: alternative systems to intensive agrochemical production. *Revista brasileira de agroecologia* **7**(1), 25–38. (in Portuguese).

Martello, M., Molin, J.P., Bazame, H.C., Tavares, T.R. & Maldaner, L.F. 2022. Use of Active Sensors in Coffee Cultivation for Monitoring Crop Yield. *Agronomy* **12**(9), 2118. doi: 10.3390/agronomy12092118

Mendonça, R., Rodrigues, W., Martins, L. & Tomaz, M.A. 2011. Approach to biennial production in coffee plants. *Enciclopédia Biosfera* **7**(13) (in Portuguese).

Mesquita, C.M., Rezende, J.E., Carvalho, J.S., Fabri Júnior, M.A., Moraes, N.C., Dias, P.T., Carvalho, R.M. & Araújo, W.G. 2016. Coffee manual: management of coffee plantations in production. Belo Horizonte: EMATER-MG, 2016, 72 pp. (in Portuguese).

Molin, J.P., Motomiya, A.V.D.A., Frasson, F.R., Faulin, G.D.C. & Tosta, W. 2010. Test procedure for variable rate fertilizer on coffee. *Acta Scientiarum. Agronomy* **32**, 569–575. doi: 10.4025/actasciagron. v32i4.5282

Piri, I., Moosavi, M., Taheri, A.Z., Alipur, H., Shojaei, S. & Mousavi, S.A. 2019. The spatial assessment of suitable areas for medicinal species of Astragalus (Astragalus hypsogeton Bunge) using the Analytic Hierarchy Process (AHP) and Geographic Information System (GIS). *Remote sensing and space sciences* **22**(2), 193–201. doi: 10.1016/j.ejrs.2018.02.003

Ribeiro Júnior, P.J. & Diggle, P. 2001. GeoR: a package for geostatistical analysis. *R-News* **1**(2), 15–18.

Sá Júnior, A., de Carvalho, L.G., Da Silva, F.F. & de Carvalho Alves, M. 2012. Application of the Köppen classification for climatic zoning in the state of Minas Gerais, Brazil. *Theoretical and Applied Climatology* **108**, 1–7. doi:10.1007/s00704-011-0507-8

Santana, L.S., Ferraz, G.A., Santos, S.A.D. & Dias, J.E.L. 2022. Precision coffee growing: a review. *Coffee Science* **17**. doi:10.25186/.v17i.2007

Santos, S.A., Ferraz, G.A.S., Figueiredo, V.C., Volpato, M.M.L., Machado, M.L. & Silva, V.A. 2023. Evaluation of the water conditions in coffee plantations using RPA. *AgriEngineering* **5**, 65–84. doi: 10.3390/agriengineering5010005

Scalco, M.S., Alvarenga, L.A., Guimarães, R.J., Dominghetti, A.W., Colombo, A., Assis, G.A. & Abreu, G.F. 2014. Leaf contents of phosphorus and zinc, productivity, and growth of irrigated coffee. *Pesquisa Agropecuária Brasileira* **49**, 95–101 (in Portuguese). doi: 10.1590/S0100-204X2014000200003

Silva, F.M.D., Souza, Z.M.D., Figueiredo, C.A.P.D., Marques Júnior, J. & Machado, R.V. 2007. Spatial variability of chemical attributes and productivity in coffee crops.*Ciência Rural* **37**, 401–407 (in Portuguese).

Silva, F.M.D., Souza, Z.M.D., Figueiredo, C.A.P.D., Vieira, L.H.D.S. & Oliveira, E.D. 2008. Spatial variability of chemical attributes and productivity of the coffee crop in two agricultural seasons. *Ciência e Agrotecnologia* **32**, 231–241 (in Portuguese). doi: 10.1590/S1413-70542008000100034

Silva, F.M.D., Alves, M.D.C., Souza, J.C.S. & Oliveira, M.S.D. 2010. Effects of manual harvesting on coffee biennial in Ijaci, Minas Gerais. *Ciência e Agrotecnologia* **34**, 625–632 (in Portuguese). doi: 10.1590/S1413-70542010000300014

Wadt, P.G.S. & Dias, J.R.M. 2012. Regional and interregional DRIS norms in the nutritional assessment of Conilon coffee.*Pesquisa Agropecuária Brasileira* **47**, 822–830 (in Portuguese). doi: 10.1590/S0100-204X2012000600013

Agronomy Research **21**(S3), 1581–1596, 2023
https://doi.org/10.15159/AR.23.090

Carbohydrate and protein metabolism of marandu grass affected by nitrogen fertilisation and number of cuts

A.A. Seixas[1,*], D.D. Fries[2], D.L.S. Dias[3], I. A.P.S. Santos[1], N.T. Cruz[1], F.A. Teixeira[2], P. Bonomo[2] and F.P. Amaral Júnior[4]

[1]State University of Southwest Bahia, Post-graduate programme in Animal Science, Spring Square, 40, Spring, BR45700000, Itapetinga, Bahia, Brazil
[2]State University of Southwest Bahia, Department of Exact and Natural Science, Spring Square, 40, Spring, BR45700000, Itapetinga, Bahia, Brazil
[3]State University of Feira of Santana, Department of Biological Sciences, New Horizon, BR44036900, Feira of Santana, Bahia, Brazil
[4]State University Paulista Júlio of Mesquita Filho, Faculty of Agricultural and Veterinary Scienses of Jaboticabal, Vila Industrial, BR14884900, Jaboticabal, São Paulo, Brazil
[*]Correspondence: angelseixas11@hotmail.com

Received: June 18th, 2023; Accepted: September 30th, 2023; Published: October 23rd, 2023

Abstract. Understanding the metabolism of tropical grasses in response to management practises imposed in pastoral environments allows for improvements in the management and use of mineral fertilisers. This study aimed to quantify metabolite content in different plant parts of Marandu grass (*Urochloa brizantha*), with a specific focus on the influence of nitrogen fertilisation and its effects following successive cuts. The treatments corresponded to four nitrogen (N) rates (0, 75, 150, and 225 kg N ha^{-1}) and the number of cuts (one, two and three cuts). The plants were fractionated into leaves, stems, and roots to assess the content of water-soluble carbohydrates (WSC), starch, albumin, globulin, prolamin, and glutelin content. N fertilisation influenced the WSC and starch content in different parts of the plant, varying according to the cuts made. In the leaves and roots, fertilisation reduced the content of WSC and starch with one cut, as these were utilised as energy sources for assimilating the excess nitrogen in the soil. There was an increase in the concentration of all protein groups with nitrogen fertilisation in all parts of the plant with one cut. In plants cut two and three times, N fertilisation led to specific increases and decreases in different parts of the plants as an adaptive strategy for allocating resources as the number of cuts increased. Our results broaden our understanding of carbohydrate and protein metabolism in tropical grasses, thereby providing subsidies for the rational use of nitrogen fertilisers.

Key words: cuttings, grasses, nitrogen, regrowth, reserves.

INTRODUCTION

Pastures cover approximately 67% of the areas used for global farming activity, with an emphasis on tropical and subtropical regions (FAO, 2020). In Brazil, pastures occupy approximately 21% of its territory, with the *Urochloa* genus standing out, with

the marandu cultivar (*Urochloa brizantha*) currently being the most cultivated forage crop in the country (Lapig, 2020). Marandu grass is a forage grass of significant economic importance because of its remarkable adaptability to different soil and climate conditions, favoured its spread and application in animal production systems in the tropics (Jank et al., 2014). However, optimising the sustainable production of marandu grass requires a deep understanding of the complex interactions resulting from the management practises often employed in pastoral environments.

In these environments, forage plants are often subjected to leaf area loss and fertilisation strategies aimed at increasing productivity (Pereira et al., 2015). The primary studies related to Marandu grass have focused on the impacts of N fertilisation and defoliation practices on morphogenic, structural, productive, and nutritional characteristics (Alexandrino et al., 2004; Pereira et al., 2015; Pontes et al., 2017). These investigations reveal that the application of nitrogen, when combined with an appropriate approach to cutting intensity and frequency, plays a significant role in boosting growth rates (Alexandrino et al., 2004; Pereira et al., 2015), biomass production, and nutritional quality (Benett et al., 2008; Pontes et al., 2017).

Despite the scientific progress made, there are still substantial gaps in the understanding of these factors related to the metabolism of tropical grasses, especially concerning the synthesis, allocation, and remobilisation of carbohydrates and proteins in different parts of the plant and during different growth stages. Studies on the metabolism of grasses of this genus are scarce and use the content of non-structural carbohydrates and the content of total nitrogen and free amino acids as parameters to assess N and carbon metabolism (Fulkerson & Donaghy, 2001; Da Silva et al., 2014; Ferro et al., 2015; Garcez & Monteiro, 2022). However, these analyses do not delve into the necessary details and fail to consider specific types of carbohydrates, such as starch, which also plays a significant role in plant metabolism (Weise et al., 2011).

Soluble carbohydrates serve as an immediate source of energy produced during photosynthesis and are rapidly utilised to sustain vital metabolic processes like growth and stress response (Rosa et al., 2009). Conversely, starch functions as a storage carbohydrate that plants accumulate as an energy reserve, mobilised when needed-such as during the night or under unfavourable photosynthetic conditions (Volenec & Nelson, 2020). Furthermore, relying solely on the total N content or free amino acids to assess protein metabolism proves inadequate, as different proteins fulfil distinct functions in different plant parts (Taiz et al., 2018). Addressing these gaps could enhance our understanding of the metabolic adaptation of these grasses, facilitating improvements in pasture management and the efficient utilisation of mineral fertilisers.

Our study aims to quantify metabolite content in different segments of Marandu grass, with a specific focus on the influence of N fertilisation and its effects following successive cuts. Our hypothesis is that the application of N to the soil and its effects on successive cuts significantly influence the metabolism of carbohydrates and proteins in different parts of Marandu grass.

MATERIALS AND METHODS

The experiment was conducted in greenhouse belonging to the Forage and Pasture sector of the State University of Southwest Bahia in Itapetinga, Bahia, Brazil (15º14'S, 40º14'W) from February to July 2017. During the experimental period, the minimum,

maximum, and average temperatures recorded inside the greenhouse were 12.2 °C, 37.2 °C and 26.1 °C, respectively. The study was conducted in a 4×3 factorial design, with four nitrogen rates (0, 75, 150, and 225 kg N ha^{-1}) and three cutting regimes (one, two and three cuts) arranged in a completely randomised design, with four replications totalling 48 pots.

Plastic pots with a capacity of 12 litres each were used and filled with 9 dm^3 of sandy loam soil collected from a depth of 0 to 20 cm. The soil underwent chemical analysis covering different parameters, such as pH (hydrogen potential in water), nutrient levels such as phosphorus (P), potassium (K), calcium (Ca), and magnesium (Mg), as well as the presence of aluminium (Al) and hydrogen (H). Base sum (BS), cations exchange capacity at pH 7.0 (T) and effective (t), base saturation (V), and the quantity of organic matter (O.M.) were also assessed, as shown in Table 1.

Table 1. Chemical analysis of soil collected at a depth of 0–20 cm

pH	P	K^+	Ca^{2+}	Mg^{2+}	Al^{3+}	H^+	BS	T	t	V	O.M.
(H_2O)	mg dm^{-3}	----------			$cmol_c$ dm^{-3}	----------				%	g dm^{-3}
5.3	6	0.08	2.4	1.8	0.2	3.6	4.3	8.1	4.5	53	10

To determine the soil's water retention capacity, pots with dry soil were weighed and saturated with water for three days. After draining the excess water, the pots were weighed again, and the difference in weight between the wet and dry soil after draining was determined as the maximum water-holding capacity of the soil. This value was used to replenish the water in each pot each day. Based on the soil analysis, there was no need for liming. The levels of phosphorus (P) and potassium (K) were below those required by the species; therefore, 22 kg P ha^{-1} and 25 kg K ha^{-1} were applied. Four plants of *Urochloa brizantha* cv. Marandu were used per pot, produced from commercial seeds with 80% cultural value.

When the plants reached 30 cm in height, all pots were cut 10 cm from the soil and nitrogen rates 75, 150, and 225 kg N ha^{-1} were applied according to each treatment. After 28 days of fertilisation, 16 pots were divided into leaves, stems and roots. Two grammes of fresh mass were collected from each fraction, wrapped in aluminium foil, and frozen for protein fractionation analysis. The remaining material was placed in a forced-circulation (Solidsteel SSDCR 40L220V environment +5 °C to 200 °C with capacity of 40 litres) oven at 65 °C for 72 h. After pre-drying, the dried material was ground in a ball mill and then subjected to final drying in an oven at 105 °C for 24 h. The remaining pots were cut at a height of 10 cm, and the cut aerial part was discarded. The process was repeated twice more, as shown in Fig. 1.

The two grams of leaves, stem, and roots collected from the pots at each cutting were extracted and fractionated into globulins, prolamins, albumins, and basic glutelins according to their solubility in distilled water, sodium chloride (NaCl), ethanol, and sodium hydroxide (NaOH), respectively, as proposed by Osborne (1924) and shown in Fig. 2. The content of soluble proteins present in the different protein fractions was quantified by the method described by Bradford (1976) using Coomassie blue G-250 solution and read in a spectrophotometer (Broadband 4NM) at 595 nm absorbance. The protein content was calculated in milligrams per gram of dry matter as a function of the dry matter content of the samples.

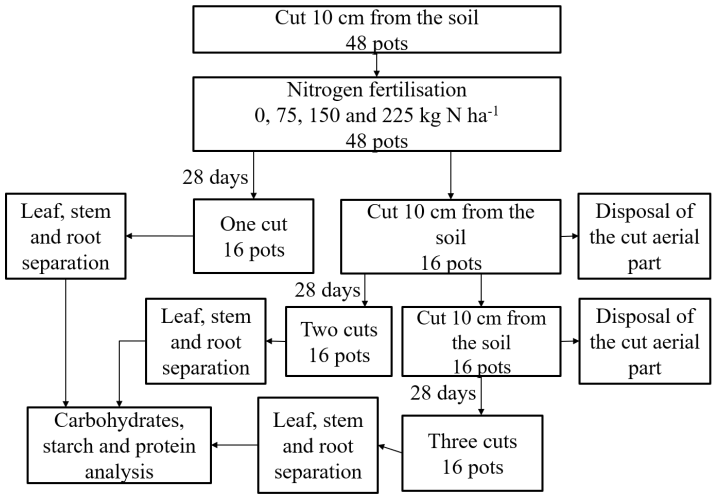

Figure 1. Schematic of cuts and sample collection in the experiment.

To quantify the carbohydrates, 0.3 g of the dry mass of leaf, stem, and root was subjected to the extraction of soluble sugar in distilled water by mixing the sample with water, followed by centrifugation. This process was repeated twice more and the supernatant was collected and used to quantify water-soluble carbohydrates (WSC). The resulting pellet was suspended in 5 mL of 200 mM potassium acetate buffer (pH 4.8) and placed in a water bath at 100 °C for 5 min to neutralise the enzymes. A solution containing amyloglucosidase enzyme was then added (0.08 mL), and the homogenate was incubated under the optimum conditions for 2 h under constant stirring. After incubation, centrifugation was performed at 9,000 g for 20 min, and the supernatant was collected for starch quantification. The content of WSC and starch was quantified using the Antrona method (Dische, 1962).

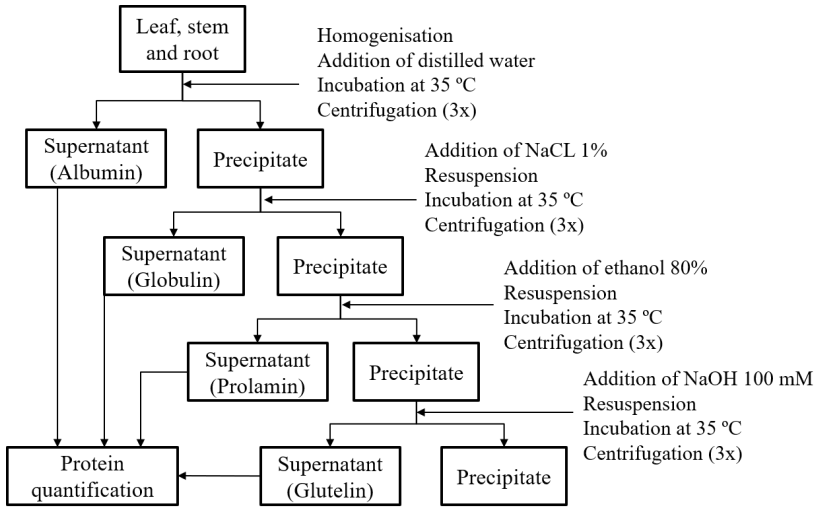

Figure 2. Schematic diagram of protein extraction.

The data were subjected to analysis of variance using the Statistical Analysis System (SAS) OnDemand for Academics programme (SAS Institute Inc., Cary, NC), considering nitrogen rates (N), cuttings (C) and the interaction of N and C as sources of variation. The effects of nitrogen fertilisation were assessed by simple regression analysis using an orthogonal decomposition of the nitrogen effect, the coefficients of which were assessed using the *F* test ($\alpha = 0.05$). Comparisons between cuts were made using the *Tukey's test*, with $\alpha = 0.05$.

RESULTS AND DISCUSSION

The interaction between N fertilisation and the number of cuts had a significant influence ($p < 0.0001$) on the content of WSC in the leaves, stems and roots (Table 2).

Table 2. Content of water-soluble carbohydrates (WSC) in leaves, stems and roots of marandu grass according to nitrogen rates and number of cuts

	Nitrogen rate (kg ha^{-1})				*P*-value					s.e.m.
	0	75	150	225	N*	C*	N×C*	L[1]	Q[1]	
WSC leaves (mg g^{-1} of DM)										
Cuts										
One	50^{a}	50^{b}	31^{c}	22^{c}	<.0001	<.0001	<.0001	<.0001	0.0009	
Two	18^{c}	96^{a}	86^{a}	85^{a}				<.0001	<.0001	1.21
Three	29^{b}	53^{b}	58^{b}	63^{b}				<.0001	<.0001	
WSC stem (mg g^{-1} of DM)										
Cuts										
One	20^{c}	37^{c}	42^{c}	36^{c}	<.0001	<.0001	<.0001	<.0001	<.0001	
Two	62^{a}	68^{b}	60^{b}	53^{b}				0.0016	0.0097	2.30
Three	48^{b}	97^{a}	105^{a}	92^{a}				<.0001	<.0001	
WSC roots (mg g^{-1} of DM)										
Cuts										
One	23^{b}	18^{c}	15^{c}	13^{c}	<.0001	<.0001	<.0001	<.0001	0.2238	
Two	14^{c}	26^{b}	31^{b}	23^{b}				<.0001	<.0001	1.40
Three	34^{a}	47^{a}	61^{a}	55^{a}				<.0001	<.0001	

Means followed by different letters, comparing the effect of cuts, are different by the *Tukey test* ($P < 0.05$). *Probability of significant for nitrogen fertilisation (N), number of cuts (C) and interaction (N×C). [1]Probability of significant effect due to nitrogen rate (L = linear effect; Q = quadratic effect; $P < 0.05$). s.e.m. = standard error of means.

In response to N fertilisation, a reduction of 57% in WSC content was observed in the leaves when fertilised with 225 kg N ha^{-1} in plants with one cut (Table 2). This decrease suggests that the plant reallocates its energy resources to maximise the assimilation of excess N (Bloom et al., 1992; Nunes-Nesi et al., 2010). According to Huppe & Turpin (1994), the capacity of the roots to absorb N and convert it into amino acids and N compounds in the leaves is directly conditioned by the amount of carbohydrates supplied through photosynthesis. The reallocation of energy resources to the synthesis of proteins represents a common adaptive mechanism in grasses (Conaghan et al., 2012; Olszewska, 2021). Conaghan et al. (2012) documented a 37% reduction in WSC content with 120 kg N ha^{-1}, whereas Olszewska (2021) observed a decrease of up to 32% with the

application of 240 kg N ha^{-1}. These results corroborate our findings, indicating a similar and even more pronounced response in grasses from tropical climates.

In plants cut two and three times, the WSC content in the leaves increased with fertilisation, reaching maximum values with the application of 148 kg N ha^{-1} and 209 kg N ha^{-1}, respectively (Table 2). The content of WSC in the leaves decreased in the unfertilised plants with two and three cuts, unlike the fertilised plants, in which they increased at rates of 75, 150, and 225 kg N ha^{-1}. This response is associated with the internal remobilisation of N to recover the photosynthetic leaf area (Meuriot et al., 2018). Lu et al. (2017) observed a positive relationship between the content of soluble proteins and N compounds in the roots and the regeneration capacity of the aerial part of alfalfa (*Medicago sativa* L.). According to Gloser et al. (2007), plants fertilised with N have higher concentrations of proteins and N compounds, which are used as a N reserve, accelerating the recovery of photosynthetic leaf area and, consequently, WSC content in the plant.

The WSC content in the stem increased with fertilisation, reaching maximum values at rates of 143, 67, and 148 kg N ha^{-1} in plants that were cut one, two, and three times, respectively (Table 1). N fertilisation improves the photosynthetic capacity of the plant, increasing the synthesis of soluble carbohydrates (Rufty et al., 1989), even after three cuts. The plant directs part of the carbohydrates produced in the aerial part to supply the energy demand necessary for the assimilation of N by the roots, increasing the flow in that part of the plant (Bredemeier & Mundstock, 2000), or to store the surplus in permanent organs, such as the stem (Volenec & Nelson, 2020).

In contrast to the stem, fertilisation with 225 kg N ha^{-1} reduced the WSC content in the roots in plants with one cut by 51% (Table 1). The decrease in WSC content in the roots is due to the energy-intensive process of N assimilation (Masclaux-Daubresse et al., 2010). The proximity of the root to the nutrient and the greater availability of N in the soil allows the plant to redirect its energy resources towards the absorption and incorporation of N into amino acids (Huppe & Turpin, 1994; Bredemeier & Mundstock, 2000). De Faria et al. (2019) also found a reduction in WSC content in the roots of piatã grass (*Urochloa brizantha*) when fertilised with 100 mg N dm^{-3}.

However, in plants cut two and three times, there was an increase in WSC content in the roots, reaching maximum values with the application of 131 kg N ha^{-1} and 149 kg N ha^{-1}, respectively. Plants fertilised with N tend to accumulate greater N reserves at the base of the stem and in the roots (Gloser et al., 2007). The reserves act as a source of N and energy for the rapid restoration of the plant's photosynthetic capacity (Dierking et al., 2017). Restoring leaf area and carbohydrate synthesis allows carbohydrates to be directed to other parts of the plant, such as the roots (Vantini et al., 2005). This adaptive strategy helps plants cope with repeated cutting cycles more efficiently (Avice et al., 1996; Aranjuelo et al., 2014).

The interaction between N fertilisation and the number of cuts was significant ($p < 0.0001$) for starch content in the stem and roots (Table 3). In the stem, the starch content increased by 5.5 mg g^{-1} of DM when fertilised with 225 kg N ha^{-1} in plants with one cut. N potentiates the recovery of leaf area, increasing photosynthetic activity, and stimulating WSC synthesis in the plant (Bassi et al., 2018). These WSCs are then used for the synthesis of reserve carbohydrates, such as starch in the stem (Vantini et al., 2005). In leaves, starch is considered transitory, since all the starch produced during the day is decomposed during the night (Weise et al., 2011). In contrast, starch stored in

permanent organs, such as stems and roots of grasses, serves as a source of energy in the medium and long term (Volenec & Nelson, 2020).

In plants cut two and three times, there was an increase in stem starch content, reaching maximum estimated values with the application of 128 kg N ha^{-1} and 91 kg N ha^{-1}, respectively (Table 3). The increase of starch in the stems of fertilised plants is linked to the increase of WSC in plants, as previously observed. The internal redistribution of N in fertilised plants during subsequent cuts results in a more efficient recovery after cutting (Gloser et al., 2007; Dierking et al., 2017), resulting in an increase in the production of carbohydrates that can be stored in the form of starch in the stem (Slewinski, 2012).

Table 3. Starch content in stems and roots of marandu grass according to nitrogen rates and number of cuts

	Nitrogen rate (kg ha^{-1})				*P*-value					s.e.m.
	0	75	150	225	N*	C*	N×C*	L[1]	Q[1]	
Starch stem (mg g^{-1} of DM)										
Cuts										
One	2.5[c]	3.8[c]	5.8[c]	7.9[a]	<.0001	<.0001	<.0001	<.0001	0.0702	
Two	5.9[b]	6.2[b]	6.8[b]	5.9[b]				0.5177	0.0056	0.20
Three	7.9[a]	11.7[a]	11.5[a]	4.8[c]				<.0001	<.0001	
Starch root (mg g^{-1} of DM)										
Cuts										
One	3.8[b]	1.4[c]	1.4[c]	2.5[b]	<.0001	<.0001	<.0001	<.0001	<.0001	
Two	3.8[b]	3.5[b]	2.5[b]	2.4[b]				<.0001	0.2363	0.11
Three	5.4[a]	5.1[a]	3.9[a]	3.3[a]				<.0001	0.2891	

Means followed by different letters, comparing the effect of cuts, are different by the *Tukey test* ($P < 0.05$). * Probability of significant for nitrogen fertilisation (N), number of cuts (C) and interaction (N×C). [1]Probability of significant effect due to nitrogen rate (L = linear effect; Q = quadratic effect; $P < 0.05$). s.e.m. = standard error of means.

Unlike the stem, the starch content in the roots decreased by 54% with N fertilisation, reaching minimum estimated value with the application of 101 kg N ha^{-1} in plants with one cut (Table 3). The trend of reducing starch content in the roots in response to N fertilisation was also observed in plants cut two and three times, with reductions of 41% and 42%, respectively, when fertilised with 225 kg N ha^{-1}. The removal in leaf area reduces the aerial part's capacity to generate energy for N assimilation (Gomide et al., 2002). As an adaptive response to take advantage of excess N, the plant uses its energy reserves in the roots to absorb and assimilate inorganic N (Morcuende et al., 2011; Soares Filho et al., 2013; Guo et al., 2017). This adaptive response was also confirmed by Soares Filho et al. (2013), who observed a 19% reduction in non-structural carbohydrates in the roots of Tanzânia grass (*Megathyrsus maximus*) treated with 150 kg N ha^{-1}. Similar results were reported by Vantini et al. (2005), demonstrating a reduction in root starch content of Tanzânia grass (*Megathyrsus maximus*) when exposed to 150 mg N dm^{-3}.

Even after three cuts, a higher starch content was observed in the roots and stem of all the plants (Table 3). When plants are cut frequently, they may allocate more resources to the root system as a survival strategy (Wiley et al., 2013). In fertilised plants, this

increase is related to the greater availability of WSC and root growth, contributing to the increase in starch in these parts of the plant (Lawlor, 2002; Kakabouki et al., 2020).

The interaction between N fertilisation and the number of cuts had a significant effect ($p < 0.0001$) on albumin content in the leaves, stems and roots (Table 4). Albumin concentration in leaves increased by 7, 16 and 5 mg g^{-1} of DM when fertilised with 225 kg N ha^{-1} in plants that were cut one, two and three times, respectively.

Table 4. Content of albumin in leaves, stems and roots of marandu grass according to nitrogen rates and number of cuts

	Nitrogen rate (kg ha^{-1})				*P*-value					s.e.m.
	0	75	150	225	N*	C*	N×C*	L[1]	Q[1]	
Albumin leaves (mg g^{-1} of DM)										
Cuts										
One	8.3[a]	10.7[a]	13.4[b]	15.2[b]				<.0001	0.3202	
Two	5.9[b]	9.9[a]	15.1[a]	21.5[a]	<.0001	<.0001	<.0001	<.0001	0.0001	0.28
Three	7.8[a]	8.5[b]	11.6[c]	12.3[c]				<.0001	0.9148	
Albumin stem (mg g^{-1} of DM)										
Cuts										
One	1.4[b]	3.7[a]	4.9[a]	7.8[a]				<.0001	0.1719	
Two	2.4[a]	3.2[a]	3.6[b]	3.7[b]	<.0001	<.0001	<.0001	<.0001	0.1345	0.22
Three	1.8[ab]	2.3[b]	2.6[c]	3.6[b]				<.0001	0.3138	
Albumin root (mg g^{-1} of DM)										
Cuts										
One	0.9[a]	3.4[a]	4.8[a]	3.7[a]				<.0001	<.0001	
Two	0.9[a]	1.5[b]	2.2[b]	2.4[b]	<.0001	<.0001	<.0001	<.0001	0.0931	0.12
Three	0.9[a]	1.6[b]	2.1[b]	2.5[b]				<.0001	0.2558	

Means followed by different letters, comparing the effect of cuts, are different by the *Tukey test* ($P < 0.05$). * Probability of significant for nitrogen fertilisation (N), number of cuts (C) and interaction (N×C). [1]Probability of significant effect due to nitrogen fertilisation (L = linear effect; Q = quadratic effect; $P < 0.05$). s.e.m. = standard error of means.

Hojilla-Evangelista et al. (2016) observed that when extracting proteins from alfalfa (*Medicago sativa*) leaves, albumins constituted the main fraction of the total protein. According to Rasheed et al. (2020), the greater participation of albumins in the leaves is due to the presence of enzymes such as Rubisco, ATP synthase, PEP-carboxylase, and glutamate synthase, all of which are soluble in water. When N is application to plants through fertilisation, the concentration of enzymes in the leaves increases because N stimulates enzyme synthesis and activity (Bassi et al., 2018; Yasuoka et al., 2018; Kocheva et al., 2020).

Despite the decrease in albumins in fertilised plants as the number of cuts increased, they remained highly concentrated in the leaves, particularly in plants with two cuts. This suggests that the plant prioritises the allocation of internal resources to maintain the concentration and activity of enzymes that act in primary metabolism as a way of maximising photosynthetic activity (Thornton & Millard, 1996; Masclaux-Daubresse et al., 2010).

The beneficial effect of N fertilisation on albumin content was also observed in the stem, with an increase of 6, 1 and 2 mg g^{-1} DM when fertilised with 225 kg N ha^{-1} in plants that were cut one, two and three times, respectively (Table 4). This response demonstrates the significant impact of N on this specific protein group, particularly in

the plant stem under conditions of high N availability. This influence can be attributed to the positive effect of N, which amplifies the synthesis of enzymes responsible for nutrient transport and growth, contributing to the increase in albumins content in the stem (Bassi et al., 2018; Taiz et al., 2018). The decrease in albumin content in the stem of fertilised plants as the number of cuts increased may indicate that these proteins can be remobilised during regrowth for the synthesis of new enzymes in the leaves (Volenec et al., 1996; Masclaux-Daubresse et al., 2010; Dierking et al., 2017).

In the roots, the albumin content increased with N fertilisation, reaching maximum estimated value with the application of 123 kg N ha^{-1} in plants with one cut. In plants cut two and three times, the albumin content in the roots increased by 2 mg g^{-1} DM when fertilised with 225 kg N ha^{-1} (Table 4). The application of N tends to increase the synthesis of enzymes involved in nutrient assimilation and protein synthesis in the roots (Garcez & Monteiro, 2022). These proteins, in turn, contribute to increasing the albumin fraction in the roots of fertilised plants (Rasheed et al., 2020). Garcez & Monteiro (2022) observed an increase in glutamine synthetase (GS) activity and total free amino acid concentrations in the roots of grasses from the *Urochloa* and *Megathyrsus* genera in response to N fertilisation. It is important to note that, despite the reduction in albumins after three cuts, the plants fertilised with N maintained elevated albumin content (Table 4). The reduction in this protein group may be associated with the plant's adaptive mechanism, which, with greater internal N availability, prioritises the remobilisation of amino acids from other parts of the plant in order to maintain the levels and activity of the enzymes involved in primary metabolism in subsequent cuts (Masclaux-Daubresse et al., 2010).

The interaction between N fertilisation and the number of cuts had a significant effect ($p < 0.0001$) on the content of globulins in the leaves, stems and roots (Table 5). Globulins in leaves with one cut increased by 6 mg g^{-1} DM with the application of 225 kg N ha^{-1}. In plants cut twice, N fertilisation also increased the globulins content in the leaves, reaching maximum value with the application of 103 kg N ha^{-1}. However, in plants cut three times, the globulins content in the leaves decreased by 52% when fertilised with 225 kg N ha^{-1}.

Globulins are predominantly composed of hydrophobic proteins because of their association with the lipid layer of the membrane and their solubility in saline solution (Teng & Wang, 2012; Rasheed et al., 2020). In the leaves, there is a considerable increase in globulins with N fertilisation, possibly due to the effect of N in stimulating the synthesis of membrane proteins of the photosynthetic complex, which act together with chlorophylls and enzymes in carbon assimilation processes (Bassi et al., 2018; Taiz et al., 2018). This increase may have contributed to the increase in globulin content in this part of the plant.

In the stem, N fertilisation increased the globulin content by 2 and 0.7 mg g^{-1} DM with the application of 225 kg N ha^{-1} in plants cut one and three times. However, the globulin content in the stem decreased by 44% when fertilised with 225 kg N ha^{-1} in plants cut twice (Table 5). In the roots, N fertilisation also led to an increase of 2 mg g^{-1} DM in globulin content when fertilised with 225 kg N ha^{-1} in plants with one cut. There was no effect of fertilisation on subsequent cuts. It is important to emphasize the significant reduction in the content of this protein group in the leaves at a rate of 225 kg N ha^{-1} with three cuts. In both the stem and roots, there was a reduction in globulins in the evaluated N rates as the number of cuts increased.

Table 5. Content of globulin in leaves, stems and roots of marandu grass according to nitrogen rates and number of cuts

	Nitrogen rate (kg ha^{-1})				*P*-value					s.e.m.
	0	75	150	225	N*	C*	N×C*	L[1]	Q[1]	
Globulin leaves (mg g^{-1} of DM)										
Cuts										
One	4.8^{c}	6.1^{b}	8.5^{ab}	10.5^{a}	0.1112	<.0001	<.0001	<.0001	0.4002	
Two	6.9^{b}	8.9^{a}	9.7^{a}	8.1^{b}				0.0114	<.0001	0.37
Three	12.8^{a}	9.5^{a}	8.2^{b}	6.1^{c}				<.0001	0.0873	
Globulin stem (mg g^{-1} of DM)										
Cuts										
One	2.8^{a}	3.8^{a}	3.8^{a}	4.8^{a}	0.0001	<.0001	<.0001	<.0001	0.9689	
Two	1.6^{b}	1.5^{b}	1.1^{b}	0.9^{c}				0.0010	0.8945	0.16
Three	1.2^{b}	1.1^{b}	1.6^{b}	1.9^{b}				0.0006	0.1665	
Globulin root (mg g^{-1} of DM)										
Cuts										
One	2.7^{a}	3.2^{a}	4.6^{a}	4.5^{a}	0.0213	<.0001	<.0001	<.0001	0.1576	
Two	0.7^{b}	1.0^{b}	0.6^{b}	0.6^{b}				0.3735	0.3906	0.21
Three	1.2^{b}	1.0^{b}	0.9^{b}	0.9^{b}				0.2910	0.6011	

Means followed by different letters, comparing the effect of cuts, are different by the *Tukey test* ($P < 0.05$). * Probability of significant for nitrogen fertilisation (N), number of cuts (C) and interaction (N×C). [1]Probability of significant effect due to nitrogen rate (L = linear effect; Q = quadratic effect; $P < 0.05$). s.e.m. = standard error of means.

To date, there are no studies in the literature that offer a better understanding of globulins in different plant tissues. Since these proteins are associated with the membrane, they can perform multiple functions in plants, including photosynthesis, transport, nutrient absorption, signalling, and storage in plant tissues (Shewry et al., 1995; Taiz et al., 2018). In our study, we observed that globulins are highly responsive to N fertilisation. Their reduction in stems and roots as the number of cuts increased may be linked to the internal remobilisation of this protein group as an adaptive process to the loss of leaf area, varying according to its concentration in each part of the plant (Volenec et al., 1996).

The interaction between N fertilisation and the number of cuts was significant ($p < 0.0001$) for the content of prolamins in the leaves, stems and roots (Table 6). N fertilisation increased the prolamins content in the leaves, reaching maximum estimated value with the application of 230 kg N ha^{-1} and 100 kg N ha^{-1} in plants cut one and two times, respectively. With three cuts, the prolamins content in the leaves decreased by 58% when fertilised with 225 kg N ha^{-1}.

The unfertilised plants increased prolamins in the leaves after the second and third cuts, unlike the fertilised plants, which showed a reduction with the third cut. Prolamins are considered to be storage proteins unique to plants and play a fundamental role as the main source of amino acids during germination and the initial phase of plant growth (Shewry & Tatham, 1990; Shewry et al., 1995). Abbaraju et al. (2022) observed that N fertilisation increased the concentration of vegetative storage proteins in maize (*Zea mays*) leaves. According to Abbaraju et al. (2022), the concentration of storage proteins is influenced by the availability of N in the soil, which represents a strong drain on surplus assimilated N.

Vegetative storage proteins in grasses are produced by plants to store N during periods of growth, acting as a source of N and energy to survive in unfavourable conditions (Avice et al., 1996; Meuriot et al., 2018). The presence of prolamins in leaves may represent an adaptive strategy to optimise the use of nutrients and resources due to the greater availability of N.

Table 6. Content of prolamin in leaves, stems and roots of marandu grass according to nitrogen rates and number of cuts

	Nitrogen rate (kg ha^{-1})				*P*-value					s.e.m.
	0	75	150	225	N*	C*	N×C*	L[1]	Q[1]	
Prolamin leaves (mg g^{-1} of DM)										
Cuts										
One	2.4^{b}	3.7^{b}	5.2^{a}	5.7^{a}	<.0001	<.0001	<.0001	<.0001	0.0079	
Two	3.6^{a}	5.3^{a}	5.8^{a}	3.6^{b}				0.7343	<.0001	0.15
Three	3.8^{a}	2.7^{c}	2.1^{b}	1.6^{c}				<.0001	0.0910	
Prolamin stem (mg g^{-1} of DM)										
Cuts										
One	2.1^{a}	3.1^{a}	3.0^{a}	4.0^{a}	<.0001	<.0001	0.0091	<.0001	0.9337	
Two	1.8^{a}	2.3^{b}	2.2^{b}	2.6^{b}				0.0017	0.7280	0.16
Three	0.8^{b}	1.1^{c}	1.2^{c}	1.4^{c}				0.0144	0.6722	
Prolamin root (mg g^{-1} of DM)										
Cuts										
One	5.0^{a}	7.5^{a}	7.7^{a}	6.4^{a}	0.0011	<.0001	<.0001	0.0041	<.0001	
Two	3.6^{b}	3.1^{b}	2.8^{b}	1.6^{b}				<.0001	0.2896	0.31
Three	2.2^{c}	1.5^{c}	1.5^{c}	1.1^{b}				0.0152	0.6452	

Means followed by different letters, comparing the effect of cuts, are different by the *Tukey test* ($P < 0.05$). * Probability of significant for nitrogen fertilisation (N), number of cuts (C) and interaction (N×C). [1]Probability of significant effect due to nitrogen rate (L = linear effect; Q = quadratic effect; $P < 0.05$). s.e.m. = standard error of means.

In the stem, N fertilisation resulted in a linear increase in the prolamins content when fertilised with 225 kg N ha^{-1} in plants cut one, two and three times (Table 6). In the roots, the prolamins content in plants with one cut increased with N fertilised, reaching maximum estimated value with the application of 109 kg N ha^{-1}. In plants cut two and three times, N fertilisation led to a significant reduction in prolamins content in the roots, with reductions of 55% and 53% observed at application rates of 225 kg N ha^{-1}, respectively. The positive response of N fertilisation on prolamin synthesis with one cut may indicate a greater investment of the excess N assimilated in the accumulation of reserve proteins in the stem and roots (Dierkung et al., 2017). These proteins were used in subsequent cuts as a source of N to restore the plant's photosynthetic capacity (Gloser et al., 2007). According to Lehmeier et al. (2013), organic reserves made up of N provide almost half of the N used during grass regrowth, indicating the importance of reserve proteins in plant regrowth.

The interaction between N fertilisation and the number of cuts was significant ($p < 0.0001$) for the glutelin content in the leaves, stem and roots of the Marandu grass (Table 7). The glutelin content in the leaves increased by 60% when fertilised with 225 kg N ha^{-1} in plants with one cut.

Table 7. Content of glutelin in leaves, stems and roots of marandu grass according to nitrogen rates and number of cuts

	Nitrogen rate (kg ha^{-1})				*P*-value					s.e.m.
	0	75	150	225	N*	C*	N×C*	L[1]	Q[1]	
Glutelin leaves (mg g^{-1} of DM)										
Cuts										
One	11.1^{a}	12.3^{a}	16.6^{a}	17.7^{a}	0.0168	<.0001	<.0001	<.0001	0.8788	
Two	12.1^{a}	10.8^{a}	9.8^{b}	10.7^{b}				0.0676	0.0694	0.61
Three	11.1^{a}	7.6^{b}	6.3^{c}	7.2^{c}				<.0001	0.0013	
Glutelin stem (mg g^{-1} of DM)										
Cuts										
One	3.7^{b}	5.5^{a}	7.2^{a}	9.6^{a}	<.0001	<.0001	<.0001	<.0001	0.4274	
Two	7.0^{a}	4.7^{a}	4.4^{b}	5.2^{b}				0.0025	0.0003	0.38
Three	3.2^{b}	3.5^{b}	3.9^{b}	4.8^{b}				0.0047	0.3734	
Glutelin root (mg g^{-1} of DM)										
Cuts										
One	8.2^{b}	11.8^{a}	14.6^{a}	9.4^{a}	0.0036	<.0001	<.0001	0.0088	<.0001	
Two	10.4^{a}	9.8^{b}	8.5^{b}	8.4^{a}				0.0051	0.6399	0.52
Three	9.3^{ab}	6.5^{c}	6.6^{c}	6.9^{b}				0.0055	0.0068	

Means followed by different letters, comparing the effect of cuts, are different by the *Tukey test* ($P < 0.05$). * Probability of significant for nitrogen fertilisation (N), number of cuts (C) and interaction (N×C). [1]Probability of significant effect due to nitrogen rate (L = linear effect; Q = quadratic effect; $P < 0.05$). s.e.m. = standard error of means.

However, in plants cut twice, there was no significant difference. In plants cut three times, there was a reduction of glutelin in the leaves with N fertilised, reaching maximum estimated value with the application of 150 kg N ha^{-1}. In the stem, glutelin content increased by 159% and 50% when fertilised with 225 kg N ha^{-1} in plans cut one and three times, respectively. Unlike the others, in plants cut twice, there was a reduction in glutelin content in the stem of fertilised plants, reaching minimum estimated value with the application of 190 kg N ha^{-1}. The glutelin content increased in the roots of the plants fertilised with one cut, reaching maximum estimated value with the application of 121 kg N ha^{-1}. However, for the other cuts, there was a reduction in glutelin content in the roots, reaching minimum estimated value with the application of 200 kg N ha^{-1} for plants cut two and three times.

The function of glutelin in different parts of plants is not yet fully understood, and more studies are needed to gain a deeper understanding of their role in different plant parts, as well as their involvement in the metabolism of tropical grasses. In the literature, glutelins are identified as proteins with a storage function exclusive to plants, but they possess larger and more complex structures than prolamins, and play a specific role as amino acid reservoirs in seeds during plant germination (Osborne, 1924; D'ovidio & Masci, 2004). However, due to their extraction using sodium hydroxide, they may include proteins with structural functions in plant tissues (Rasheed et al., 2020). In our study, we found that glutelins represent the predominant group of proteins in different parts of Marandu grass and respond significantly to N fertilisation. We observed a marked reduction in glutelin content in the stems and roots of fertilised plants, as well as in the leaves at rates of 150 and 225 kg N ha^{-1}, as the number of cuts increased. This indicates that, at high content, this group of proteins can also act as a N reserve during regrowth.

Although our results offer valuable insights into how N fertilisation and the number of cuts impact carbohydrate and protein metabolism in Marandu grass, further research is necessary to enhance our understanding. This necessity is justified by the fact that the growth conditions within a greenhouse environment might not entirely replicate the natural habitat of the plants, potentially influencing the outcomes. To mitigate these potential effects, conducting experiments that closely simulate field conditions is recommended. These findings can serve as a foundation for future investigations, including studies on specific fertilisation and management strategies, interactions with other nutrients, effects on different soil types and climates, and contributing to the reduction of the dependency on N fertilisers.

CONCLUSIONS

The Marandu grass demonstrates a remarkable ability to adapt to leaf area loss through the strategic allocation of resources. In situations of energy imbalance due to leaf area loss, the plant directs its carbon reserves towards the assimilation of excess nitrogen in the soil, increasing the synthesis of different protein groups in the plant. These proteins play a fundamental role in the growth and recovery of the plant after subsequent cuts. These findings contribute to a better understanding of resource allocation and adaptive strategies of tropical forage plants, especially concerning carbohydrate and protein metabolism, with significant implications for proper plant management and the use of nitrogen fertilisers.

ACKNOWLEDGEMENTS. This study was financed in part by the Coordenação de Aperfeiçoamento de Pessoal de Nível Superior - Brasil (CAPES) - Finance Code 001, and by Fundação de Amparo à Pesquisa do Estado da Bahia (FAPESB).

REFERENCES

Abbaraju, H.K.R., Gupta, R., Appenzeller, L.M., Fallis, L.P., Hazebroek, J., Zhu, G., Bourett, T.M., Howard, R.J., Weers, B., Lafitte, R.H., Hakimi, S.M., Schussler, J.R., Loussaert, D.F., Habben, J.E. & Dhugga, KS. 2022. A vegetative storage protein improves drought tolerance in maize. *Plant Biotechnology Journal* **20**(2), 374–389. doi: 10.1111/pbi.13720

Alexandrino, E., Nascimento Júnior, D., Mosquim, P.R., Regazzi, A.J. & Rocha, F.C. 2004. Morphogenesis and Structural Characteristics of Regrowth ob *Brachiaria brizantha* cv. Marandu Assigned to Three Nitrogen Levels. *The Brazilian of Animal Science* **33**(6), 1372–1379. doi: 10.1590/S1516-35982004000600003 (in Portuguese).

Aranjuelo, I., Molero, G., Erice, G., Aldasoro, J., Arrese-igor, C. & Nogués, S. 2014. Effect of shoot removal on remobilisation of carbon and nitrogen during regrowth of nitrogen-fixing alfalfa. *Physiologia plantarum* **153**(1), 91–104. doi: 10.1111/ppl.12222

Avice, J.C., Ourry, A., Lemaire, G. & Boucaud, J. 1996. Nitrogen and carbon flows estimated by 15N and 13C pulse-chase labeling during regrowth of alfalfa. *Plant Physiology* **112**(1), 281–290. doi: 10.1104/pp.112.1.281

Bassi, D., Menossi, M. & Mattiello, L. 2018. Nitrogen supply influences photosynthesis establishment along the sugarcane leaf. *Scientific Reports* **8**, 2327. doi: 10.1038/s41598-018-20653-1

Benett, C.G.S., Buzetti, S., Silva, K.S., Bergamaschine, A.F. & Fabricio, J.A. 2008. Yield and bromatologic composition of Marandu grass as function of sources and doses of nitrogen. *Science and Agrotechnology* **32**(5), 1629–1636. doi: 10.1590/S1413-70542008000500041 (in Portuguese).

Bloom, A.J., Sukrapanna, S.S. & Warner, R.L. 1992. Root respiration associated with ammonium and nitrate absorption and assimilation by barley. *Plant Physiology* **99**(4), 1294–1301. doi: 10.1104/pp.99.4.1294

Bradford, M.M. 1976. A rapid and sensitive method for the quantitation of microgram quantities of protein utilizing the principle of protein-dye binding. *Analytical Biochemistry* **72**, 248. doi: 10.1006/abio.1976.9999

Bredemeier, C. & Mundstock, C.M. 2000. Regulation of absorption and assimilation of nitrogen in plants. *Rural Science* **30**(2), 365–372. doi: 10.1590/S0103-84782000000200029 (in Portuguese).

Conaghan, P., O'Kiely, P., Halling, M.A., O'Mara, F.P. & Nesheim, L. 2012. Yield and Quality Response of Perennial Ryegrass Selected for High Concentration of Water-Soluble Carbohydrate to Nitrogen Application Rate. *Crop Science* **52**(6), 2839–2851. doi: 10.2135/cropsci2012.02.0100

D'ovidio, R. & Masci, S. 2004. The low-molecular-weight glutenin subunits of wheat gluten. *Journal of Cereal Science* **39**(3), 321–329. doi: 10.1016/j.jcs.2003.12.002

Da Silva, S.C., Pereira, L.E.T., Sbrissia, A.F. & Hernandez-Garay, A. 2014. Carbon and nitrogen reserves in marandu palisade grass subjected to intensities of continuous stocking management. *Journal of Agricultural Science* **153**(8), 1449–1463. doi: 10.1017/S0021859614001130

De Faria, D.A., Dallabrida Avelino, A.C., Avelino Cabral, C.E., de Abreu, J.G., de Barros, L.V., Avelino Cabral, C.H., Valiati Dantas, V.G., Guarnieri, S.F., Neto, A.B. & Barros Assis, L.M. 2019. Investigating the Optimal Day for Nitrogen Fertilisation on Piatã palisade grass and Quênia guinea grass after Defoliation. *Journal of Experimental Agriculture International* **34**(6), 1–11. doi: 10.9734/jeai/2019/v34i630192

Dierking, R.M., Allen, D.J., Cunningham, S.M., Brouder, S.M. & Volenec, J.J. 2017. Nitrogen reserve pools in two *Miscanthus x giganteus* genotypes under contrasting N Managements. *Frontier in Plant Science* **8**, 1618. doi: 10.3389/fpls.2017.01618

Dische, Z. 1962. General color reactions. In Whistler, R.L, Wolfram, M.L. *Methods Carbohydrate chemistry*. New York: Academic, pp. 477–512.

FAO. 2020. *World Food and Agriculture. Statistical Yearbook*. FAO (Rome).

Ferro, M.M., Zanine, A.M., Ferreira, D.J., Souza, A.L. & Geron, L.J.V. 2015. Organic Reserves in tropical grasses under grazing. *American Journal of Plant Sciences* **6**(14), 2329. doi: 10.4236/ajps.2015.614236

Fulkerson, W.J. & Donaghy, D.J. 2001. Plant-soluble carbohydrate reserves and senescence - key criteria for developing an effective grazing management system for ryegrass-based pastures: a review. *Australian Journal of Experimental Agriculture* **41**(2), 261–275. doi: 10.1071/EA00062

Garcez, T.B. & Monteiro, F.A. 2022. Nitrogen metabolism of two tropical forage grass species: nitrogen availability × cultivars. *Australian Journal of Crop Science* **16**(8), 1920–1029. doi: 10.21475/ajcs.22.16.08.p3239

Gloser, V., Košvancová, M. & Gloser, J. 2007. Regrowth dynamics of *Calamagrostis epigejos* after defoliation affected by the nitrogen availability. *Plantarum biology* **51**, 501–506. doi: 10.1007/s10535-007-0105-x

Gomide, C.A.M., Gomide, J.A., Huaman, C.A.M. & Paciullo, D.S.C. 2002. Photosynthesis, organic reserves and regrowth of Mombaça grass (*Panicum maximum* Jacq.) under different defoliation intensities of the main tiller. *The Brazilian of Animal Science* **31**(6), 2165–2175. doi: 10.1590/S1516-35982002000900003 (in Portuguese).

Guo, Q., Turnbull, M.H., Song, J., Roche, J., Novak, O., Späth, J., Jameson, P.E. & Love, J. 2017. Depletion of carbohydrate reserves limits nitrate uptake during early regrowth in *Lolium perenne* L. *Journal of Experimental Botany* **68**(7), 1569–1583. doi: 10.1093/jxb/erx056

Hojilla-Evangelista, M.P., Selling, G.W., Hatfield, R. & Digman, M. 2016. Extraction, composition, and functional properties of dried alfalfa (*Medicago sativa* L.) leaf protein. *Journal of the Science and Food and Agriculture* **97**(3), 882–888. doi: 10.1002/jsfa.7810

Huppe, H.C. & Turpin, D.H. 1994. Integration of carbon and nitrogen metabolism in plant and algal cells. *Annual Review of Plant Physiology and Plant Molecular Biology* **45**, 577–607. doi: 10.1146/annurev.pp.45.060194.003045

Jank, L., Barrios, S.C, Valle, C.B., Simeão, R.M. & Alves, G.F. 2014. The value of improved pastures to Brazilian beef production. *Crop and Pasture Science* **65**, 1132–1137. doi: 10.1071/CP13319

Kakabouki, I., Folina, A., Karydogianni, S., Zisi, Ch. & Efthimiadou, A. 2020. The effect of nitrogen fertilisation on root characteristics of *Camelina sativa* L. in greenhouse pots. *Agronomy Research* **18**(3), 2060–2068. doi: 10.15159/AR.20.178

Kocheva, K., Kartseva, T., Nenova, V., Georgiev, G., Brestič, M. & Misheva, S. 2020. Nitrogen assimilation and photosynthetic capacity of wheat genotypes under optimal and deficient nitrogen supply. *Physiology Molecular Biology of Plants* **26**(11), p. 2139–2149. doi: 10.1007/s12298-020-00901-3

Lapig. 2020. *Image Processing and Geoprocessing Laboratory. Dynamics of Brazilian pastures: Occupation of areas and signs of degradation - 2010 a 2018*. Goiânia: LAPIG/UFG. (in Portuguese).

Lawlor, D.W. 2002. Carbon and nitrogen assimilation in relation to yield: mechanisms are the key to understanding production systems. *Journal of Experimental Botany* **370**(57), 773–787. doi: 10.1093/jexbot/53.370.773

Lehmeier, C.A., Wild, M., Schnyder, H., Grünlandlehre, L., Pflanzenwissenschaften, D. & München, T.U. 2013. Nitrogen stress affects the turnover and size of nitrogen pools supplying leaf growth in a grass. *Plant Physiology* **162**(4), 2095–2105. doi: 10.1104/pp.113.219311

Lu, X., Ji, S., Hou, C., Qu, H., Li, P. & Shen, Y. 2017. Impact of root C and N reserves on shoot regrowth of defoliated alfalfa cultivars differing in fall dormancy. *Grassland Science* **64**(2), 83–90. doi: 10.1111/grs.12190

Masclaux-Daubresse, C., Daniel-Vedele, F., Dechorgnat, J., Chardon, F. & Suzuki, A. 2010. Nitrogen uptake, assimilation and remobilisation in plants: challenges for sustainable and productive agriculture. *Annals of Botany* **105**(7), 1141–1157. doi: 10.1093/aob/mcq028

Meuriot, F., Morvan-Bertrand, A., Noiraud-Romy, N., Decau, M., Escobar-Gutiérrez, A.J., Gastal, F. & Prud'homme, M. 2018. Short-term effects of defoliation intensity on sugar remobilisation and N fluxes in ryegrass. *Journal of Experimental Botany* **69**(16), 3975–3986. doi: 10.1093/jxb/ery211

Morcuende, R., Pérez, P., Martínez-Carrasco, R. & Gutiérrez, E. 2011. Nitrogen Modulates the Diurnal Regulation in Wheat Plants – Projections Towards Climate Change. *Agronomy Research* **9**(Special Issue II), 443–450. https://agronomy.emu.ee/wp-content/uploads/2011/12/p09s211.pdf#abstract-2827

Nunes-Nesi, A., Fernie, A. R. & Stitt, M. 2010. Metabolic and Signaling Aspects Underpinning the Regulation of Plant Carbon Nitrogen Interactions. *Molecular Plant* **3**(6), 973–996. doi:10.1093/mp/ssq049

Olszewska, M. 2021. Effects of Cultivar, Nitrogen Rate and Harvest Time on the Content of Carbohydrates and Protein in the Biomass of Perennial Ryegrass. *Agronomy* **11**(3), 468. doi: 10.3390/agronomy11030468

Osborne, T.B. 1924. *The vegetable proteins*. 2.ed. London: Longmans Green and company, 154 pp.

Pereira, L.E.T., Paiva, A.J., Guarda, V.D., Pereira, P.M., Caminha, F.O. & Da Silva, S.C. 2015. Herbage utilisation efficiency of continuously stocked marandu palisade grass subjected to nitrogen fertilisation. *Scientia Agricola* **72**(2), 114–123. doi: 10.1590/0103-9016-2014-0013

Pontes, L.S., Baldissera, T.C., Giostri, A.F., Stafin, G., Santos, B.R.C. & Carvalho, P.C.F. 2017. Effects of nitrogen fertilisation and cutting intensity on the agronomic performance of warm-season grasses. *Grass and Forage Science* **72**(4), 663–675. doi: 10.1111/gfs.12267

Rasheed, F., Markgren, J., Hedenqvist, M. & Johansson, E. 2020. Modeling to Understand Plant Protein Structure-Function Relationships—Implications for Seed Storage Proteins. *Molecules* **25**(4), 1–17. doi: 10.3390/molecules25040873

Rosa, M., Prado, C., Podazza, G., Interdonato, R., González, J.A., Hilal, M. & Prado, F.E. 2009. Soluble sugars--metabolism, sensing and abiotic stress: a complex network in the life of plants. *Plant Signaling & Behavior* **4**(5), 388–93. doi: 10.4161/psb.4.5.8294

Rufty, T.W., Mackown, C.T. & Volk, R.J. 1989. Effects of altered carbohydrate availability on whole-plant assimilation of $^{15}NO_3^-$. *Plant Physiology* **89**(2), 457–463. doi: 10.1104/pp.89.2.457

SAS Institute Inc. SAS OnDemand for Academics: Accessed: https://www.sas.com/en_us/software/on-demand-for-academics.html.

Shewry, P.R. & Tatham, A.S. 1990. The prolamin storage proteins of cereal seeds – structure and evolution. *Biochemical Journal* **267**(1), 1–12. doi: 10.1042/bj2670001

Shewry, P.R., Napier, J.A. & Tatham, A.S. 1995. Seed storage proteins: Structures and biosynthesis. *Plant Cell* **7**(7), 945–956. doi: 10.1105/tpc.7.7.945

Slewinski, T. 2012. No-structural carbohydrate partitioning in grass stems: a target to increase yield stability, stress tolerance, and bioful production. *Journal Of Experimental Botany* **63**(13), 4647–4670. doi: doi:10.1093/jxb/ers124

Soares Filho, C.V., Cecato, U., Ribeiro, O.L., Roma, C.F.C., Jobim, C.C., Beloni, T. & Perri, S.H.V. 2013. Root system and root and stem base organic reserves of pasture Tanzania grass fertiliser with nitrogen under grazing. *Semina: Ciências Agrárias* **34**(5), 2415–2426. doi: 10.5433/1679-0359.2013v34n5p2415 (in Portuguese).

Taiz, L., Zeiger, E., Møller, I.M., & Murphy, A.S. 2018. *Plant physiology and development*. New York, Oxford Universtity Press, 761 pp.

Teng, Z. & Wang, Q. 2012. Extraction, identification and characterisation of the water-insoluble proteins from tobacco biomass. *Journal of the Science and Food and Agriculture* **92**(7), 1368–1374. doi: 10.1002/jsfa.4708

Thornton, B. & Millard, P. 1996. The effect of severity of defoliation on root functioning ins grasses. *Journal of Range Management* **49**(5), 443–447. doi: 10.2307/4002927

Vantini, P.P., Rodrigues, T.J.D., Cruz, M.C.P., Rodrigues, L.R.A. & Malheiros, E.B. 2005. Total non-structural carbohydrate content of Tanzania grass fertilised with different doses of nitrogen. *Acta Scientiarum. Animal Sciences* **27**(4), 425–432. doi: 10.4025/actascianimsci.v27i4.1144 (in Portuguese).

Volenec, J.J. & Nelson, C.J. 2020. Carbon Metabolism in Forage Plants. In: Moore, K.J.; Collins, M.; Nelson, C.J. & Redfearn, D.D. (Ed.). *Forage: The Science Of Grassland Agriculture.* Croydon: Willey Blackwell, 65–84.

Volenec, J.J., Ourry, A. & Joern, B.C. 1996. A role for nitrogen reserves in forage regrowth and stress tolerance. *Physiologia Plantarum* **97**(1), 185–193. doi: 10.1111/j.1399-3054.1996.tb00496.x

Weise, S.E., Wijk, K.J. & Sharkey, T.D. 2011. The role of transitory starch in C3, CAM, and C4 metabolism and opportunities for engineering leaf starch accumulation. *Journal of Experimental Botany* **62**(9), 3109–3118. doi: 10.1093/jxb/err035

Wiley, E., Huepenbecker, S., Casper, B.B. & Helliker, B.R. 2013. The effects of defoliation on carbon allocation: can carbon limitation reduce growth in favour of storage? *Tree Physiology* **33**(11), 1216–1228. doi: 10.1093/treephys/tpt093

Yasuoka, J.I., Pedreira, C.G.S., Da Silva, V.J., Alonso, M.P., Da Silva, L.S. & Gomes, F.J. 2018. Canopy height and N affect herbage accumulation and the relative contribution of leaf categories to photosynthesis of grazed *Brachiaria* grass pastures. *Grass and Forage Science* **73**(1), 183–192. doi: 10.1111/gfs.12302

Agronomy Research **21**(S3), 1597–1606, 2023
https://doi.org/10.15159/AR.23.075

Physicochemical properties of goat milk yoghurt with synbiotics from inulin of mangrove apple and *Lactobacillus plantarum*

J.M.W. Wibawanti[1,3], S. Mulyani[2], R. Hartanto[1] and A.M.Legowo[2,*]

[1]Universitas Diponegoro, Faculty of Animal and Agricultural Sciences, Department of Animal Science, Semarang 50275, Central Java, Indonesia
[2]Universitas Diponegoro, Faculty of Animal and Agricultural Sciences, Department of Food Technology, Semarang 50275, Central Java, Indonesia
[3]Universitas Muhammadiyah Purworejo, Faculty of Agricultural Science, Department of Animal Science, Purworejo 54151, Central Java, Indonesia
[*]Correspondence: anangmohlegowo@lecturer.undip.ac.id

Received: March 19th, 2023; Accepted: August 14th, 2023; Published: August 23rd, 2023

Abstract. Physicochemical changes could affect the quality of goat milk yoghurt. Yoghurt quality has been improved by incorporating a synbiotic derived from a prebiotic combined with probiotics. This study aimed to evaluate the effect of different concentrations of synbiotics (inulin of mangrove apple and *Lactobacillus plantarum*) in the physicochemical properties of goat's milk yoghurt. This study used a Completely Randomized Design (CRD) with 5 treatments and 4 replications, with differences in the concentration of synbiotics as much as 0, 2, 4, 6, and 8%. The addition of synbiotics was significant ($p < 0.05$) in the sugar reduction, colour, and syneresis of yoghurt products. They did not significantly affect ($p > 0.05$) the firmness of yoghurt texture. This study provides support for the addition of synbiotics to improve physicochemical properties of goat's milk yogurt.

Key words: inulin, mangrove apple, physicochemical, synbiotics, yogurt.

INTRODUCTION

The addition of synbiotics to yoghurt products is one of the development trends for dairy products in Indonesia. Yoghurt has benefited as a portion of healthy food due to the beneficial effects of its bacteria which are typically attributed to the presence of probiotics and bioactive peptides (Mantzourani et al., 2022; Wang et al., 2022; Zahid et al., 2022). *Streptococcus thermophilus* and *Lactobacillus bulgaricus* combine their bacterial cultures to produce yoghurt (Sharma & Ramanathan, 2021; Mitra et al., 2022). Synergistic synbiotics, which contain prebiotics that can specifically stimulate probiotic growth, also have beneficial effects on digestive health (Lim, 2018). Yoghurt that contains both beneficial bacteria (probiotic microorganisms) and indigestible carbohydrates (prebiotic compounds) to encourage the growth of those bacteria is known as a synbiotic yoghurt (El-Kholy et al., 2020; Sakr & Massoud, 2021).

Several studies were related to synbiotic yoghurt including synbiotic yoghurt using puree banana and *Lactobacillus* (Fidina et al., 2018), goat milk of synbiotic yoghurt with sorghum flour and *Lactobacillus acidophilus* (Sukarmimah et al., 2019), synbiotic yoghurt containing *Bifidobacterium* and konjac mannan oligosaccharides (Li et al., 2021b), and synbiotic yoghurt with lactitol and *Lacticaseibacillus paracasei* (Li et al., 2022). Synbiotics could increase the effectiveness of probiotics (Shafi et al., 2019, Li et al., 2022). Prebiotics including inulin can promote the development of probiotic product (El-Kholy et al., 2020). Mangrove apples (*Sonneratia caseolaris*), have an inulin content of up to 5.08% (Wibawanti et al., 2021).

Yoghurt is one of the most popular fermentation products made from goat's milk (Park et al., 2019). Yoghurt is the preferred dairy product because of its unique qualities (Ehsani et al., 2018). One of the determinants of yoghurt quality are its physicochemical properties yoghurt (Wibawanti & Rinawidiastuti., 2018; Khalifa & Zakaria, 2019; Prayitno et al., 2020). The texture and appearance of yoghurt are important indicators of its quality and structure (Li et al., 2021a; Hu et al., 2022; Mitra et al., 2022). Yoghurt quality also varies based on colour, affecting how well consumers will accept the product (Ścibisz et al., 2019; Marand et al., 2020). Therefore, this study aimed to evaluate the effect of different concentrations of synbiotics from inulin of mangrove apple and *Lactobacillus plantarum* on the physicochemical properties of goat's milk yoghurt.

MATERIALS AND METHODS

Synbiotic preparation

The synbiotics were prepared by combining *Lactobacillus plantarum* and inulin extract of mangrove apple as a prebiotic according to Setyaningrum et al. (2019), with a few modifications. Mangrove apple inulin was extracted using the procedure reported by Wibawanti et al. (2022). The mangrove apple was divided into tiny pieces and heated to 90 °C. Mangrove apple was extracted in hot water at 90 °C for 60 minutes using a 1:4 ratio of fruit to water. The filtrates were kept at -18 °C after being precipitated with 40% ethanol. The filtrate was thawed to room temperature. The filtrate of the mangrove apple's inulin was centrifuged at 5,000 rpm for five minutes before the supernatant was taken out. The synbiotics were made from 10 mL *Lactobacillus plantarum* and 9% inulin from mangrove apples. They were incubated anaerobically in Man Rogosa and Sharpe (MRS) Broth for 24 hours at 37 °C.

Yoghurt preparation

Freeze-dried bacterial cultures, namely *Lactobacillus bulgaricus* (FNCC 0041) (2.89×10^8 CFU/mL), *Streptococcus thermophilus* (FNCC 0040) (9.6×10^7 CFU mL^{-1}), and *Lactobacillus plantarum* (FNCC 0026) (2.25×10^8 CFU mL^{-1}), were purchased from Gadjah Mada University. These strains were thawed at room temperature in a Man Rogosa and Sharpe (MRS) Broth at the ideal temperature (37 °C) before the experiments to produce fresh cultures from frozen stocks (Fan et al., 2022).

Five different yoghurts were produced using a combination of the *Streptococcus thermophilus* and *Lactobacillus bulgaricus* strains, with four replications. Synbiotic yoghurt was done by method Sharma & Ramantha's (2021). The fresh milk from the goat was heated at 80 °C for 15 min. It was cooled at a temperature of 45–42 °C for 20 minutes. The starter culture consisting of *Streptococcus thermophilus* and

Lactobacillus bulgaricus was added with the ratio of maximum 5%. The treatment of synbiotics (*Lactobacillus plantarum* and inulin of mangrove apple) was applied with different concentrations of as much as 0 (control), 2, 4, 6, and 8% (v/v). For five hours, the incubation was carried out at 42 °C. The yoghurt synbiotic was kept at refrigeration temperature (4 ± 1 °C) to calculate coagulation.

Reducing sugar

Reducing sugar in the synbiotic yoghurt was determined using the Somogyi - Nelsen method previously described by Wibawanti et al. (2022). One gram of synbiotic yoghurt samples was prepared. The samples were added to the volume with distilled water until it reached 100 mL. The samples were centrifuged and then filtered. One mL of the filtrate was dissolved in one mL of Nelson reagent. The solution was heated over a waterbath with a temperature of 100 ℃ for 30 minutes. The mixture was cooled to 25 °C, 1 mL of the arsenomolybdate reagent was added, and it was agitated. Then, 10 mL of distilled water was added. The absorbance of the vortex solution was then measured using a spectrophotometer with a wavelength of 540 nm.

The firmness texture

The firmness texture of yoghurt were analysed using a texture analyser, according to Al-Sahlany et al. (2022), with modification. The yoghurt samples were served in cylindrical glass cups (50 mm diameter, 75 mm high) and then measured immediately after being removed from the fridge (4 °C). The sample compression was performed to 50% of their original height with probe P/35. A 50-kg load cell was used at a crosshead speed of 1 $mmVs^{-1}$.

Colour measurement

The yoghurt samples were poured into tubes and colour analysis was carried out using Colorimeter as previously described by Qiu et al. (2021). Values of L* (lightness), a*(red-green) and b* (yellow-blue) were evaluated.

Syneresis yoghurt

The syneresis of the yoghurt was evaluated using the centrifugation method, which was modified from the method proposed by Pereira et al. (2021).Yoghurt samples of 10 mL were placed in 15 mL Falcone tubes previously weighed and centrifuged at 3,500 rpm for 15 min at 4 °C. The syneresis index was calculated as a percentage of the weight of the serum in relation to the initial weight of the yoghurt after the supernatant serum was removed and weighed.

Statistical analysis

The mean value of four measurements was taken for each parameter assessed in the study. Data obtained from the Completely Randomized Design (CRD) study were evaluated statistically using variance analysis (ANOVA) and Duncan's new multiple-range tests. SPSS 16.0 software was used to statistically analyze all of the results.

RESULTS AND DISCUSSION

Reducing Sugar

Statistical analysis showed that the addition of synbiotics had a significant effect ($p < 0.05$) on reducing sugar from yoghurt. The results of the reducing sugar is presented in Fig. 1. Goat milk yoghurt with synbiotic treatment had a significant effect ($p < 0.05$)on the value of reducing sugar. The addition of synbiotics resulted in lower reducing sugar content ($p < 0.05$) compared to the yoghurt control. Reducing sugar in yoghurt without treatment (control) of 4.06% ± 0.28 was not significantly different ($p > 0.05$) with the addition of 2% or 4% synbiotic with a value of 3.86% ± 0.15. The addition of synbiotics with a concentration of 6% showed results that were not significantly different ($p > 0.05$) with a concentration of 8% with a value of 3.53% ± 0.16 and 3.68 ± 0.08, respectively.

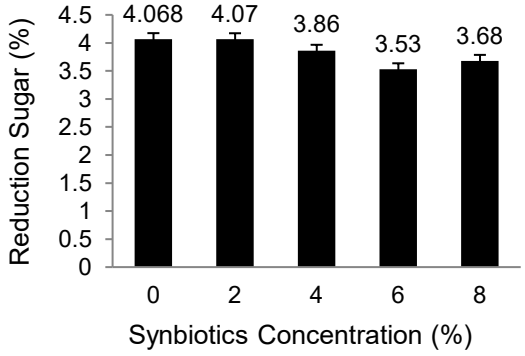

Figure 1. The sugar reduction of synbiotic yoghurt.

The reduced sugar content of synbiotic goat milk yoghurt was significantly lower than that of yoghurt without synbiotics. The decrease in sugar reduction value is thought to be due to inulin from mangrove apple extract contained in prebiotics used as a source for the growth of lactic acid bacteria, both *Lactobacillus bulgaricus*, *Streptococcus thermophilus*, and *Lactobacillus plantarum* in yoghurt, in order to increase the viability of probiotics. Krasaekoopt & Watcharapoka, (2014) reported that the use of prebiotics is a factor that can increase the viability of probiotics. Hartati et al. (2012) reported that the total amount of reduced sugar in yoghurt can support the growth of lactic acid bacteria.

The firmness texture of synbiotics yoghurt

Firmness texture is one of the determining factors for assessing the physical characteristics of yoghurt. Firmness texture is used to measure the maximum force of the material at a certain deformation in the sample, which directly reflects the yoghurt's gel strength (Li et al., 2022). The firmness results are shown in Fig. 2. Statistical analysis revealed that the addition of synbiotics did not have a significant ($p > 0.05$) effect on the firmness of yoghurt. The addition of 0, 2, 4, 6, and 8% synbiotics showed results that were not significantly different with value of 10.64 ± 2.25, 10.67 ± 1.00, 11.65 ± 1.44, 10.65 ± 1.53, and 8.5 ± 0.73 g, respectively.

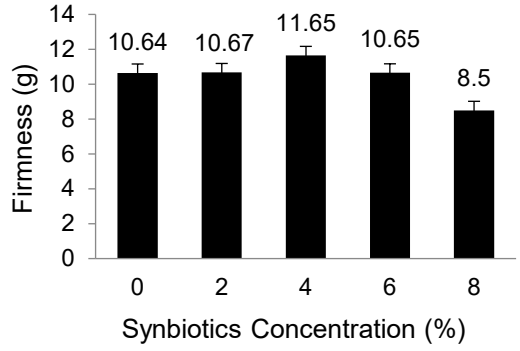

Figure 2. The Firmness texture of synbiotic yoghurt.

The inulin content of mangrove apples as a polysaccharide in synbiotics influences the texture of yoghurt. Synbiotic yoghurt's firmness is also influenced by the protein content. Nadtochii et al. (2020) reported that polysaccharides could be used in dairy products to modify the rheological properties. The texture of yoghurt is directly dependent on the type of protein, the protein content, and the total solids yoghurt (Ścibisz et al., 2019). The texture is also caused by the interaction of proteins, fats, and water in the food matrix (Mitra et al., 2022). Hu et al. (2022) reported that during yoghurt production, stabilizers were added to bind free water as hydration and stabilize protein molecules in the network through covalent or electrostatic interactions.

Colour property

The lightness (L) of synbiotic yoghurt is shown in Fig. 3. Results based on the research showed that the addition of synbiotics had an effect on the colour of the lightness (L) of yoghurt ($p < 0.05$). The addition of synbiotics showed significantly different results ($p < 0.05$) on the lightness colour of synbiotic yoghurt. The addition of synbiotics with concentrations of 0, 2, 4, and 6% showed no different results between treatments ($p > 0.05$) with average values of 88.41 ± 3.81; 88.53 ± 1.03; 89.19 ± 0.56; 89.65 ± 0.14, respectively. The addition of synbiotics with a concentration of 8% showedsignificantly different results ($p < 0.05$) when compared to other treatments with a value of 81.31 ± 8.53. The results showed that an 8% synbiotic concentration decreased the lightness value of yogurt. This is because inulin from mangrove apples has a brownish color, which causes the lightness value to be lower when added to goat's milk yogurt. Qiu et al. (2021) reported that the the addition of rose extracts can reduce the lightness of the yogurt color.

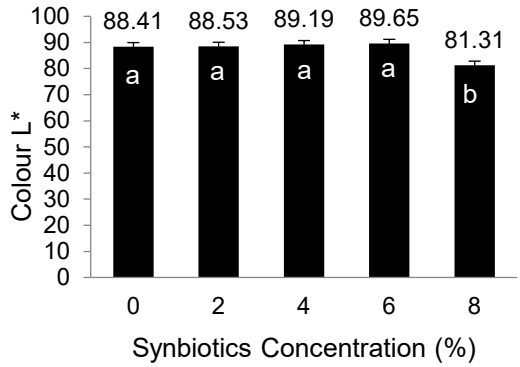

Figure 3. The lightness (L) colour of synbiotic yoghurt.

The redness (a*) colour of synbiotic yoghurt is presented in Fig. 4. The addition of synbiotics showed no significant ($p > 0.05$) effect on the redness colour of symbiotic.

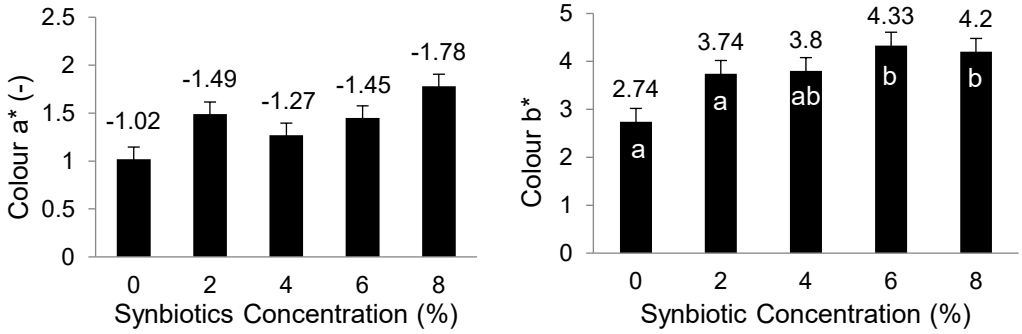

Figure 4. The redness (a*) and yellowness (b*) color of synbiotic yoghurt.

The redness (a*) colour of synbiotic yoghurt is presented in Fig. 4. The addition of synbiotics showed no significant ($p > 0.05$) effect on the redness colour of synbiotic yoghurt. The redness of yoghurt with the different concentrations of 0, 2, 4, 6, and 8% was the value -1,02 ± 0.52; -1.49 ± 0.23; -1.27 ± 0.26; -1.45 ± 0.43; and -1.78 ± 1.9, respectively. The yellowness (b*) colour of synbiotic yoghurt is shown in Fig. 4. The addition of synbiotics showed significant results ($p < 0.05$) on the yellowness colour of synbiotic yoghurt. The yellowness colour of yoghurt with the different concentrations of 0, 2, and 4% was the value 2.74 ± 1.0; 3.74 ± 0.52; 3.8 ± 0.28. The addition of synbiotics at concentrations of 6 and 8% did not result in a statistically significant difference, with values of 4.33 ± 1.0 and 4.2 ± 0.5. The addition of synbiotics at concentrations of 0 and 2% resulted in a statistically significant difference when compared to concentrations of 6 and 8%. This is due to the presence of pigments in mangrove apples as a source of prebiotics. Mangrove apples contain phenol components that may contribute to the colour of yoghurt. Pourjavid et al. (2022) reported a change in the colour parameters of a synbiotic yoghurt in the presence of natural prebiotics and *Lactobacillus paracasei* microencapsulation. The colour of yoghurt can also be influenced by adding natural plants that contain pigments (Fan et al., 2022). Ścibisz et al. (2019) reported that the colour of yoghurt indicates the concentration of pigments in the product. The water-soluble plant pigments anthocyanins are among the phenolic compounds (Khoo et al., 2017).

Yoghurt syneresis

The results of the study on the syneresis value of synbiotic yoghurt are presented in Fig. 5. The results showed that the synbiotic addition of inulin of mangrove apple with *Lactobacillus plantarum* with different concentrations had a significant effect ($p < 0.05$) on the syneresis value of yoghurt. It caused may be due to the extensive protein-carbohydrate interactions produced by inulin. It can extend its branched structure more evenly into casein aggregates. According to Gomes et al. (2022) that protein and carbohydrate interaction results in a decrease in syneresis and an increase in gel stability. Milk protein exposed to lactic acid (LA) produced by lactic acid bacteria coagulates to form a compact structure (Hosseini & Behbahani, 2021). Zakaria et al. (2020) reported that the decreased syneresis in the yoghurt can occur with an increase in total solids content and absorption of excess whey by lactoferrin powder.

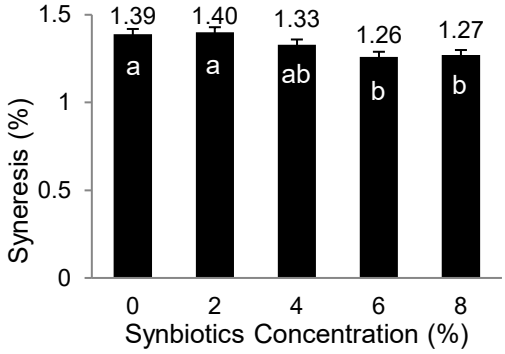

Figure 5. The syneresis of synbiotic yoghurt.

The addition of synbiotics showed significantly different results ($p < 0.05$) on the syneresis value of yoghurt. The addition of synbiotics with concentrations of 0, 2, and 4% showed non-significant results between treatments ($p > 0.05$) with syneresis values of 1.39 ± 0.01, 1.4 ± 0.13, and 1.33 ± 0.11%. The addition of synbiotics with concentrations of 6 and 8% showed significantly different results ($p < 0.05$) when compared to other treatments with syneresis values of 1.26 ± 0.05 and 1.27 ± 0.01%.

The addition of synbiotics to yoghurt showed lower syneresis results. The addition of synbiotics to yoghurt with various concentrations affects the total dissolved solids, thus causing differences in syneresis yoghurt. The syneresis was lower in yoghurts with the addition of synbiotics 6 and 8% compared with control yoghurt. Inulin in the synbiotics has a stabilizer in yoghurt products. Benmeziane et al. (2021) reported that stabilizers like pectin, starches, gums, or whey protein concentrate can be added to prevent syneresis. Setyawardani et al. (2020) stated that high-quality fermented products with low syneresis. Park et al. (2019) reported that syneresis can be avoided by increasing stabilizers such as pectin, starches, gums, or whey protein concentrate. In the literature, Celik & Temiz, (2022) reported that syneresis in yoghurt was associated with the dry matter content, more specifically the protein content.

CONCLUSIONS

The addition of 8% synbiotic (inulin of mangrove apple and *Lactobacillus plantarum*) to goat milk yoghurt could improve the quality of physicochemical properties including reduced sugar, colour, and syneresis. However, the addition of synbiotics to the firmness texture was not significant.

ACKNOWLEDGEMENTS. The research was supported by the Ministry of Education, Culture, Research, and Technology of the Republic of Indonesia. Contract No.187-48/UN7.6.1/PP/2022.

REFERENCES

Al-Sahlany, S.T.G., Khassaf, W.H., Niamah, A.K. & Al-Manhel, A.J.A. 2022. Date juice addition to bio-yoghurt: The effects on physicochemical and microbiological properties during storage, as well as blood parameters in vivo. *J. the Saudi Society of Agric. Sci*. **22**, 71–77. https://doi.org/10.1016/j.jssas.2022.06.005

Benmeziane, F., Raigar, R.K., Ayat, N.E.H., Aoufi, D, Djermoune-Arkoub, L. & Chala, A. 2021. Lentil (*Lens culinaris*) flour addition to yoghurt: Impact on physicochemical, microbiological and sensory attributes during refrigeration storage and microstructure changes. *Lwt*. **140**, 110793. https://doi.org/10.1016/j.lwt.2020.110793

Celik, O.F. & Temiz, H. 2022. *Lactobacilli* isolates as potential aroma producer starter cultures: Effects on the chemical, physical, microbial, and sensory properties of yoghurt. *Food Biosci*. **48**(April). https://doi.org/10.1016/j.fbio.2022.101802

Ehsani, J., Mohsenzadeh, M., Khomeiri, M. & Ghasemnezhad, A. 2018. Chemical characteristics, and effect of inulin extracted from artichoke (*Cynara scolymus* L.) root on biochemical properties of synbiotic yoghurt at the end of fermentation. *Iranian J. Chem. Chem. Engineering* **37**(2), 219–230.

El-Kholy, W.M., Aamer, R.A. & Ali, A.N.A. 2020. Utilization of inulin extracted from chicory (*Cichorium intybus* L.) roots to improve the properties of low-fat synbiotic yoghurt. *Annals Agric. Sci*. **65**(1), 59–67. https://doi.org/10.1016/j.aoas.2020.02.002

Fan, X., Du, L., Xu, J., Shi, Z., Zhang, T., Jiang, S., Zeng, X., Wu, Z. & Pan, D. 2022. Effect of single probiotics *Lacticaseibacillus casei* CGMCC1.5956 and *Levilactobacillus brevis* CGMCC1.5954 and their combination on the quality of yoghurt as fermented milk. *Lwt-Food Sci. Technol*. **163**, 113530. https://doi.org/10.1016/j.lwt.2022.113530

Fidina, N., Sukarminah, E. & Sumanti., D.M. 2018. The effects of the addition of banana puree to the total number of total probiotic bacteria, ph value and organoleptic characteristics of the synbiotic yoghurt made from goat milk and banana puree. *J. Industrial Inform. Technol.Agric*. **2**(1), 12–21. https://doi.org/10.24198/jiita.v2i1.17649

Hartati, A.I, Mulyani, S. & Legowo, A.M. 2012. Lactose and reduction sugar concentration, pH, and the sourness of date flavored yoghurt drink as probiotic baverage. *J. App. Food. Technol*. **1**(1), 1–3.

Gomes, E.R., Carneiro, L.C.M., Stephani, R., Carvalho, A.F., Renhe, I.R.T., Wolfschoon-Pombo, A.F. & Perrone, Í.T. 2022. Effect of sugar reduction and addition of corn fibre and polydextrose on pore size and syneresis of yoghurt. *Inter. Dairy J*. **129**. https://doi.org/10.1016/j.idairyj.2021.105298

Hosseini, S.M. & Behbahani, M. 2021. Enhancement of probiotics viability and lactic acid production in yoghurts treated with *Prangos ferulaceae* and *Carum copticum* plant extracts.*Biocatalys. Agric. Biotechnol*. **35**(July),102084.https://doi.org/10.1016/j.bcab.2021.102084

Hu, L., Ding, F., Liu, W., Cheng, Y., Zhu, J., Ma, L., Zhang, Y. & Wang, H. 2022. Effect of enzymatic-ultrasonic hydrolyzed chitooligosaccharide on rheology of gelatin incorporated yoghurt and 3D printing. *Food Hydrocolloids* **132**(2), 107851. https://doi.org/10.1016/j.foodhyd.2022.107851

Krasaekoopt, W. & Watcharapoka, S. 2014. Effect of addition of inulin and galactooligosaccharide on the survival of microencapsulated probiotics in alginate beads coated with chitosan in simulated digestive system, yoghurt and fruit juice. *Lwt-Food Sci. Technol*. **57**, 761–766. http://dx.doi.org/10.1016/j.lwt.2014.01.037

Khalifa, M.I. & Zakaria, A.M. 2019. Physiochemical, sensory characteristics and acceptability of a new set yoghurt developed from camel and goat milk mixed with buffalo milk. *Anim. Vet. Sci*. **7**(3), 172–177. http://dx.doi.org/10.17582/journal.aavs/2019/7.3.172.177

Khoo, H.E., Azlan, A., Tang, S.T. & Lim, S.M. 2017. Anthocyanidins and anthocyanins: colored pigments as food, pharmaceutical ingredients, and the potential health benefits. *Food Nutr. Res*. **61**. https://doi.org/10.1080/16546628.2017.1361779

Li, H., Liu, T., Yang, J., Wang, R., Li, Y., Feng, Y., Liu, D., Li, H. & Yu, J. 2021a. Effect of a microencapsulated synbiotic product on microbiology, microstructure, textural and rheological properties of stirred yoghurt. *Lwt*. **152**(29), 112302. https://doi.org/10.1016/j.lwt.2021.112302

Li, H., Song, W., Liu, T., Xu, S., Zhang, S., Zhang, Y., Liu, D., Li, H. & Yu, J. 2022. Developing novel synbiotic yoghurt with *Lacticaseibacillus paracasei* and lactitol: Investigation of the microbiology, textural and rheological properties. *Inter. Dairy J*. **135**, 105475. https://doi.org/10.1016/j.idairyj.2022.105475

Li, T., Yan, Q., Wen, Y, Liu, J, Sun, J. & Jiang, Z. 2021b. Synbiotic yoghurt containing konjac mannan oligosaccharides and *Bifidobacterium animalis* ssp. lactis BB12 alleviates constipation in mice by modulating the stem cell factor (SCF)/ c-Kit pathway and gut microbiota. *J. Dairy Sci*.**104**(5), 5239–5255. https://doi.org/10.3168/jds.2020-19449

Lim, E.S. 2018. Preparation and functional properties of probiotic and oat-based synbiotic yoghurts fermented with lactic acid bacteria. *Applied Bio. Chem*. **61**(1), 25–37. https://doi.org/10.1007/s13765-017-0333-5

Mantzourani, C., Batsika, C.S., Kokotou, M.G. & Kokotos, G. 2022. Free fatty acid profiling of Greek yoghurt by liquid chromatography-high resolution mass spectrometry (LC-HRMS) analysis. *Food Res. Inter.* **160**(April), 111751. https://doi.org/10.1016/j.foodres.2022.111751

Marand, A., Amjadi, M., Marand, A.S., Roufegarinejad, M., Jafari, S.M. 2020. Fortification of yoghurt with flaxseed powder and evaluation of its fatty acid profile, physicochemical, antioxidant, and sensory properties. *Powder Technol*. **359**, 76–84. https://doi.org/10.1016/j.powtec.2019.09.082

Mitra, P., Nepal, K. & Tavade, P. 2022. Effect of whey and soy proteins fortification on the textural and rheological properties of value-added yoghurts. *Applied Food Res*. **2**(2), 1–6. https://doi.org/10.1016/j.afres.2022.100195

Nadtochii, L.A., Baranenko, D.A., Lu, W., Safronova, A.V., Lepeshkin, A.I. & Ivanova, V.A. 2020. Rheological and physical chemical properties of yogurt with oat chia seeds composites. *Agronomy Research* **18**(S3), 1816–1828. https://doi.org/10.15159/AR.20.142

Park, Y.W., Oglesby, J., Hayek, S.A., Aljaloud, S.O., Gyawali, R. & Ibrahim, S.A. 2019. Impact of different gums on textural and microbial properties of goat milk yoghurts during refrigerated storage. *Foods*. **8**(5), 1–7. https://doi.org/10.3390/foods8050169

Pereira, C.T.M., Pereira, D.M., Medeiros, A.C., Hiramatsu, E.Y., Ventura, M.B. & Bolini, H.M.A. 2021. Skyr yoghurt with mango pulp, fructooligosaccharide and natural sweeteners: Physical aspects and drivers of liking. *Lwt*. **150**(June). https://doi.org/10.1016/j.lwt.2021.112054

Pourjavid, H., Ateai, M., Pourahmad, R., Anvar, A.A. & Behmadi, H. 2022. Improvement of the quality parameters of a novel synbiotic yoghurt sauce using microencapsulated *Lactobacillus paracasei* and natural prebiotics. *Food Sci. Technol, Campinas*. **42**, e40322. https://doi.org/10.1590/fst.40322

Prayitno, S.S., Sumarmono, J., Rahardjo, A.H.D. & Setyawardani, T. 2020. Modification of physical properties of goat milk yoghurt by addition of microbial transglutaminase enzyme and external protein sources. *Jurnal Aplikasi Teknologi Pangan*. **9**(2), 77–82. https://doi.org/10.17728/jatp.6396

Qiu, L., Zhang, M., Mujumdar, A.S. & Chang, L. 2021. Effect of edible rose (*Rosa Rugosa* Cv. Plena) flower extract addition on the physicochemical, rheological, functional and sensory properties of set-type yogurt. *Food Biosci.* **43**(July), 101249. doi: 10.1016/j.fbio.2021.101249

Sakr, E.A.E. & Massoud, M.I. 2021. Impact of prebiotic potential of stevia sweeteners-sugar used as synbiotic preparation on antimicrobial, antibiofilm, and antioxidant activities. *Lwt*. **144**(March), 111260. https://doi.org/10.1016/j.lwt.2021.111260

Ścibisz, I., Ziarno, M. & Mitek, M. 2019. Color stability of fruit yoghurt during storage. *J. Food Sci. Technol*. **56**(4), 1997–2009. https://doi.org/10.1007/s13197-019-03668-y

Setyaningrum, S., Yunianto, V.D., Sunarti, D. & Mahfudz, L.D. 2019. The Effect of synbiotic (inulin extract from gembili tuber and *Lactobacillus plantarum*) on growth performance, intestinal ecology and haematological indices of broiler chicken. *Livest. Res. Rural Develop*. **31**(11), Article #177.http://www.lrrd.org/lrrd31/11/srise31177.html

Setyawardani, T., Sumarmono, J. & Widayaka, K. 2020. Physical and microstructural characteristics of kefir made of milk and colostrum. *Bulletin of Animal Science* **44**(1), 43–49. doi: 10.21059/buletinpeternak.v44i1.49130

Shafi, A., Naeem, R.H., Farooq, U., Akram, K., Hayat, Z., Naz, A. & Nadeem, H.R. 2019. Antimicrobial and antidiabetic potential of synbiotic fermented milk: A functional dairy product. *Inter. J. Dairy Technol*. **72**(1), 15–22. https://doi.org/10.1111/1471-0307.12555

Sharma, H. & Ramanathan, R. 2021. Gas chromatography-mass spectrometry based metabolomic approach to investigate the changes in goat milk yoghurt during storage. *Food Res. Inter*. **140**(August), 110072. https://doi.org/10.1016/j.foodres.2020.110072

Sukarmimah, E., Lanti, I., Wulandari, E., Lembong, E. & Utami, R. 2019. The effect of sorghum flour (*Sorghum bicolor* L. Moench) addition to characteristic quality of goat milk synbiotic yoghurt candidate. *IOP Conf. Series: Earth Environ. Sci*. **347**, 012012. https://doi:10.1088/1755-1315/347/1/012012

Wang, J., Liu, B., Qi, Y., Wu, D., Liu, X., Liu, C., Gao, Y., Shi, J., Fang, L. & Min, W. 2022. Impact of *Auricularia cornea* var. lipolysaccharides on the physicochemical, textual, flavor, and antioxidant properties of set yoghurt. *Inter. J. Biological Macrom*. **206**(2888),148–158. https://doi.org/10.1016/j.ijbiomac.2022.02.141

Wibawanti, J.M.W., Mulyani, S., Hartanto, R., Al-Baarri, A.N., Pramono, Y.B. & Legowo, A.M. 2022. The characteristics of goat milk synbiotics-yoghurt using *Lactobacillus plantarum* as probiotic and inulin of mangrove apple (*Sonneratia caseolaris*). *Adv. Anim. Vet. Sci*. **10**(11), 2475–2463.http://dx.doi.org/10.17582/journal.aavs/2022/10.11.2457.2463

Wibawanti, J.M.W., Mulyani, S., Legowo, A.M., Hartanto, R., Al-Baarri, A.N. & Pramono, Y.B. 2021. Characteristics of inulin from mangrove apple (*Sonneratia caseolaris*) with different extraction temperatures. *Food Res*. **5**(4),99–106. https://doi.org/10.26656/fr.2017.5(4).662

Wibawanti, J.M.W. & Rinawidiastuti, R. 2018. Physical and organoleptical properties of yoghurt drink with supplementation of mangosteen rind extract (*Garcinia Mangostana* L.). *J. Anim. Product Sci. Tehnol.* (JITEK). **13**(1), 27–37. https://doi.org/10.21776/ub.jitek.2018.013.01.3

Zahid, H.F., Ali, A., Ranadheera, C.S., Fang, Z., Dunshea, F.R. & Ajlouni, S. 2022. In vitro bioaccessibility of phenolic compounds and alpha-glucosidase inhibition activity in yoghurt enriched with mango peel powder. *Food Biosci*. **50**(PA), 102011. https://doi.org/10.1016/j.fbio.2022.102011

Zakaria, A.M., Zakaria, H.M., Abdelhiee, E.Y., Fadl, S.E. & Ombarak, R. 2020. The impact of lactoferrin fortification on the health benefits and sensory properties of yoghurt. *J. Current Vet. Res*. **2**(2), 105–112.

INSTRUCTIONS TO AUTHORS

Papers must be in English (British spelling). Authors are strongly urged to have their manuscripts reviewed linguistically prior to submission. Contributions should be sent electronically. Papers are considered by referees before acceptance. The manuscript should follow the instructions below.

Structure: Title, Authors (initials & surname; an asterisk indicates the corresponding author), Authors' affiliation with postal address (each on a separate line) and e-mail of the corresponding author, Abstract (up to 250 words), Key words (not repeating words in the title), Introduction, Materials and methods, Results and discussion, Conclusions, Acknowledgements (optional), References.

Layout, page size and font

- Use preferably the latest version of **Microsoft Word**, doc., docx. format.
- Set page size to **ISO B5 (17.6×25 cm)**, all **margins at 2 cm**. All text, tables, and figures must fit within the text margins.
- Use single line spacing and **justify the text**. Do not use page numbering. Use **indent 0.8 cm** (do not use tab or spaces instead).
- Use font Times New Roman, point size for the title of article **14 (Bold)**, author's names 12, core text 11; Abstract, Key words, Acknowledgements, References, tables, and figure captions 10.
- Use *italics* for Latin biological names, mathematical variables and statistical terms.
- Use single ('…') instead of double quotation marks ("…").

Tables

- All tables must be referred to in the text (Table 1; Tables 1, 3; Tables 2–3).
- Use font Times New Roman, regular, 10 pt. Insert tables by Word's 'Insert' menu.
- Do not use vertical lines as dividers; only horizontal lines (1/2 pt) are allowed. Primary column and row headings should start with an initial capital.

Figures

- All figures must be referred to in the text (Fig. 1; Fig. 1 A; Figs 1, 3; Figs 1–3). Use only black and white or greyscale for figures. Avoid 3D charts, background shading, gridlines and excessive symbols. Use font **Arial, 10 pt** within the figures. Make sure that thickness of the lines is greater than 0.3 pt.
- Do not put caption in the frame of the figure.
- The preferred graphic format is Excel object; for diagrams and charts EPS; for half-tones please use TIFF. MS Office files are also acceptable. Please include these files in your submission.
- Check and double-check spelling in figures and graphs. Proof-readers may not be able to change mistakes in a different program.

References

- **Within the text**

In case of two authors, use '&', if more than two authors, provide first author 'et al.':

Smith & Jones (2019); (Smith & Jones, 2019);
Brown et al. (2020); (Brown et al., 2020)

When referring to more than one publication, arrange them by following keys: 1. year of publication (ascending), 2. alphabetical order for the same year of publication:

(Smith & Jones, 2019; Brown et al., 2020; Adams, 2021; Smith, 2021)

- **For whole books**

Name(s) and initials of the author(s). Year of publication. *Title of the book* (*in italics*). Publisher, place of publication, number of pages.

Behera, K.B. & Varma, A. 2019. *Bioenergy for Sustainability and Security*. Springer International Publishing, Cham, pp. 1–377.

- **For articles in a journal**

Name(s) and initials of the author(s). Year of publication. Title of the article. *Abbreviated journal title* (*in italic*) volume (in bold), page numbers.
Titles of papers published in languages other than English, should be replaced by an English translation, with an explanatory note at the end, e.g., (in Russian, English abstr.).

Bulgakov, V., Adamchuk, V., Arak, M. & Olt, J. 2018. The theory of cleaning the crowns of standing beet roots with the use of elastic blades. *Agronomy Research* **16**(5), 1931–1949. doi: 10.15159/AR.18.213

Doddapaneni, T.R.K.C., Praveenkumar, R., Tolvanen, H., Rintala, J. & Konttinen, J. 2018. Techno-economic evaluation of integrating torrefaction with anaerobic digestion. *Applied Energy* **213**, 272–284. doi: 10.1016/j.apenergy.2018.01.045

- **For articles in collections:**

Name(s) and initials of the author(s). Year of publication. Title of the article. Name(s) and initials of the editor(s) (preceded by In:) *Title of the collection (in italics)*, publisher, place of publication, page numbers.

Yurtsev, B.A., Tolmachev, A.I. & Rebristaya, O.V. 2019. The floristic delimitation and subdivisions of the Arctic. In: Yurtsev, B.A. (ed.) *The Arctic Floristic Region*. Nauka, Leningrad, pp. 9–104 (in Russian).

- **For conference proceedings:**

Name(s) and initials of the author(s). Year of publication. Name(s) and initials of the editor(s) (preceded by In:) *Proceedings name (in italics)*, publisher, place of publishing, page numbers.

Ritchie, M.E. & Olff, H. 2020. Herbivore diversity and plant dynamics: compensatory and additive effects. In: Olff, H., Brown, V.K. & Drent R.H. (eds) *Herbivores between plants and predators. Proc. Int. Conf. The 38th Symposium of the British Ecological Society*, Blackwell Science, Oxford, UK, pp. 175–204.

Please note

- Use '.' (not ',') for decimal point: 0.6 ± 0.2; Use ',' for thousands – 1,230.4;
- Use '–' (not '-') and without space: pp. 27–36, 1998–2000, 4–6 min, 3–5 kg
- With spaces: 5 h, 5 kg, 5 m, 5 °C, C : D = 0.6 ± 0.2; $p < 0.001$
- Without space: 55°, 5% (not 55 °, 5 %)
- Use 'kg ha^{-1}' (not 'kg/ha');
- Use degree sign ' ° ' : 5 °C (not 5 ^{O}C).